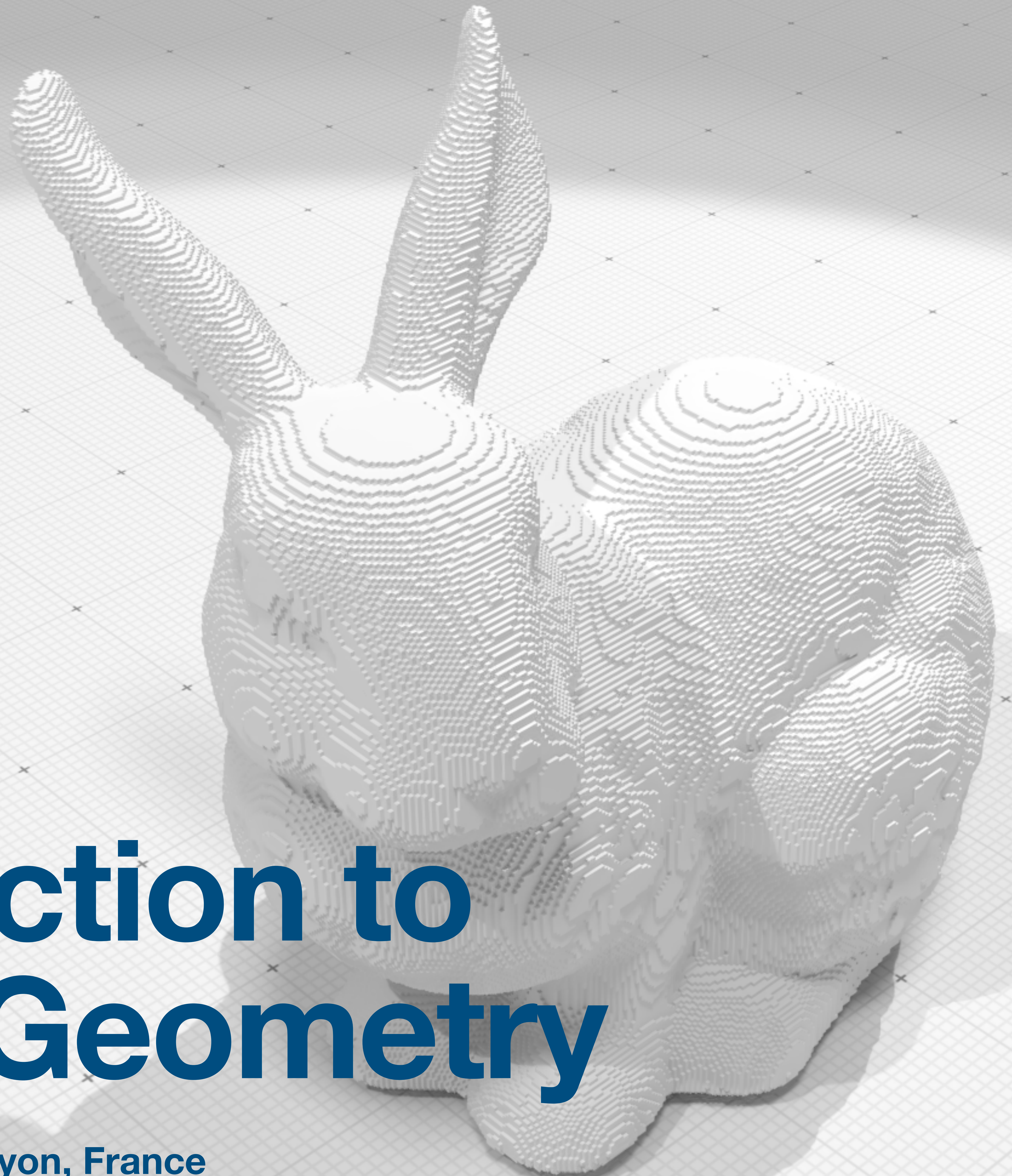

Introduction to Digital Geometry

David Coeurjolly, CNRS, Lyon, France

Jacques-Olivier Lachaud, Université Savoie Mont-Blanc, France

Outline

- context
- dgtal.org
- geometry with integers
- geometry processing on grids
- digital surface processing
- conclusion

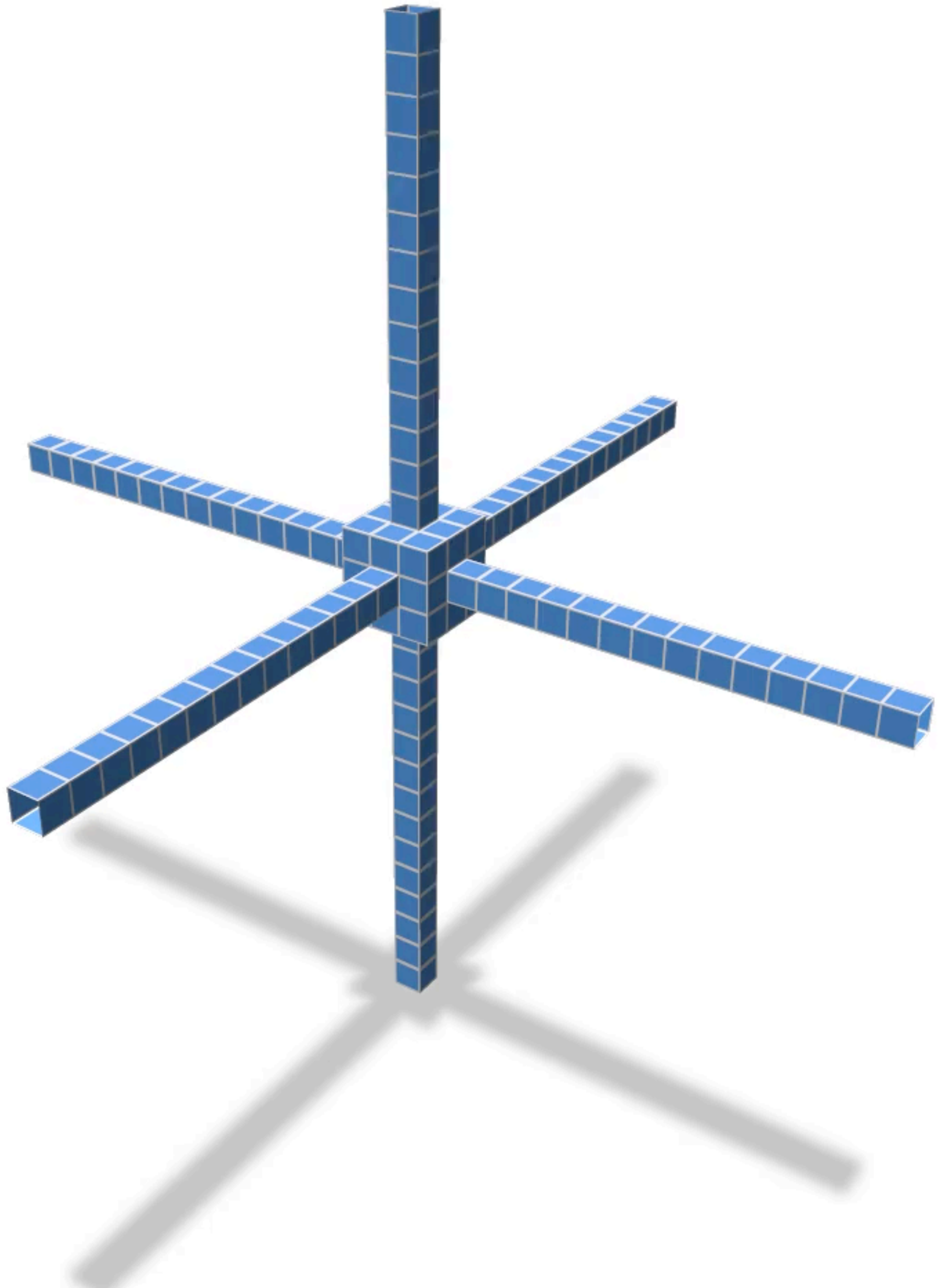

Outline

- context
- dgtal.org
- geometry with integers
- geometry processing on grids
- digital surface processing
- conclusion

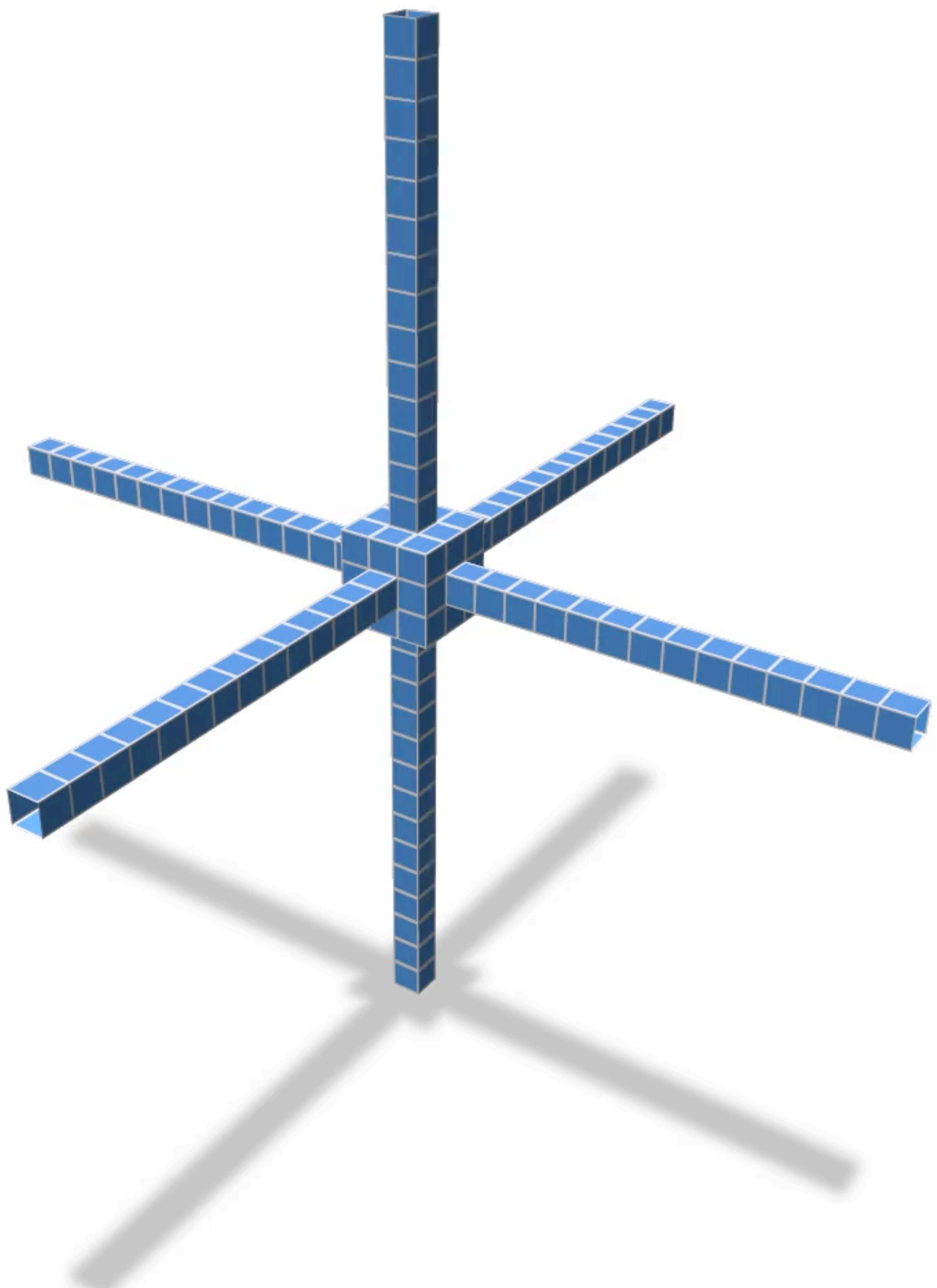

Motivations (1): devices

- Micro-tomographic images
  - material sciences
  - medical images

- Process geometry/topology of images partitions

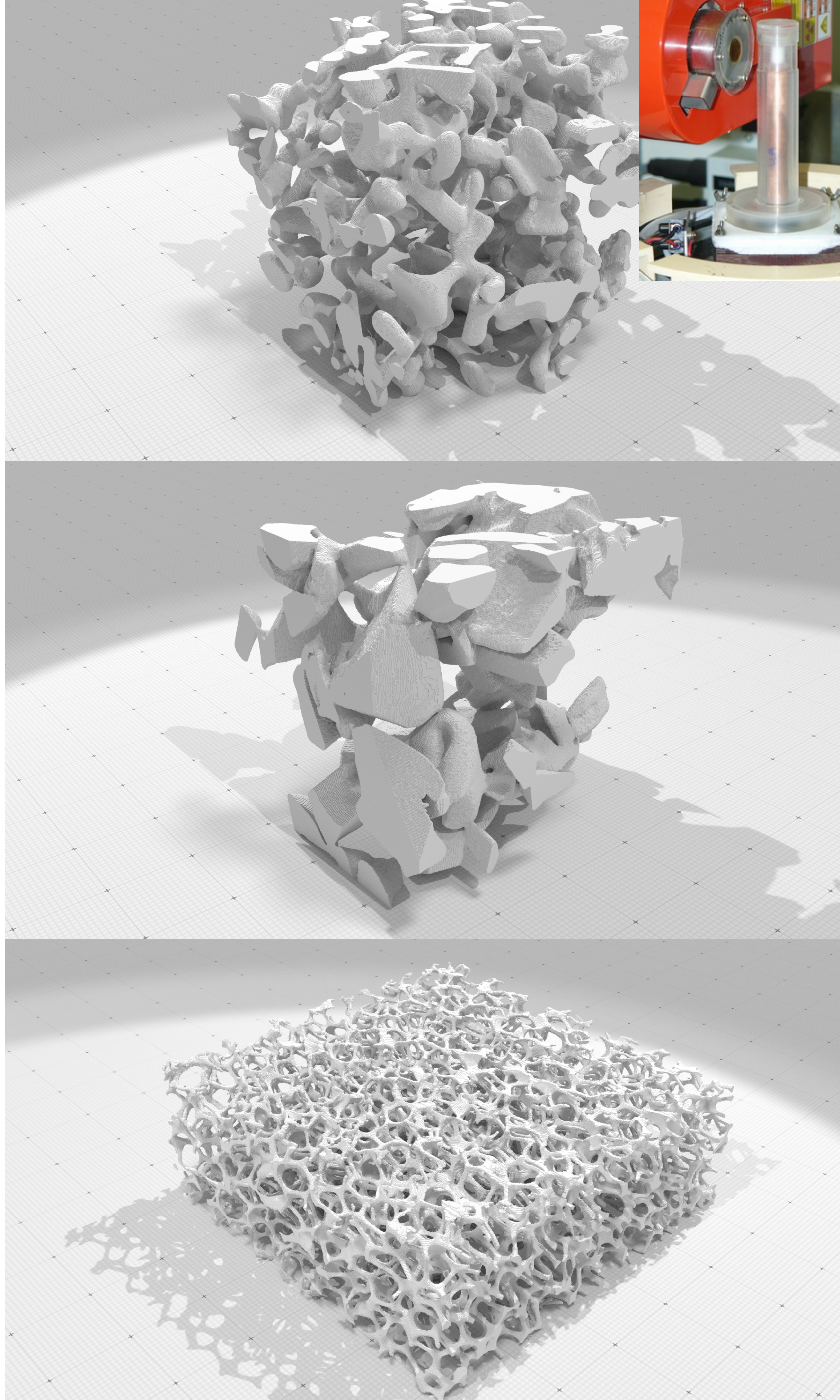

Motivations (1): devices

- Micro-tomographic images
  - material sciences
  - medical images

- Process geometry/topology of images partitions

$$\Rightarrow X \subset \mathbb{Z}^3$$

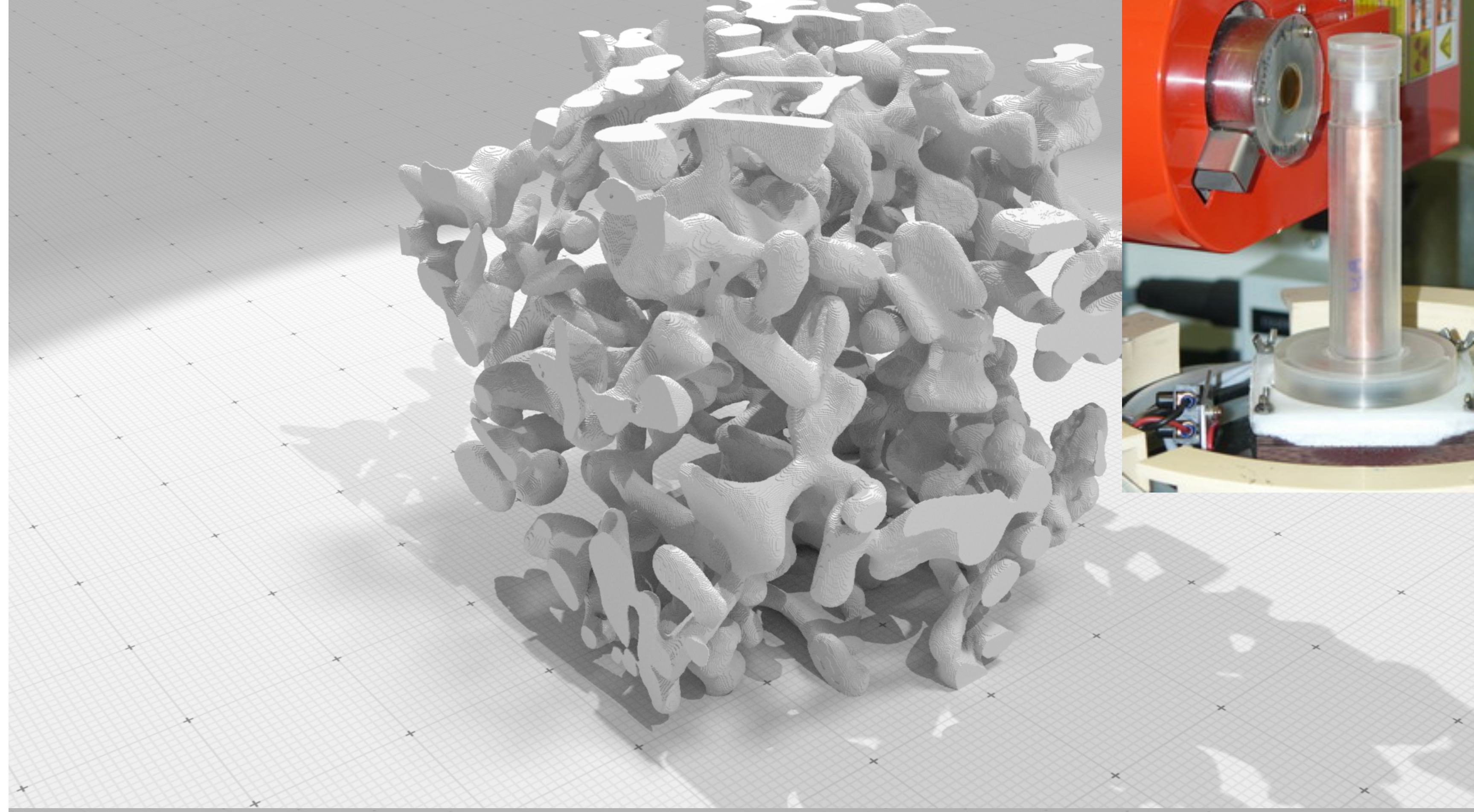
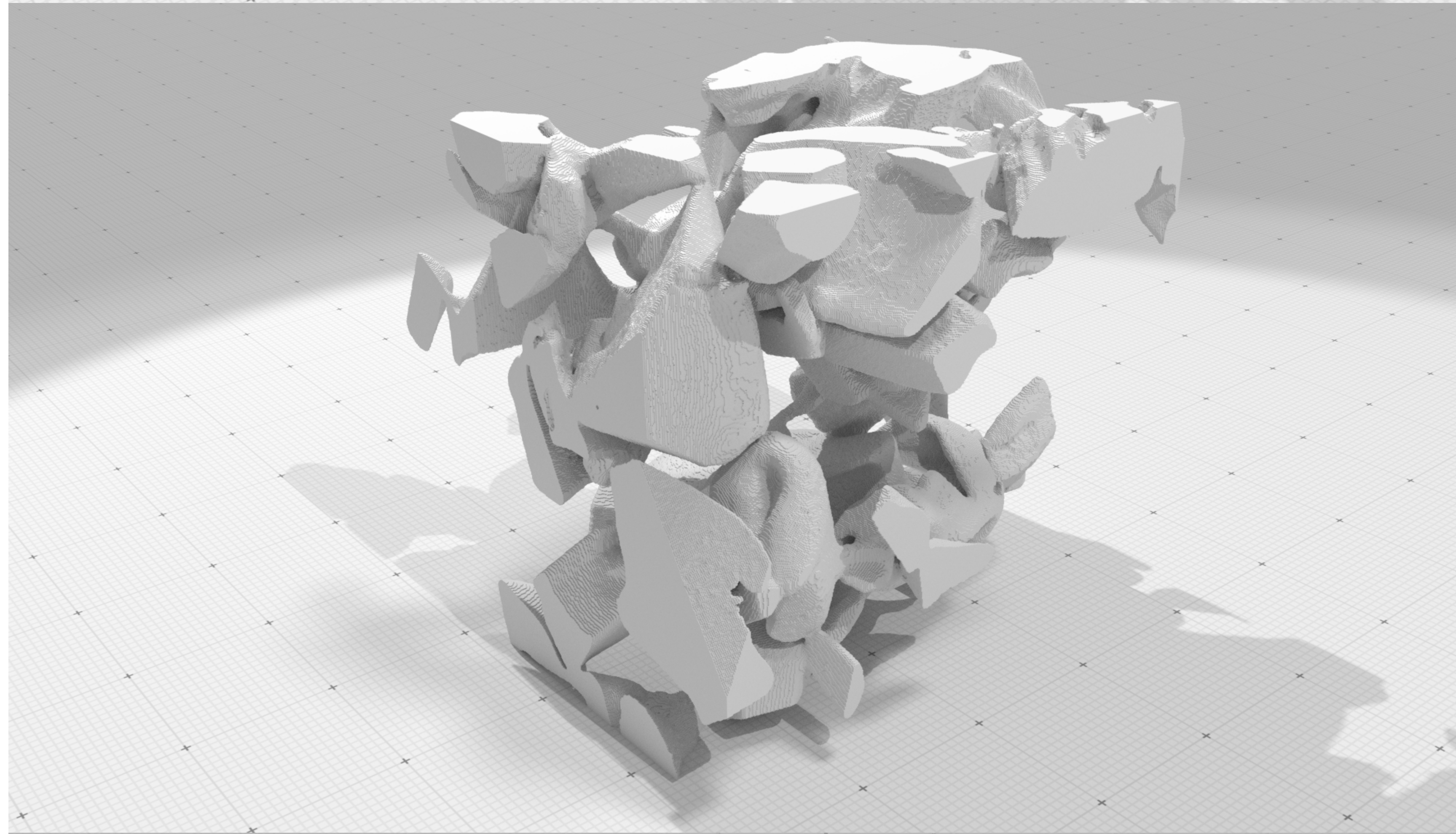
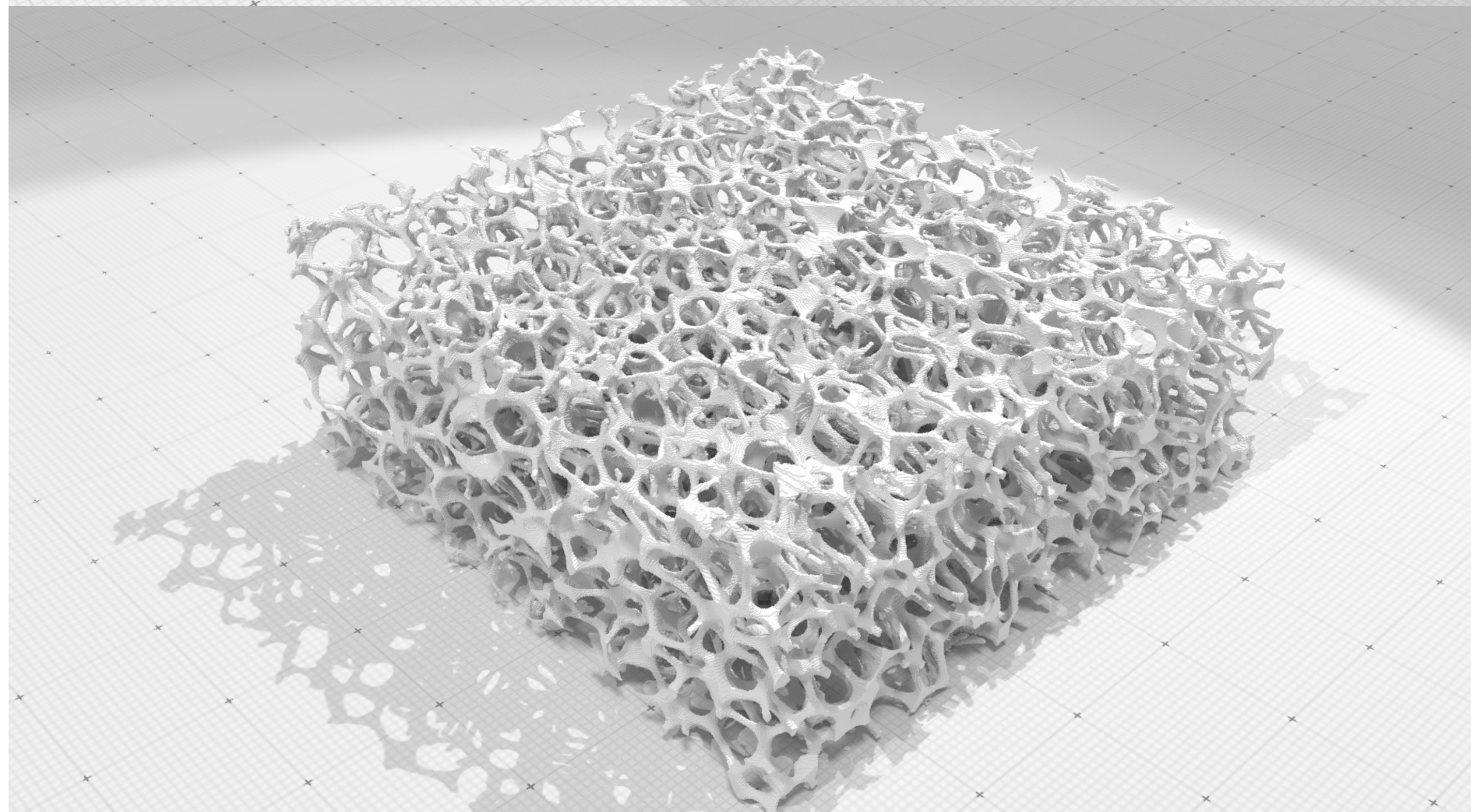

Motivations (2): $\mathbb{Z}^d$ as an efficient modelling space

- Shape optimization / fabrication

- As a proxy or an intermediate representation

  light transport simulation, booleans, medial axis, distance fields, multiple interfaces/objects tracking in a simulation loop…

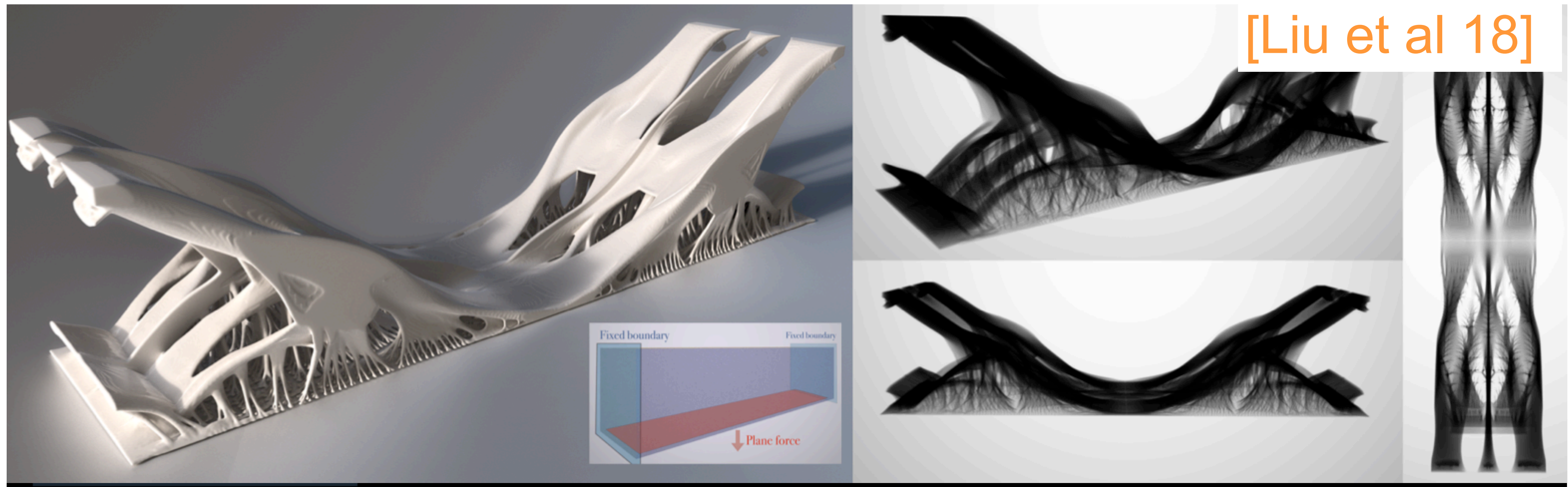

[Liu et al 18]

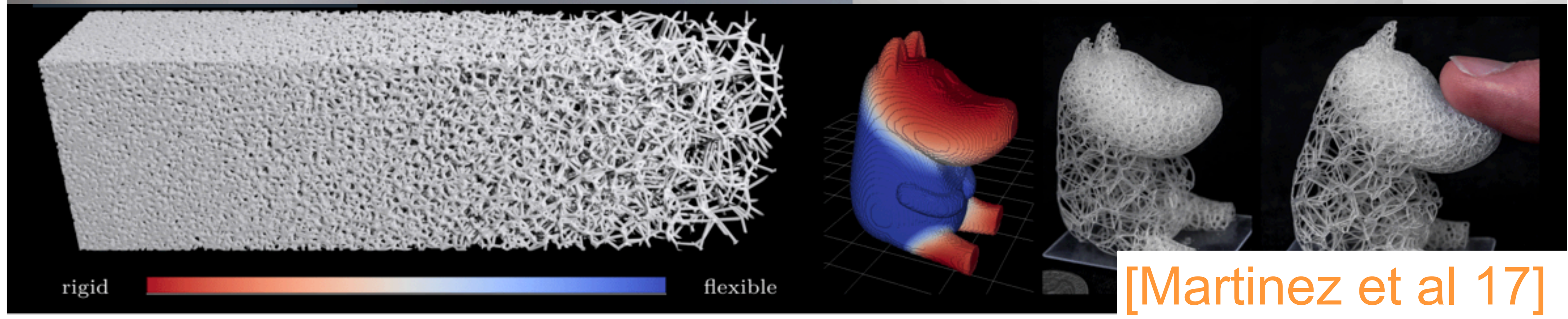

[Martinez et al 17]

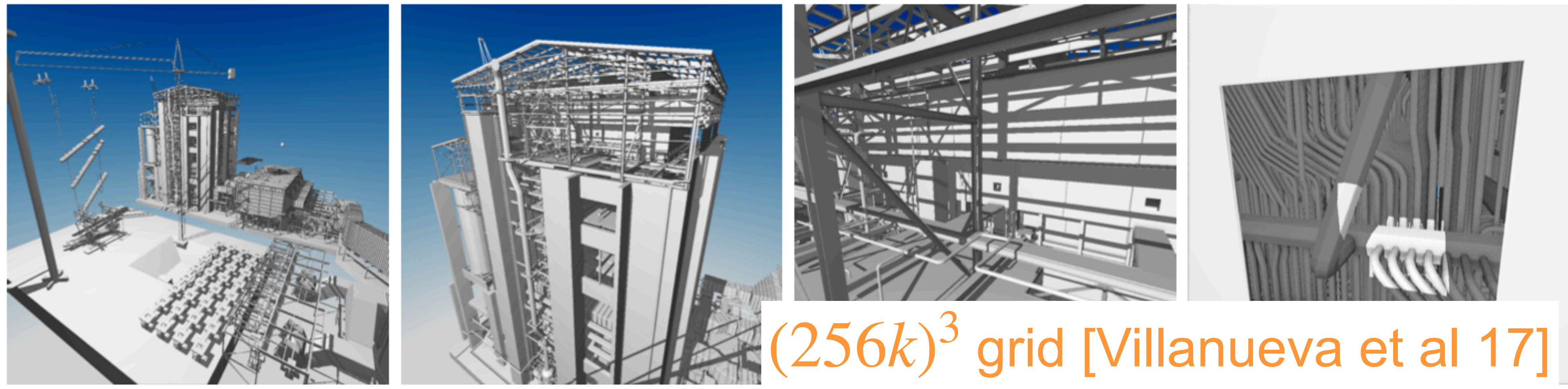

$(256k)^3$ grid [Villanueva et al 17]

Focus*: characteristic functions / labelled images / level sets / …*

Digital Geometry

Topology and geometry processing on regular data:

- fast algorithms thanks to the regularity of the data
- simple topological structure
- integer based computations
- advanced surface based geometry processing

… in $\mathbb{Z}^d$

dgtal.org

DGtal

Digital Geometry Tools and Algorithms Library

Fork me on GitHub

News

DGtal release 1.3

Posted on November 25, 2022

We are thrilled to announce the release 1.3 of DGtal and its tools. Many new features, edits and bugfixes are listed in the Changelog, and we would like to thank all devs involved in this release. In this short review, we would like to only focus on selected new features.... **[Read More]**

DGtal tutorial at DGMM 2022

https://dgtal.org

python

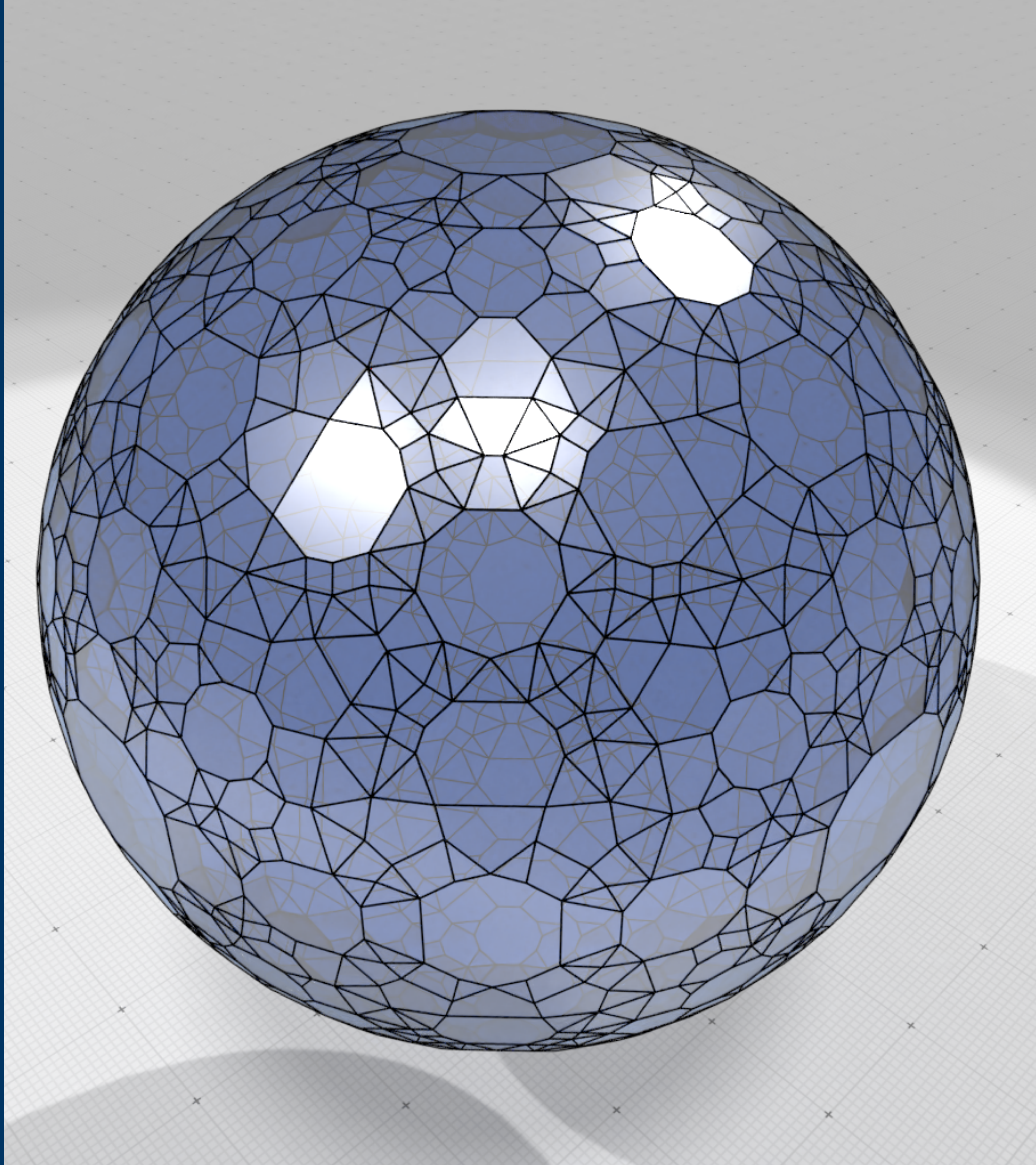

Quick example

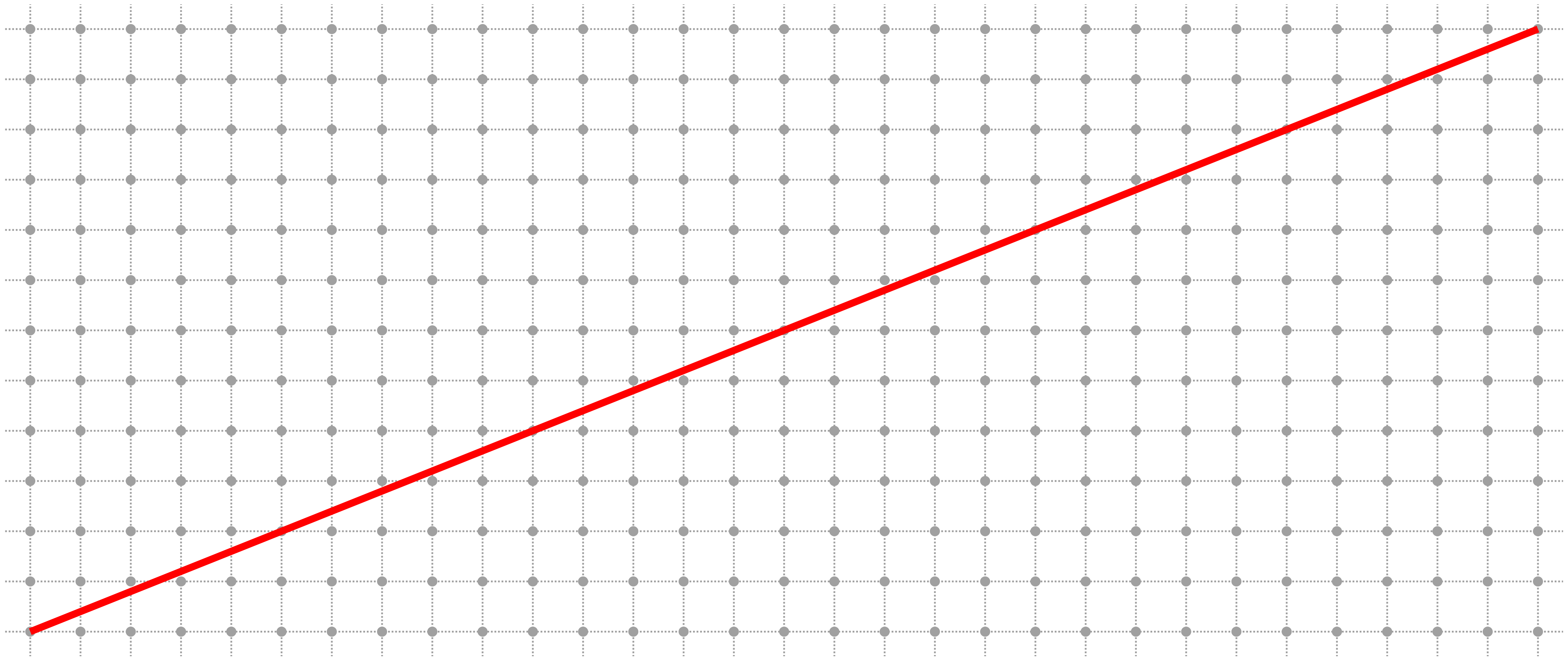

$$a_0 + \cfrac{b_1}{a_1 + \cfrac{b_2}{a_2 + \cfrac{b_3}{a_3 + \ddots}}}$$

- Rational slope ⇒ finite set of remainders ⇒ periodic structure ⇒ canonical pattern from **continued fraction**

→ *arithmetization* to speed-up tracing (e.g. fast ray marching on Sparse Voxel Octree)

→ useful to design fast recognition algorithms (pixels/voxels ⇒ digital straight lines, planes, circles…)

Quick example

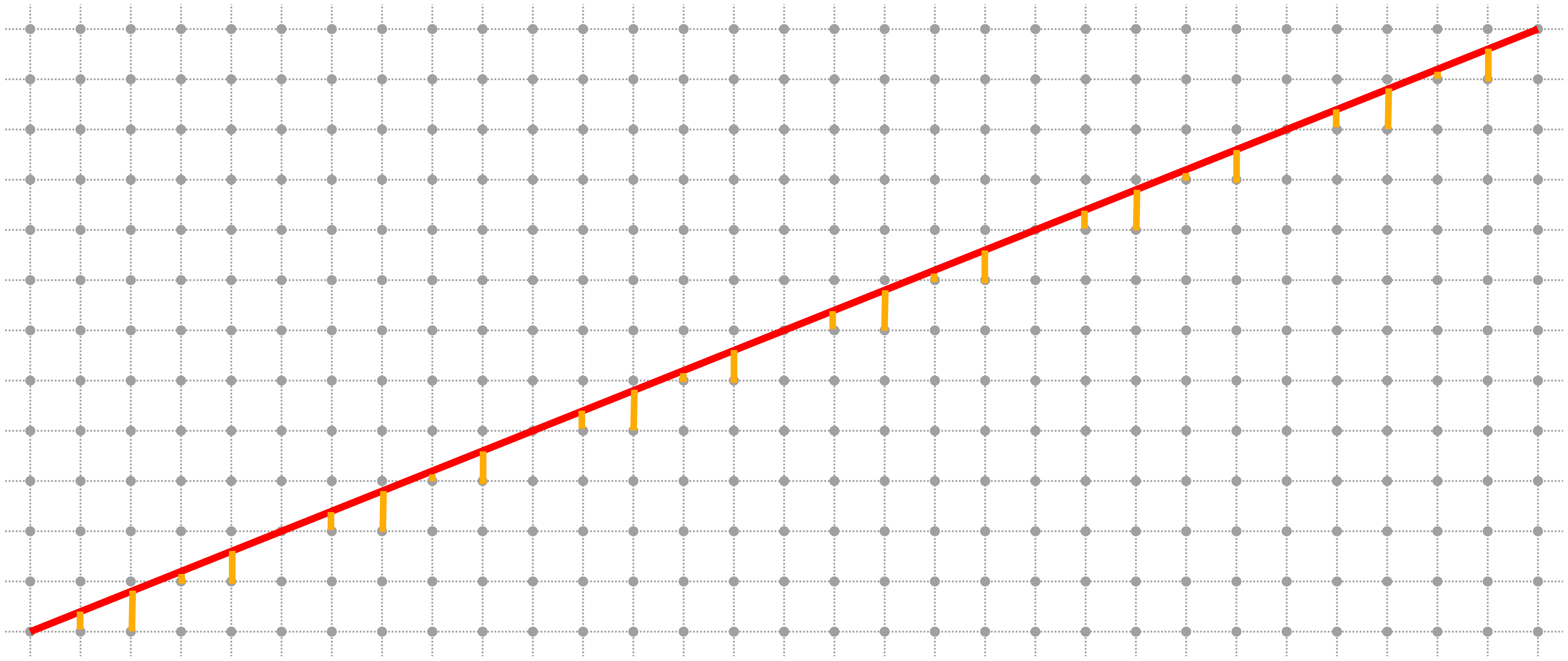

$$a_0 + \cfrac{b_1}{a_1 + \cfrac{b_2}{a_2 + \cfrac{b_3}{a_3 + \ddots}}}$$

- Rational slope ⇒ finite set of remainders ⇒ periodic structure ⇒ canonical pattern from **continued fraction**

→ *arithmetization* to speed-up tracing (e.g. fast ray marching on Sparse Voxel Octree)

→ useful to design fast recognition algorithms (pixels/voxels ⇒ digital straight lines, planes, circles…)

Quick example

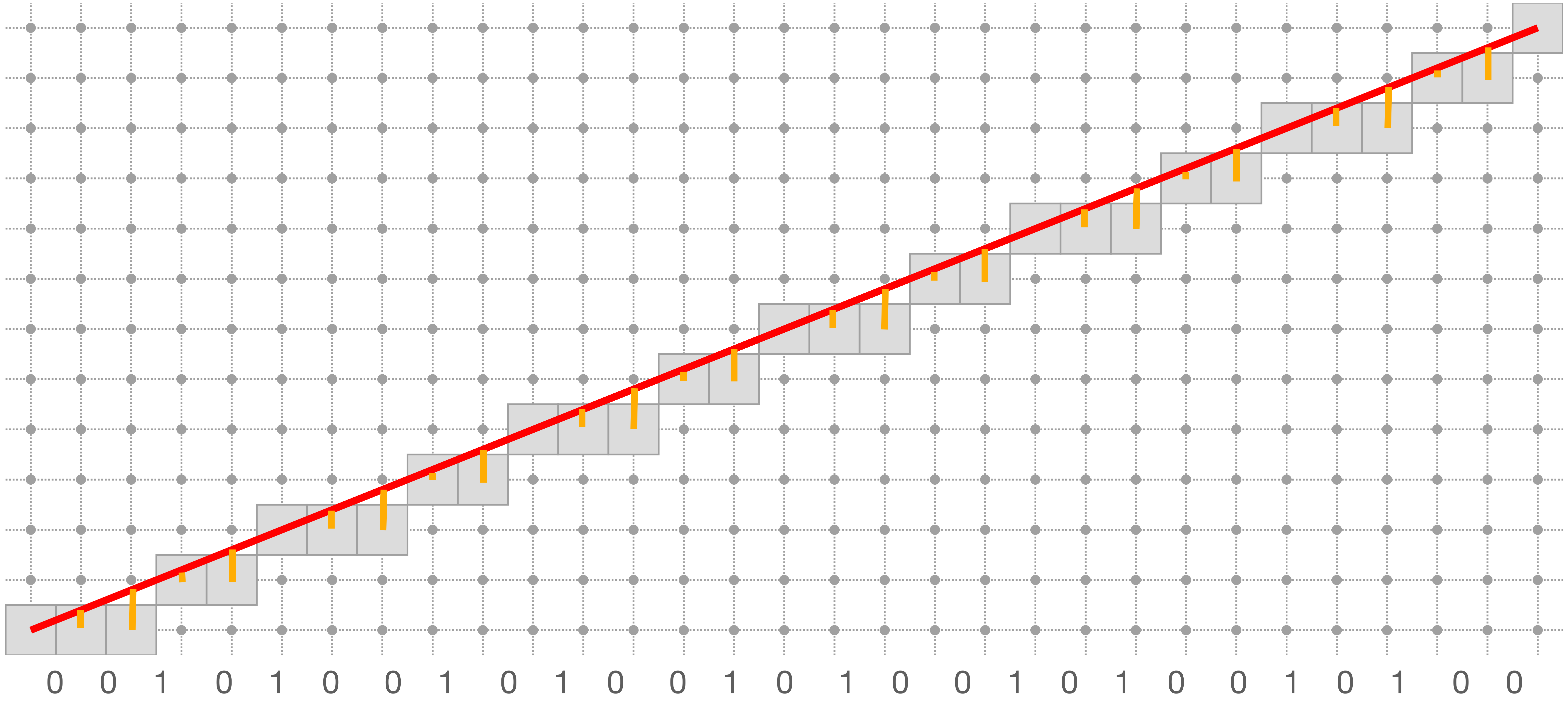

$$a_0 + \cfrac{b_1}{a_1 + \cfrac{b_2}{a_2 + \cfrac{b_3}{a_3 + \ddots}}}$$

- Rational slope ⇒ finite set of remainders ⇒ periodic structure ⇒ canonical pattern from **continued fraction**

→ *arithmetization* to speed-up tracing (e.g. fast ray marching on Sparse Voxel Octree)

→ useful to design fast recognition algorithms (pixels/voxels ⇒ digital straight lines, planes, circles…)

Quick example

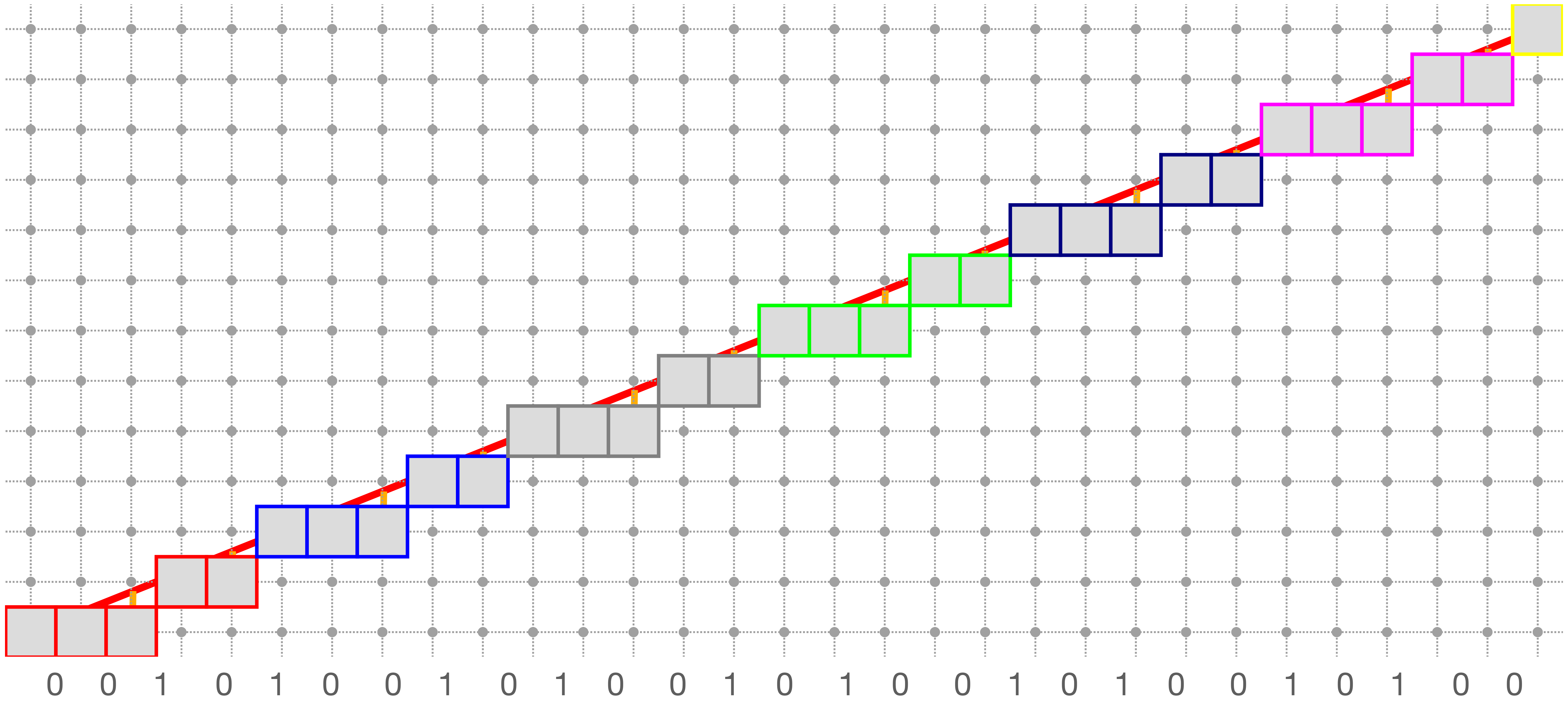

$$a_0 + \cfrac{b_1}{a_1 + \cfrac{b_2}{a_2 + \cfrac{b_3}{a_3 + \ddots}}}$$

- Rational slope ⇒ finite set of remainders ⇒ periodic structure ⇒ canonical pattern from **continued fraction**

→ *arithmetization* to speed-up tracing (e.g. fast ray marching on Sparse Voxel Octree)

→ useful to design fast recognition algorithms (pixels/voxels ⇒ digital straight lines, planes, circles…)

Further elements

Let $P \subset \mathbb{Z}^d$ a lattice polytope with non-empty interior, then: $f_k \ll c_d(Vol\,P)^{\frac{d-1}{d+1}}$

Convex on the lattice $[1,n]^2$grid has $O(n^{2/3})$ edges

Let $P \subset [1,U]^2$ (with $U \leq 2^m$) and $n := |P|$, the expected time for Voronoi diagram / Delaunay triangulation is:

$$O\left(\min\{n \log n, n\sqrt{U}\}\right)$$

⋮

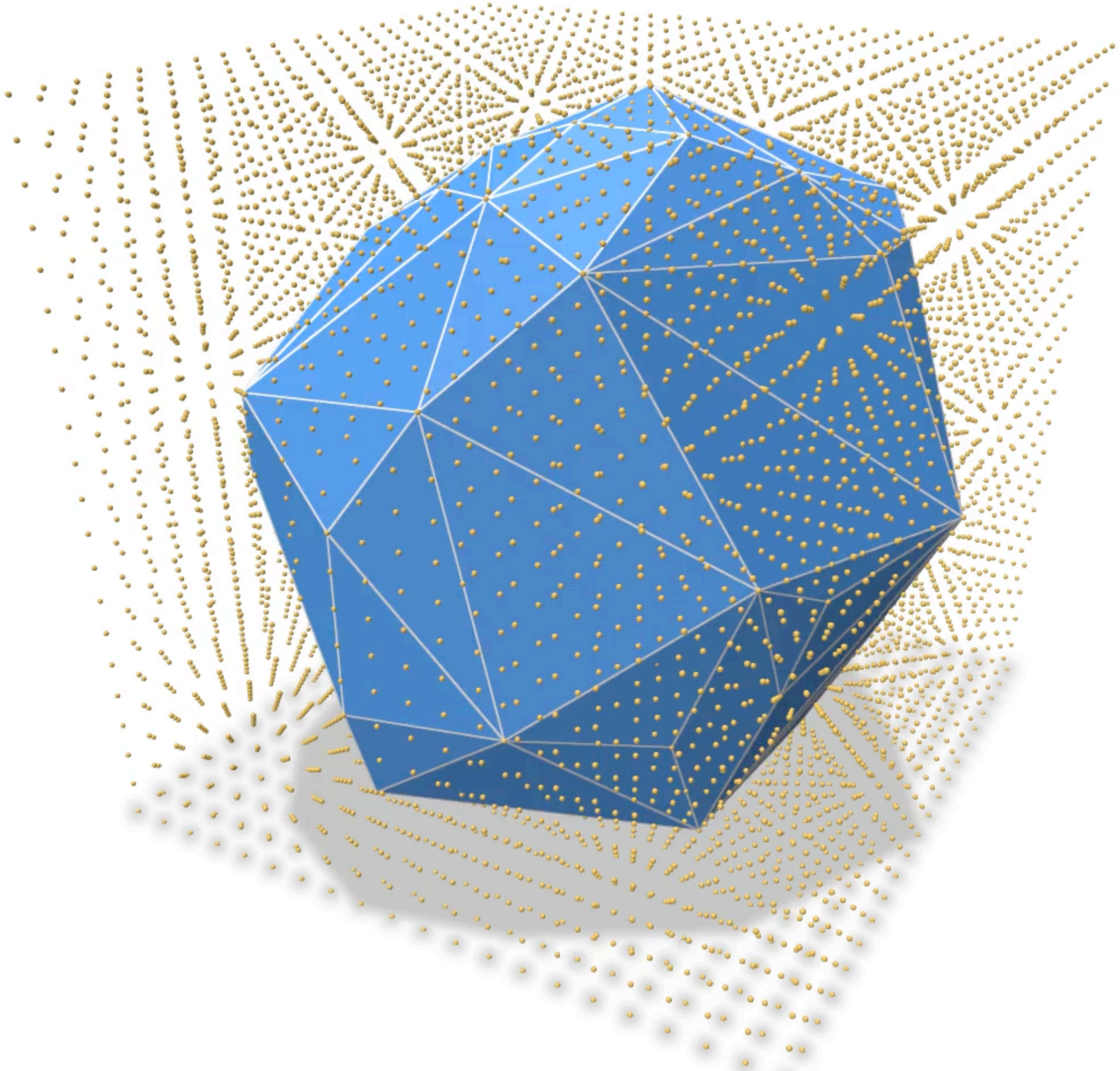

Further elements

Let $P \subset \mathbb{Z}^d$ a lattice polytope with non-empty interior, then: $f_k \ll c_d (Vol\,P)^{\frac{d-1}{d+1}}$

Convex on the lattice $[1,n]^2$grid has $O(n^{2/3})$ edges

Let $P \subset [1,U]^2$ (with $U \leq 2^m$) and $n := |P|$, the expected time for Voronoi diagram / Delaunay triangulation is:

$$O\left(\min\{n \log n, n\sqrt{U}\}\right)$$

⋮

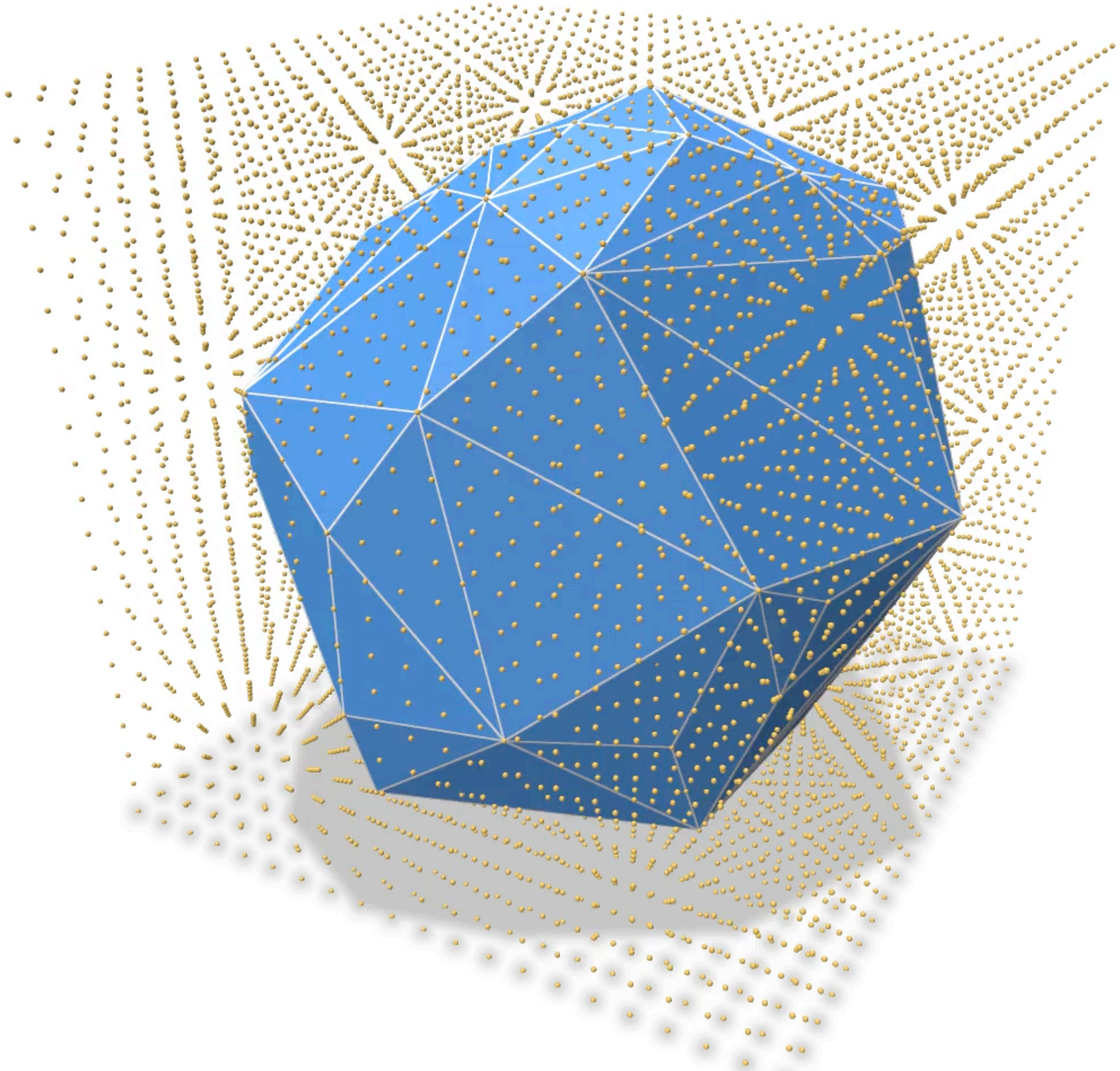

hands on…

```
void oneStep(double myh)
{
  auto params = SH3::defaultParameters();
  params( "polynomial", "sphere1" )( "gridstep", myh )
        ( "minAABB", -1.25 )( "maxAABB", 1.25 );
  auto implicit_shape  = SH3::makeImplicitShape3D  ( params );
  auto digitized_shape = SH3::makeDigitizedImplicitShape3D( implicit_shape, params );

  std::vector<Point> points;
  std::cout << "Digitzing shape" << std::endl;
  auto domain = digitized_shape->getDomain();
  for(auto &p: domain)
    if (digitized_shape->operator()(p))
      points.push_back(p);

  std::cout << "Computing convex hull" << std::endl;
  QuickHull3D hull;
  hull.setInput( points );
  hull.computeConvexHull();
  std::cout << "#points="    << hull.nbPoints()
            << " #vertices=" << hull.nbVertices()
            << " #facets="   << hull.nbFacets() << std::endl;
  std::vector< RealPoint > vertices;
  hull.getVertexPositions( vertices );
  std::vector< std::vector< std::size_t > > facets;
  hull.getFacetVertices( facets );

  polyscope::registerSurfaceMesh("Convex hull", vertices, facets)->rescaleToUnit();
}
```

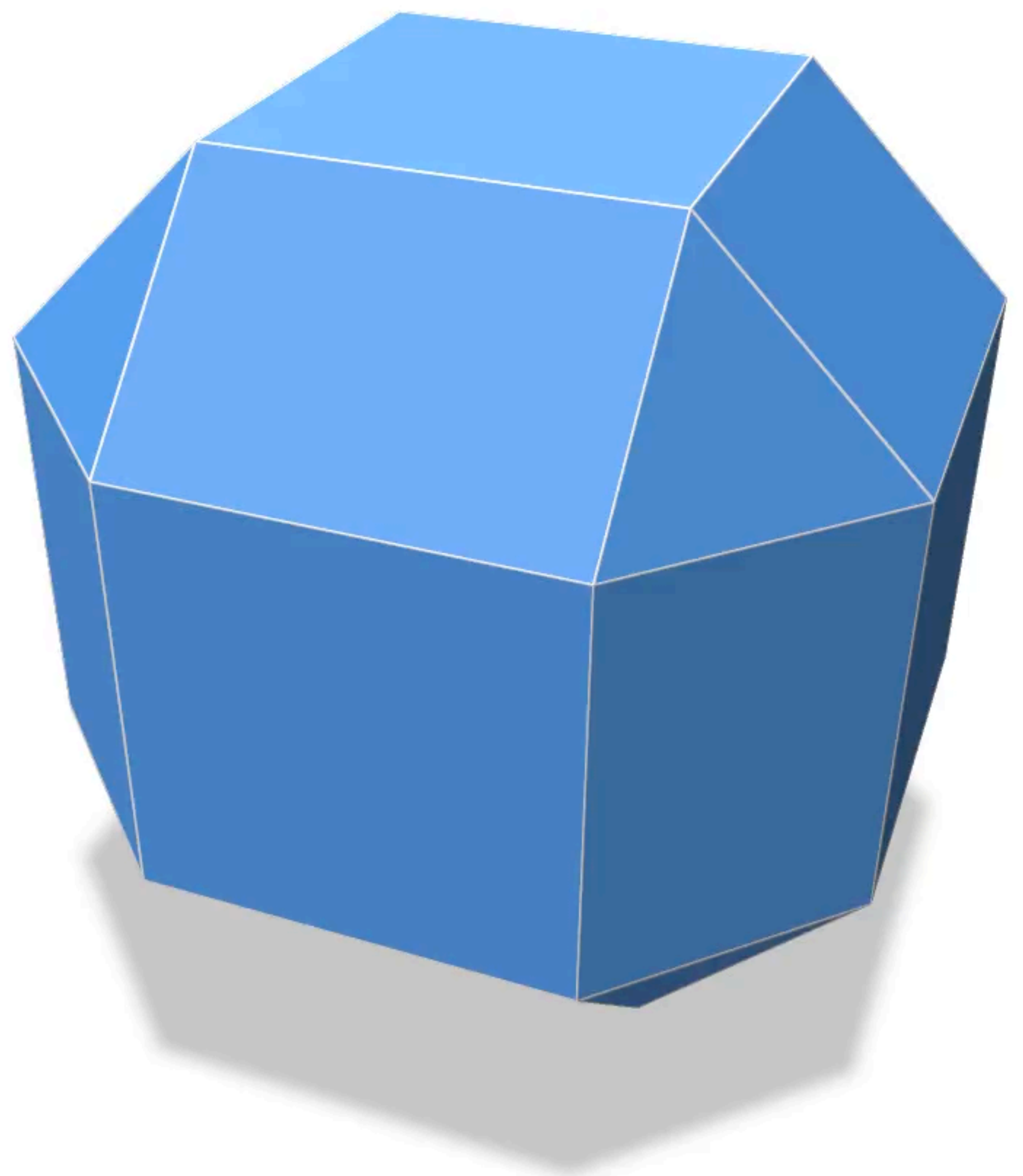

```
void oneStep(double myh)
{
  auto params = SH3::defaultParameters();
  params( "polynomial", "sphere1" )( "gridstep", myh )
        ( "minAABB", -1.25 )( "maxAABB", 1.25 );
  auto implicit_shape  = SH3::makeImplicitShape3D  ( params );
  auto digitized_shape = SH3::makeDigitizedImplicitShape3D( implicit_shape, params );

  std::vector<Point> points;
  std::cout << "Digitzing shape" << std::endl;
  auto domain = digitized_shape->getDomain();
  for(auto &p: domain)
    if (digitized_shape->operator()(p))
      points.push_back(p);

  std::cout << "Computing convex hull" << std::endl;
  QuickHull3D hull;
  hull.setInput( points );
  hull.computeConvexHull();
  std::cout << "#points="    << hull.nbPoints()
            << " #vertices=" << hull.nbVertices()
            << " #facets="   << hull.nbFacets() << std::endl;
  std::vector< RealPoint > vertices;
  hull.getVertexPositions( vertices );
  std::vector< std::vector< std::size_t > > facets;
  hull.getFacetVertices( facets );

  polyscope::registerSurfaceMesh("Convex hull", vertices, facets)->rescaleToUnit();
}
```

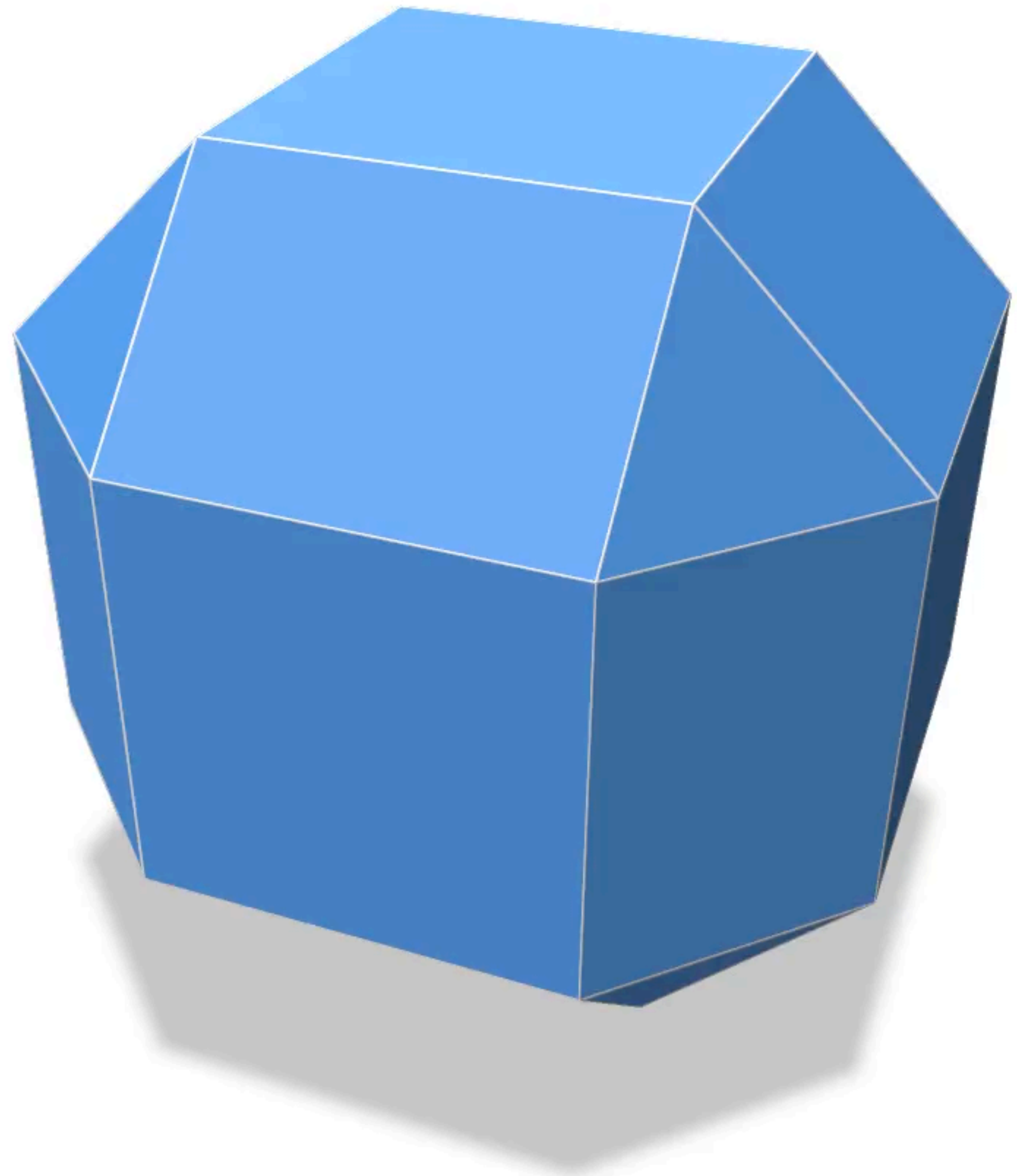

$\mathbb{Z}^d$

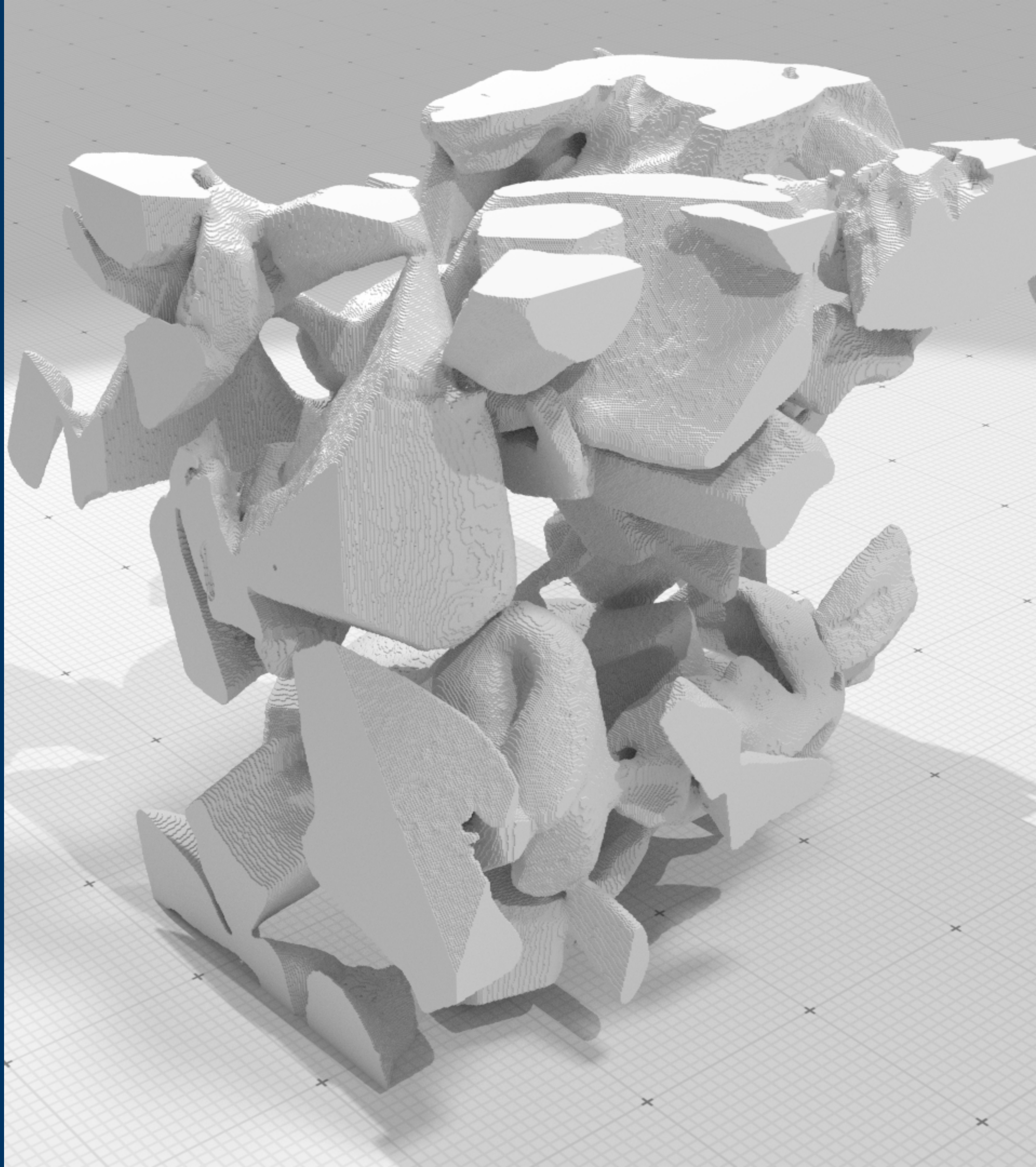

Volumetric analysis

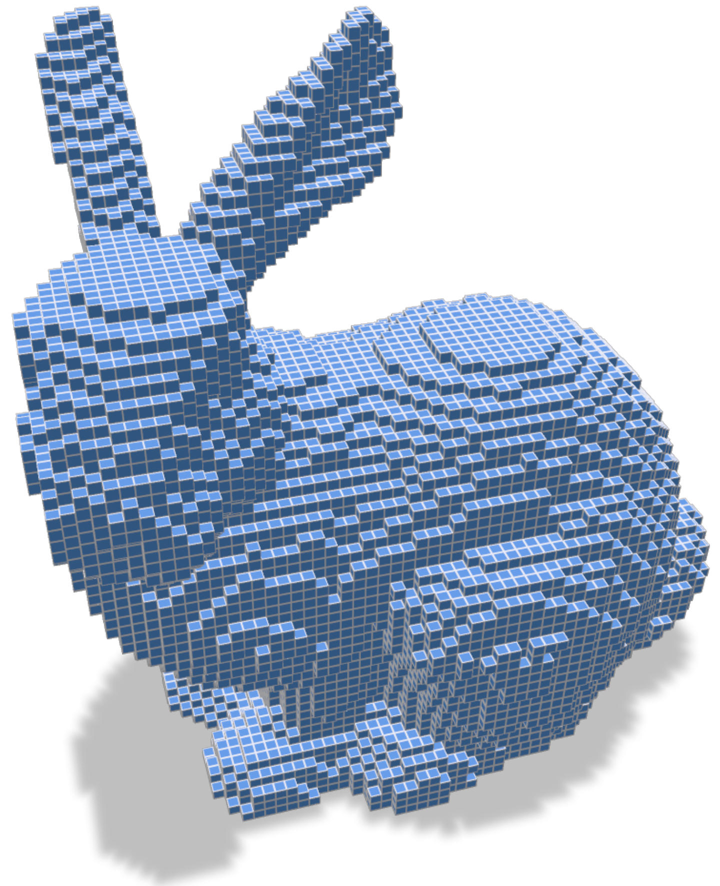

Given $X \subset \mathbb{Z}^d$ and a domain $[0,n]^d$, compute:

Volumetric analysis

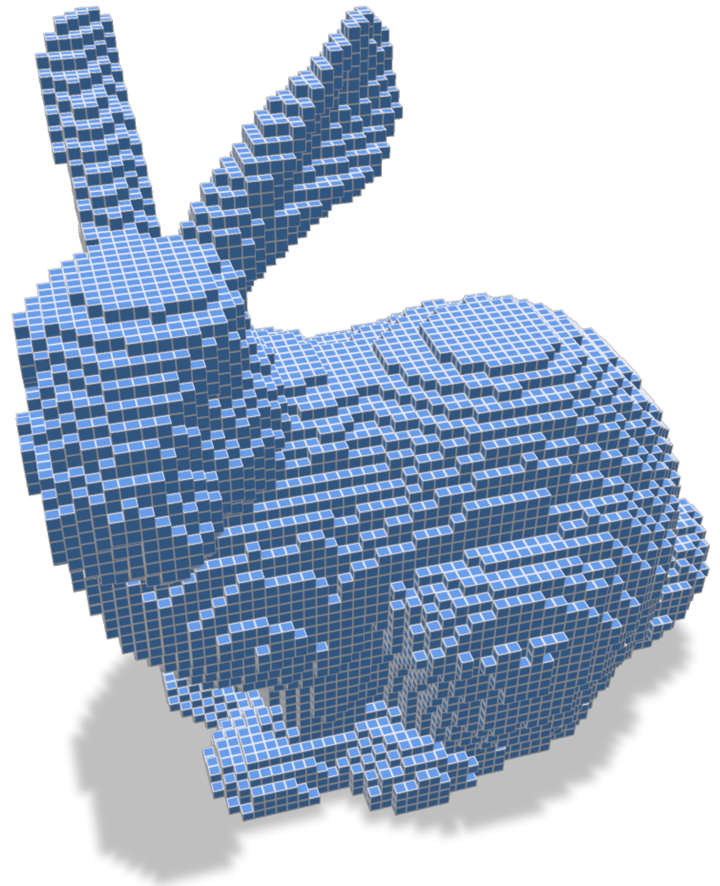

Given $X \subset \mathbb{Z}^d$ and a domain $[0,n]^d$, compute:

Volumetric analysis

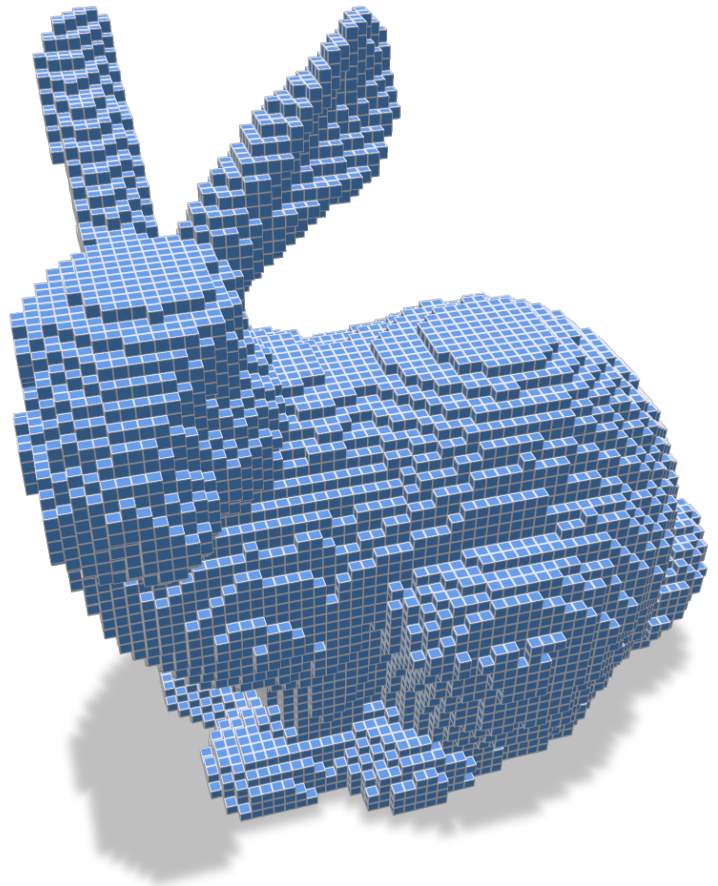

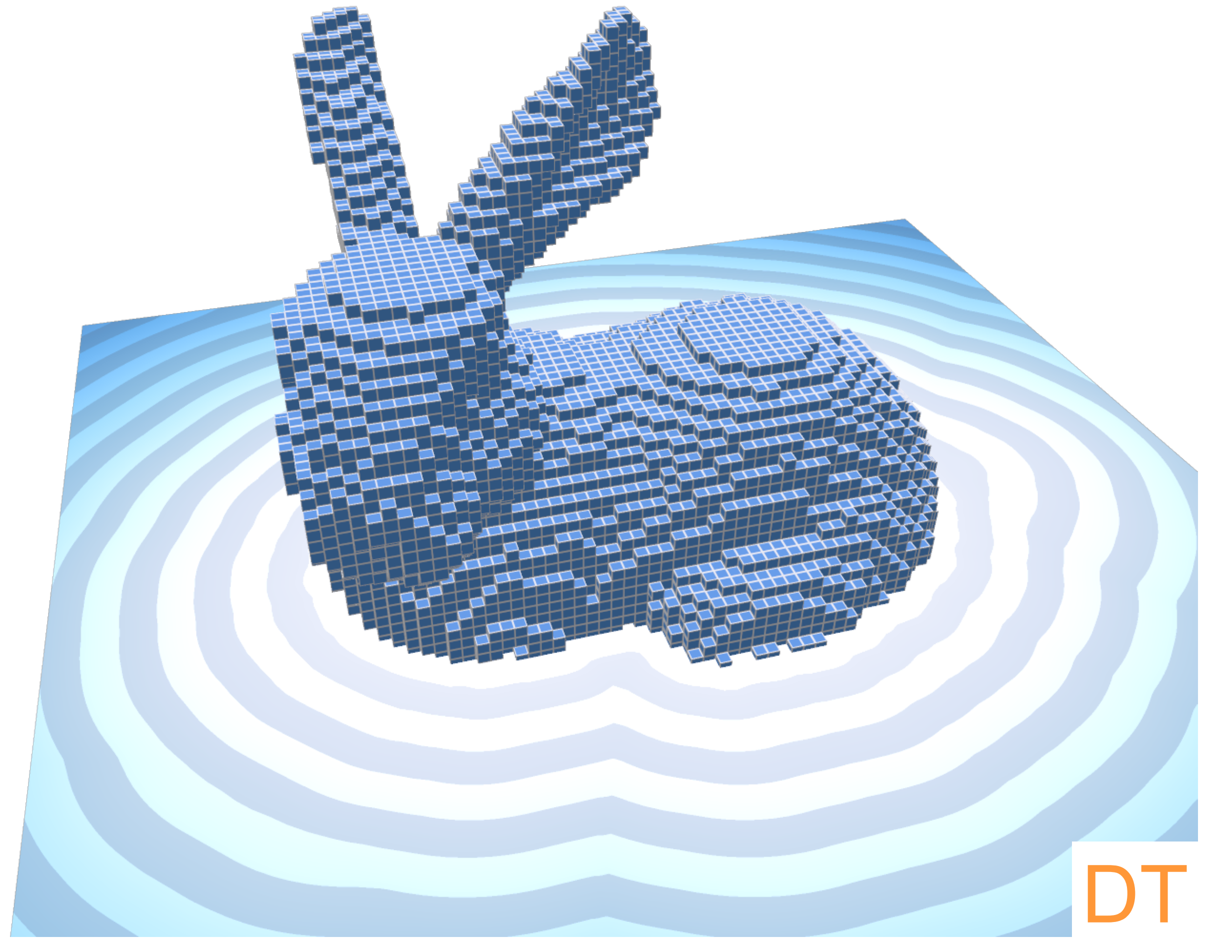

Given $X \subset \mathbb{Z}^d$ and a domain $[0,n]^d$, compute:

$$DT(x) = min_{y \in D \setminus X}\ d(x,y)$$ *(aka distance map)*

Volumetric analysis

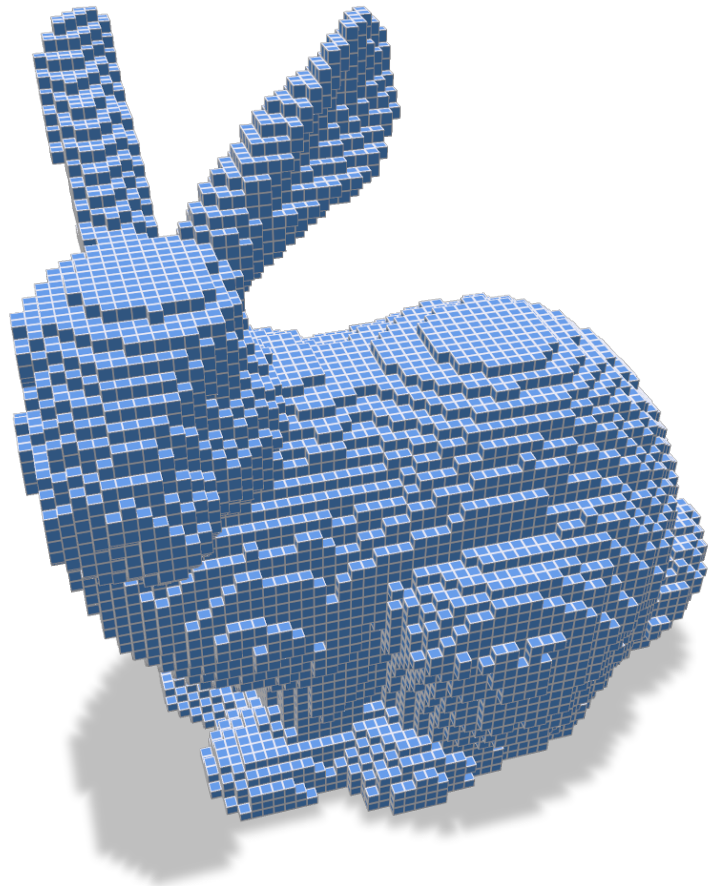
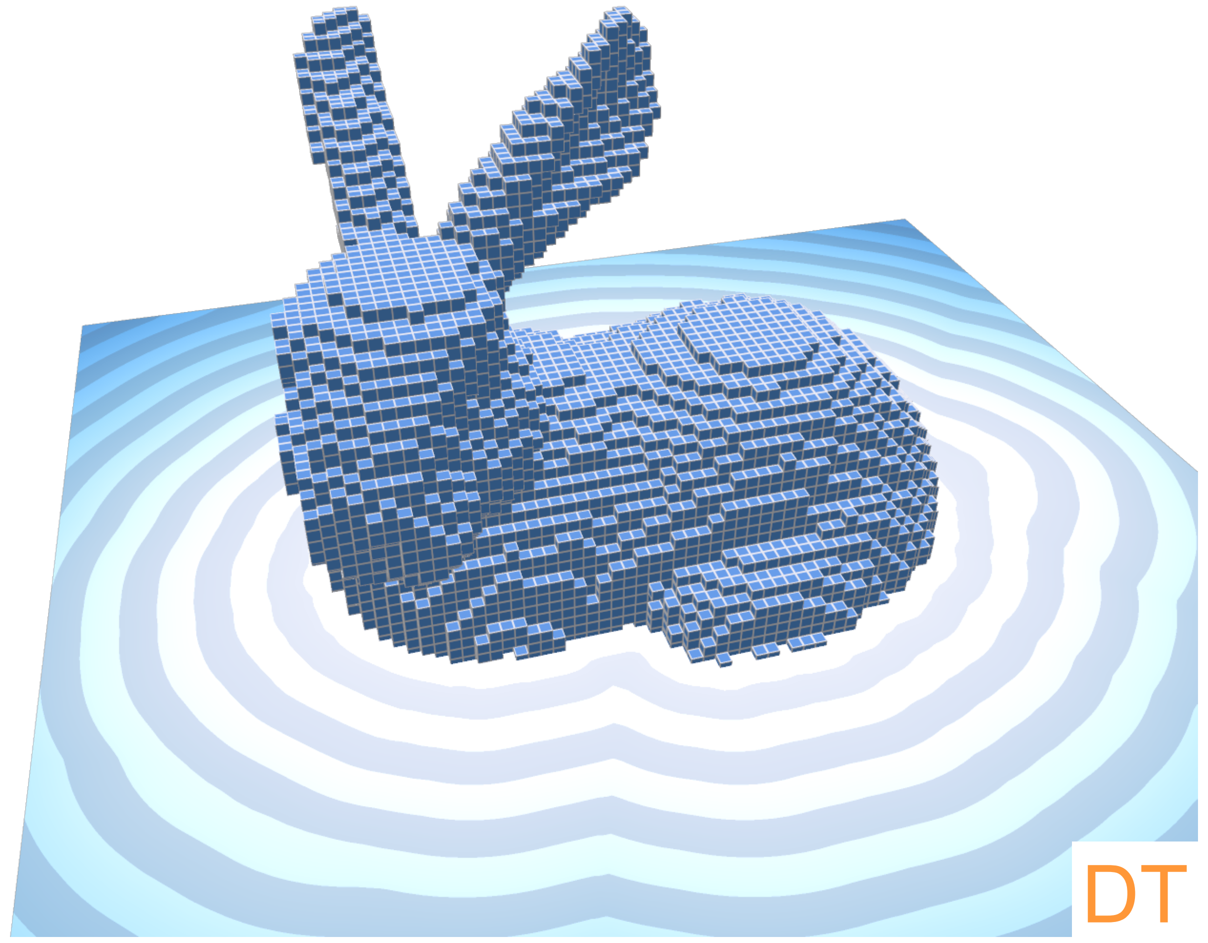

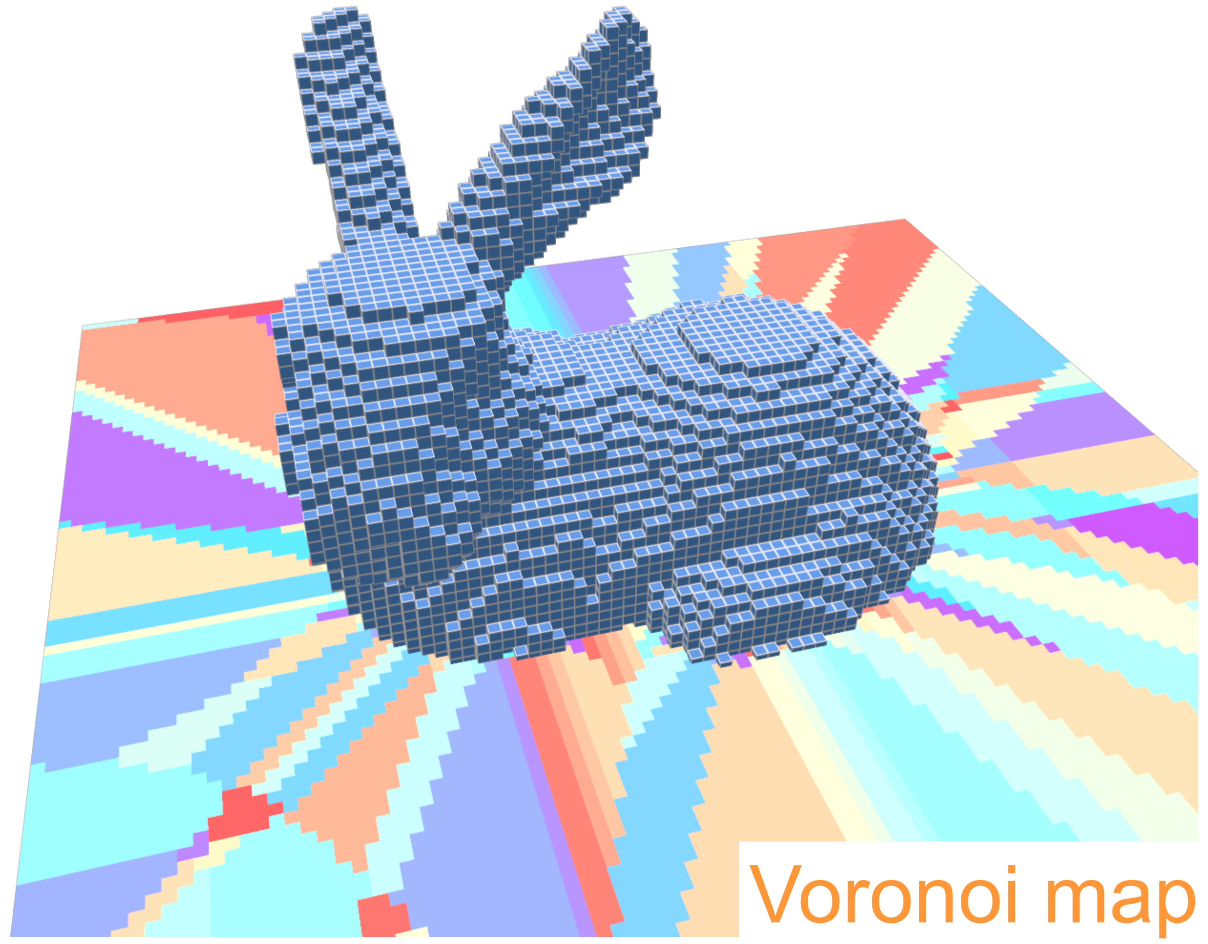

Given $X \subset \mathbb{Z}^d$ ***and a domain*** $[0,n]^d$***, compute:***

$$DT(x) = min_{y \in D \backslash X} \ d(x,y)$$ *(aka distance map)*

$$\sigma(x) = \text{argmin}_{y \in D \backslash X} \ d(x,y)$$ *(aka Voronoi map* $\mathscr{V}(X) \cap \mathbb{Z}^d$*)*

Volumetric analysis

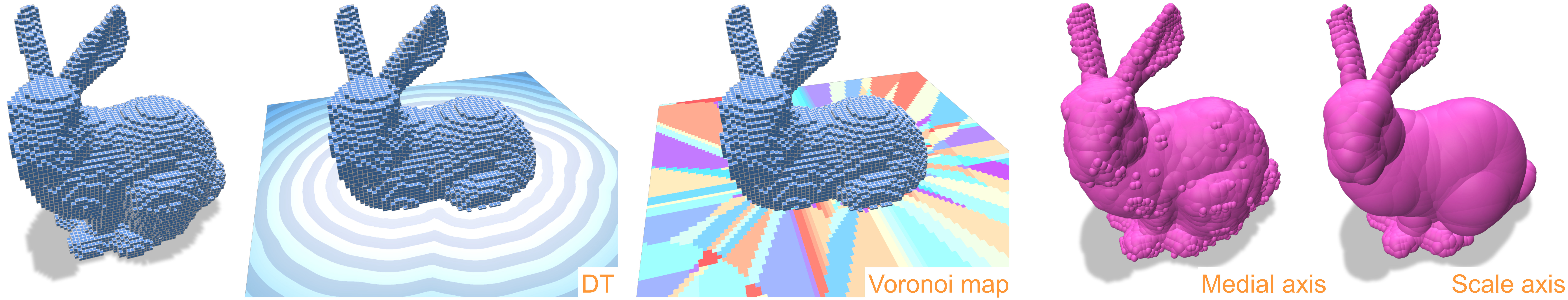

Given $X \subset \mathbb{Z}^d$ ***and a domain*** $[0,n]^d$***, compute:***

$$DT(x) = min_{y \in D \setminus X} \ d(x,y)$$ *(aka distance map)*

$$\sigma(x) = \operatorname{argmin}_{y \in D \setminus X} \ d(x,y)$$ *(aka Voronoi map* $\mathscr{V}(X) \cap \mathbb{Z}^d$*)*

$$M = \{(x,r) \in \mathbb{Z}^{d+1} \mid \mathscr{B}(x,r) \cap \mathbb{Z}^d \subset X, \textit{there is no } (x',r') \textit{ s.t. } \mathscr{B}(x,r) \subset \mathscr{B}(x',r')\}$$ *(aka discrete medial axis)*

Volumetric analysis

Given $X \subset \mathbb{Z}^d$ ***and a domain*** $[0,n]^d$***, compute:***

$DT(x) = min_{y \in D \setminus X} \; d(x,y)$ *(aka distance map)*

$\sigma(x) = \text{argmin}_{y \in D \setminus X} \; d(x,y)$ *(aka Voronoi map* $\mathscr{V}(X) \cap \mathbb{Z}^d$*)*

$M = \{(x,r) \in \mathbb{Z}^{d+1} \mid \mathscr{B}(x,r) \cap \mathbb{Z}^d \subset X,$ *there is no* (x', r') *s.t.* $\mathscr{B}(x,r) \subset \mathscr{B}(x',r')\}$ *(aka discrete medial axis)*

$\pi(x) = \text{argmin}_{(y,r) \in M} \; \|x - y\|_2^2 - r^2$ *(aka* l_2 *Power map* $\mathscr{P}(M) \cap \mathbb{Z}^d$*)*

Volumetric analysis

Given $X \subset \mathbb{Z}^d$ ***and a domain*** $[0,n]^d$***, compute:***

➡ $DT(x) = min_{y \in D \setminus X} \; d(x,y)$ *(aka distance map)*

➡ $\sigma(x) = \text{argmin}_{y \in D \setminus X} \; d(x,y)$ *(aka Voronoi map* $\mathcal{V}(X) \cap \mathbb{Z}^d$*)*

$M = \{(x,r) \in \mathbb{Z}^{d+1} \mid \mathcal{B}(x,r) \cap \mathbb{Z}^d \subset X,$ *there is no* (x',r') *s.t.* $\mathcal{B}(x,r) \subset \mathcal{B}(x',r')\}$ *(aka discrete medial axis)*

$\pi(x) = \text{argmin}_{(y,r) \in M} \; \|x-y\|_2^2 - r^2$ *(aka* l_2 *Power map* $\mathcal{P}(M) \cap \mathbb{Z}^d$*)*

Separable Volumetric approaches

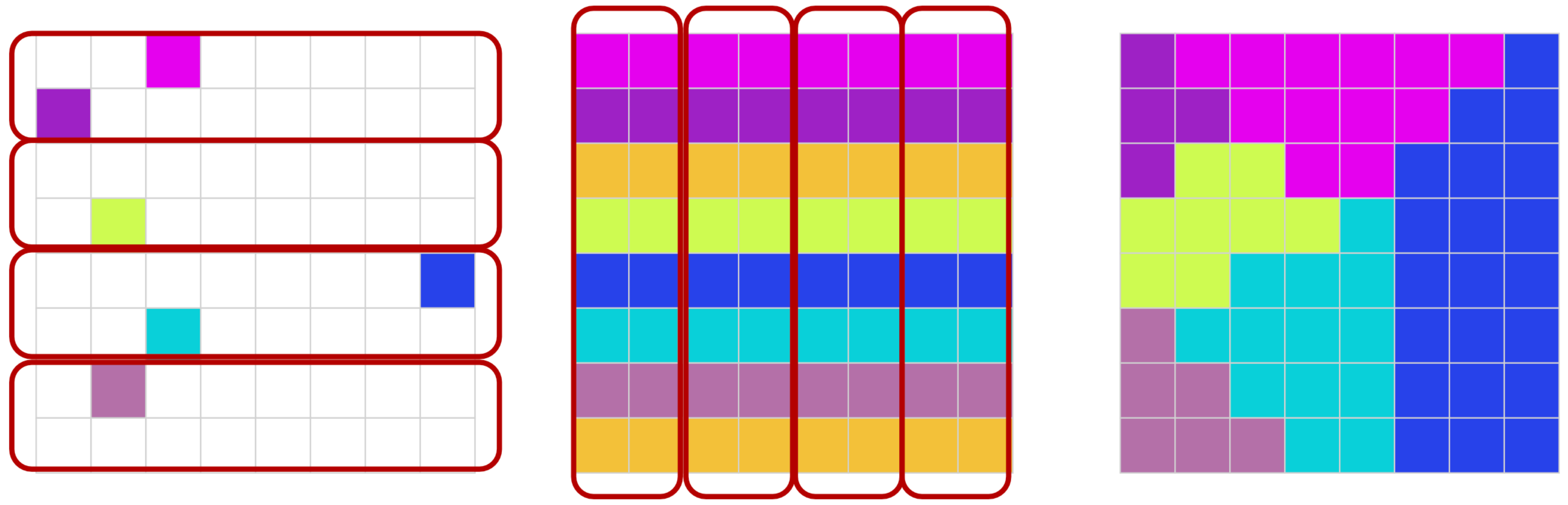

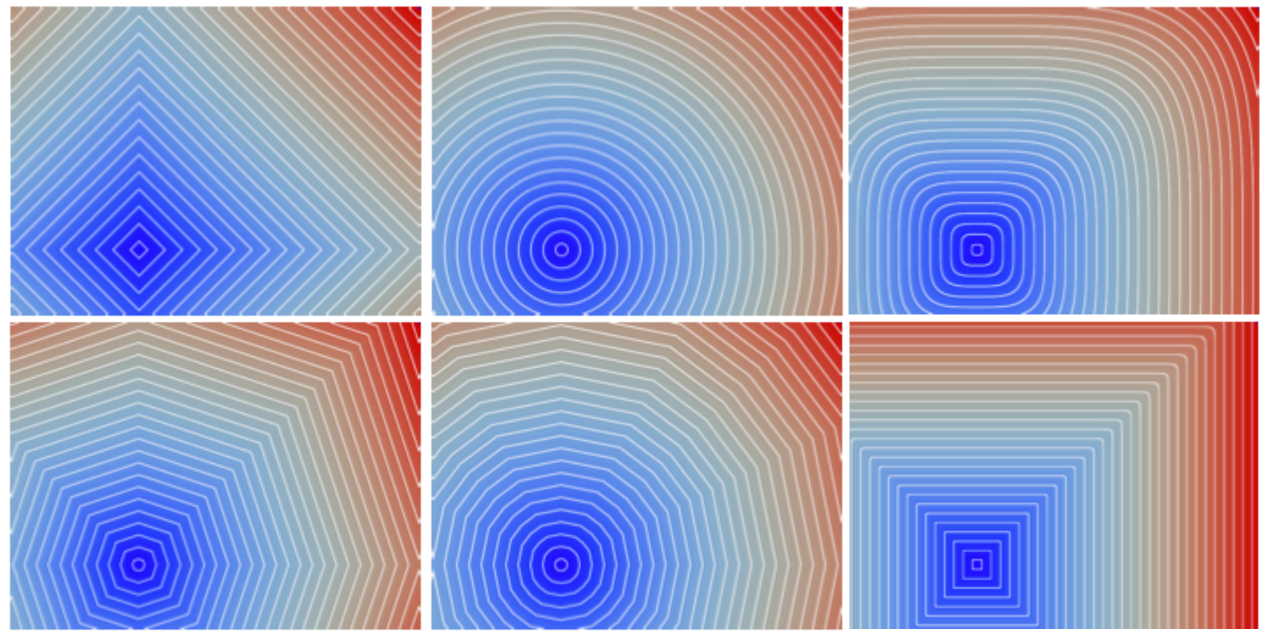

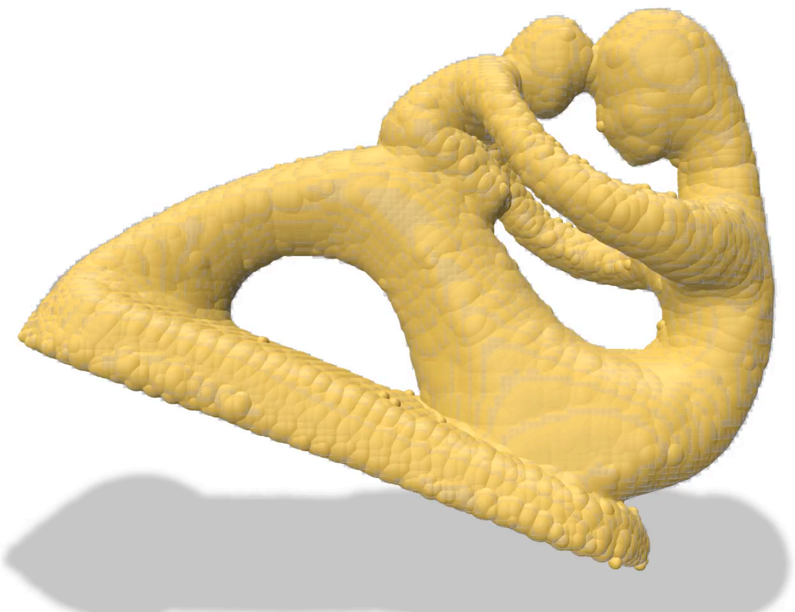

Separable Volumetric approaches

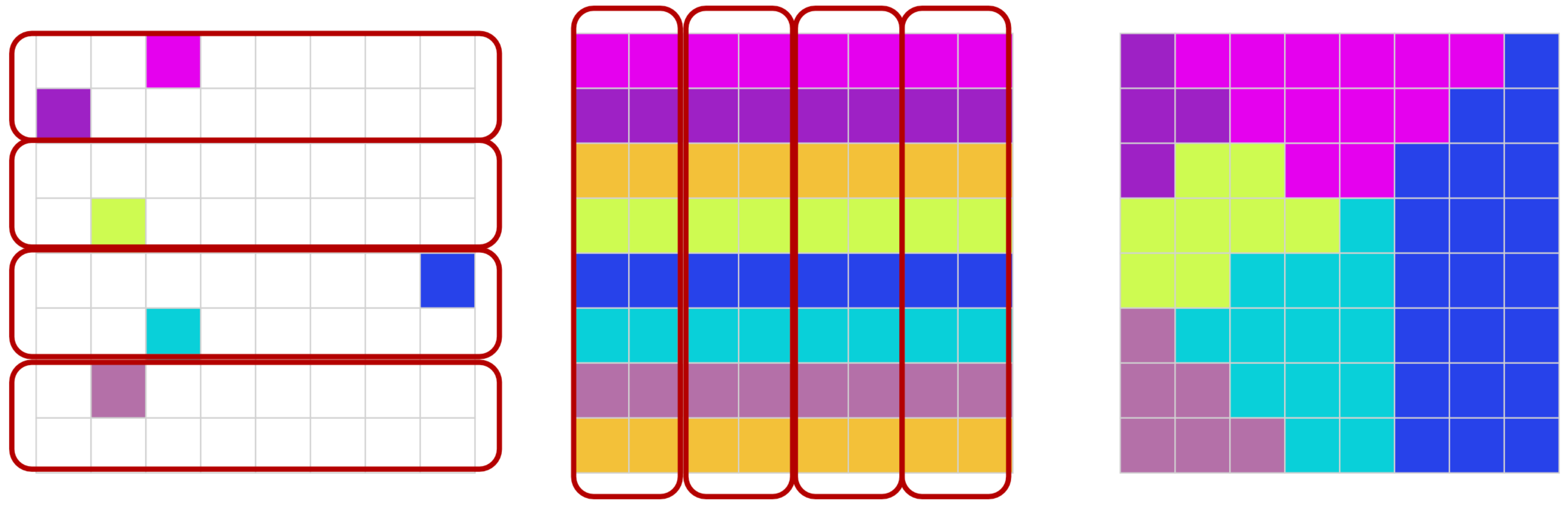

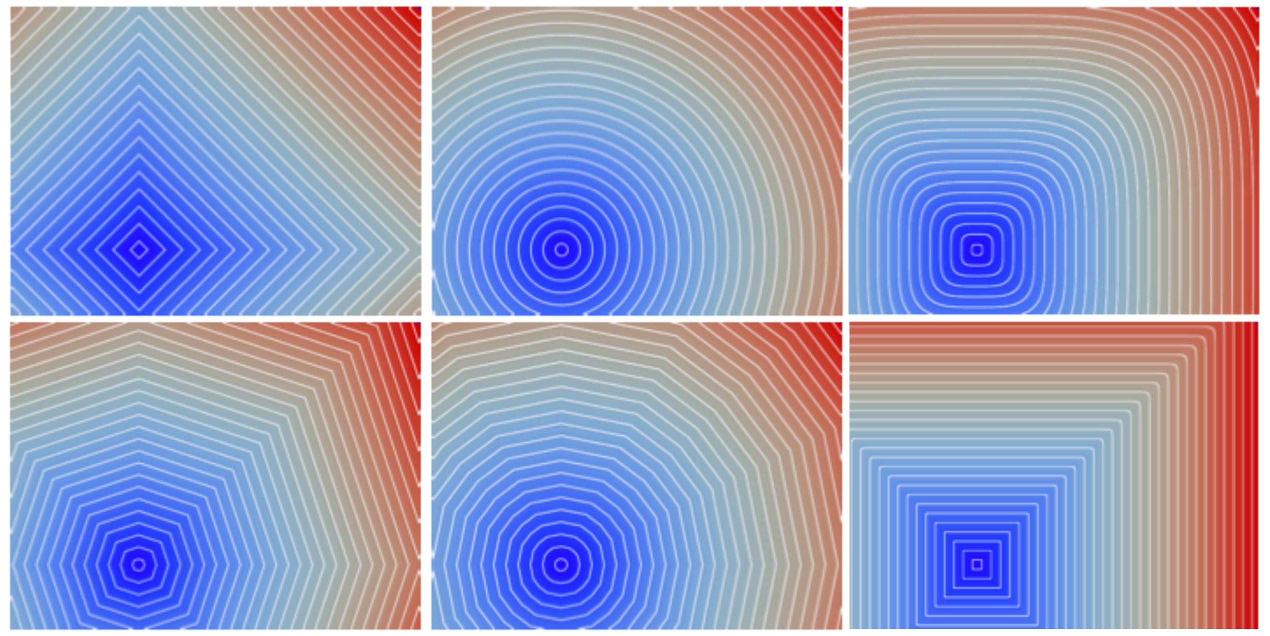

The separable algorithm is correct:

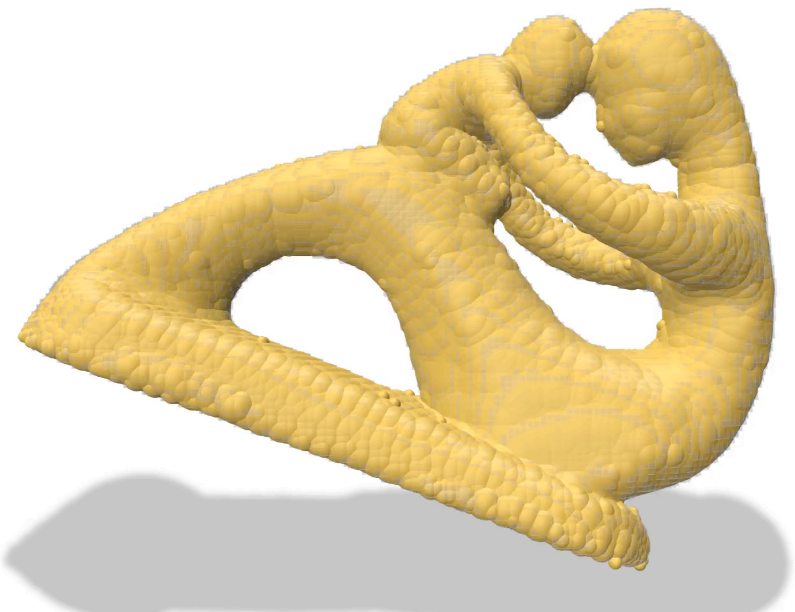

Separable Volumetric approaches

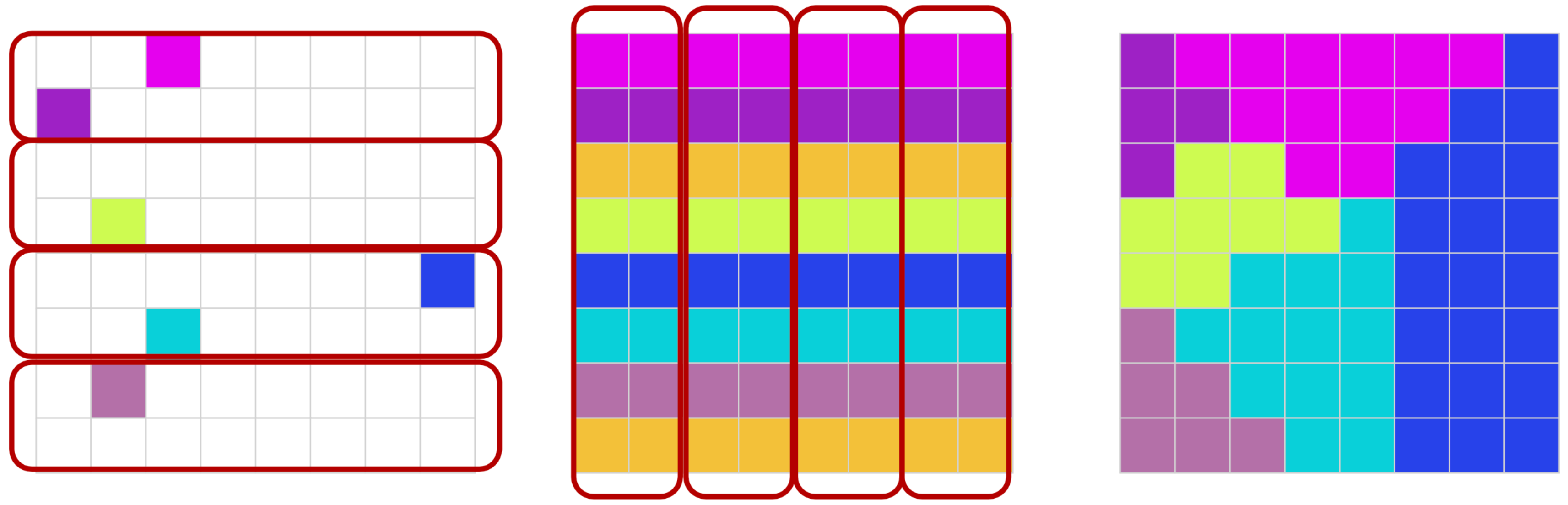

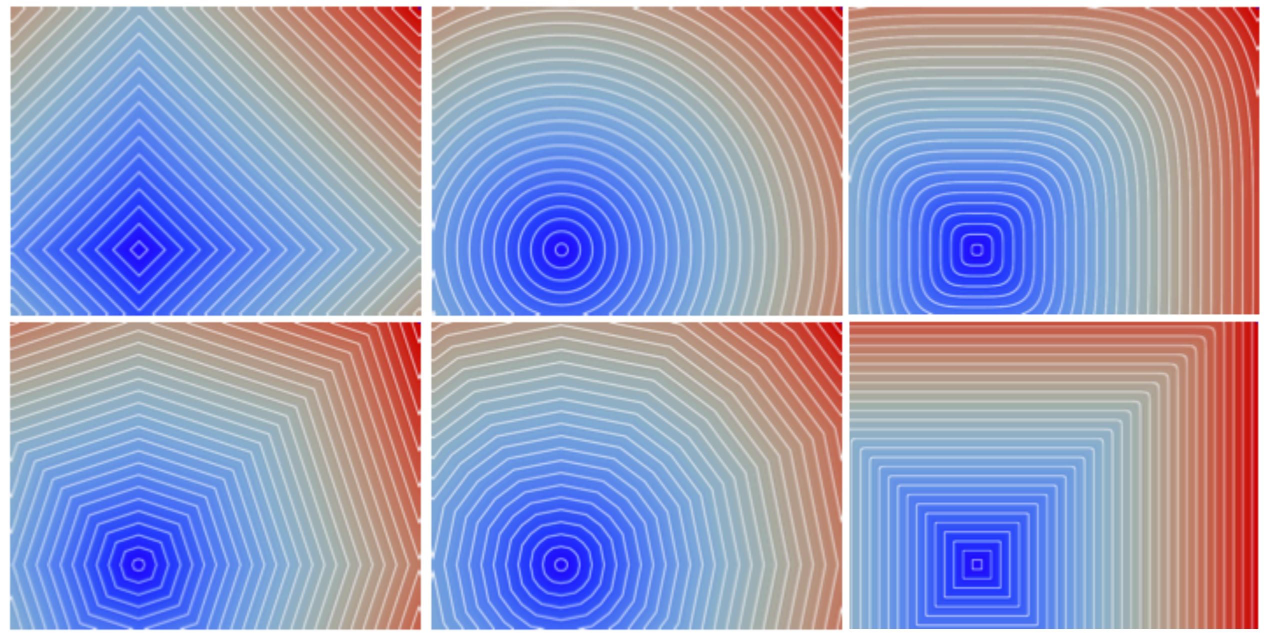

The separable algorithm is correct:

- for any dimension

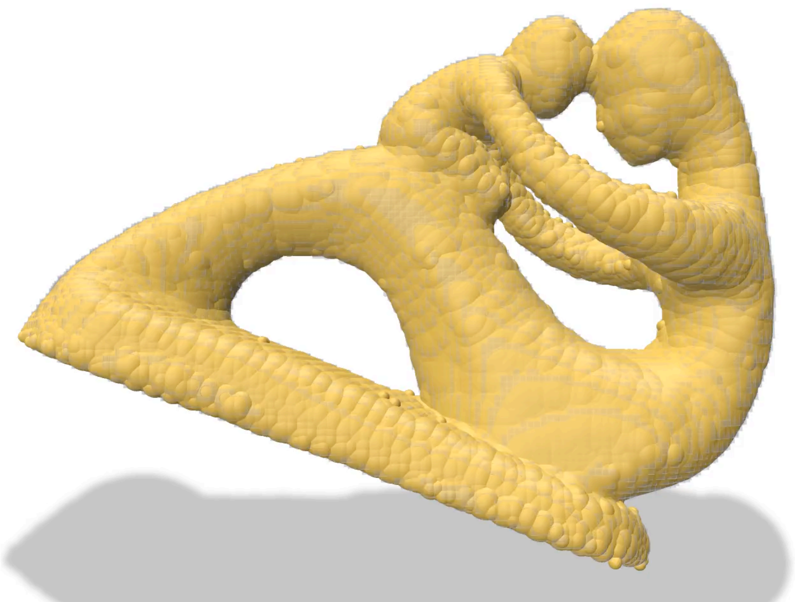

Separable Volumetric approaches

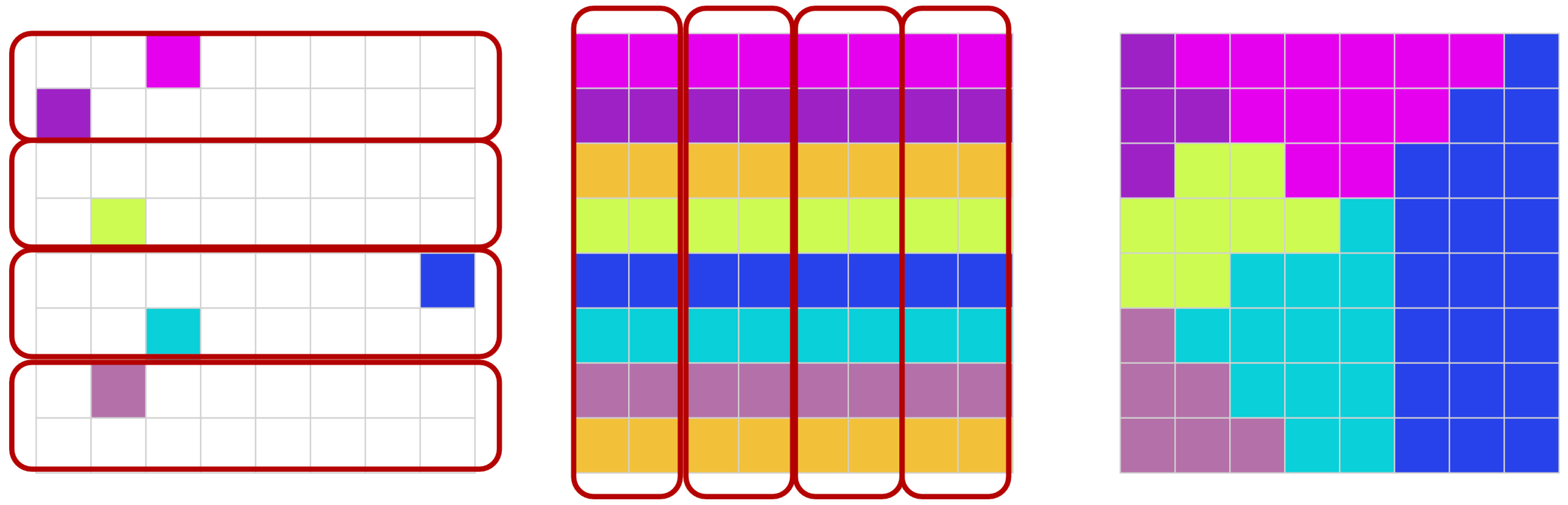

The separable algorithm is correct:

- for any dimension
- for any metric with axis symmetric unit ball (e.g. any l_p, chamfer norms)

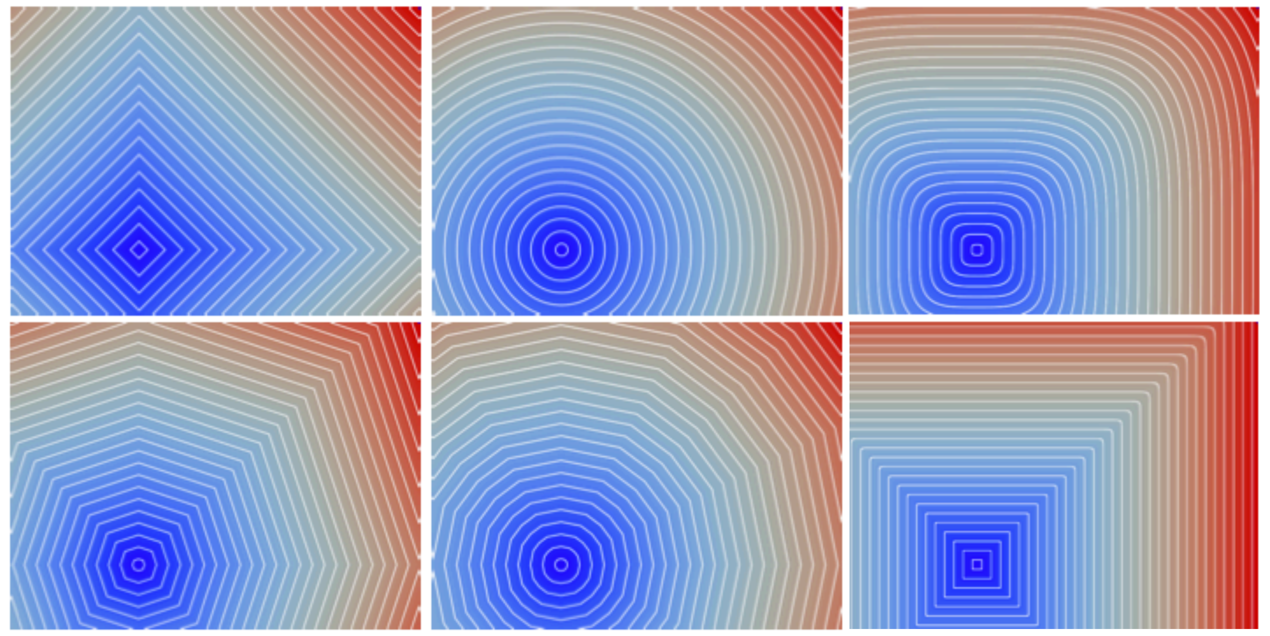

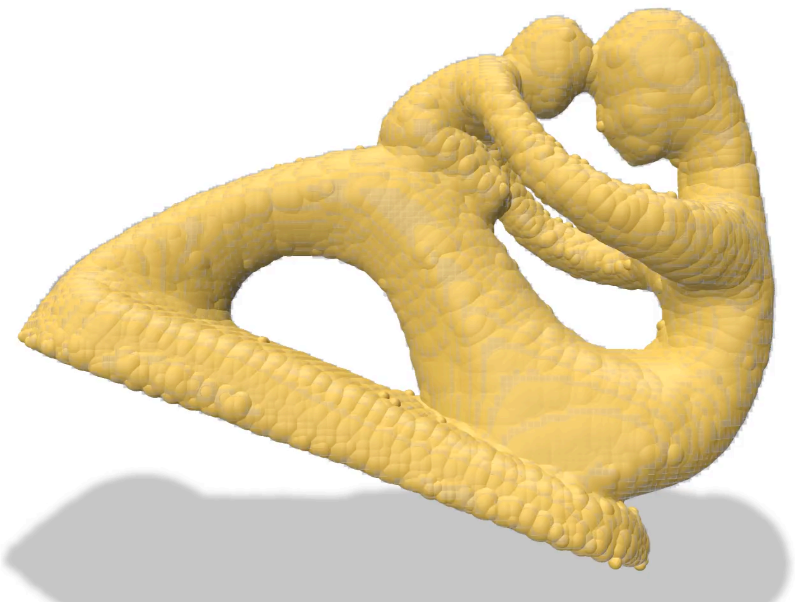

Separable Volumetric approaches

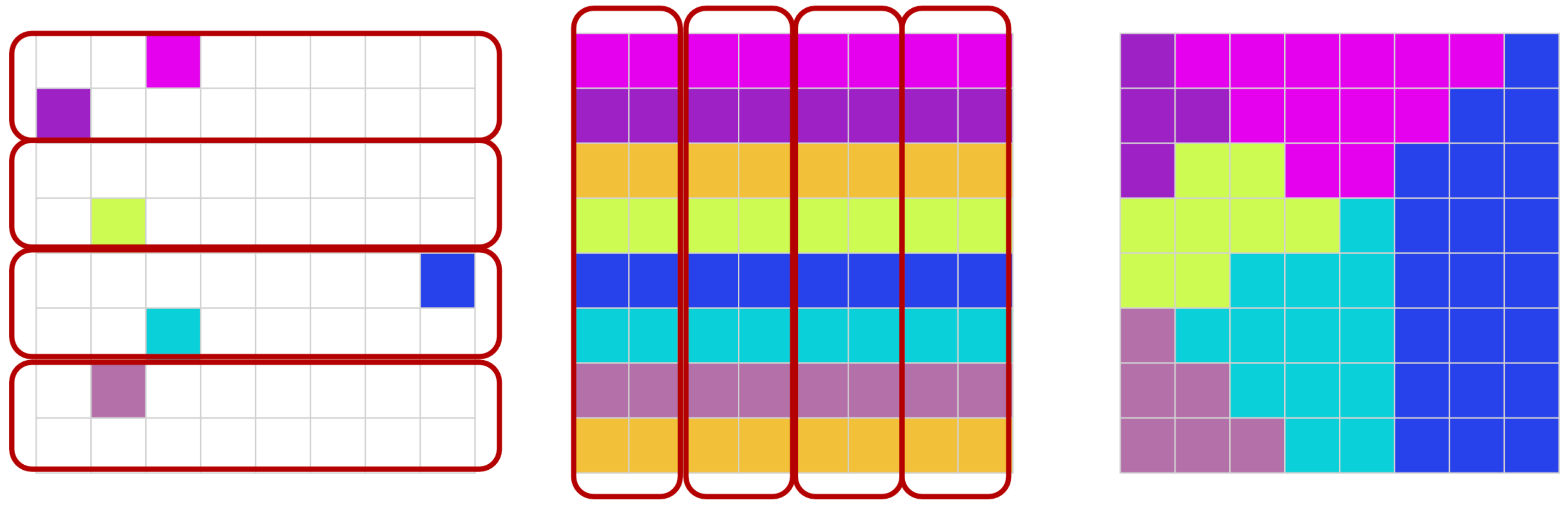

The separable algorithm is correct:

- for any dimension
- for any metric with axis symmetric unit ball (e.g. any l_p, chamfer norms)
- on any toroidal nD domains

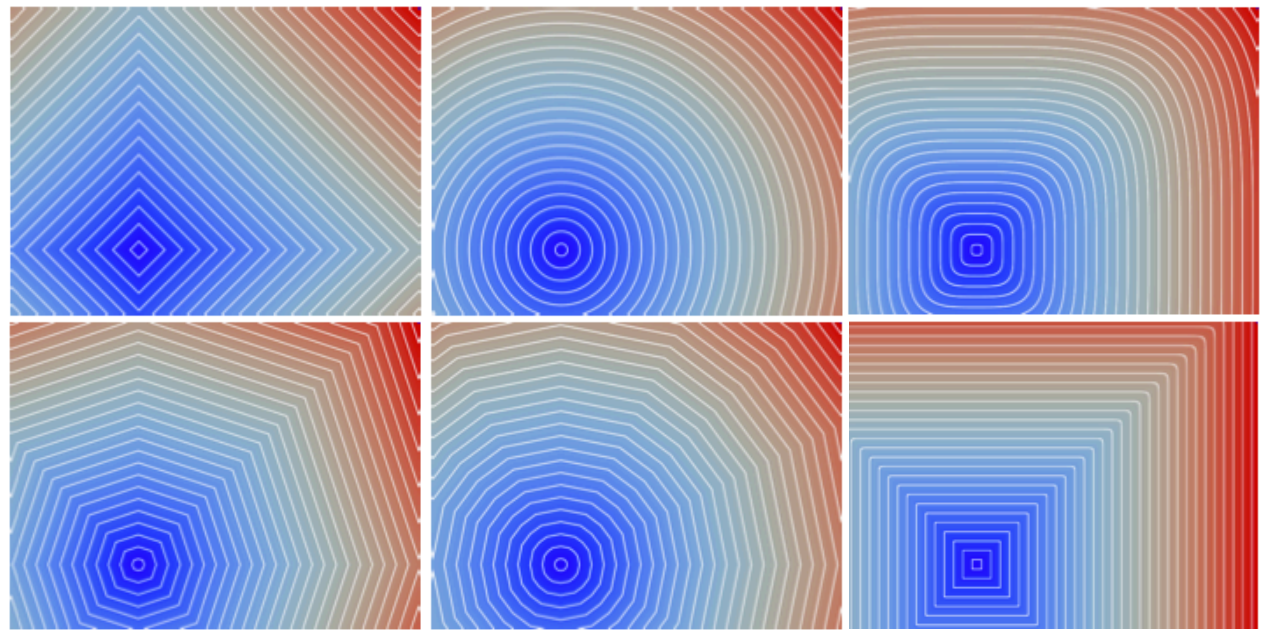

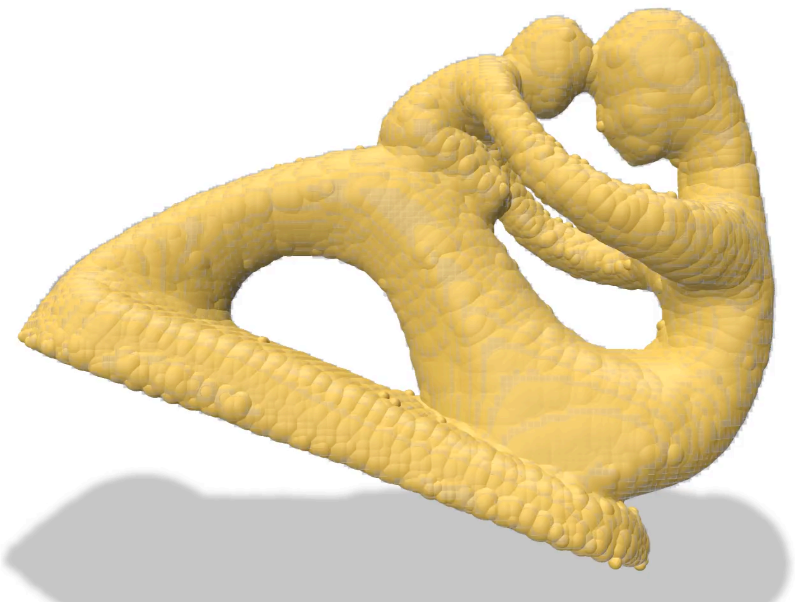

Separable Volumetric approaches

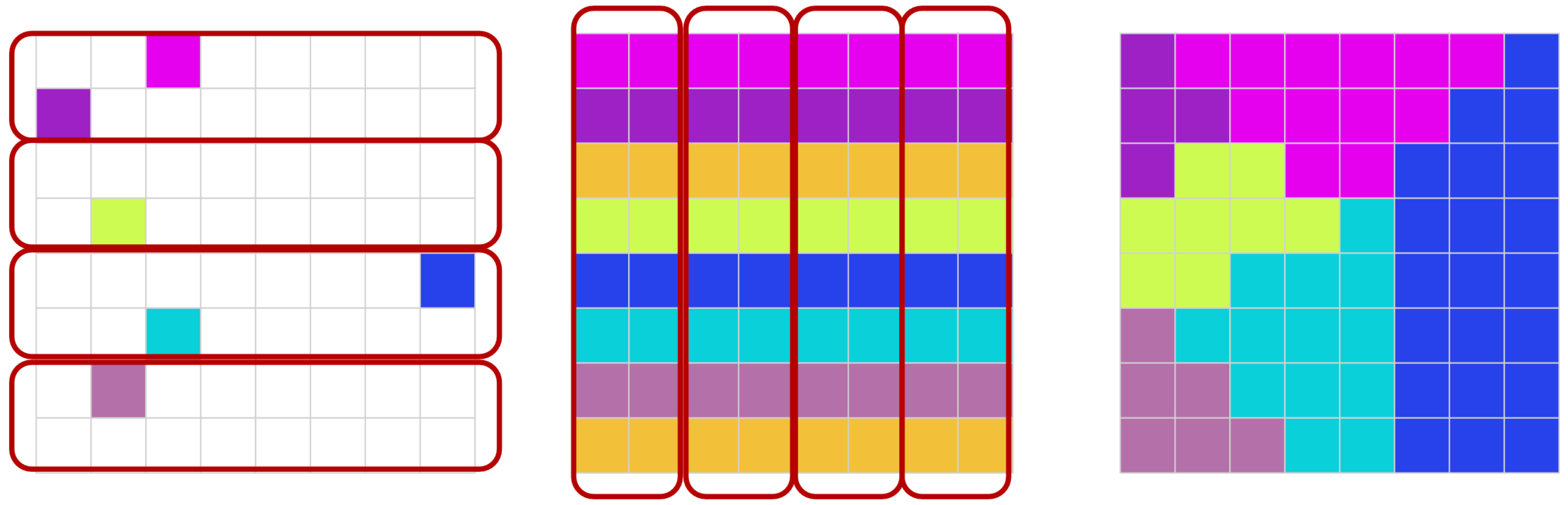

The separable algorithm is correct:

- for any dimension
- for any metric with axis symmetric unit ball (e.g. any l_p, chamfer norms)
- on any toroidal nD domains

Exact and linear in time w.r.t. the number of grid points $O(d \cdot n^d)$ for l_2

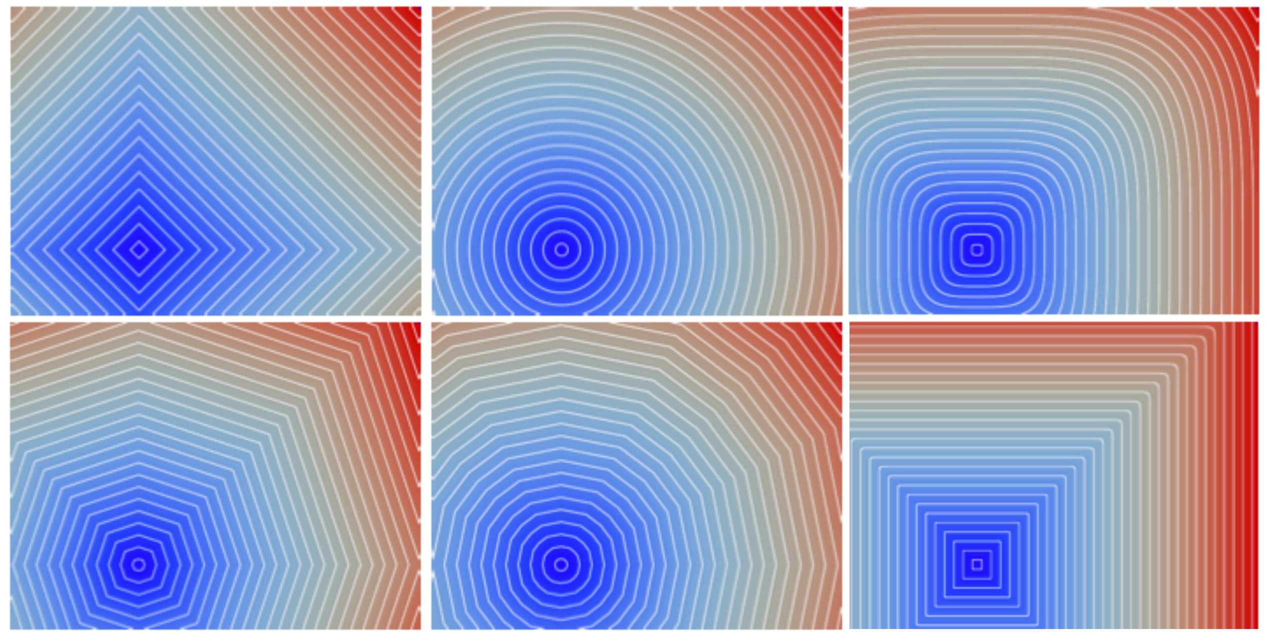

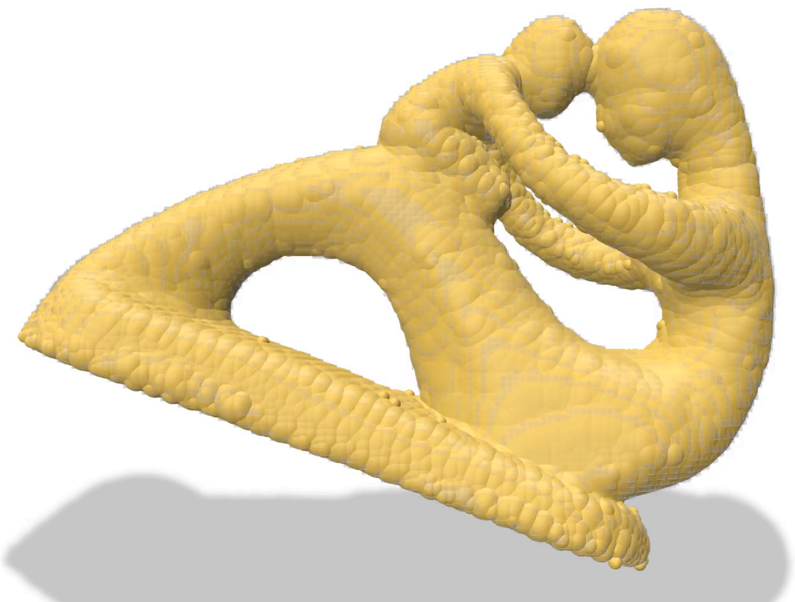

Separable Volumetric approaches

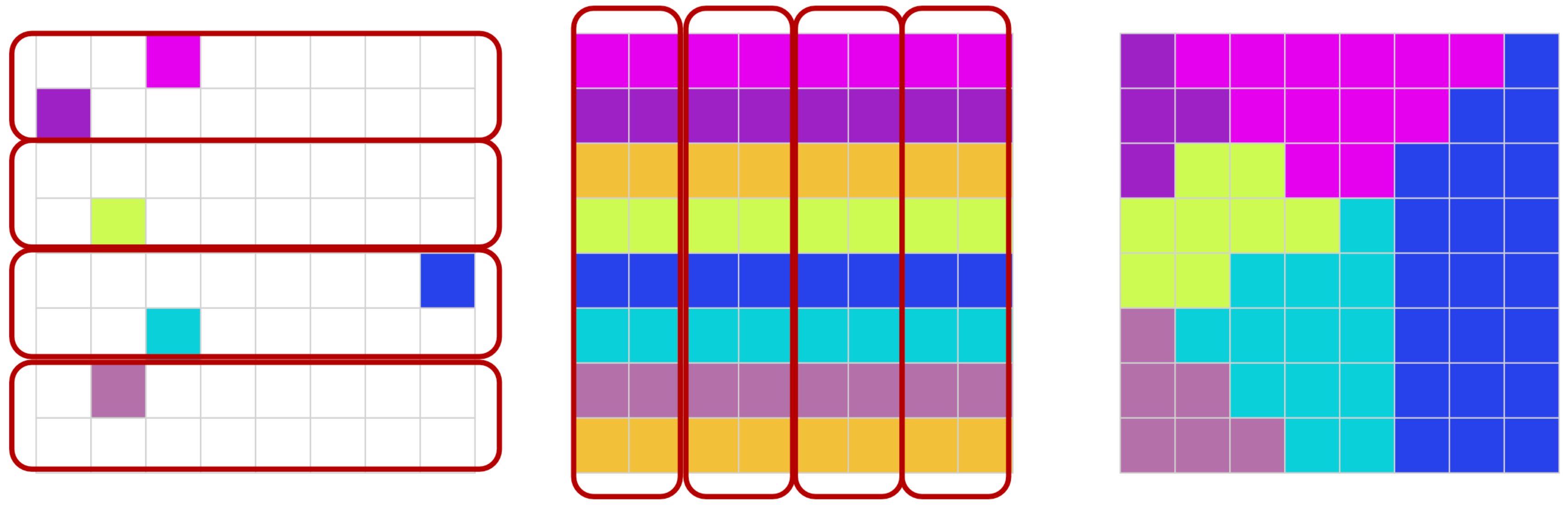

The separable algorithm is correct:

- for any dimension
- for any metric with axis symmetric unit ball (e.g. any l_p, chamfer norms)
- on any toroidal nD domains

Exact and linear in time w.r.t. the number of grid points $O(d \cdot n^d)$ for l_2

$O(d^2 \cdot \log(p) \cdot \log(n) \cdot n^d)$ for exact l_p ($p \in \mathbb{Z}^+$), $O(d \cdot n^d)$ approx.

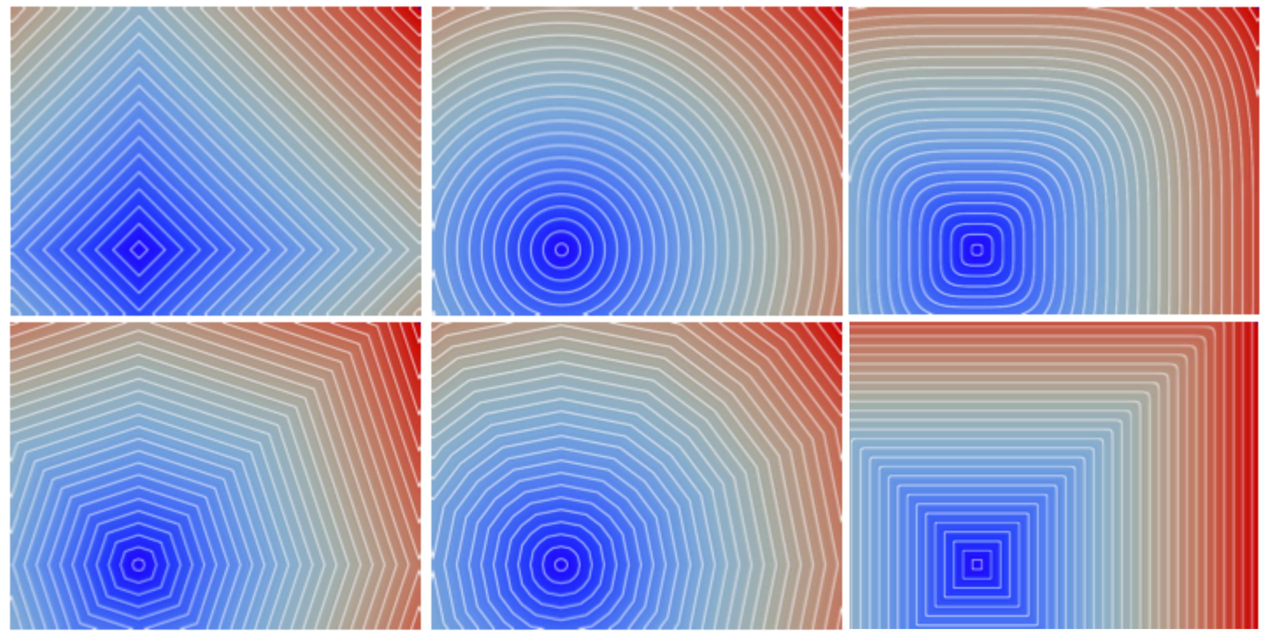

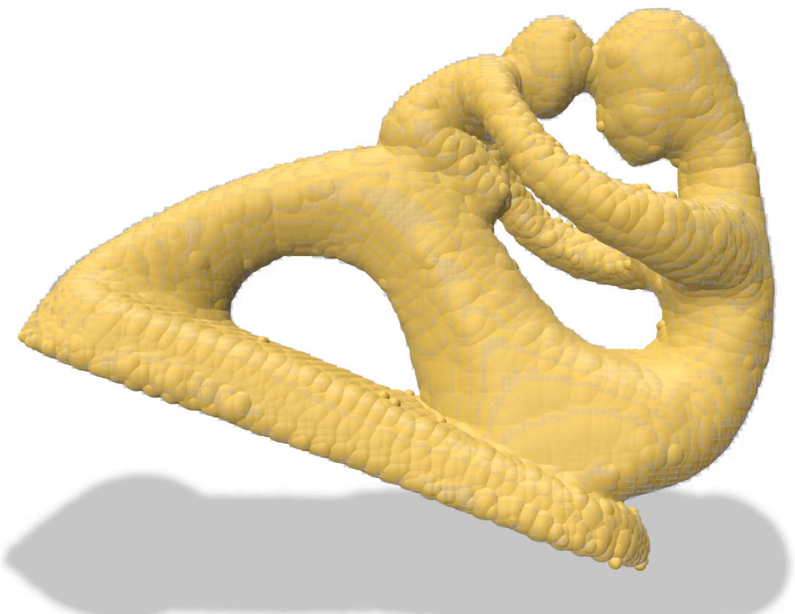

Separable Volumetric approaches

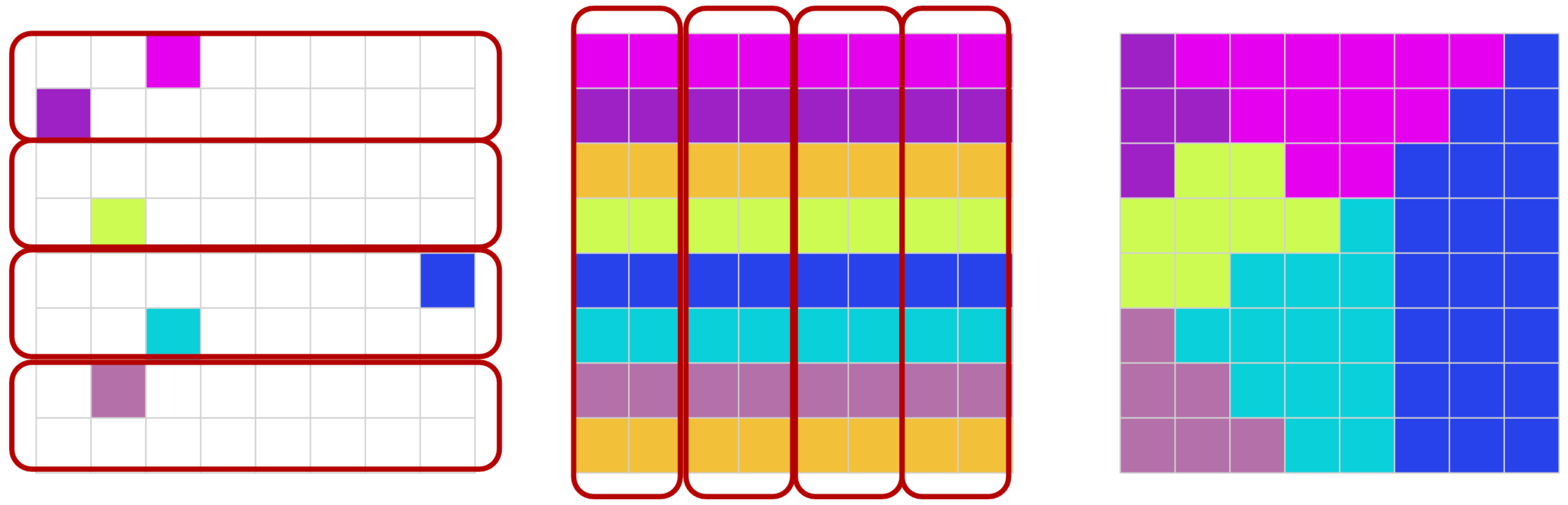

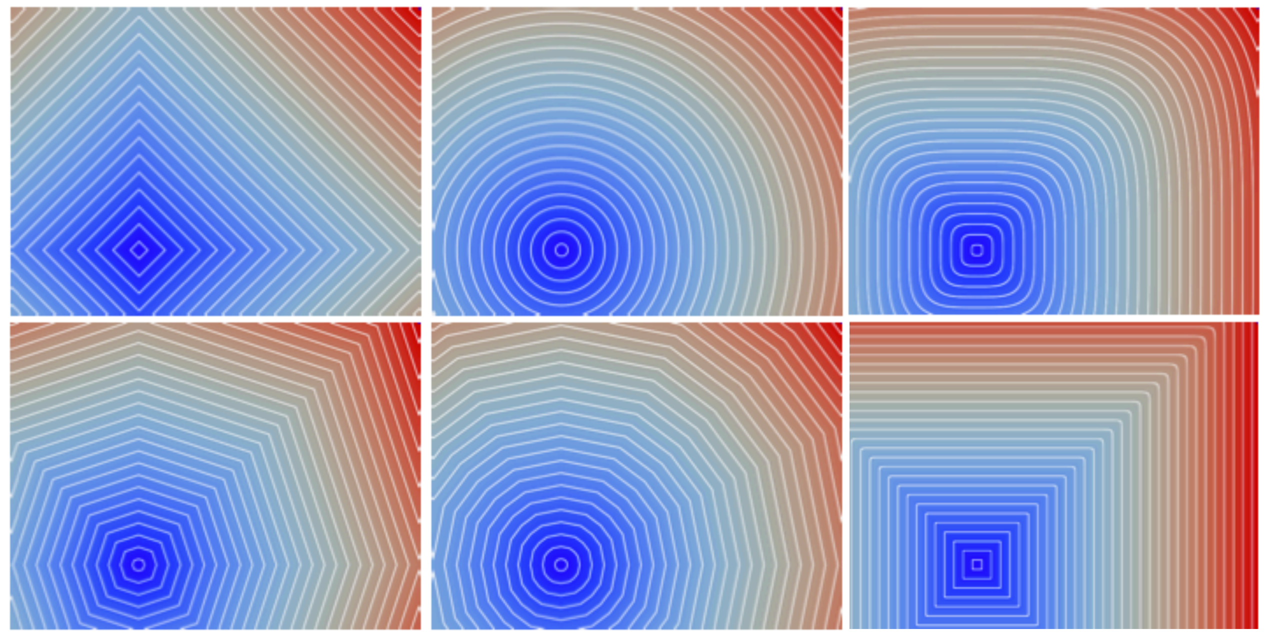

The separable algorithm is correct:

- for any dimension
- for any metric with axis symmetric unit ball (e.g. any l_p, chamfer norms)
- on any toroidal nD domains

Exact and linear in time w.r.t. the number of grid points $O(d \cdot n^d)$ for l_2

$O(d^2 \cdot \log(p) \cdot \log(n) \cdot n^d)$ for exact l_p $(p \in \mathbb{Z}^+)$, $O(d \cdot n^d)$ approx.

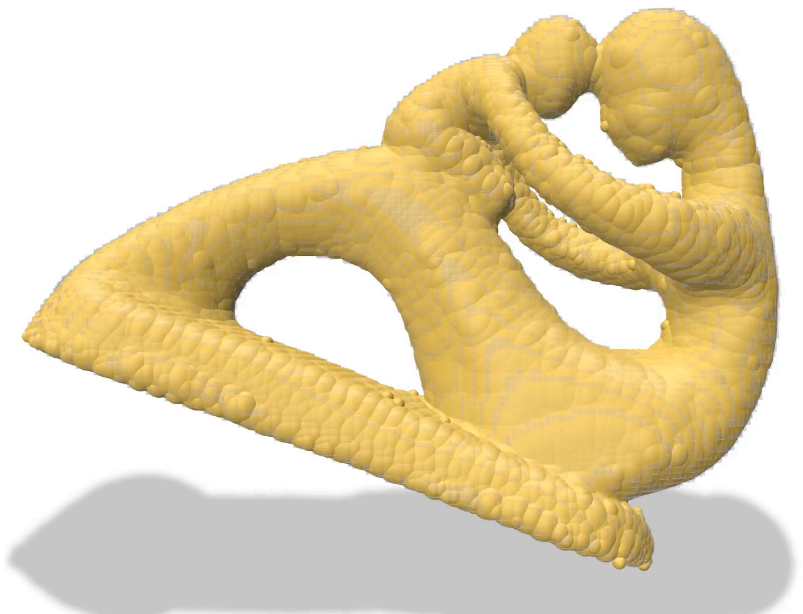

Separable Volumetric approaches

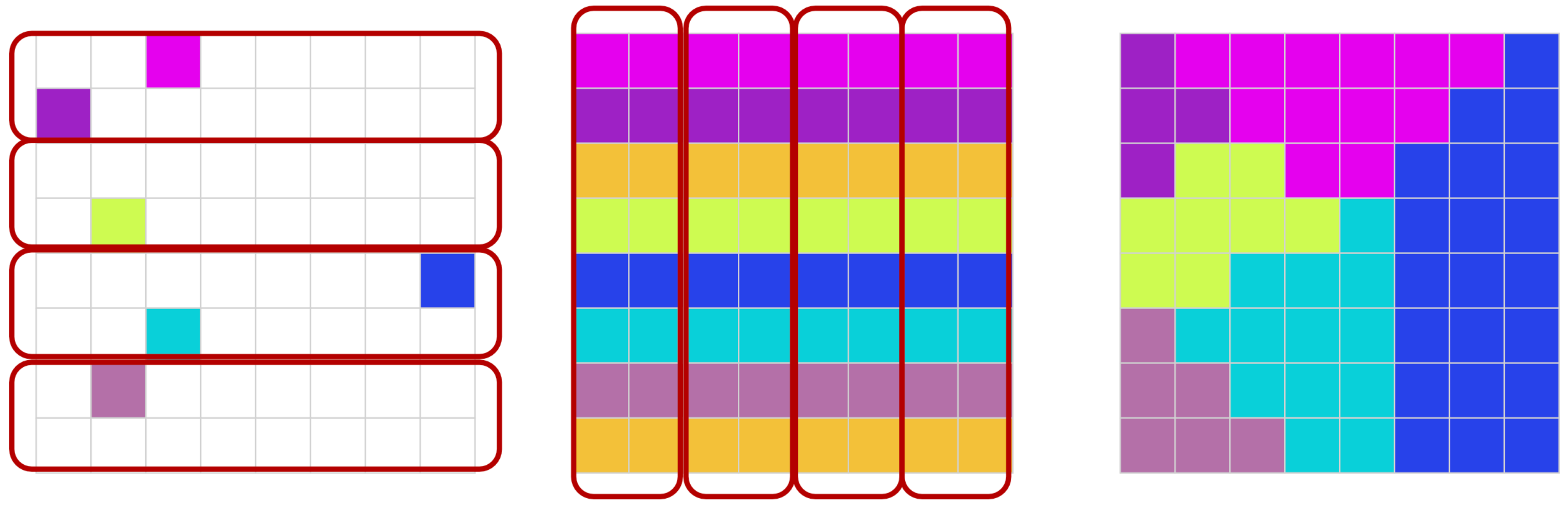

The separable algorithm is correct:

- for any dimension
- for any metric with axis symmetric unit ball (e.g. any l_p, chamfer norms)
- on any toroidal nD domains

Exact and linear in time w.r.t. the number of grid points $O(d \cdot n^d)$ for l_2

$O(d^2 \cdot \log(p) \cdot \log(n) \cdot n^d)$ for exact l_p ($p \in \mathbb{Z}^+$), $O(d \cdot n^d)$ approx.

Trivial multithread / GPU / out-of-core implementations

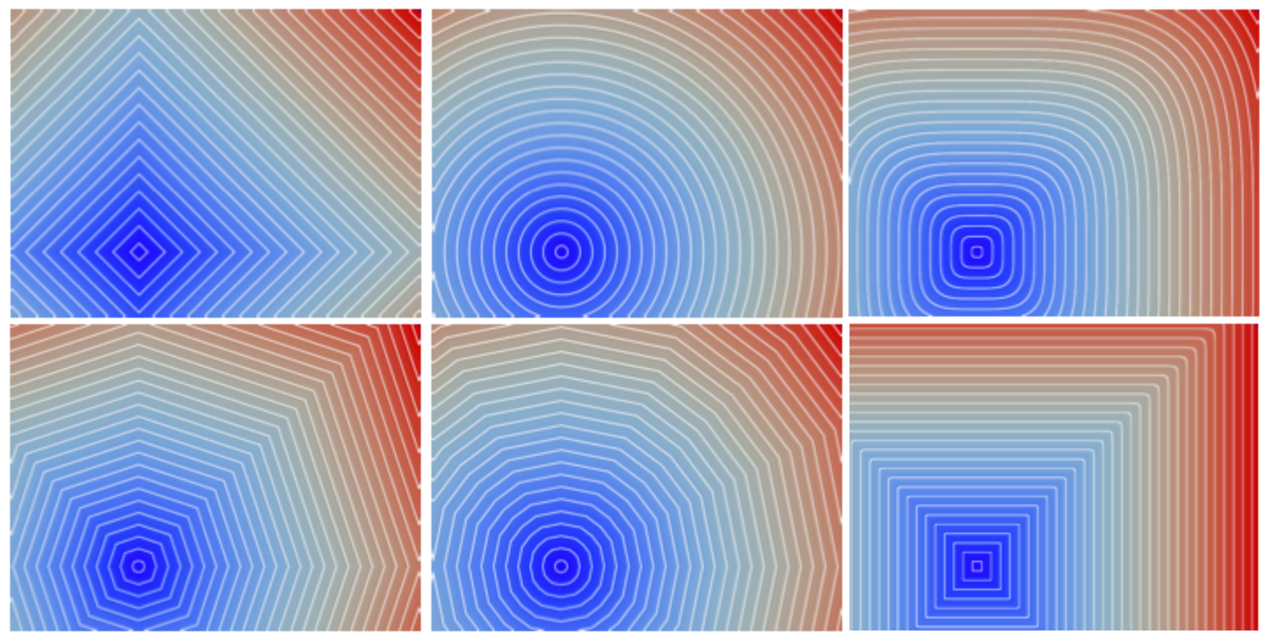

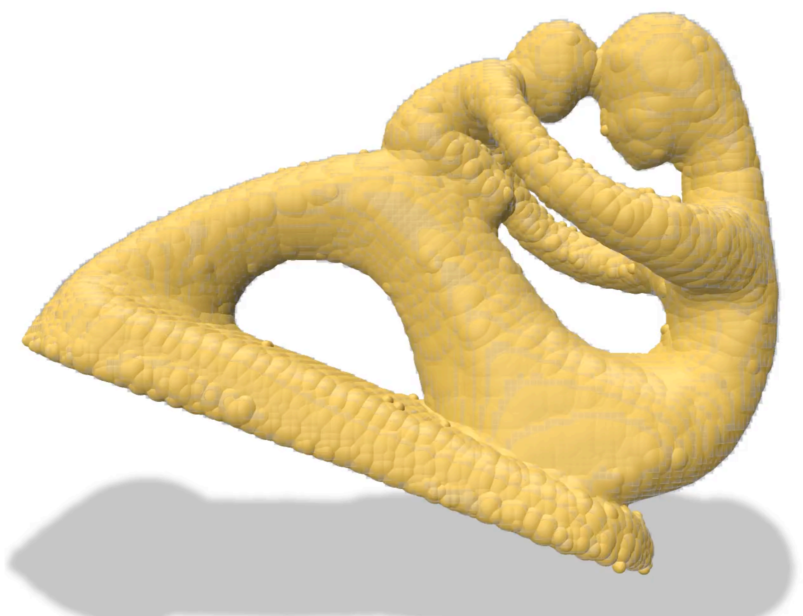

Separable Volumetric approaches

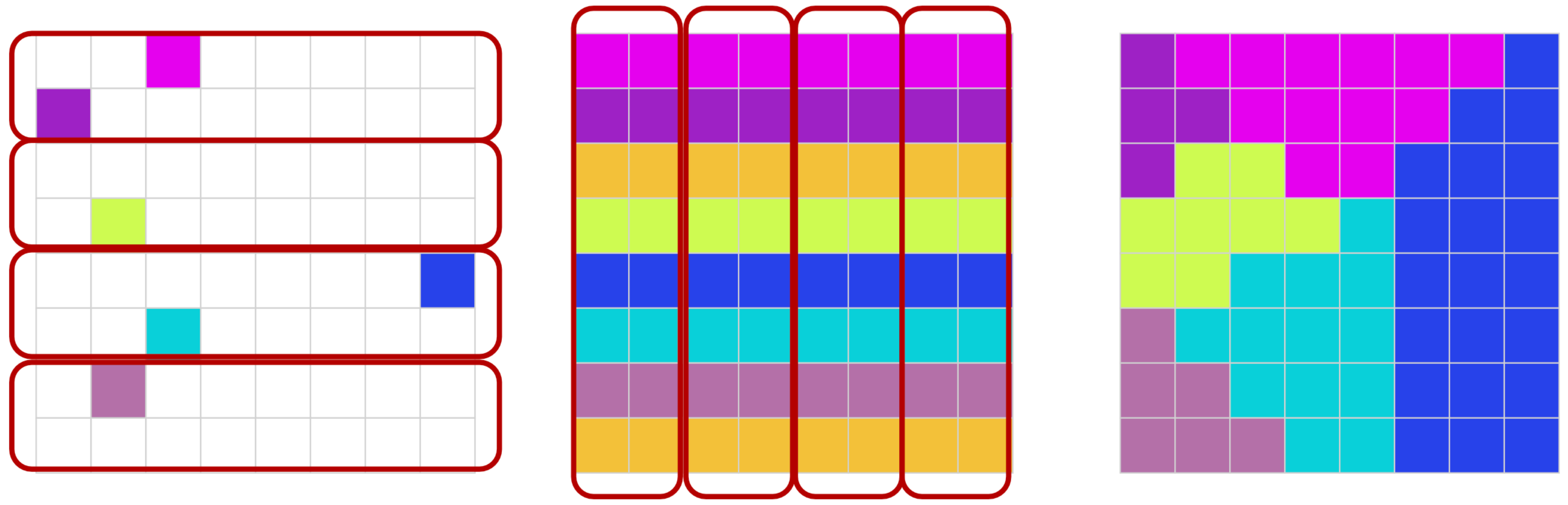

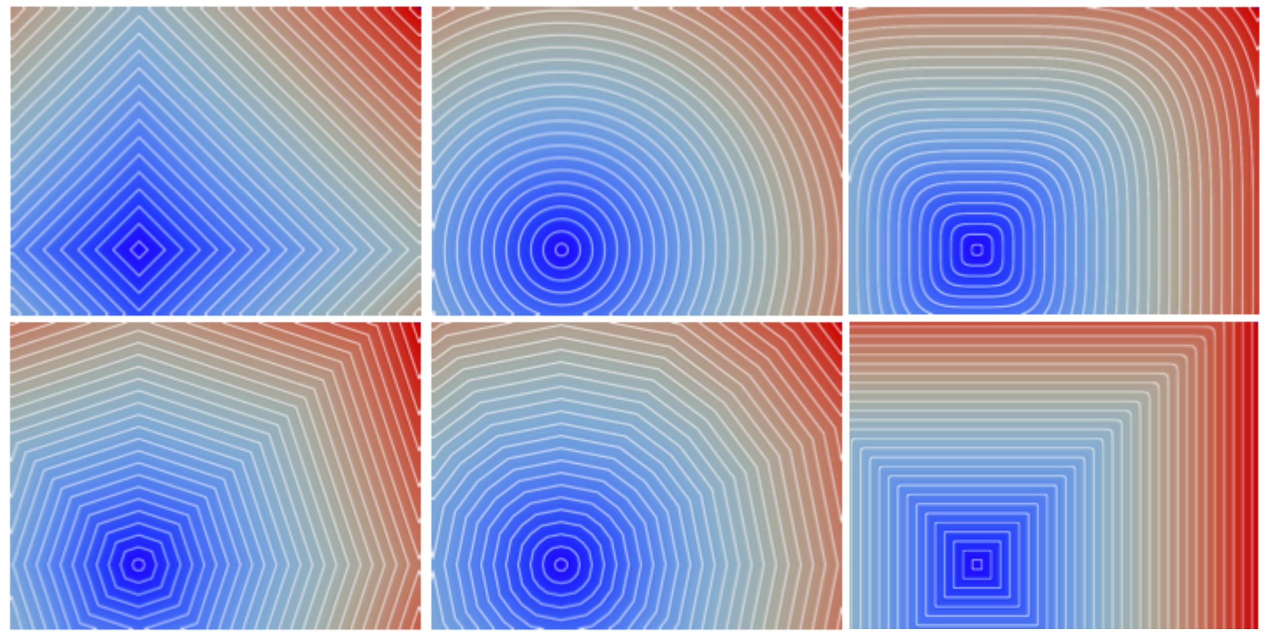

The separable algorithm is correct:

- for any dimension
- for any metric with axis symmetric unit ball (e.g. any l_p, chamfer norms)
- on any toroidal nD domains

Exact and linear in time w.r.t. the number of grid points $O(d \cdot n^d)$ for l_2

$O(d^2 \cdot \log(p) \cdot \log(n) \cdot n^d)$ for exact l_p ($p \in \mathbb{Z}^+$), $O(d \cdot n^d)$ approx.

Trivial multithread / GPU / out-of-core implementations

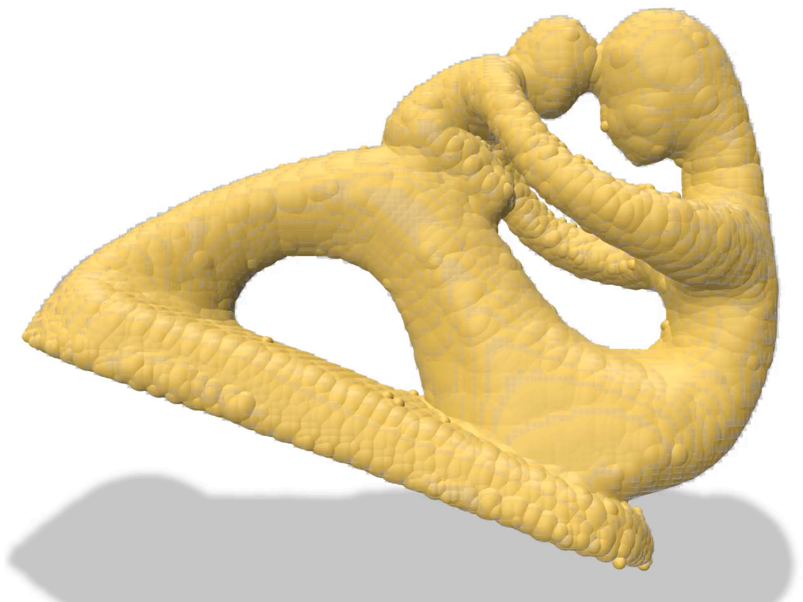

Separable Volumetric approaches

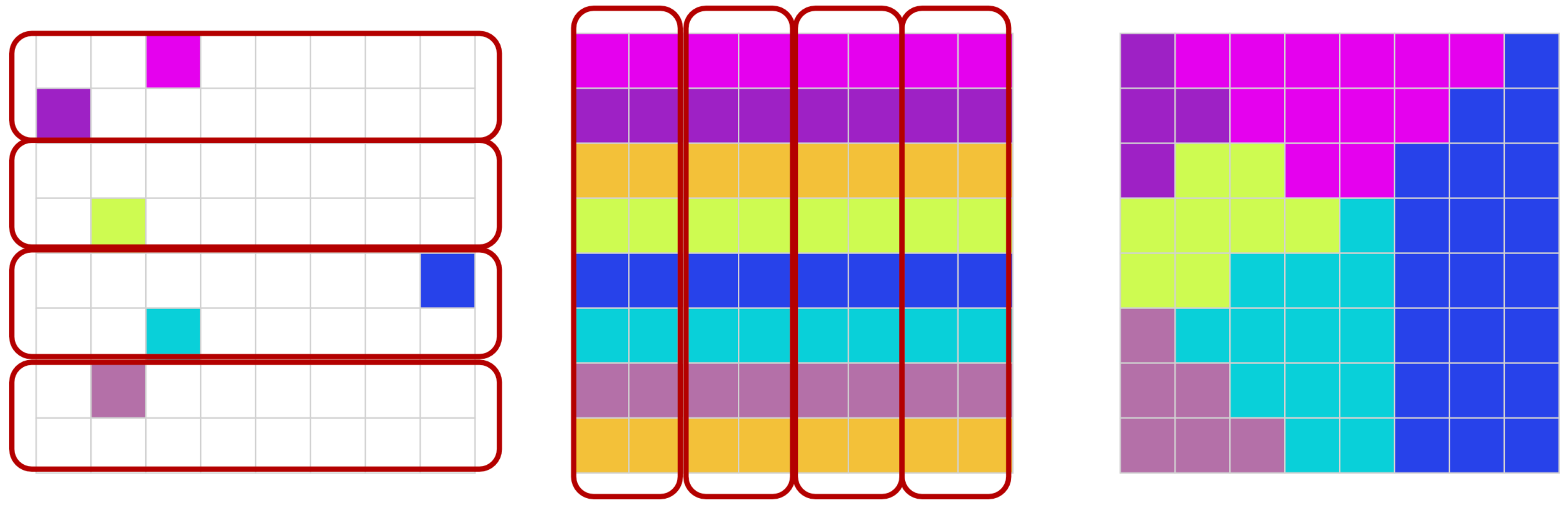

The separable algorithm is correct:

- for any dimension
- for any metric with axis symmetric unit ball (e.g. any l_p, chamfer norms)
- on any toroidal nD domains

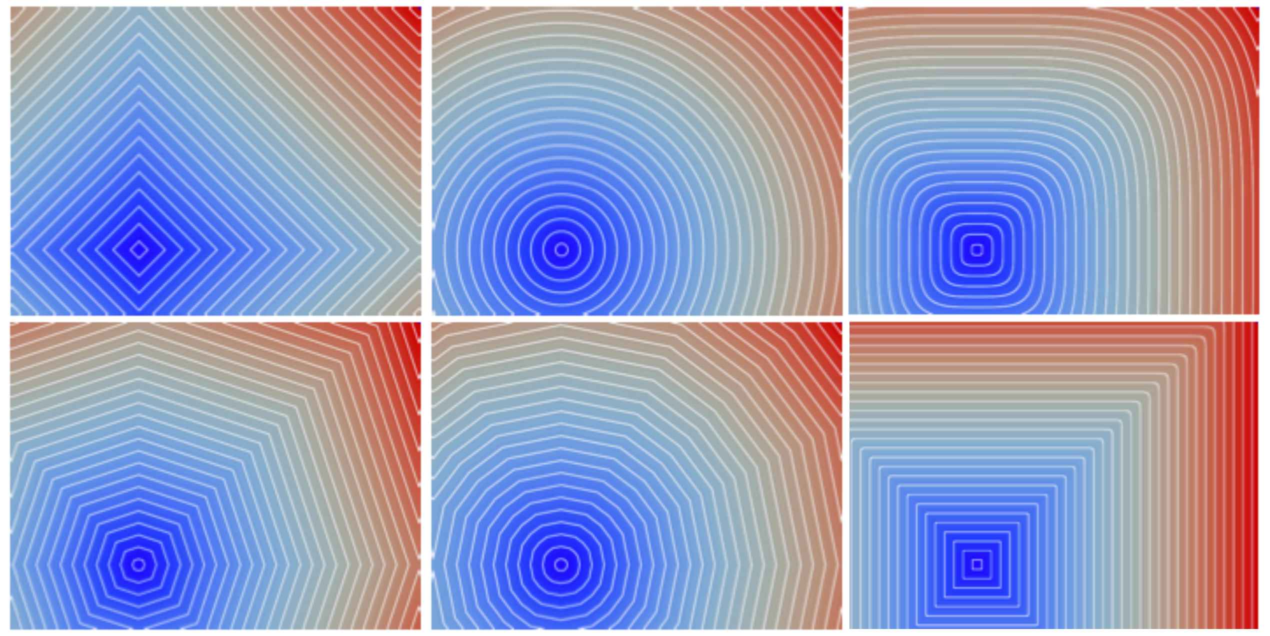

Exact and linear in time w.r.t. the number of grid points $O(d \cdot n^d)$ for l_2

$O(d^2 \cdot \log(p) \cdot \log(n) \cdot n^d)$ for exact l_p ($p \in \mathbb{Z}^+$), $O(d \cdot n^d)$ approx.

Trivial multithread / GPU / out-of-core implementations

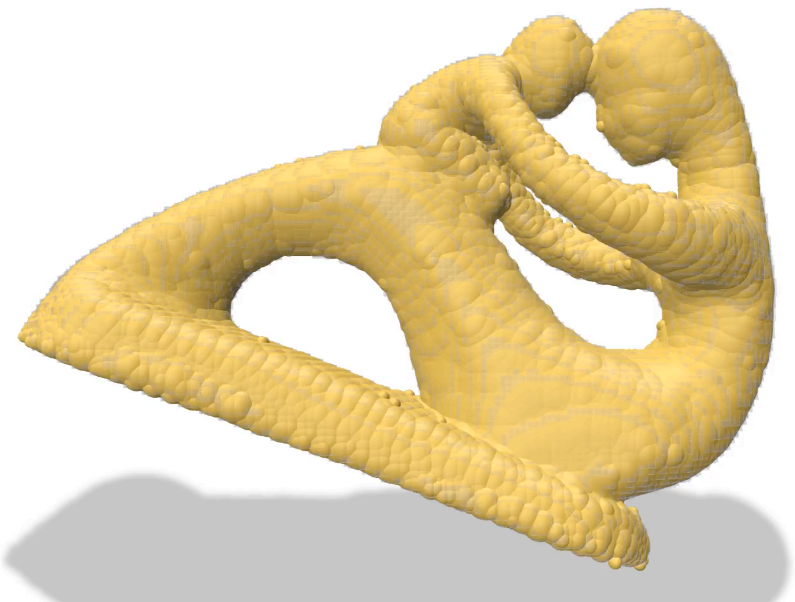

Separable Volumetric approaches

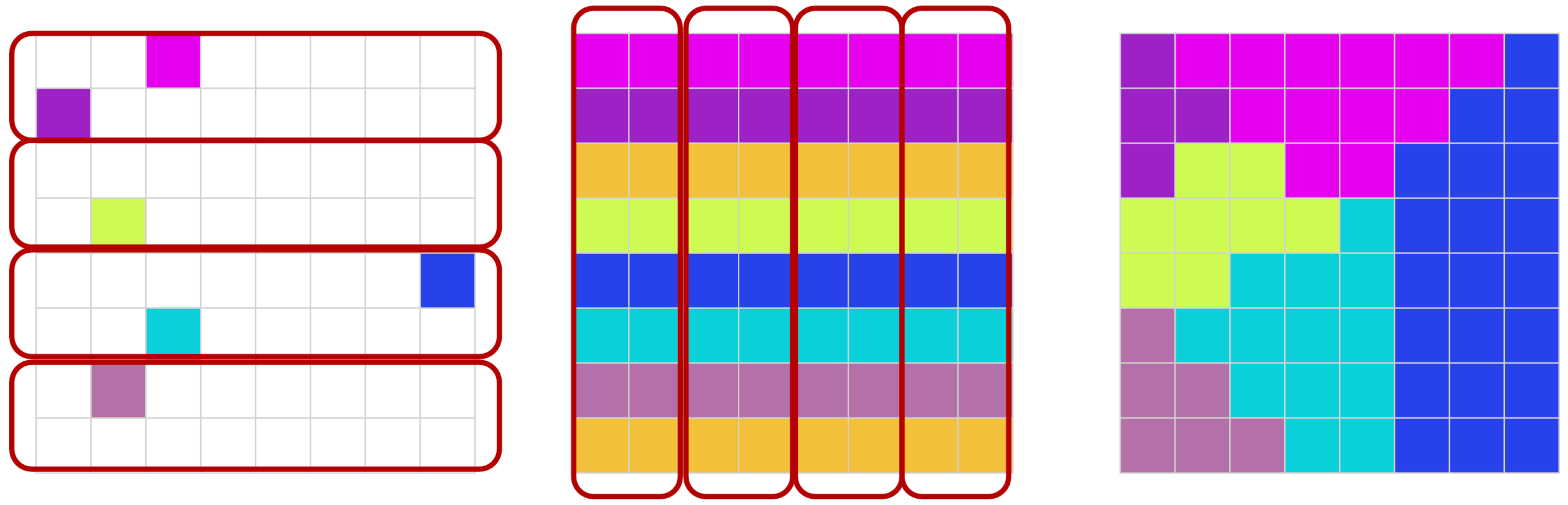

The separable algorithm is correct:

- for any dimension
- for any metric with axis symmetric unit ball (e.g. any l_p, chamfer norms)
- on any toroidal nD domains

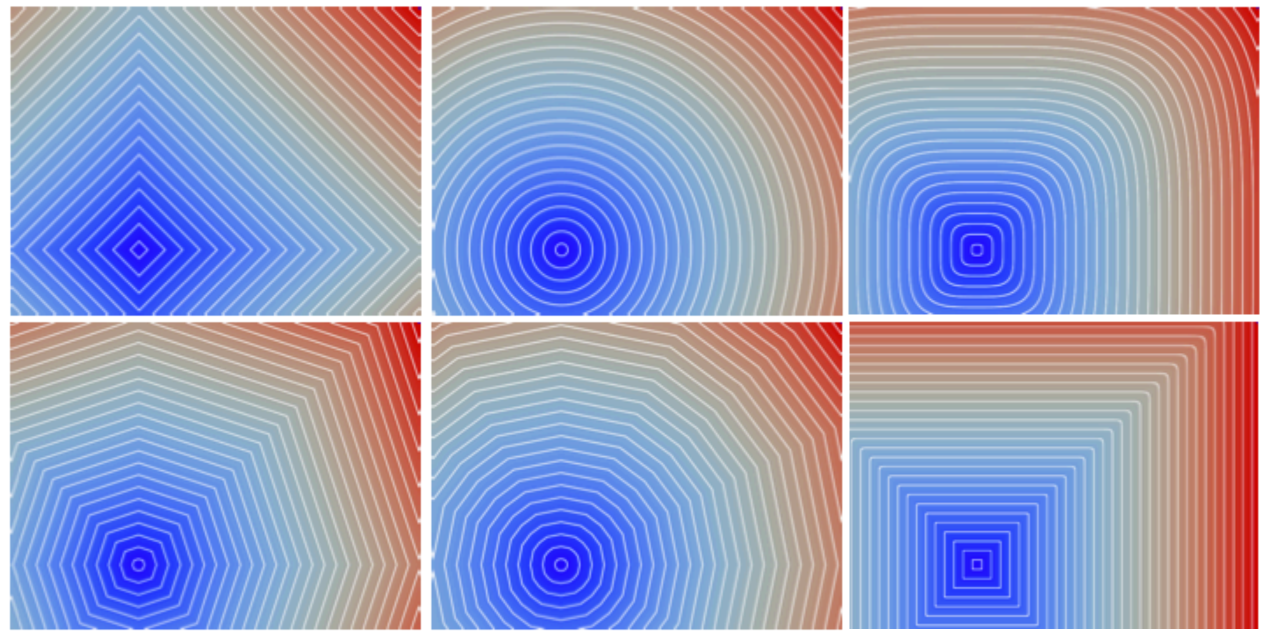

Exact and linear in time w.r.t. the number of grid points $O(d \cdot n^d)$ for l_2

$O(d^2 \cdot \log(p) \cdot \log(n) \cdot n^d)$ for exact l_p $(p \in \mathbb{Z}^+)$, $O(d \cdot n^d)$ approx.

Trivial multithread / GPU / out-of-core implementations

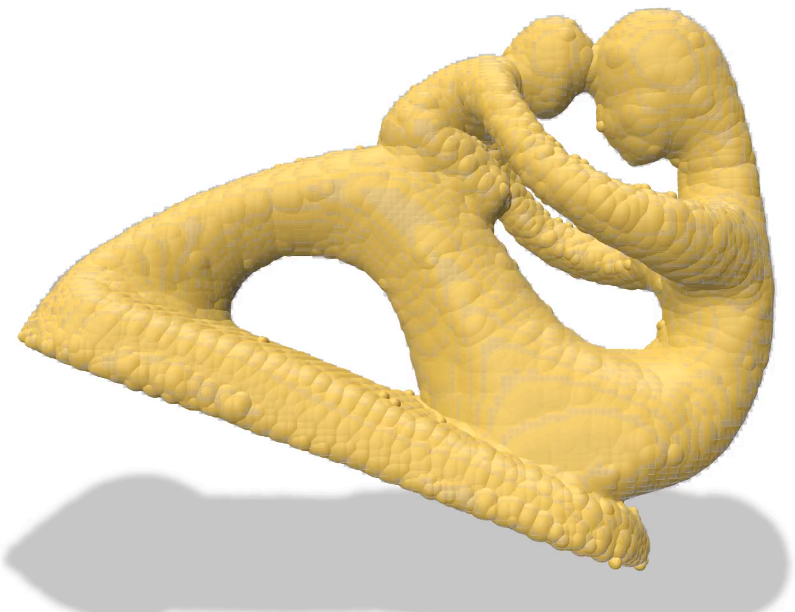

Separable Volumetric approaches

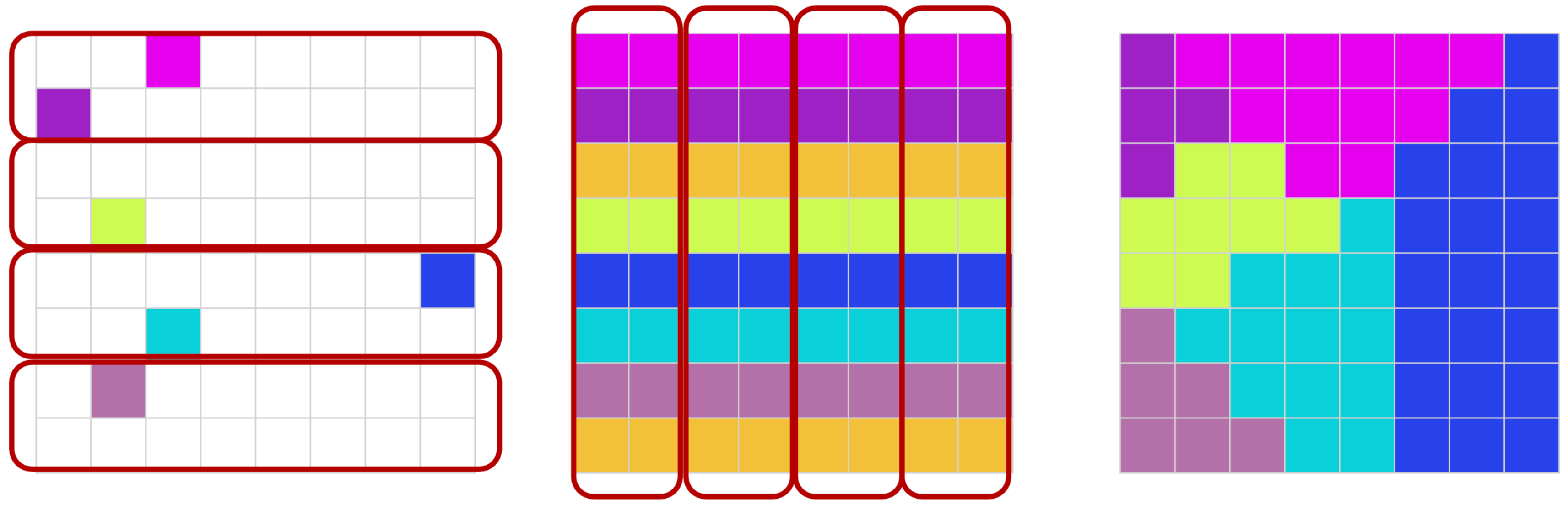

The separable algorithm is correct:

- for any dimension
- for any metric with axis symmetric unit ball (e.g. any l_p, chamfer norms)
- on any toroidal nD domains

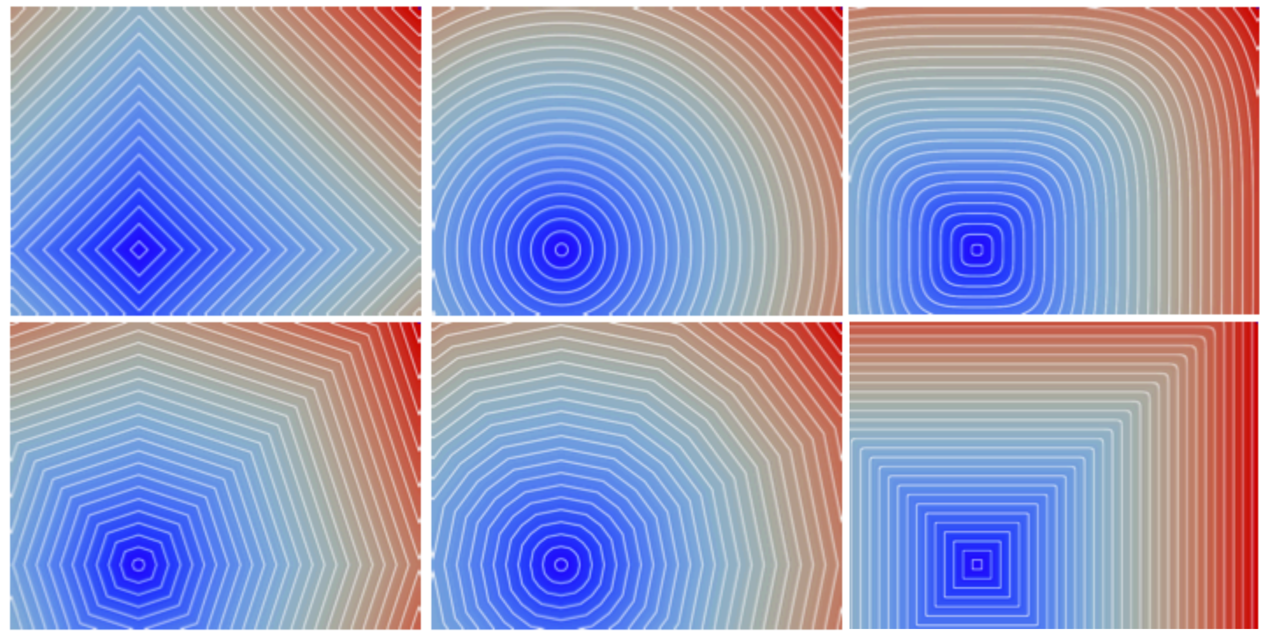

Exact and linear in time w.r.t. the number of grid points $O(d \cdot n^d)$ for l_2

$O(d^2 \cdot \log(p) \cdot \log(n) \cdot n^d)$ for exact l_p ($p \in \mathbb{Z}^+$), $O(d \cdot n^d)$ approx.

Trivial multithread / GPU / out-of-core implementations

Same techniques and computational costs for: [C. et al 07]

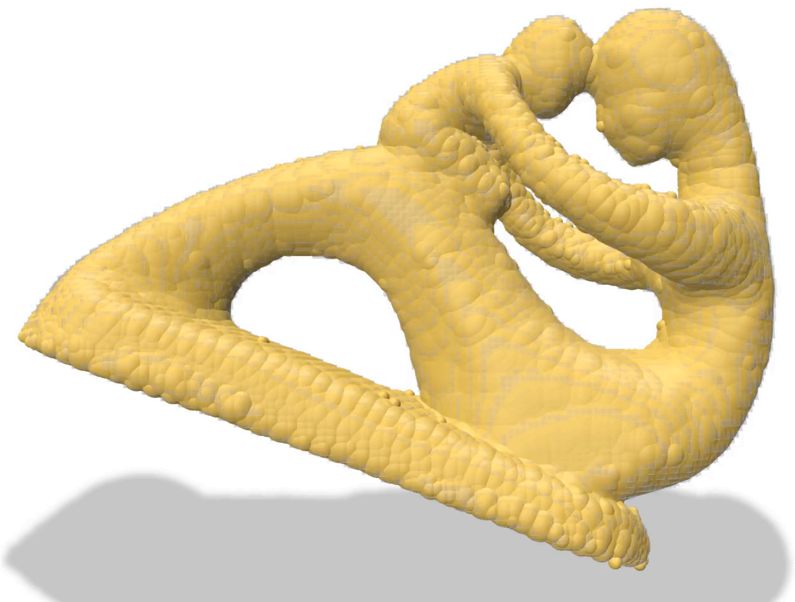

Separable Volumetric approaches

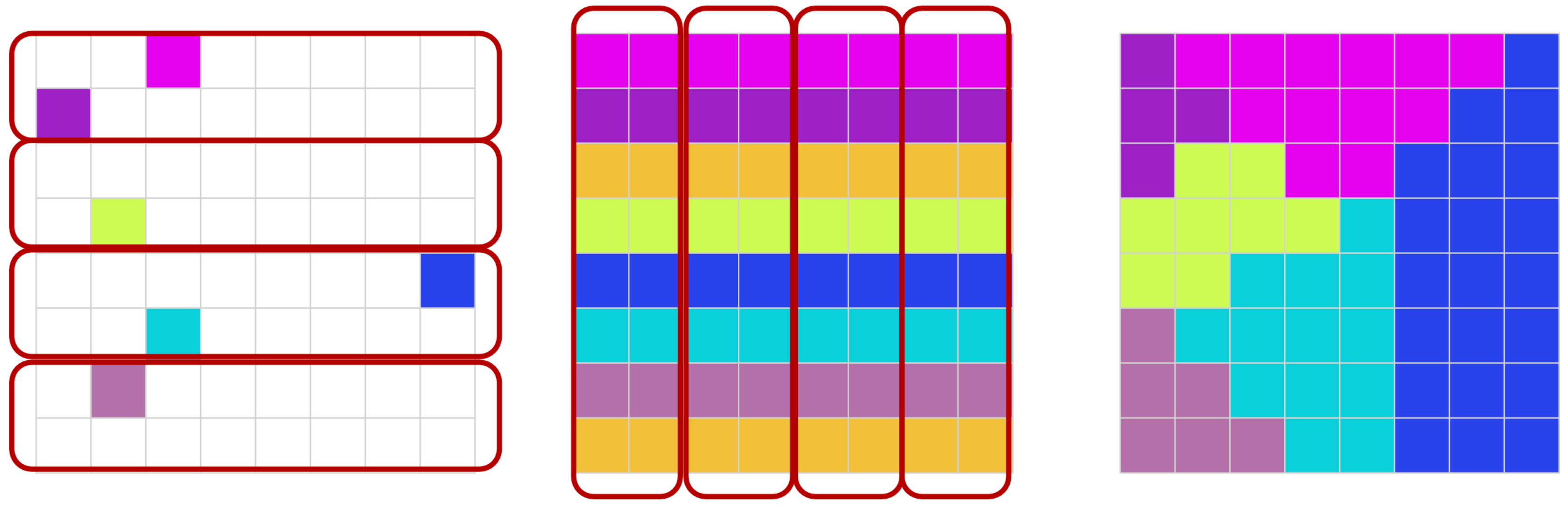

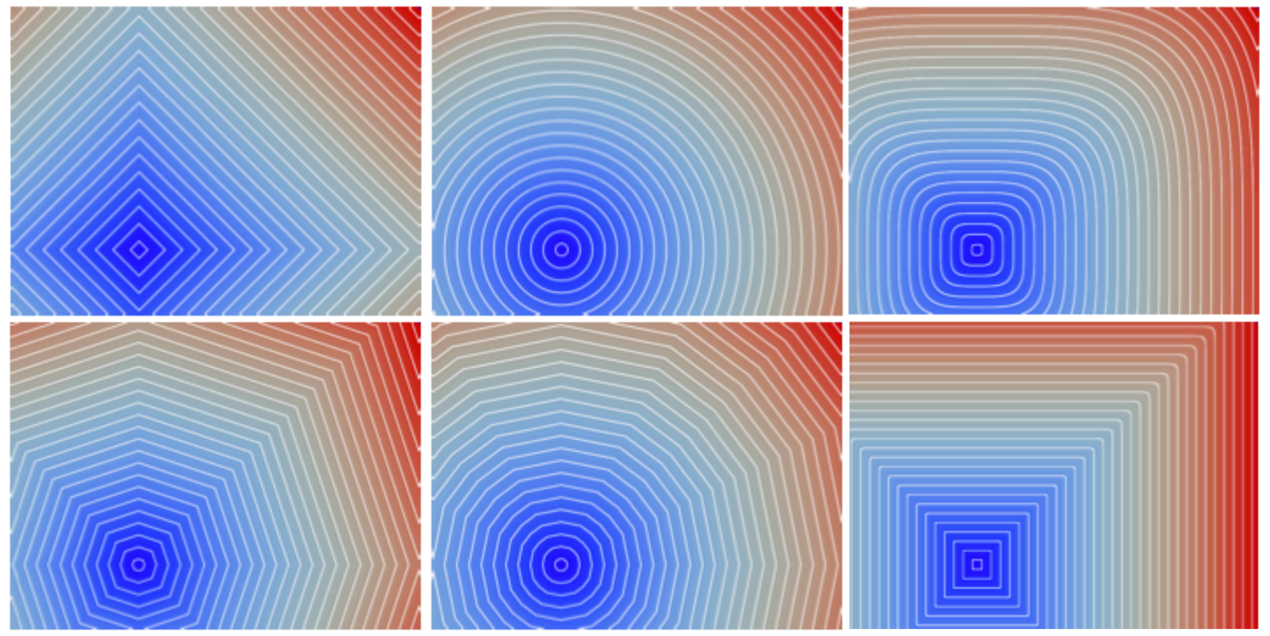

The separable algorithm is correct:

- for any dimension
- for any metric with axis symmetric unit ball (e.g. any l_p, chamfer norms)
- on any toroidal nD domains

Exact and linear in time w.r.t. the number of grid points $O(d \cdot n^d)$ for l_2

$O(d^2 \cdot \log(p) \cdot \log(n) \cdot n^d)$ for exact l_p ($p \in \mathbb{Z}^+$), $O(d \cdot n^d)$ approx.

Trivial multithread / GPU / out-of-core implementations

Same techniques and computational costs for: [C. et al 07]

- Power diagram / power maps construction

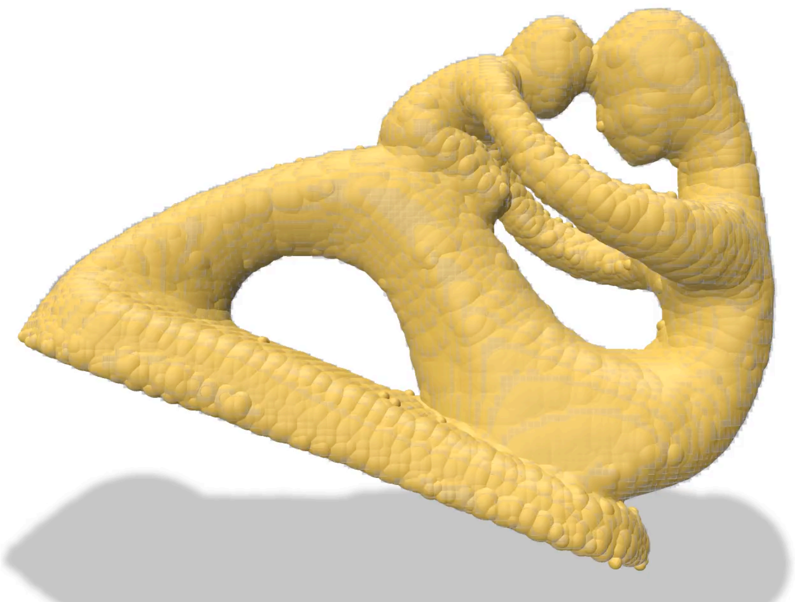

Separable Volumetric approaches

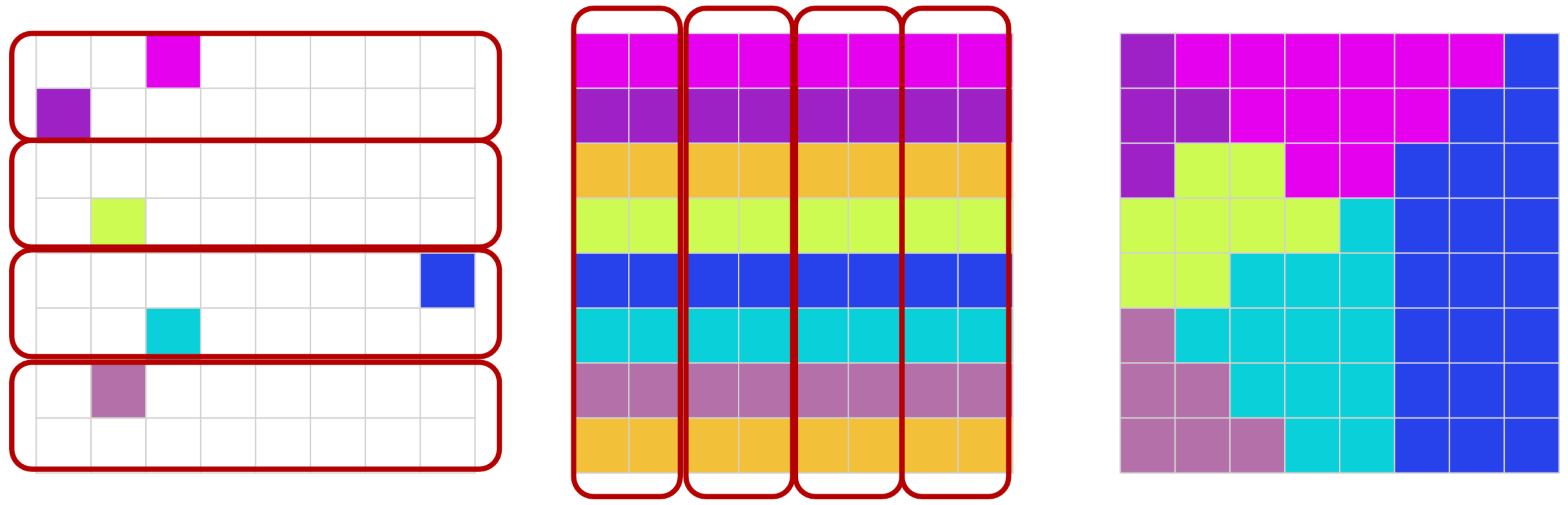

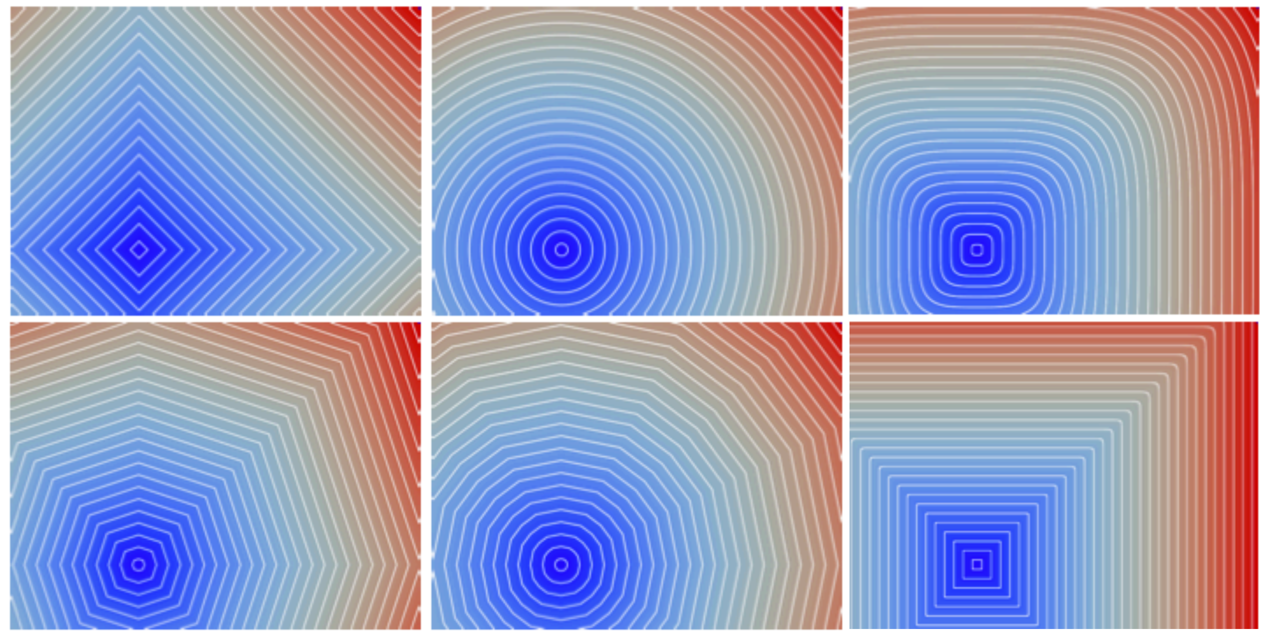

The separable algorithm is correct:

- for any dimension
- for any metric with axis symmetric unit ball (e.g. any l_p, chamfer norms)
- on any toroidal nD domains

Exact and linear in time w.r.t. the number of grid points $O(d \cdot n^d)$ for l_2

$O(d^2 \cdot \log(p) \cdot \log(n) \cdot n^d)$ for exact l_p ($p \in \mathbb{Z}^+$), $O(d \cdot n^d)$ approx.

Trivial multithread / GPU / out-of-core implementations

Same techniques and computational costs for: [C. et al 07]

- Power diagram / power maps construction
- Discrete Medial Axis extraction (aka non-empty inner power cells)

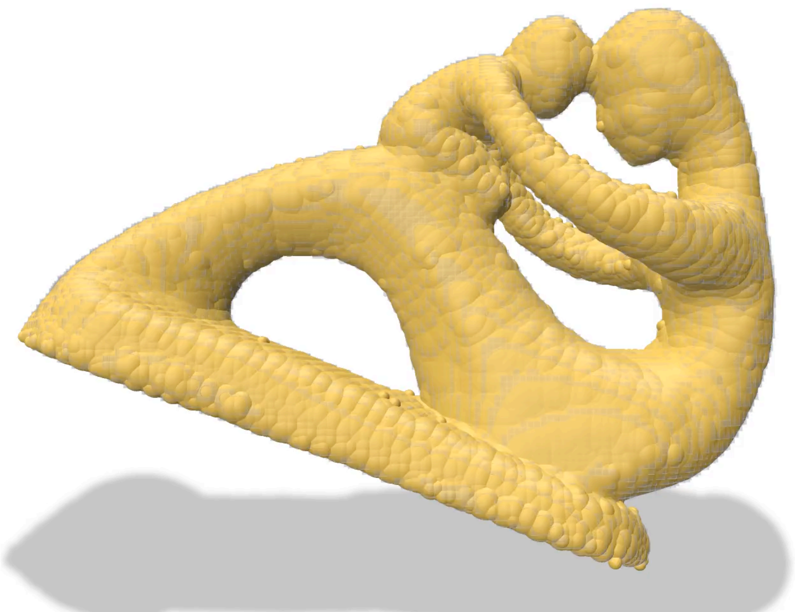

Separable Volumetric approaches

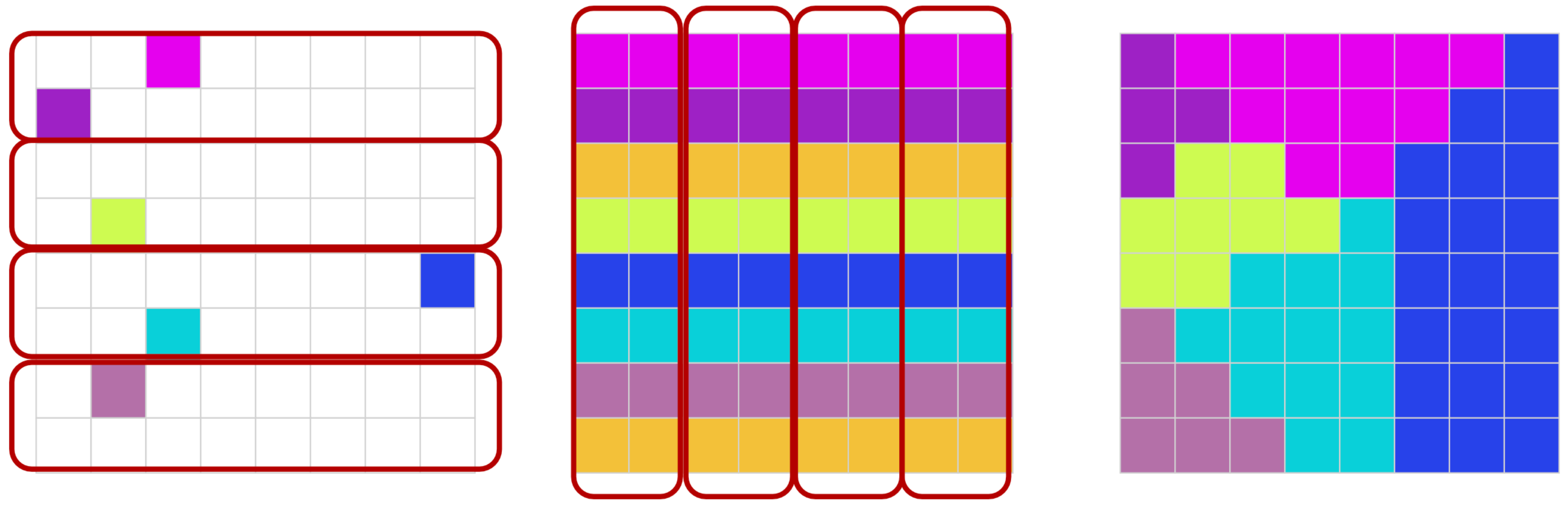

The separable algorithm is correct:

- for any dimension
- for any metric with axis symmetric unit ball (e.g. any l_p, chamfer norms)
- on any toroidal nD domains

Exact and linear in time w.r.t. the number of grid points $O(d \cdot n^d)$ for l_2

$O(d^2 \cdot \log(p) \cdot \log(n) \cdot n^d)$ for exact l_p ($p \in \mathbb{Z}^+$), $O(d \cdot n^d)$ approx.

Trivial multithread / GPU / out-of-core implementations

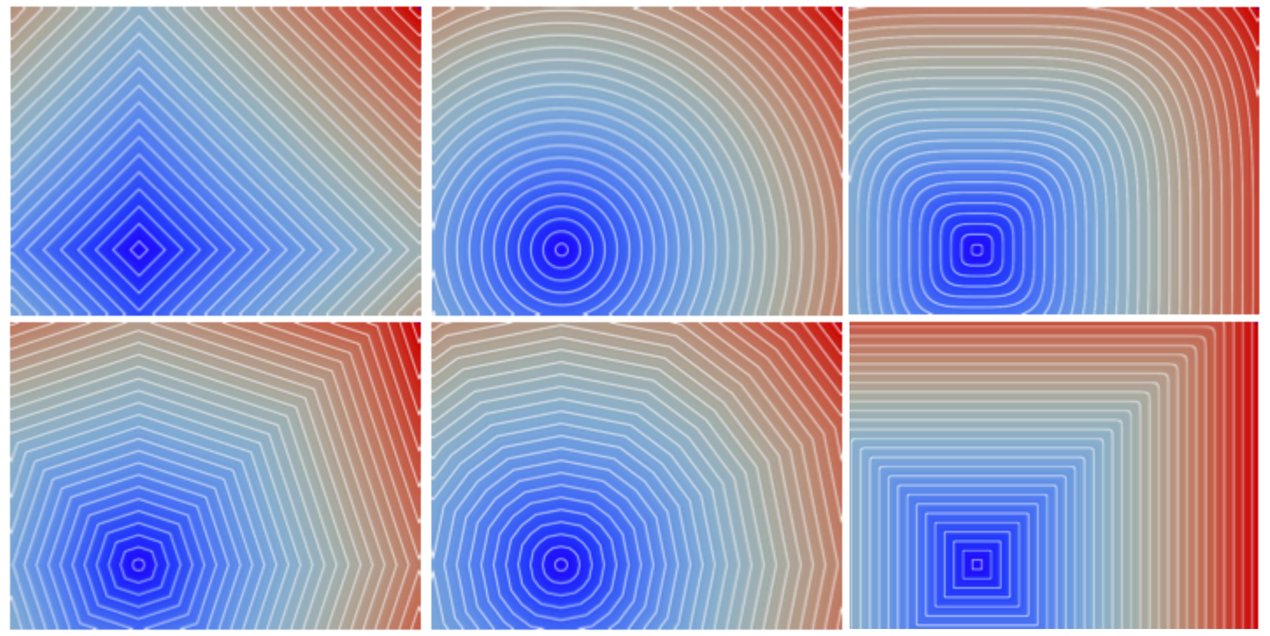

Same techniques and computational costs for: [C. et al 07]

- Power diagram / power maps construction
- Discrete Medial Axis extraction (aka non-empty inner power cells)
- Reverse reconstruction (balls$\rightarrow$shape)

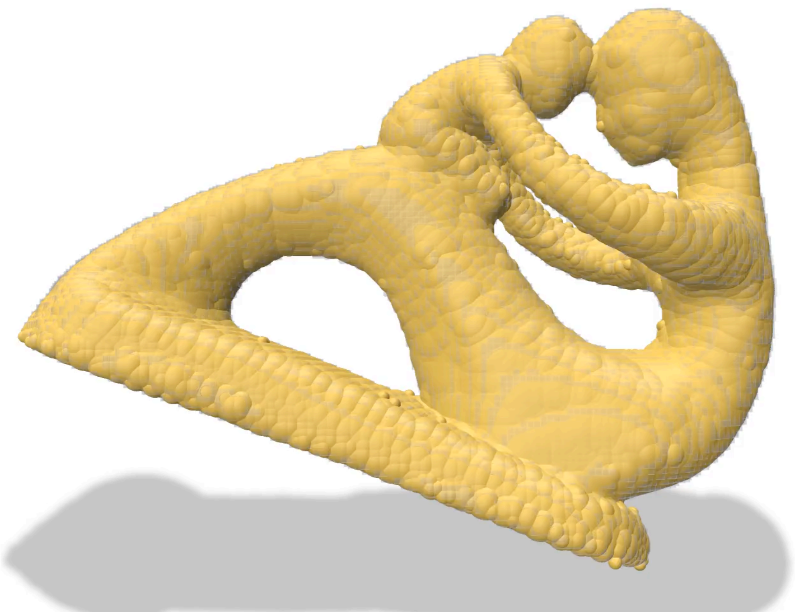

Separable Volumetric approaches

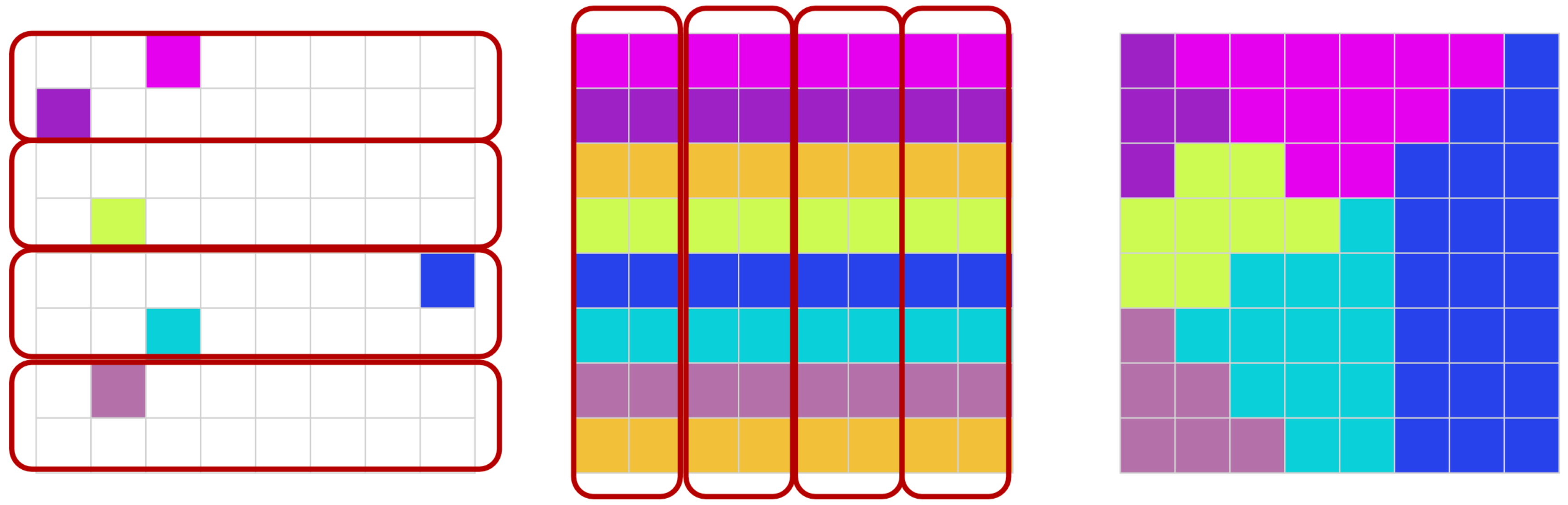

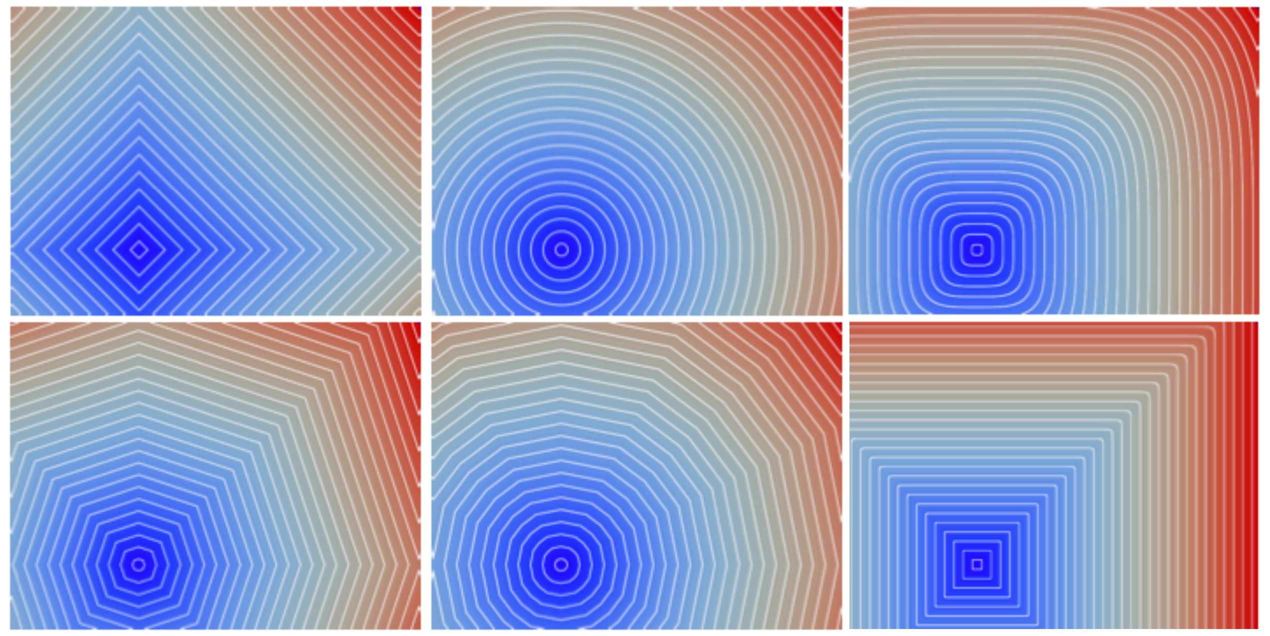

The separable algorithm is correct:

- for any dimension
- for any metric with axis symmetric unit ball (e.g. any l_p, chamfer norms)
- on any toroidal nD domains

Exact and linear in time w.r.t. the number of grid points $O(d \cdot n^d)$ for l_2

$O(d^2 \cdot \log(p) \cdot \log(n) \cdot n^d)$ for exact l_p ($p \in \mathbb{Z}^+$), $O(d \cdot n^d)$ approx.

Trivial multithread / GPU / out-of-core implementations

Same techniques and computational costs for: [C. et al 07]

- Power diagram / power maps construction
- Discrete Medial Axis extraction (aka non-empty inner power cells)
- Reverse reconstruction (balls→shape)

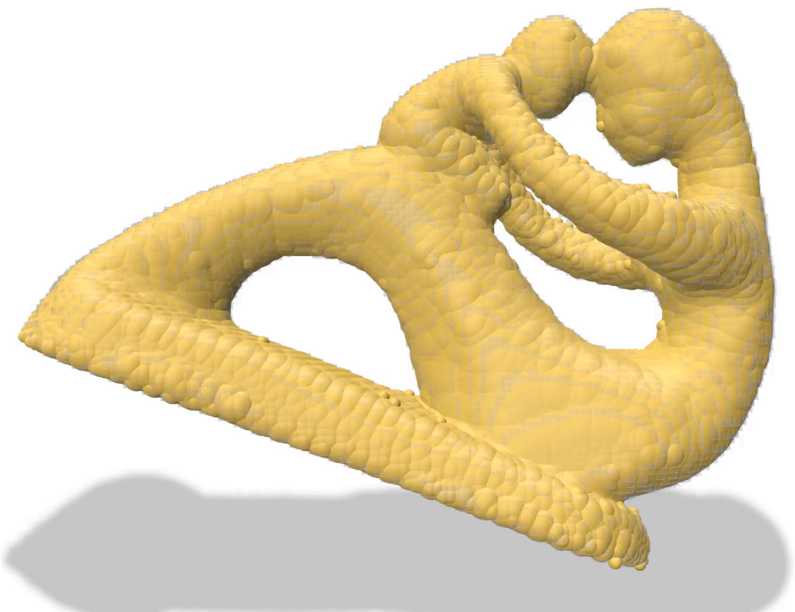

Separable Volumetric approaches

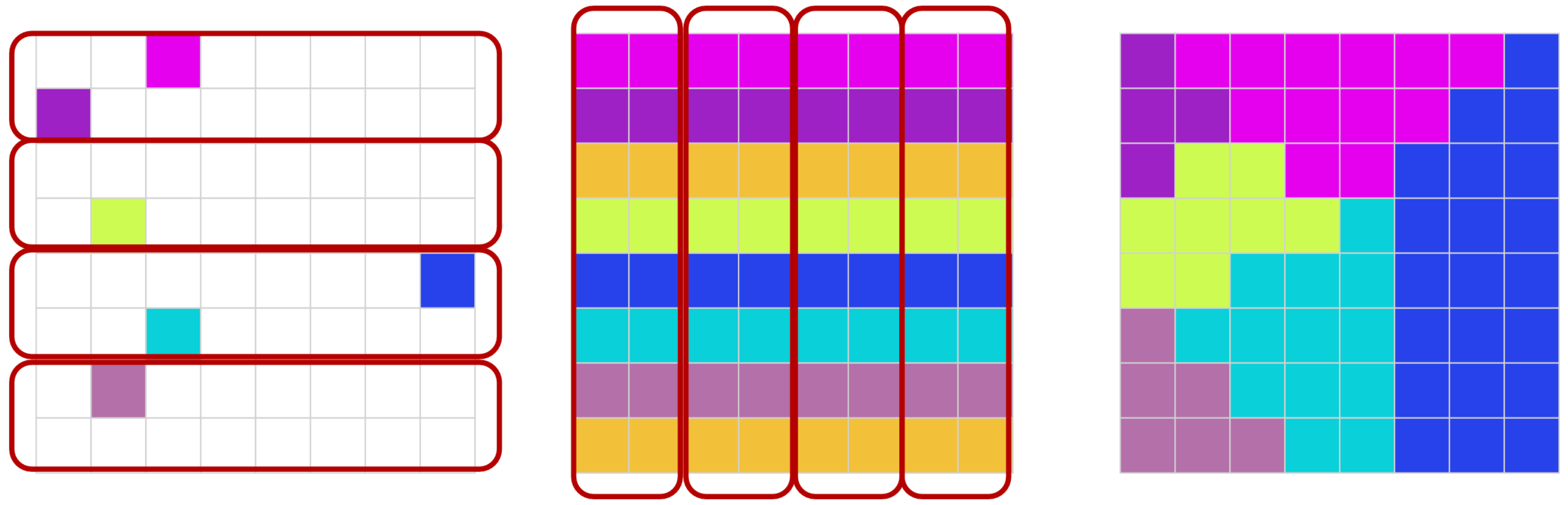

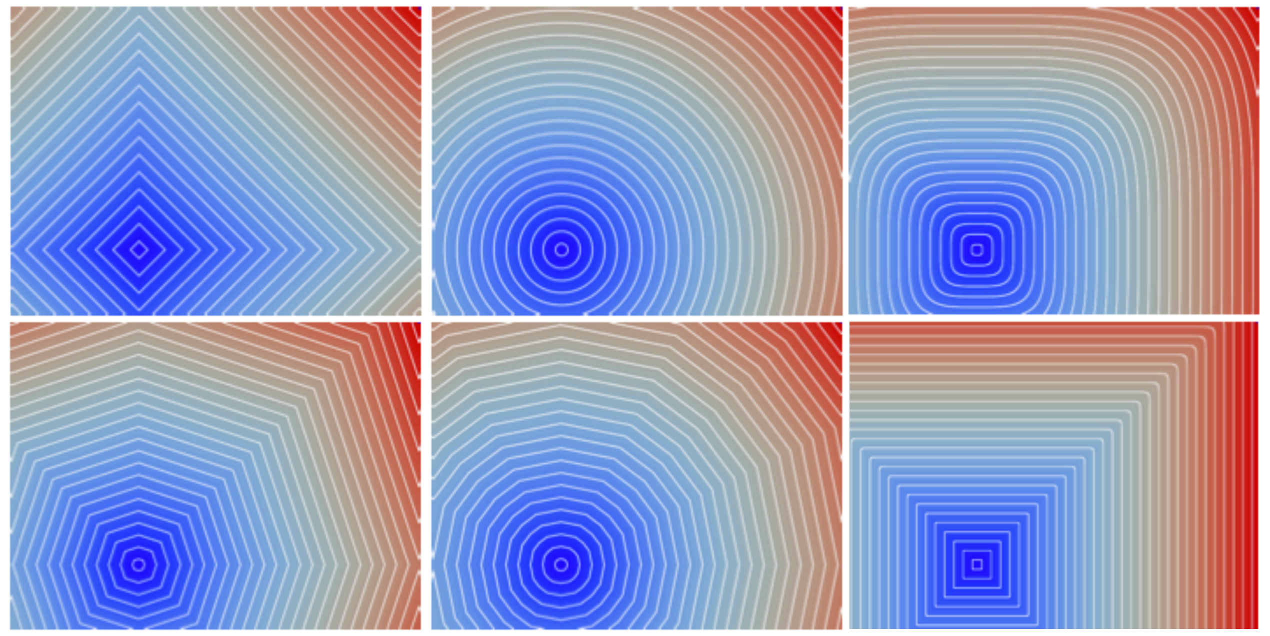

The separable algorithm is correct:

- for any dimension
- for any metric with axis symmetric unit ball (e.g. any l_p, chamfer norms)
- on any toroidal nD domains

Exact and linear in time w.r.t. the number of grid points $O(d \cdot n^d)$ for l_2

$O(d^2 \cdot \log(p) \cdot \log(n) \cdot n^d)$ for exact l_p ($p \in \mathbb{Z}^+$), $O(d \cdot n^d)$ approx.

Trivial multithread / GPU / out-of-core implementations

Same techniques and computational costs for: [C. et al 07]

- Power diagram / power maps construction
- Discrete Medial Axis extraction (aka non-empty inner power cells)
- Reverse reconstruction (balls→shape)

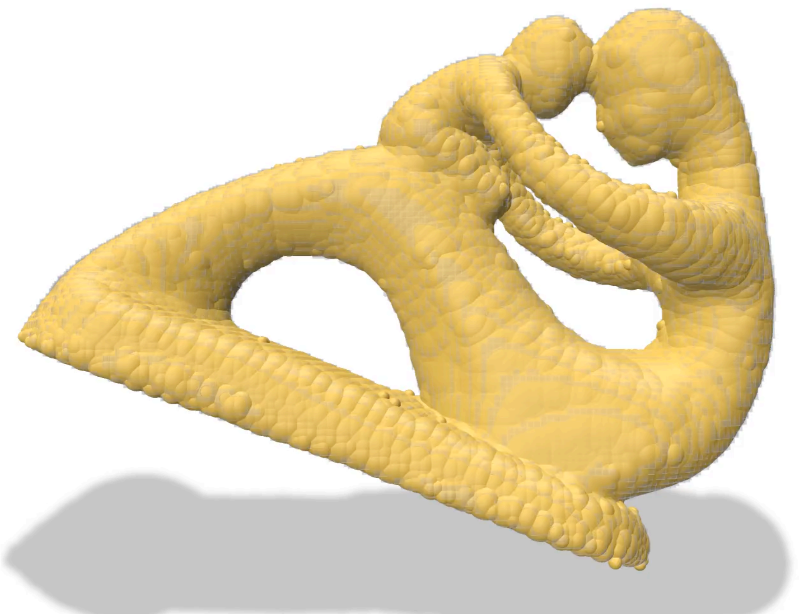

topology on $\mathbb{Z}^d$

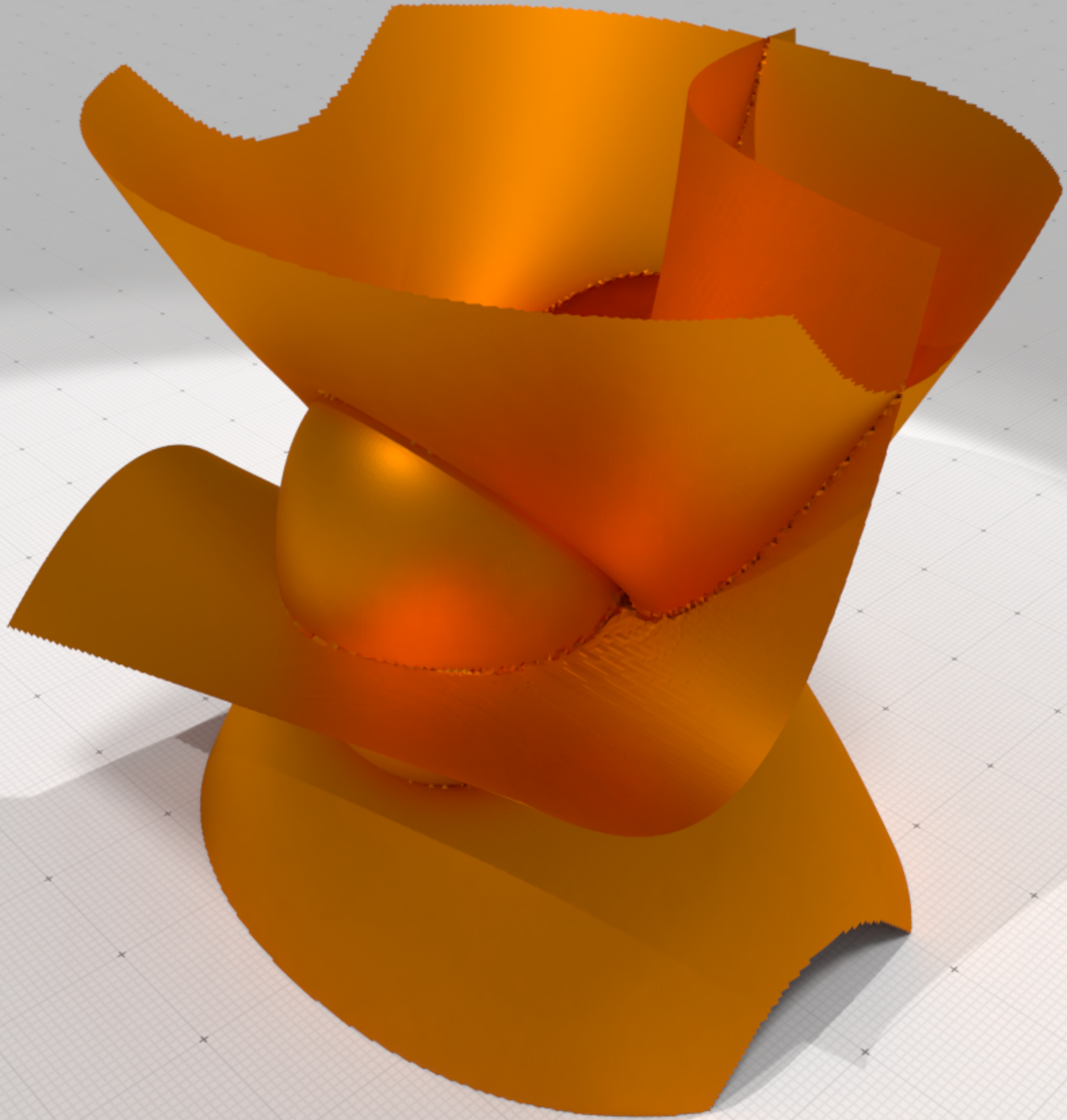

Before geometry : topological models for $\mathbb{Z}^d$

How to represent volumes, boundaries, curves, surfaces, partitions ?

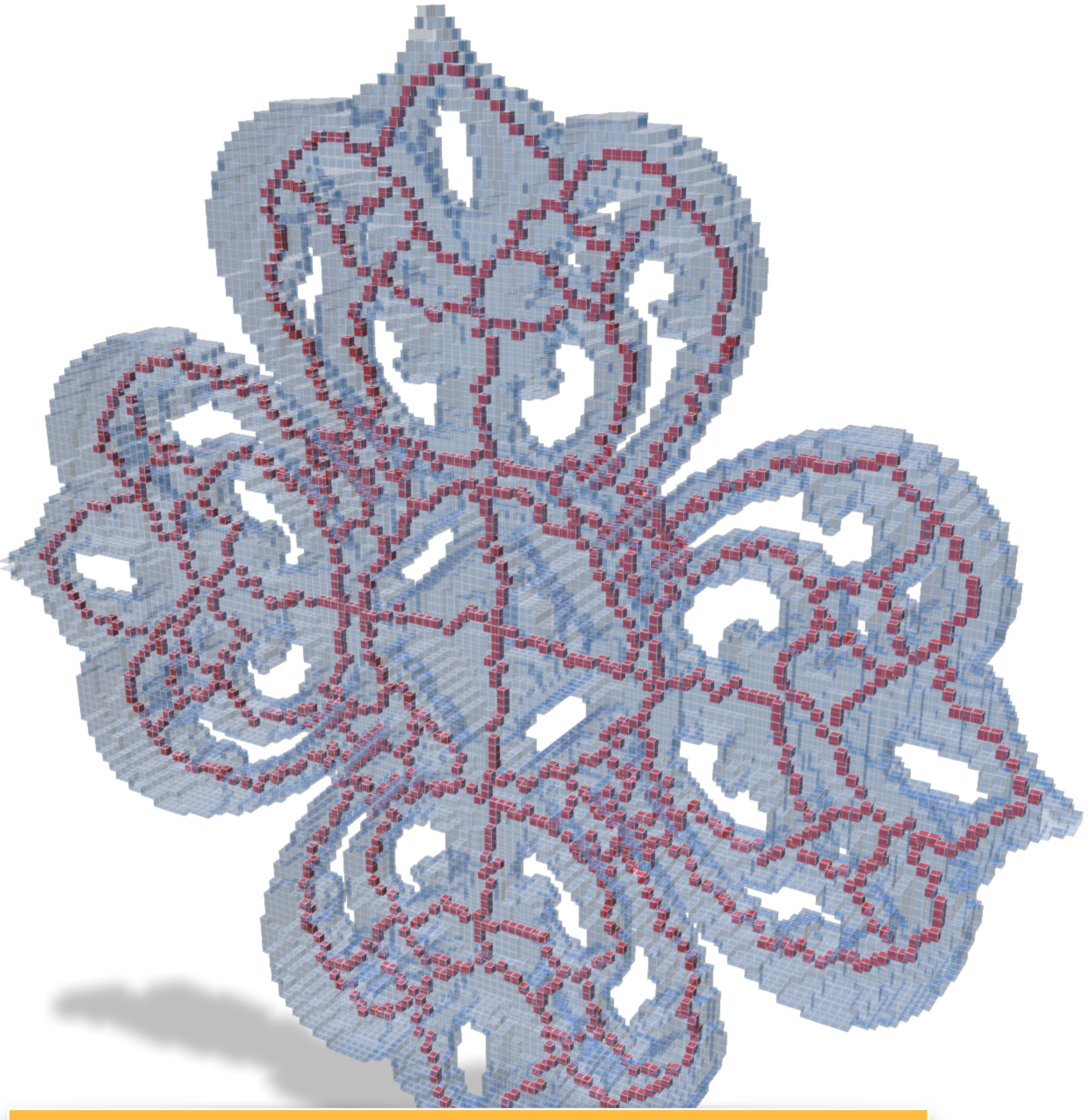

1. lattice points

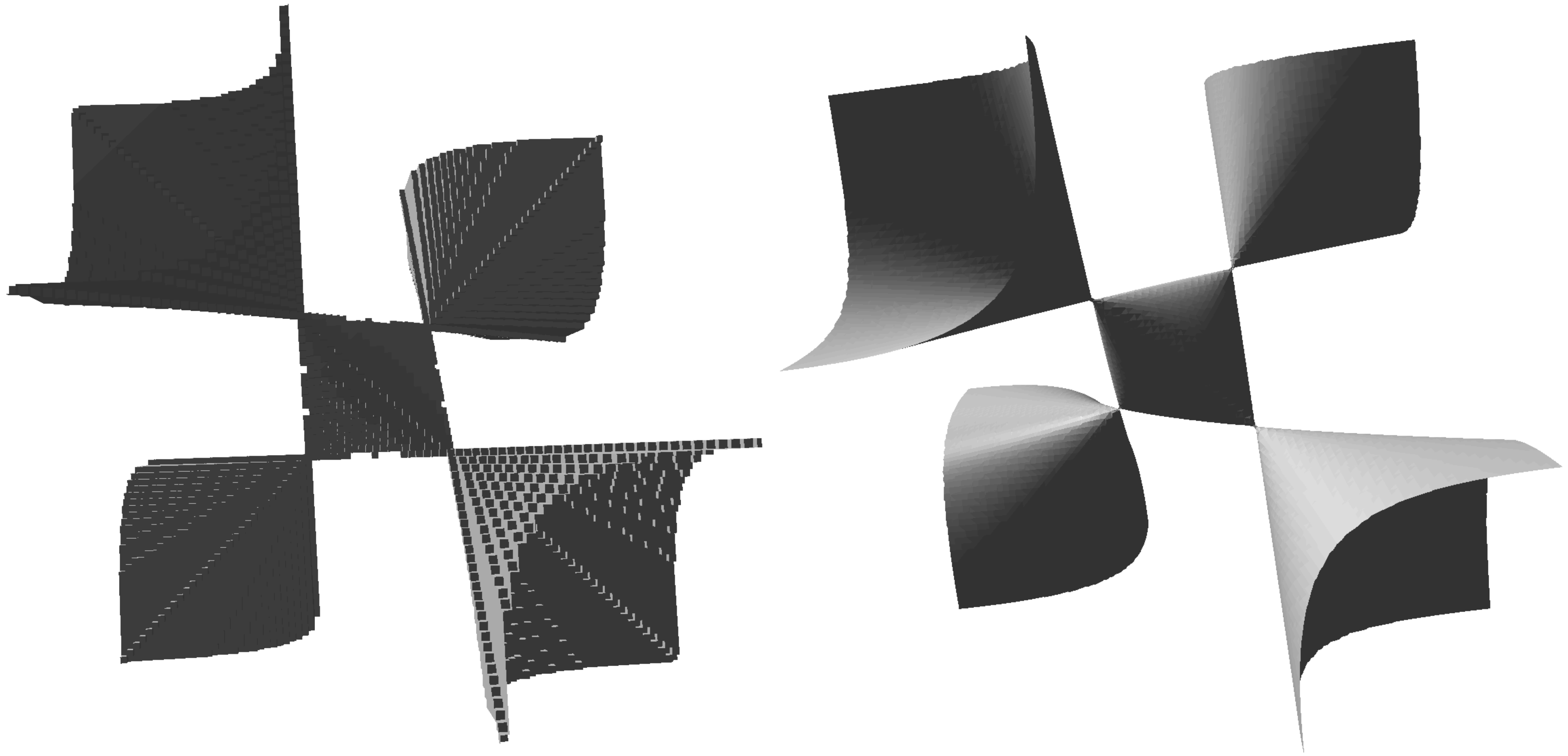

2. cubical complexes

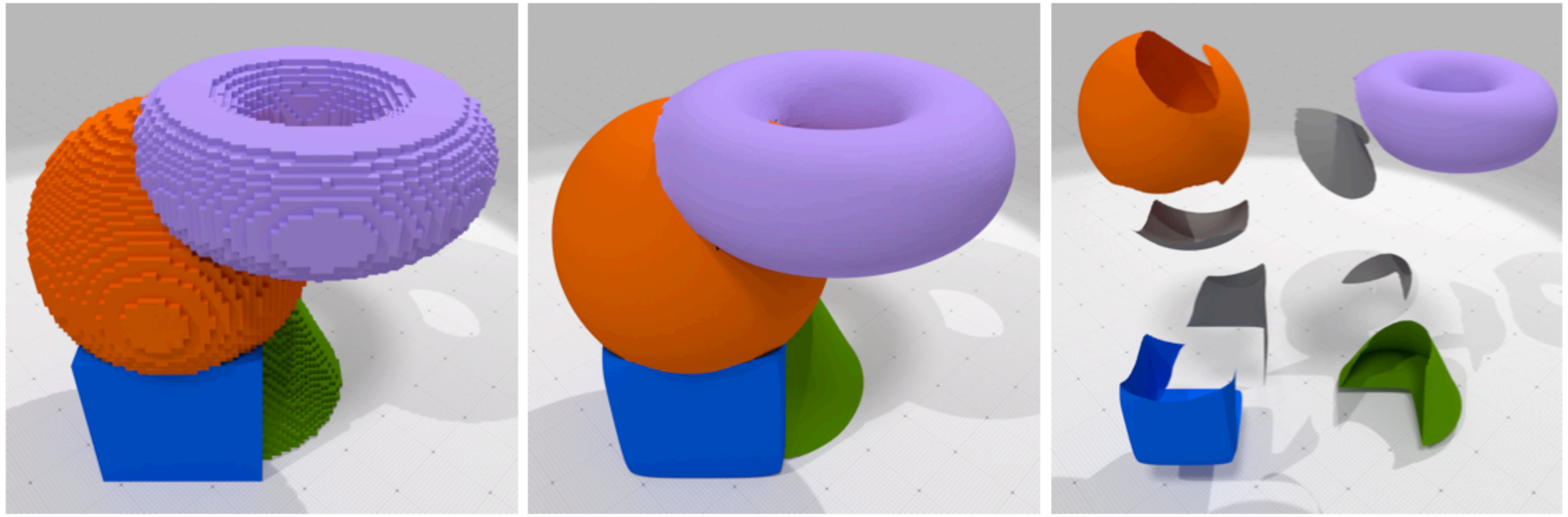

Digital topology

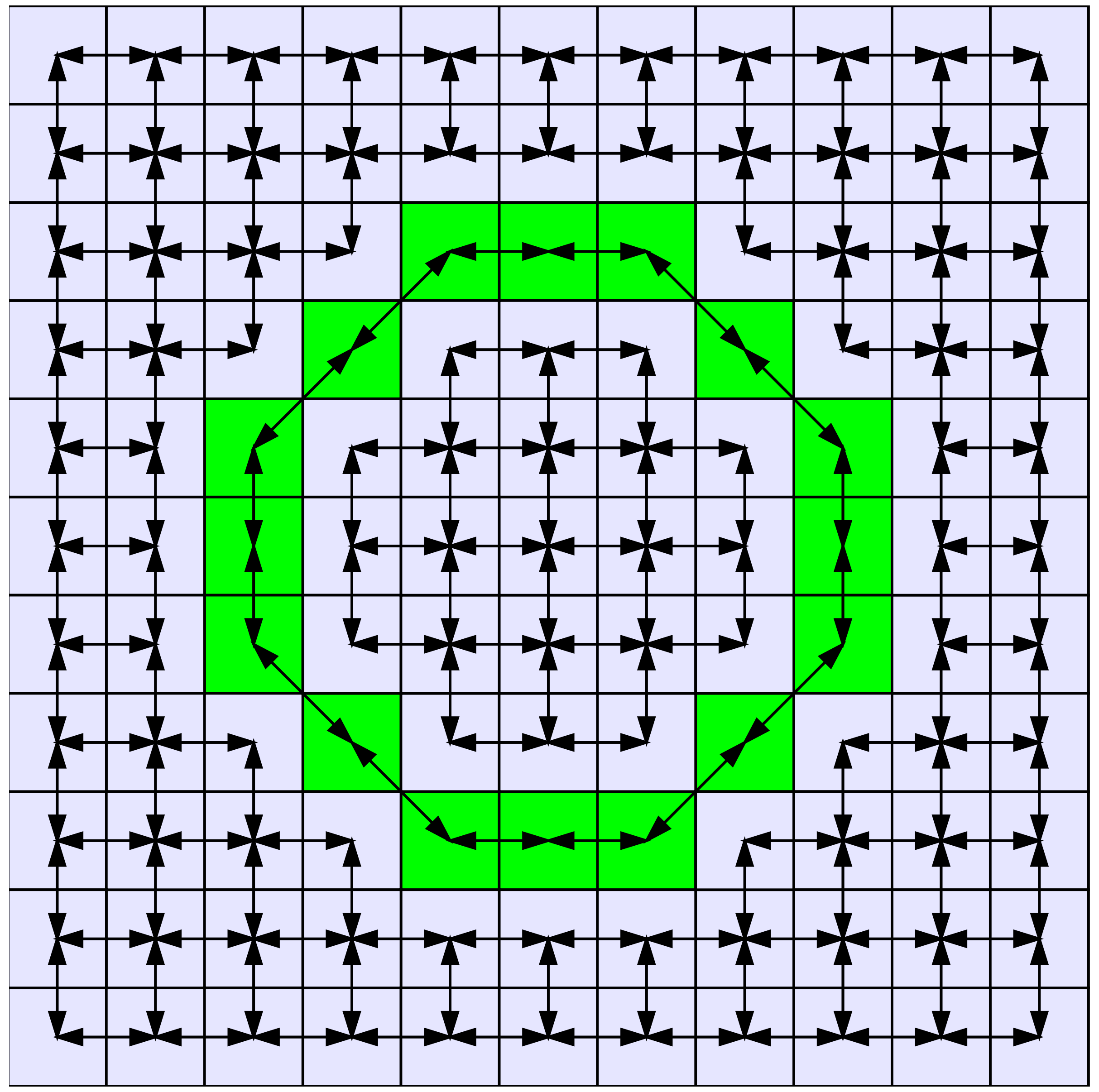

(8,4)-topology

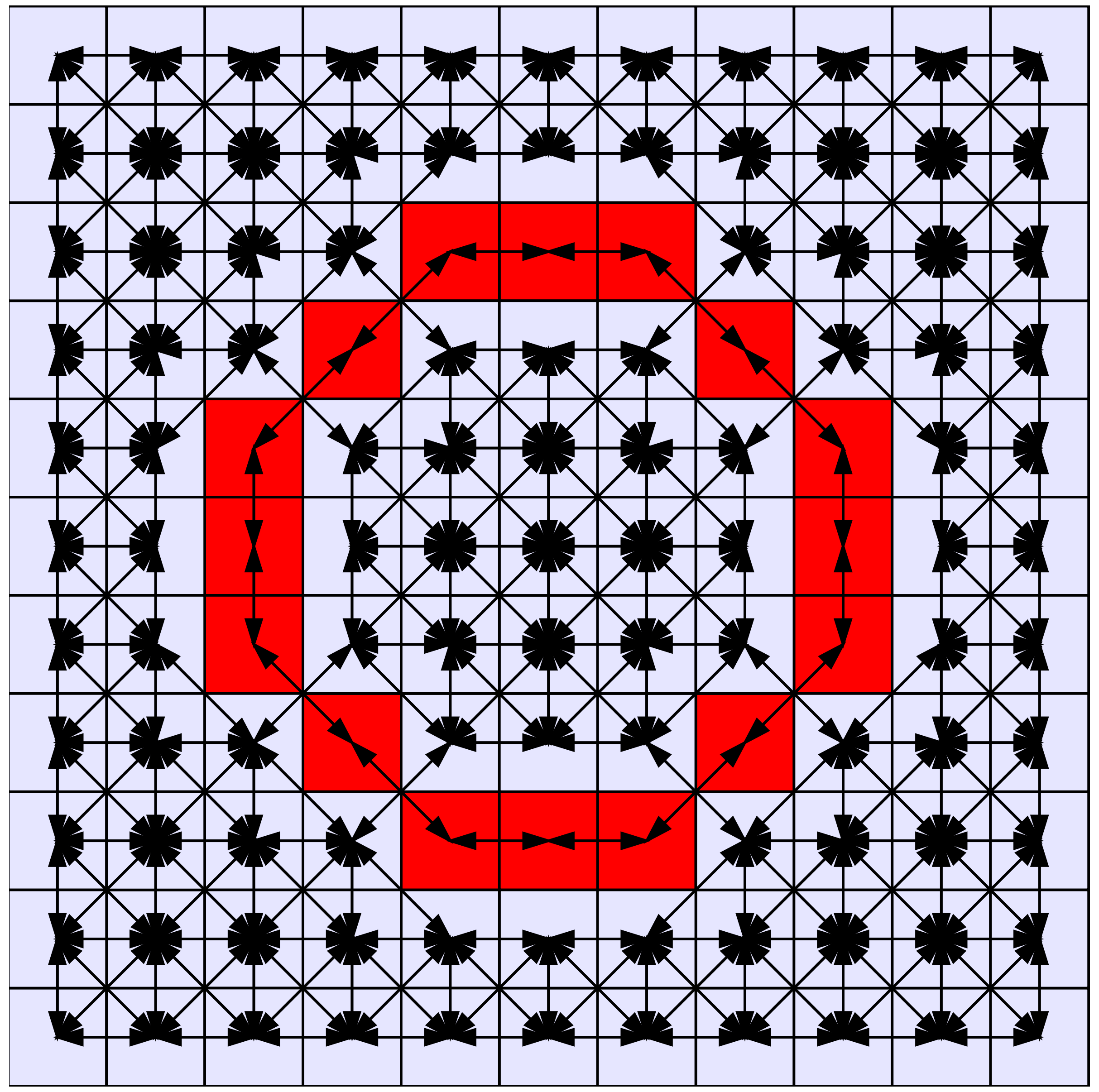

(8,8)-topology

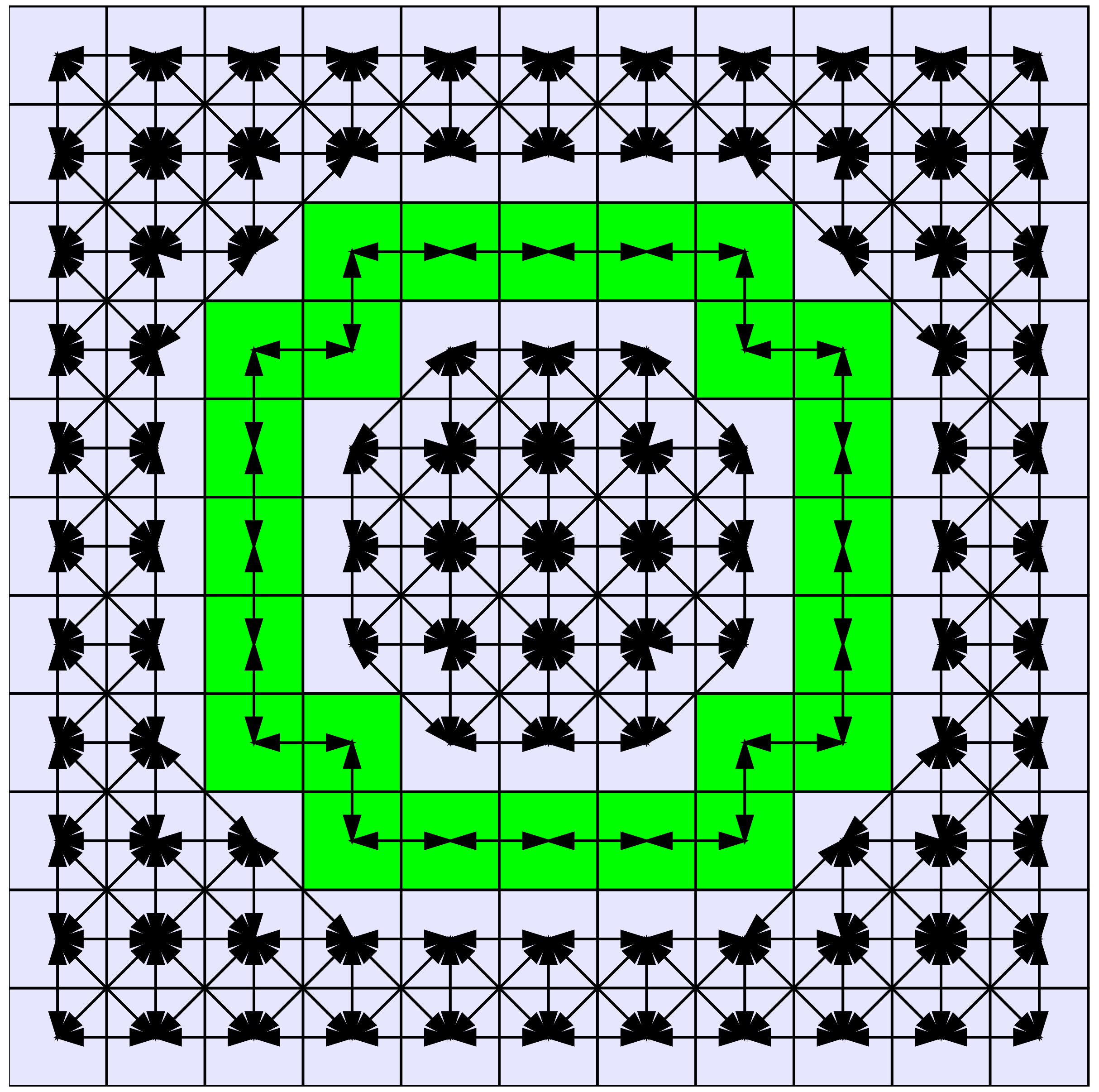

(4,8)-topology

Good adjacencies for object/background

- Jordan separation theorem
- consistence borders and interior components
- definition of surfaces in $\mathbb{Z}^d$

Topology invariance: simple points

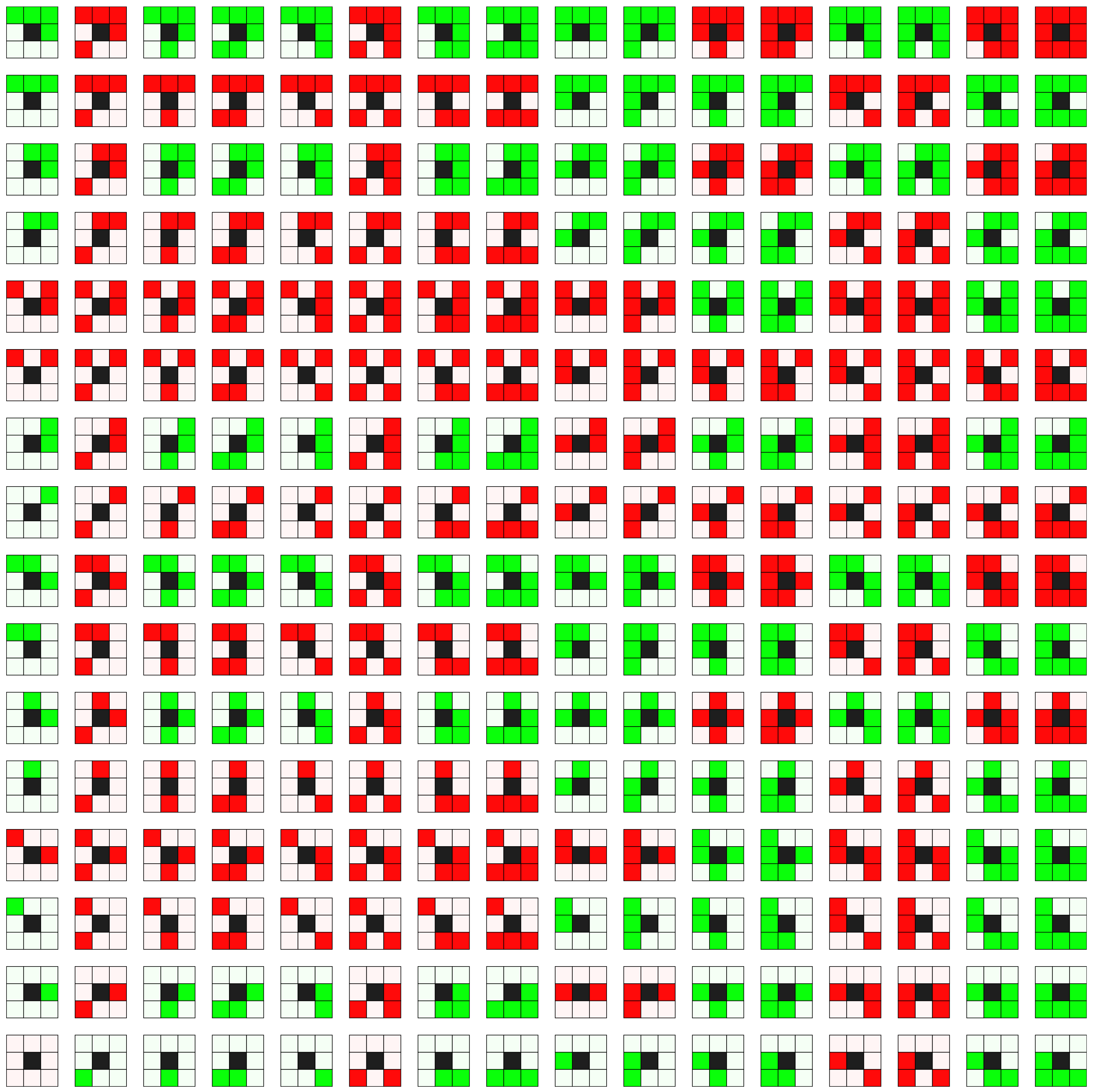

(8,4)-topology

locally keep connected components

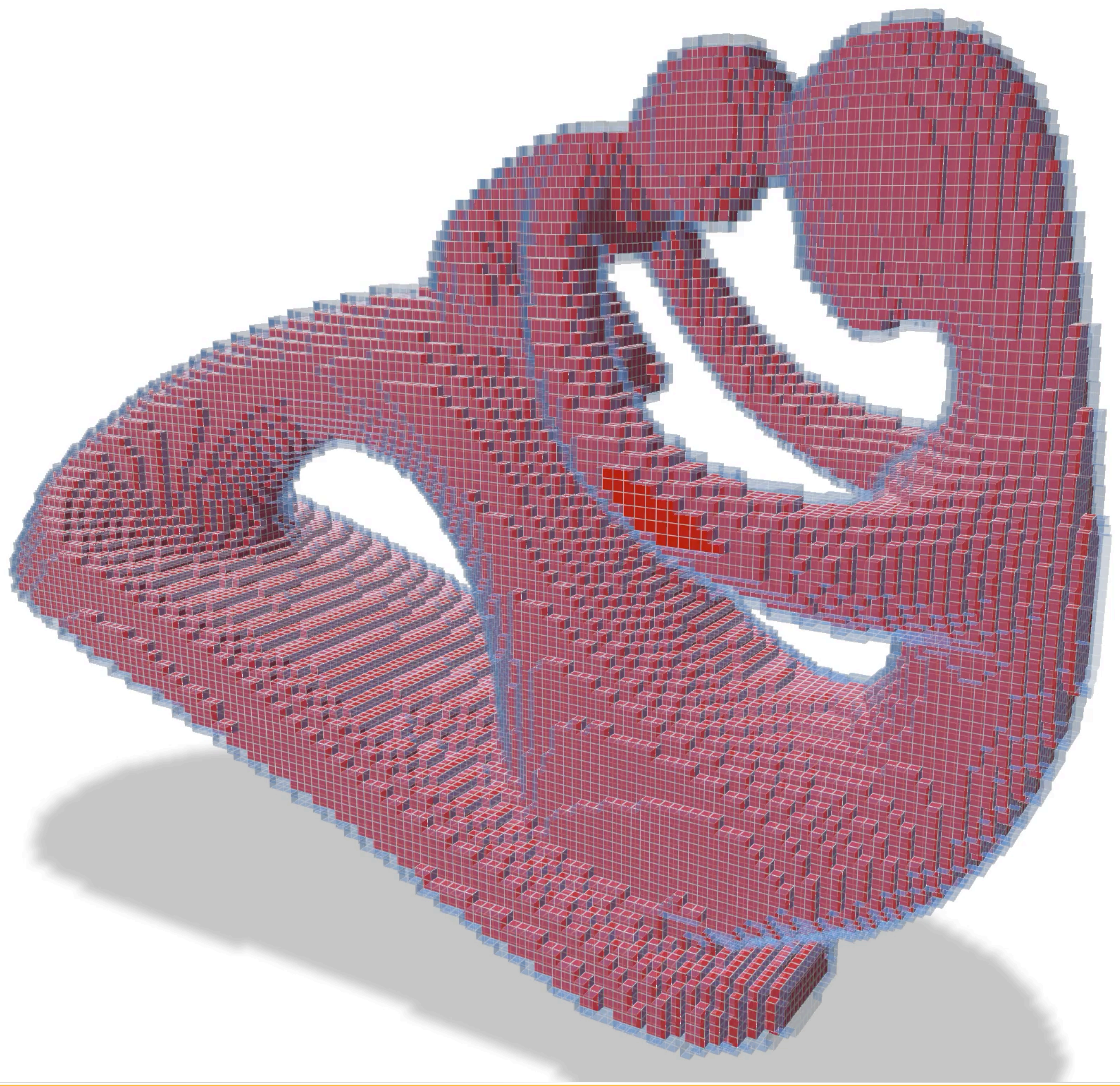

Simple points: points whose removal preserves topology

- digital topology invariance of object and background
- very fast: look-up tables in 2D and 3D
- useful for skeleton extraction / coupled with medial axis

Topology invariance: simple points

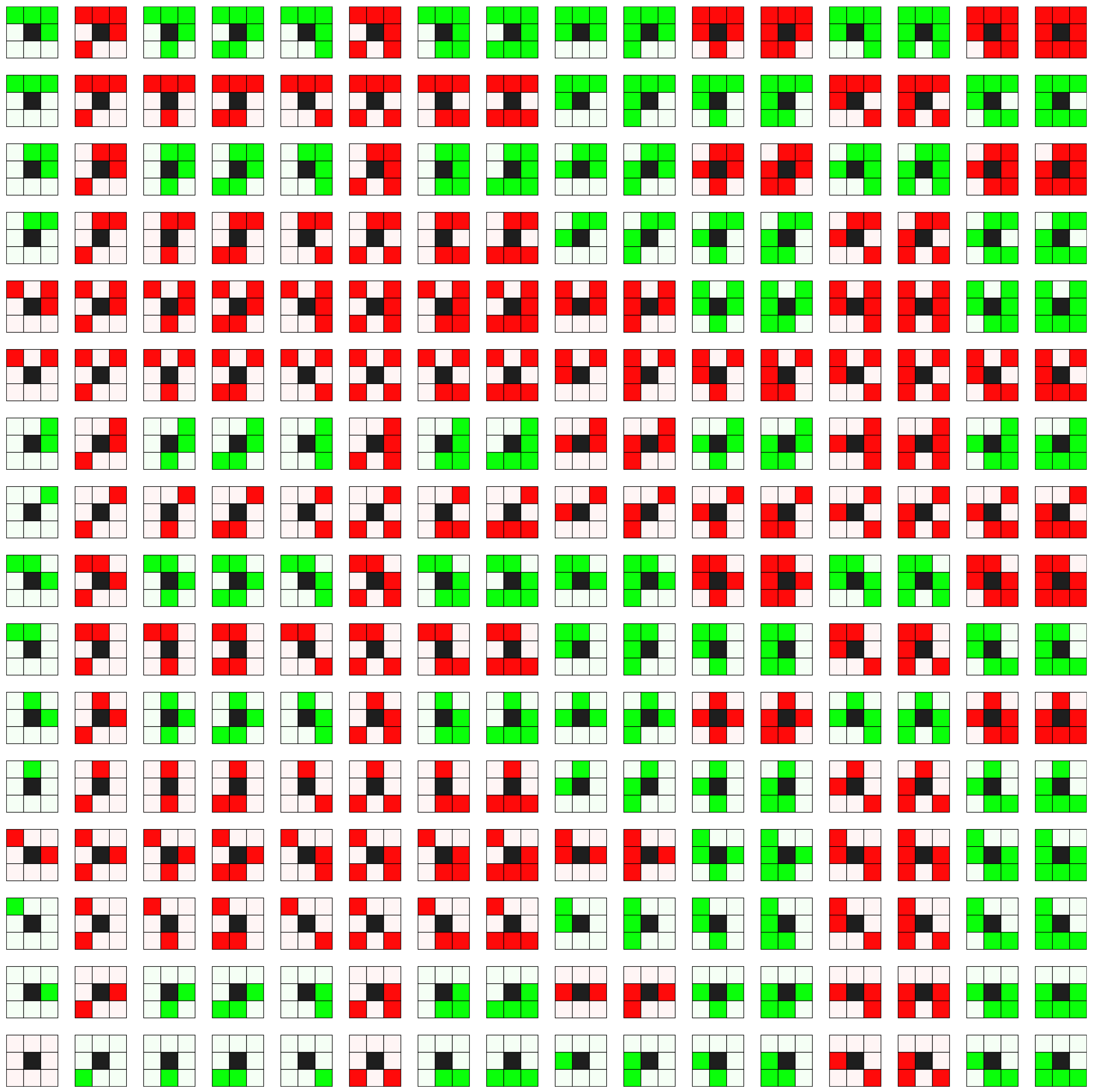

(8,4)-topology

locally keep connected components

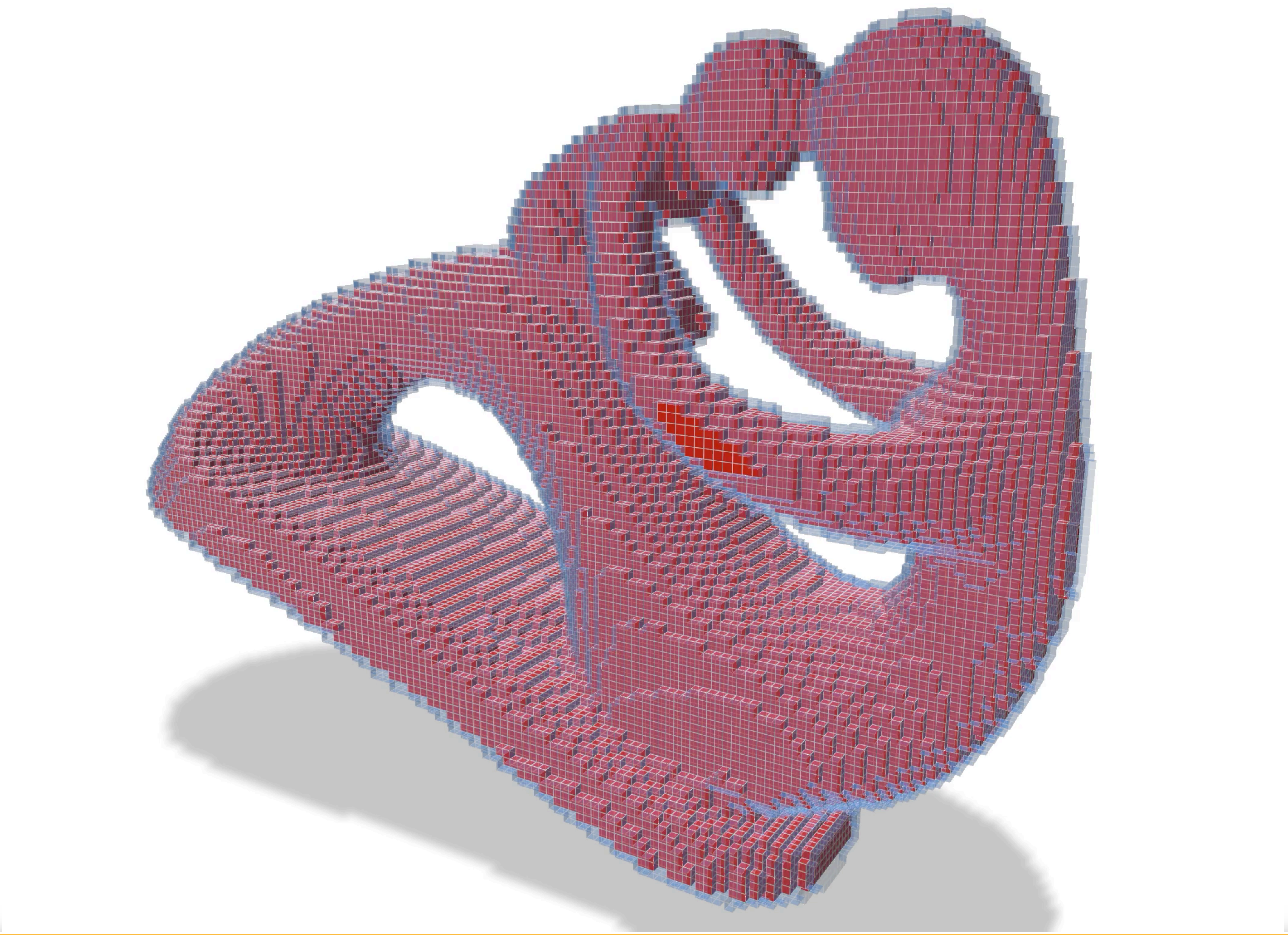

Simple points: points whose removal preserves topology

- digital topology invariance of object and background
- very fast: look-up tables in 2D and 3D
- useful for skeleton extraction / coupled with medial axis

hands on…

```
// Build object with digital topology
const auto K = SH3::getKSpace( binary_image );
Domain domain( K.lowerBound(), K.upperBound() );
Z3i::DigitalSet voxel_set( domain );
for ( auto p : domain )
  if ( (*binary_image)( p ) ) voxel_set.insertNew( p );
the_object = CountedPtr< Z3i::Object26_6 >( new Z3i::Object26_6( dt26_6, voxel_set ) );
the_object->setTable(functions::loadTable<3>(simplicity::tableSimple26_6));
```

Create object with (26,6) topology from binary image

```
// Removes a peel of simple points onto voxel object.
bool oneStep( CountedPtr< Z3i::Object26_6 > object )
{
  DigitalSet & S = object->pointSet();
  std::queue< Point > Q;
  for ( auto&& p : S )
    if ( object->isSimple( p ) )
      Q.push( p );
  int nb_simple = 0;
  while ( ! Q.empty() )
    {
      const auto p = Q.front();
      Q.pop();
      if ( object->isSimple( p ) )
        {
          S.erase( p );
          binary_image->setValue( p, false );
          ++nb_simple;
        }
    }
  trace.info() << "Removed " << nb_simple << " / " << S.size()
               << " points." << std::endl;
  registerDigitalSurface( binary_image, "Thinned object" );
  return nb_simple == 0;
}
```

Queue simple points

Remove simple points

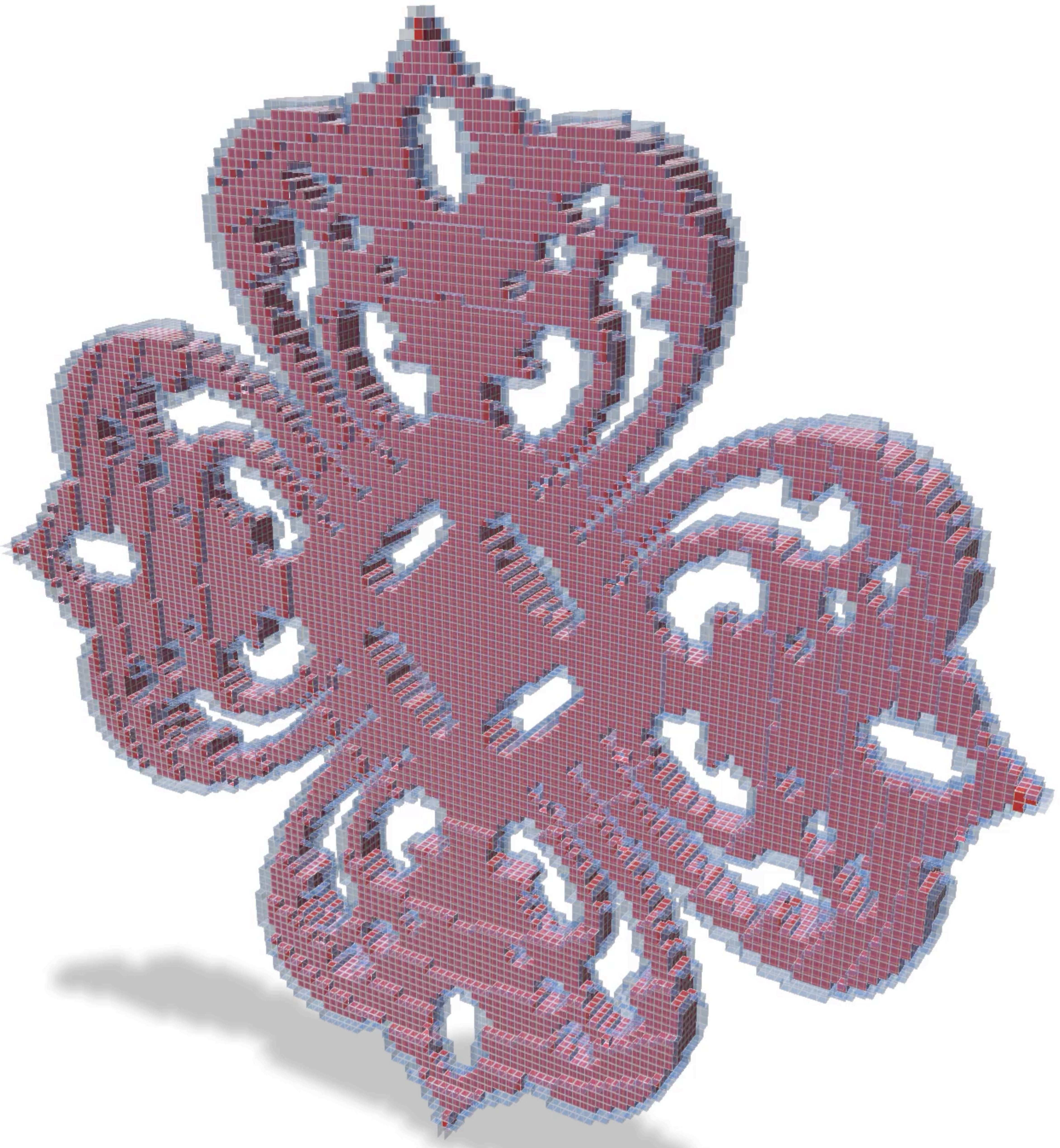

Create object with (26,6) topology from binary image

```
// Build object with digital topology
const auto K = SH3::getKSpace( binary_image );
Domain domain( K.lowerBound(), K.upperBound() );
Z3i::DigitalSet voxel_set( domain );
for ( auto p : domain )
  if ( (*binary_image)( p ) ) voxel_set.insertNew( p );
the_object = CountedPtr< Z3i::Object26_6 >( new Z3i::Object26_6( dt26_6, voxel_set ) );
the_object->setTable(functions::loadTable<3>(simplicity::tableSimple26_6));
```

Queue simple points

Remove simple points

```
// Removes a peel of simple points onto voxel object.
bool oneStep( CountedPtr< Z3i::Object26_6 > object )
{
  DigitalSet & S = object->pointSet();
  std::queue< Point > Q;
  for ( auto&& p : S )
    if ( object->isSimple( p ) )
      Q.push( p );
  int nb_simple = 0;
  while ( ! Q.empty() )
    {
      const auto p = Q.front();
      Q.pop();
      if ( object->isSimple( p ) )
        {
          S.erase( p );
          binary_image->setValue( p, false );
          ++nb_simple;
        }
    }
  trace.info() << "Removed " << nb_simple << " / " << S.size()
               << " points." << std::endl;
  registerDigitalSurface( binary_image, "Thinned object" );
  return nb_simple == 0;
}
```

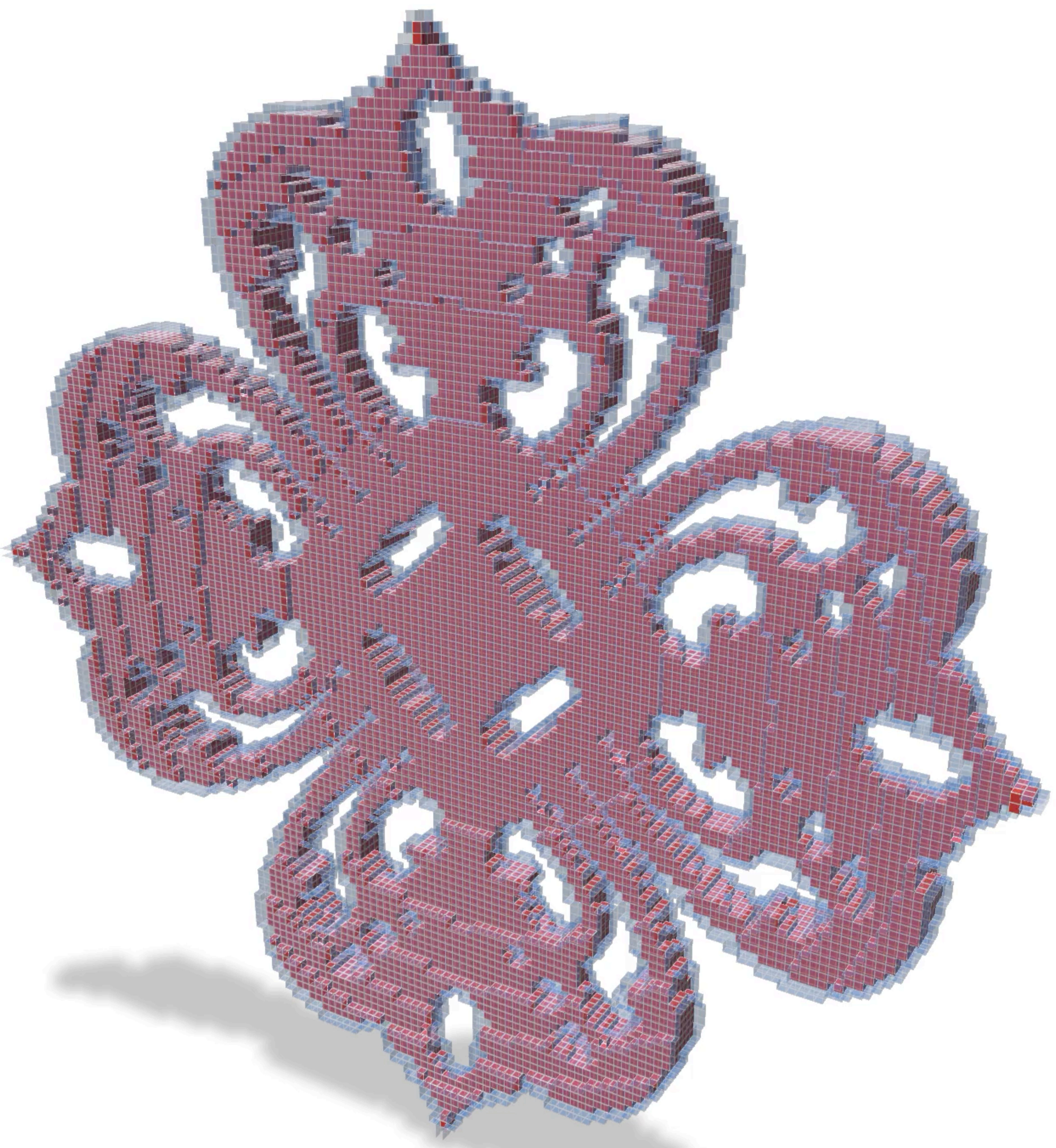

Homotopic collapses

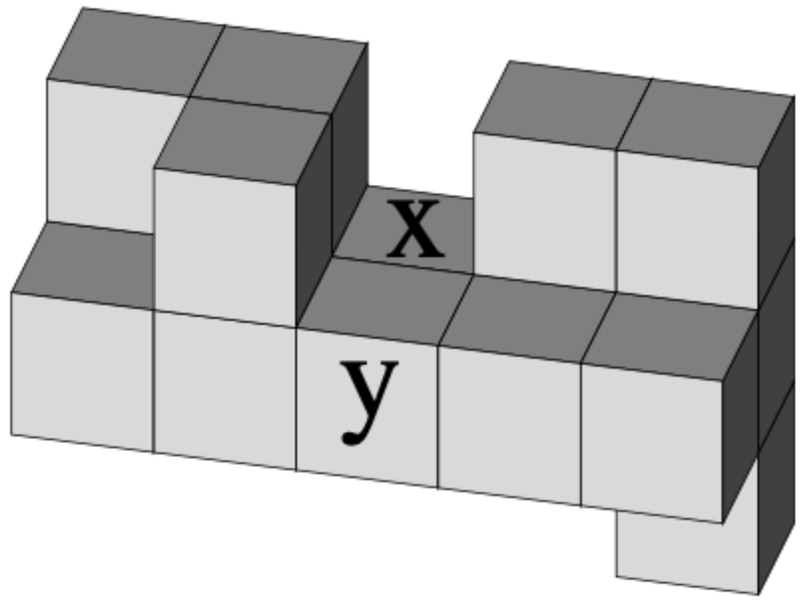

x and y are simple
but cannot be removed in parallel

Needs cubical complex representation

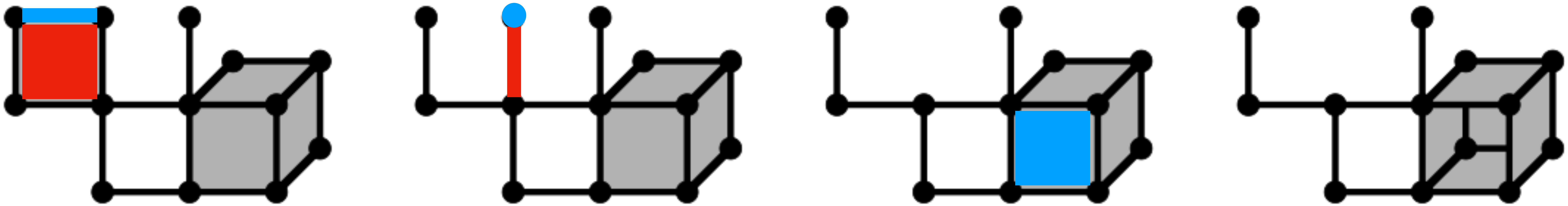

Elementary **collapse** : removing cell pairs (f,g) where g is free
preserves homotopy

Homotopic collapses and critical kernels

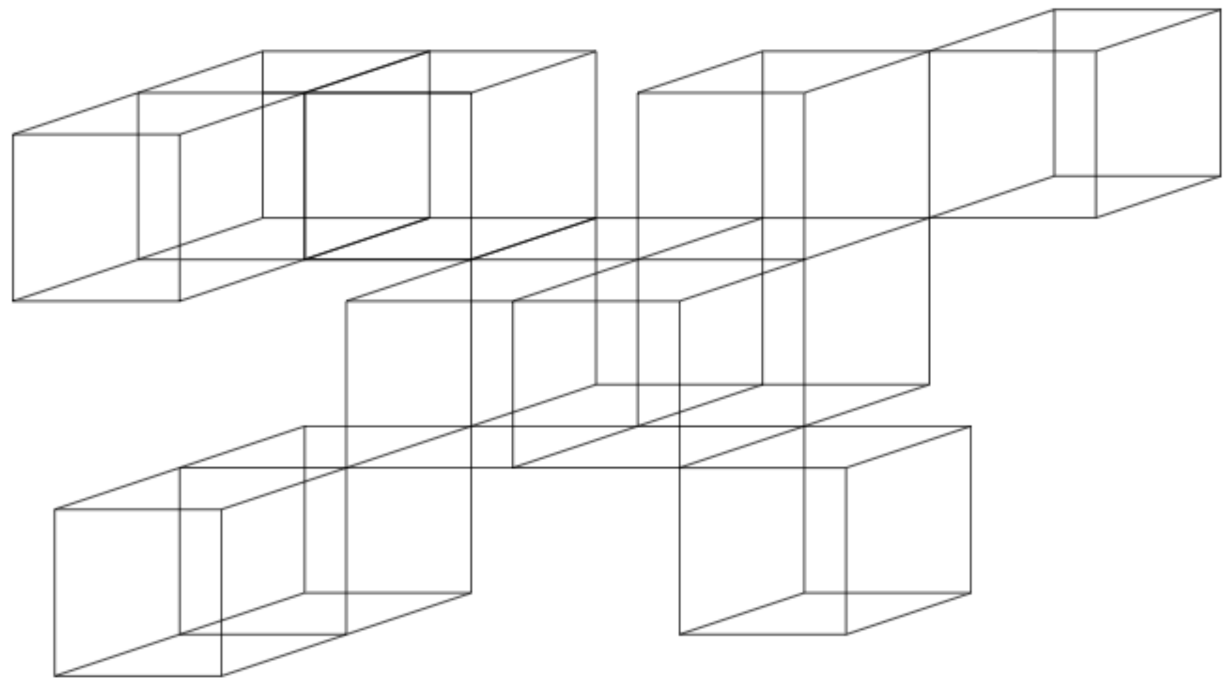

cubical complex X

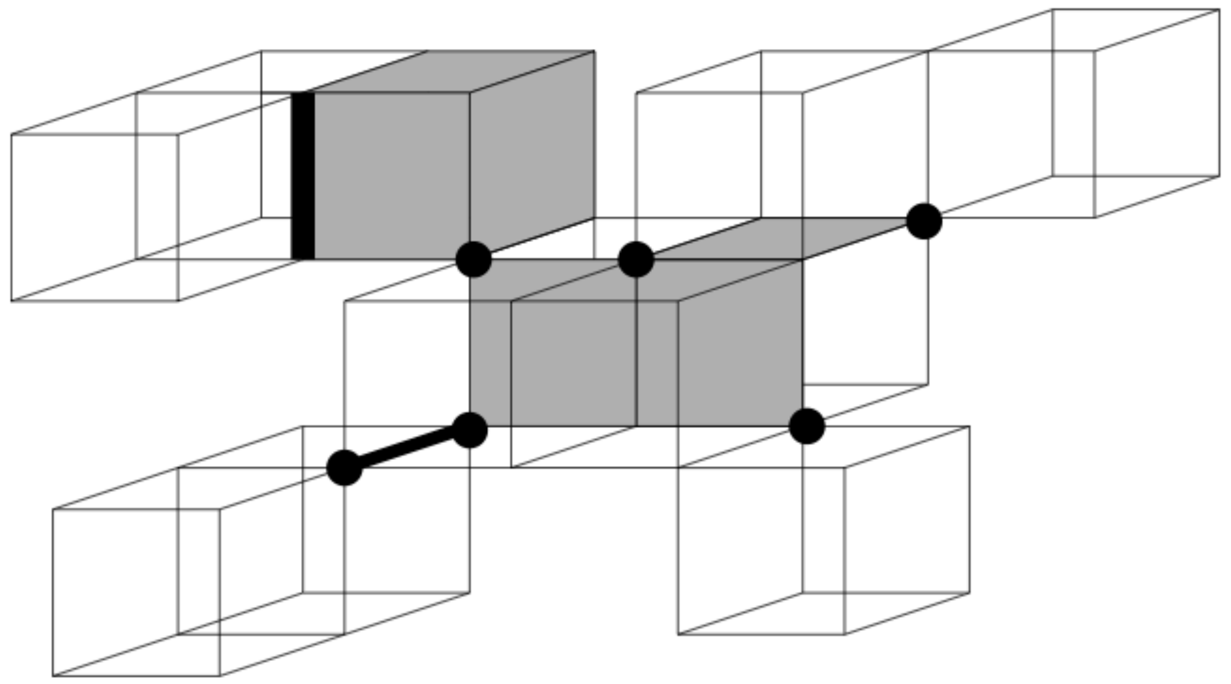

Z := critical kernel of X

critical cells : cells that do not collapse onto their neighborhood

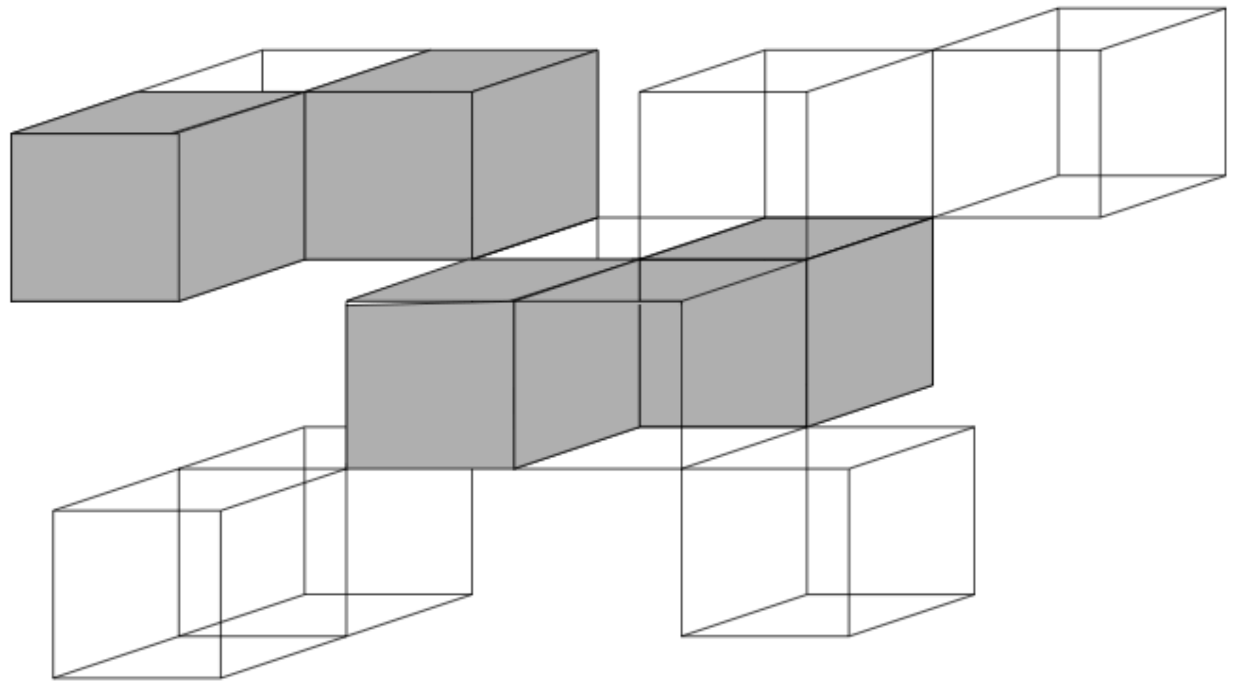

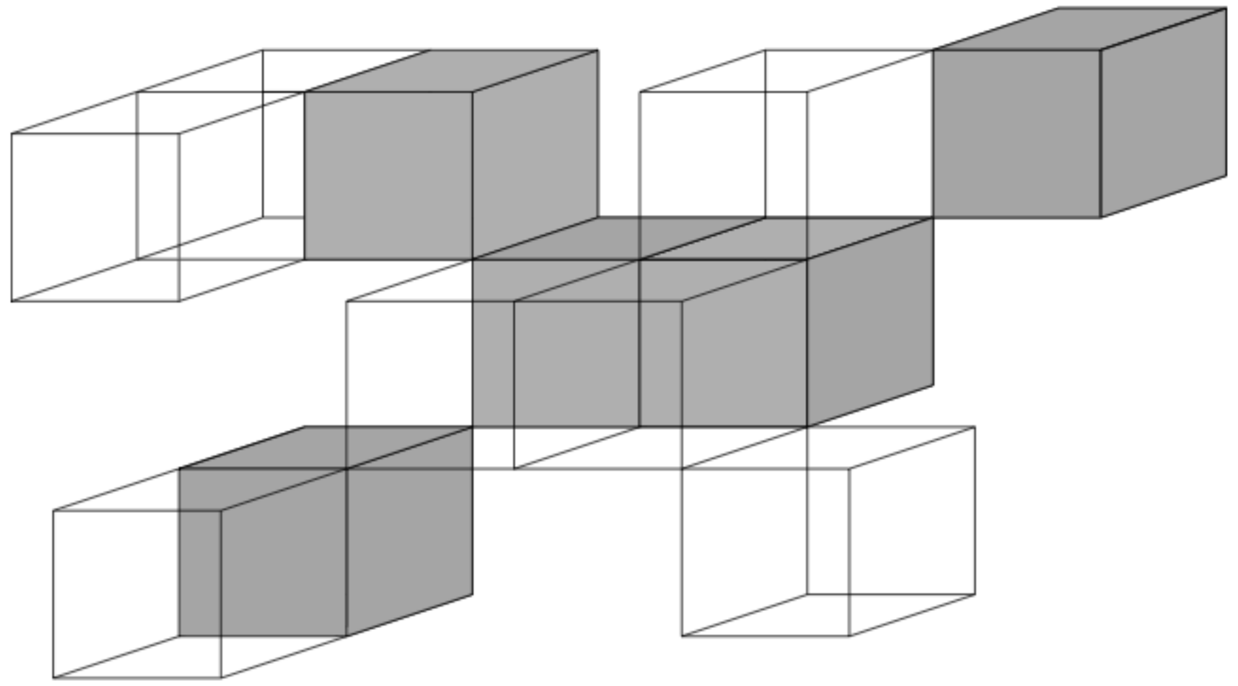

Both complexes Y_1, Y_2 are thinning, since $Z \subseteq Y_i \subseteq X$

All complexes Y, such that $Z \subseteq Y \subseteq X$ are homotopic to X !

Allows parallel algorithms for extracting skeletons

Skeletons with critical kernels

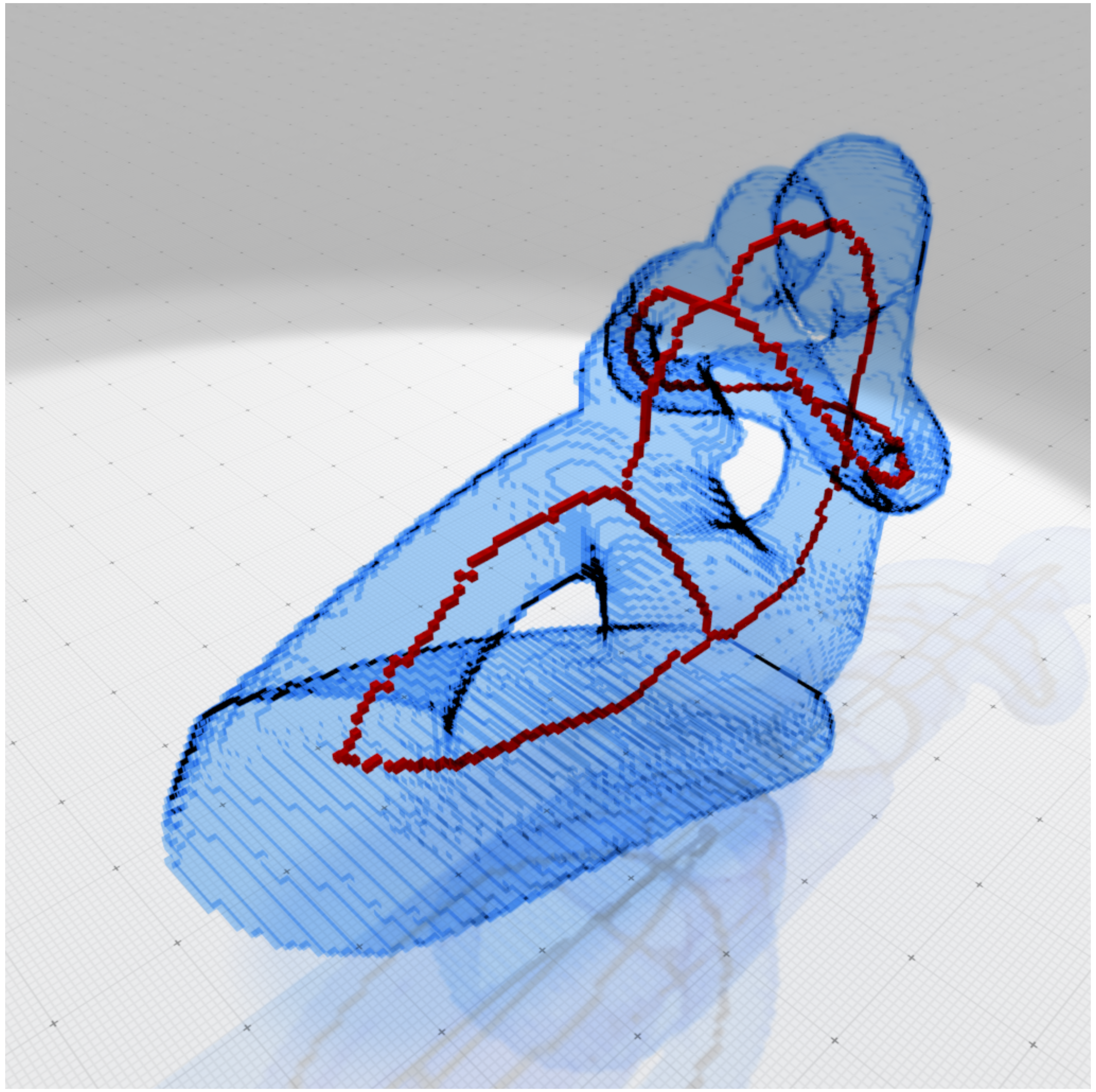

« curved » skeleton

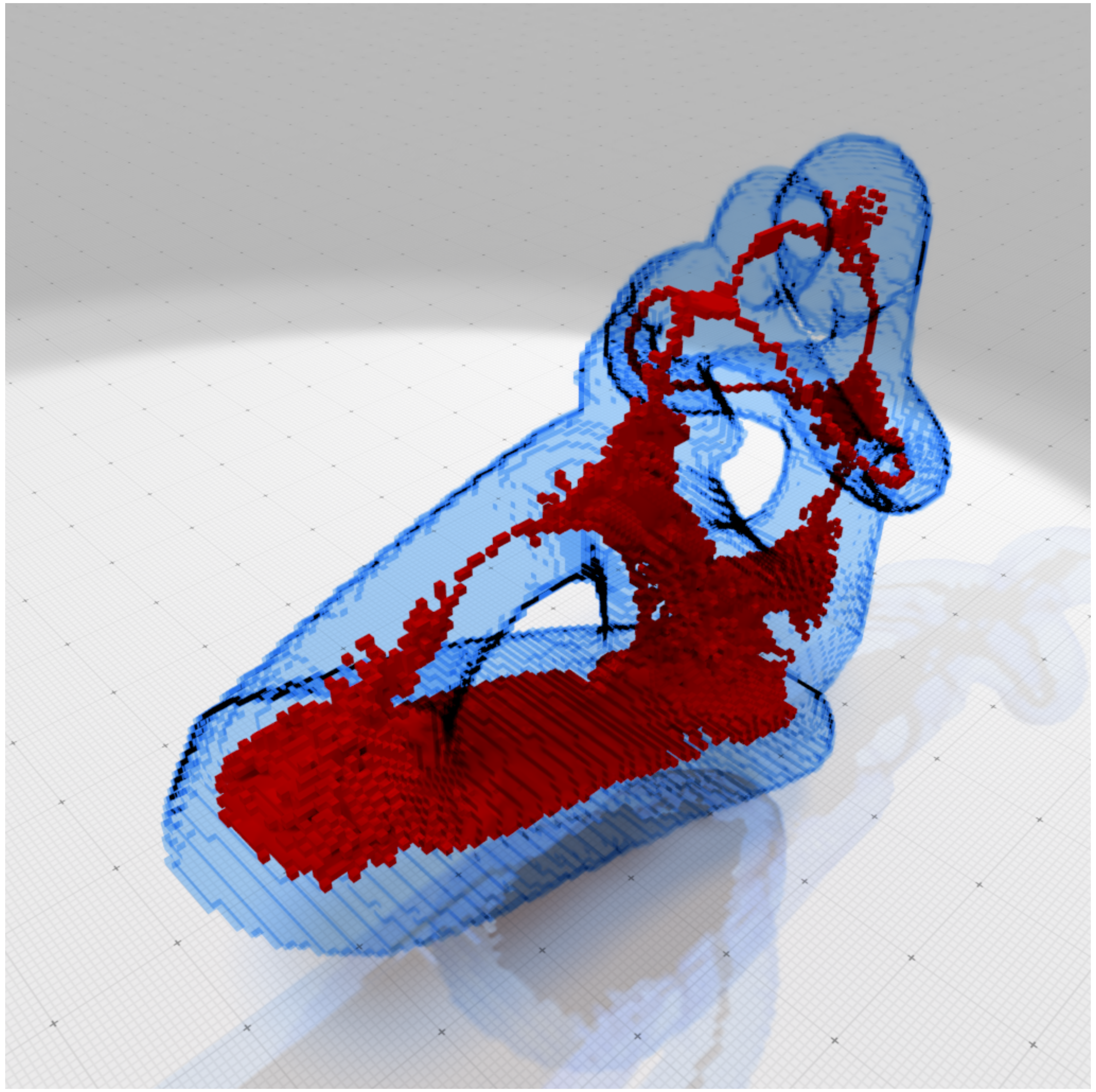

« surface » skeleton

Digital surfaces

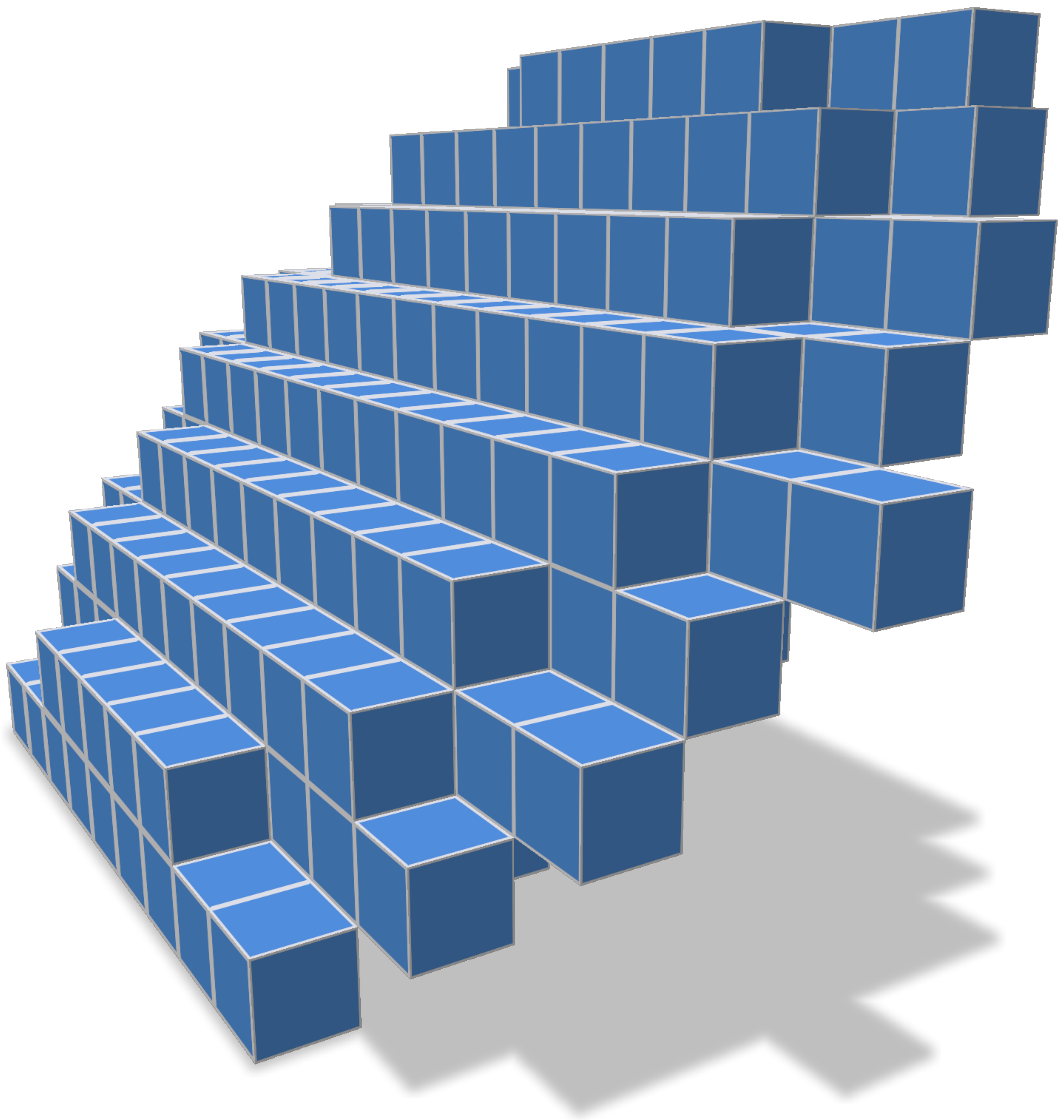

Primal surface
(here, digitization of some ellipsoid)

- digital surface ≈ set of faces of voxels
- in « ideal cases » 4-regular graph (3D)
    - vertices = surfels/faces
- generally not a manifold
    - pinched on edges and/or vertices
- not a sampling, only approximation
- only 6 different normals in 3D
    - even fine digital surface have poor normals

Digital surfaces + topology (primal ↔ dual)

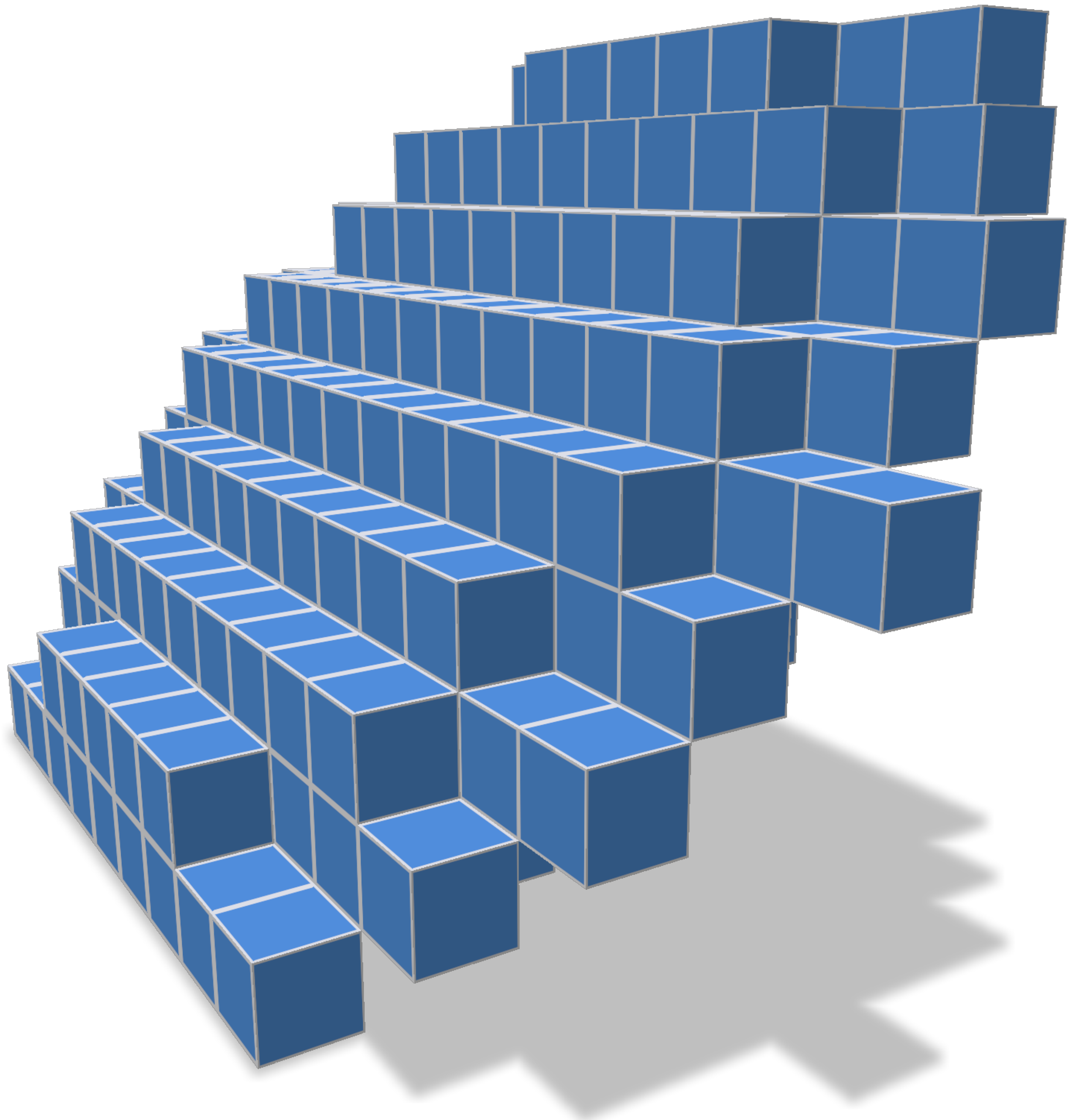

Primal surface

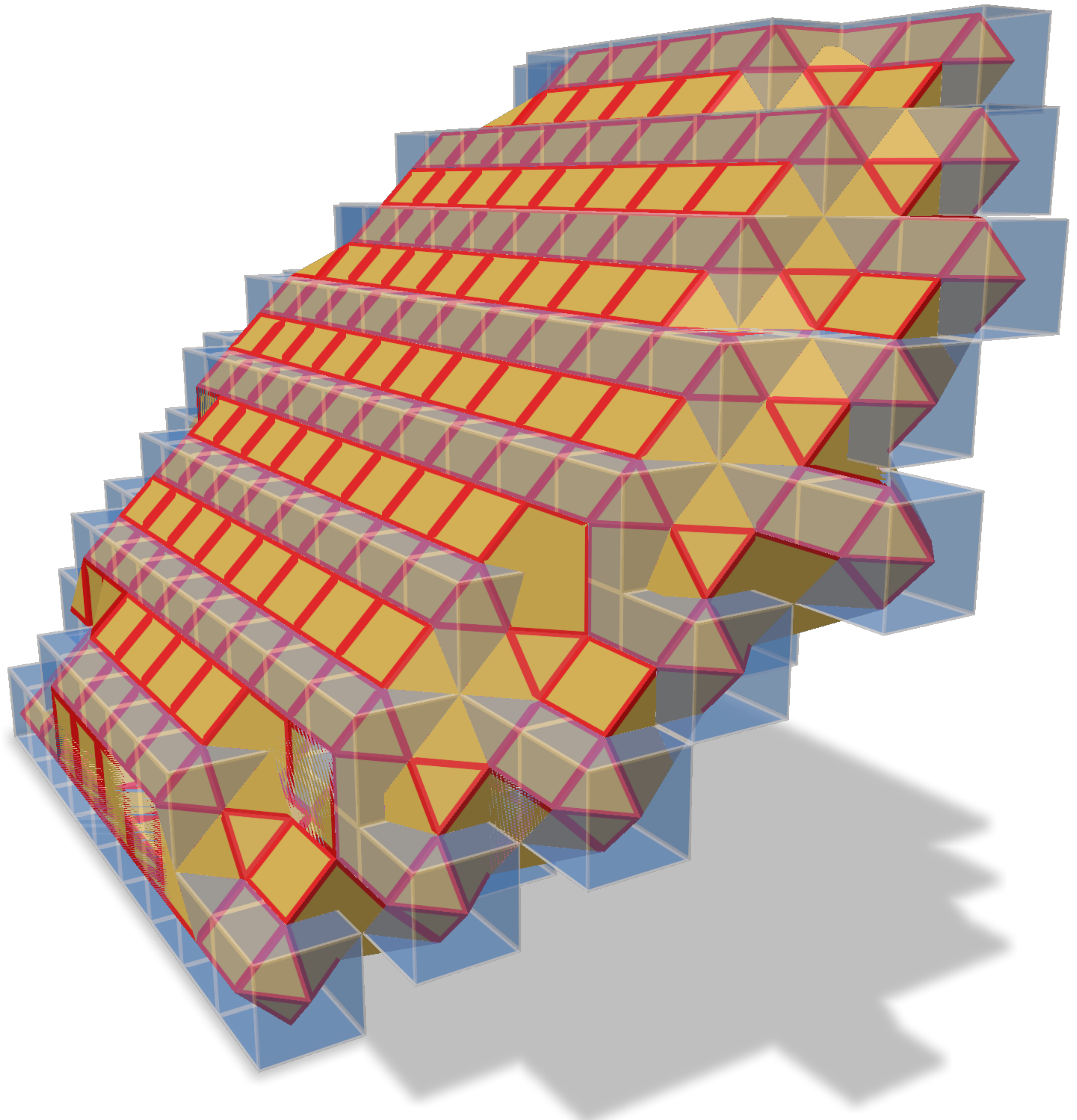

Dual surface
(26,6) topology

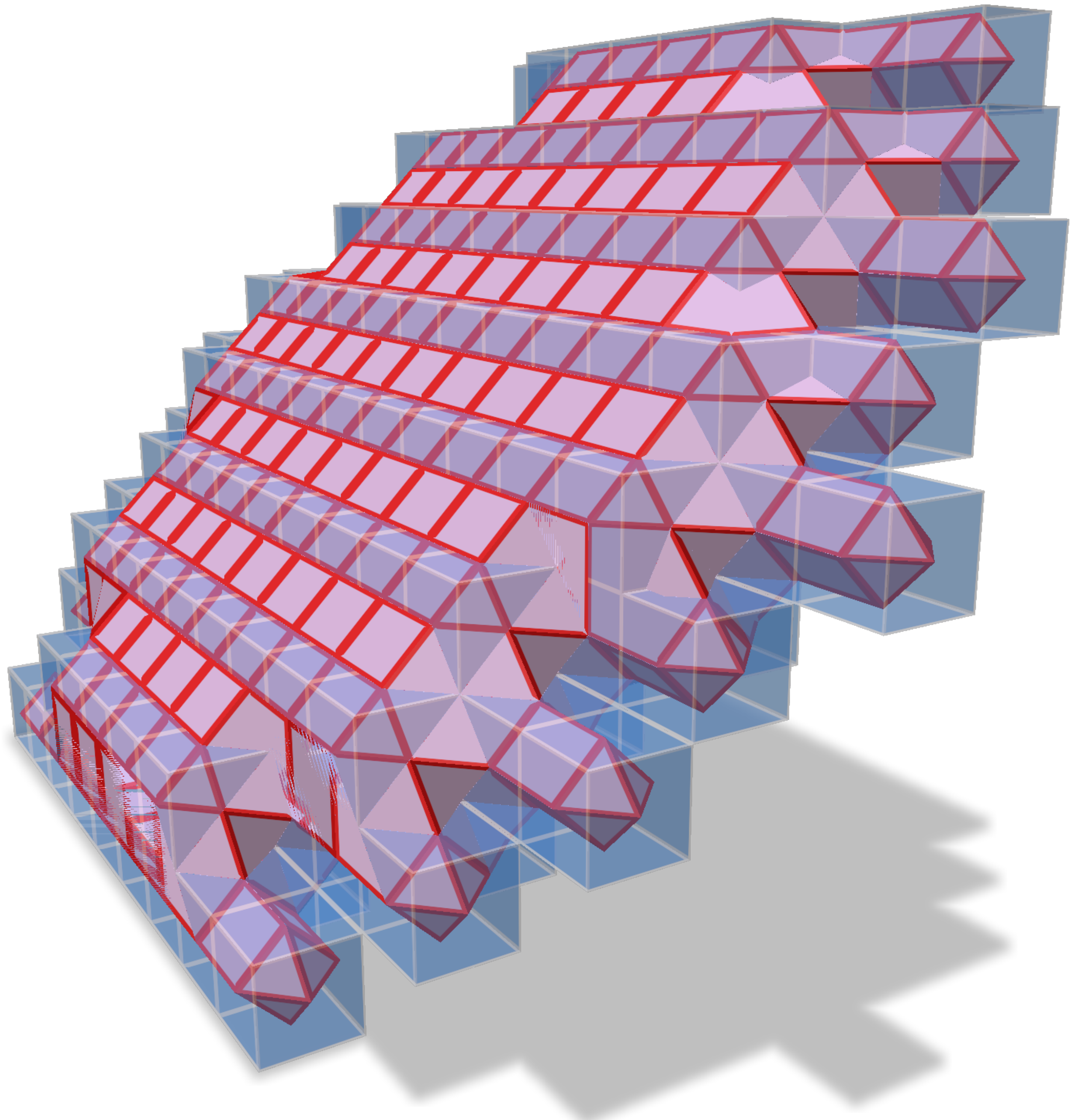

Dual surface
(6,26) topology

Adding object/background topology allows manifoldness in arbitrary dimensions - exactly d-1 paths crossing at each point

digital surface geometry

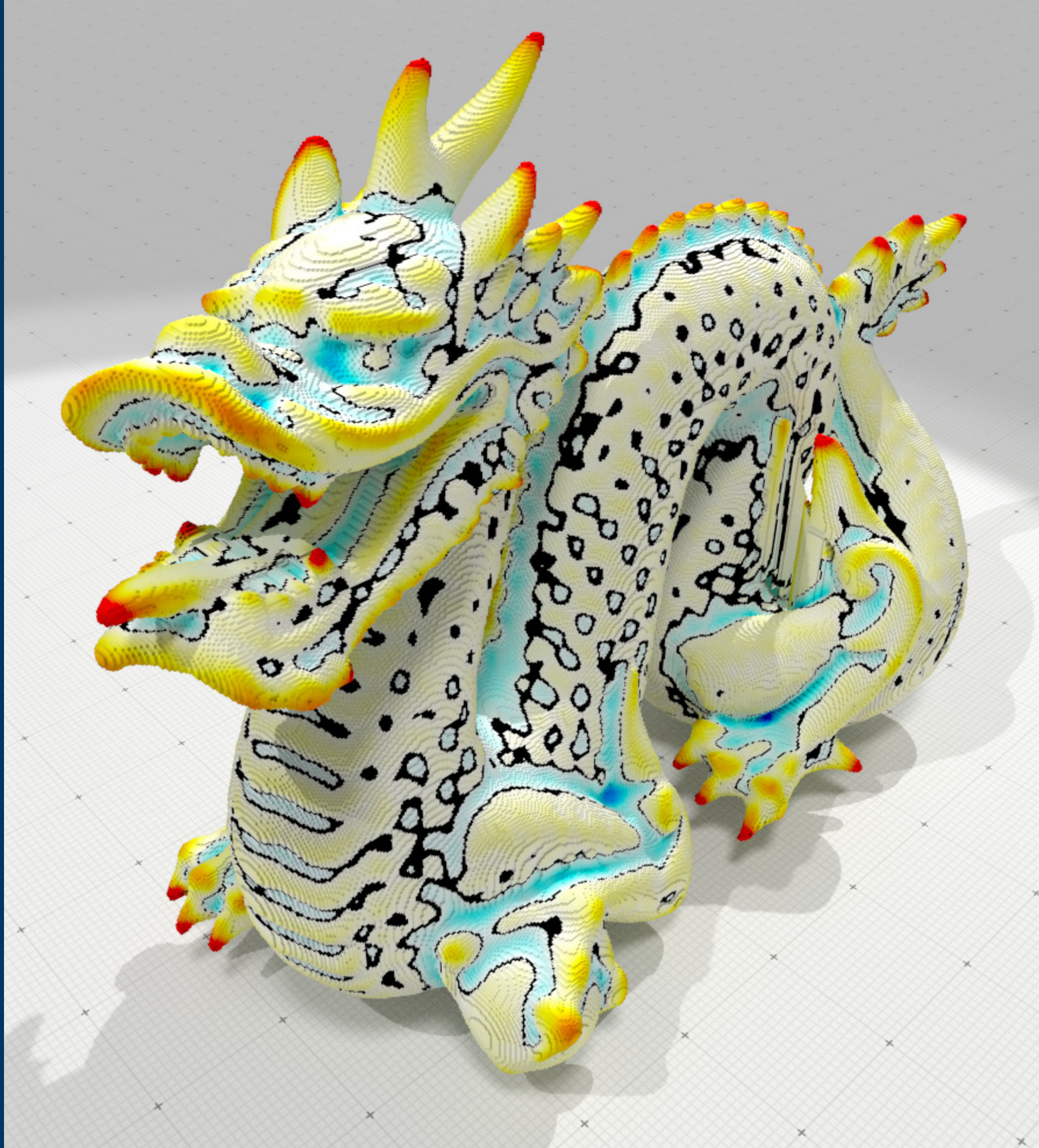

Linking continuous and digital geometry : Gauss digitization with gridstep h

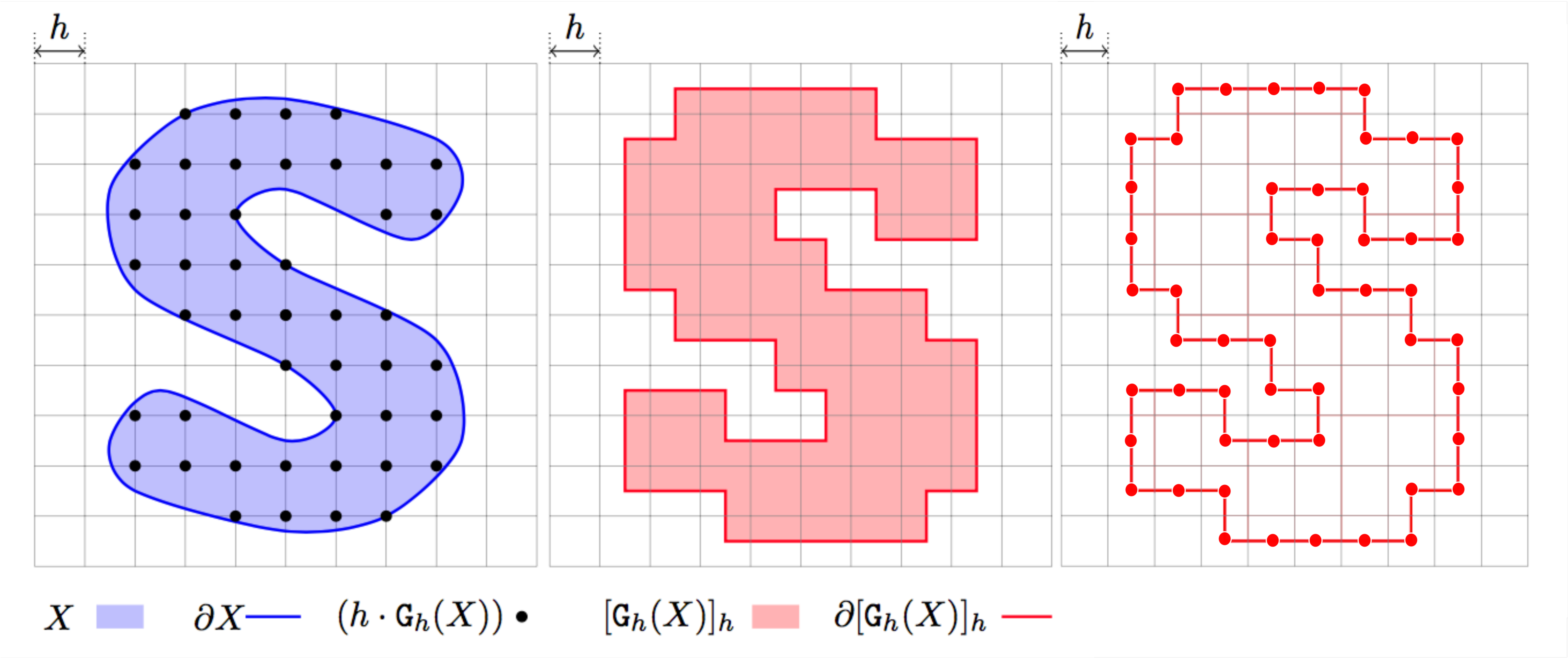

« digitization » « voxelization » « digitized surface »


What can we say for finer and finer digitization ? ($h \to 0$)

What can we say for finer and finer digitization ? ($h \to 0$)

Hausdorff closeness of digitized shapes

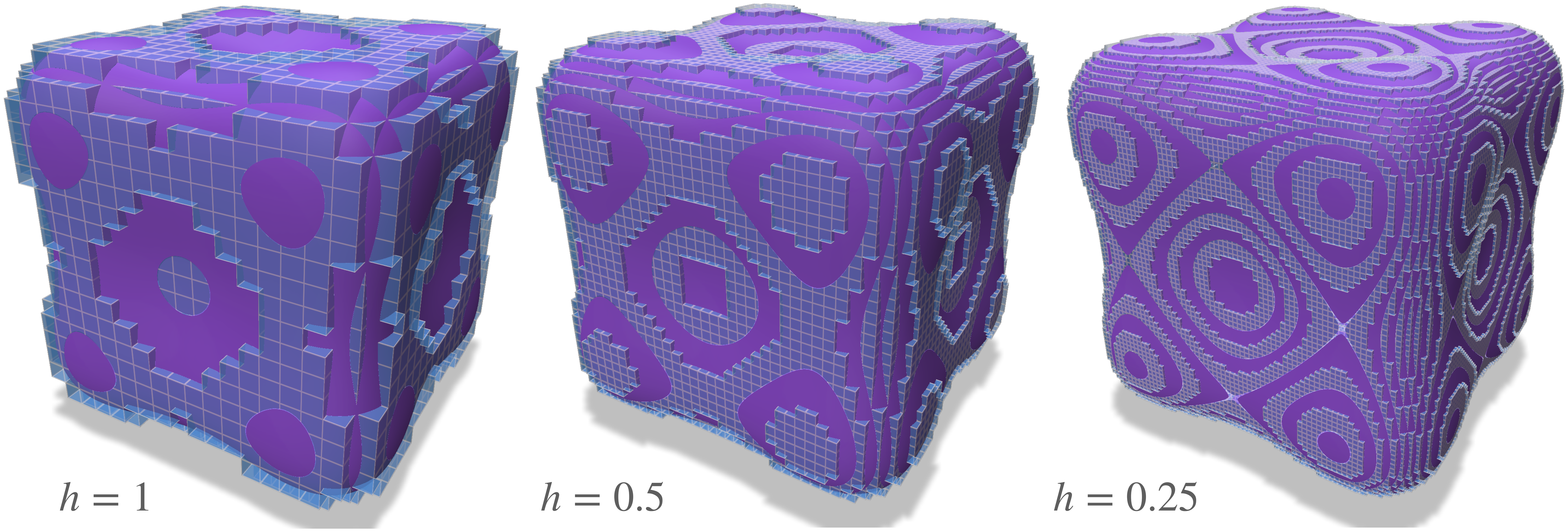

For any compact domain $X \in \mathbb{R}^d$ such that ∂X has positive reach, and its digitization $X_h := [G_h(X)]_h$ on a grid with grid-step h, then $d_H(\partial X, \partial X_h) \leq h\sqrt{d}/2$ for small enough h

[LT16]

Bijectivity of projection and manifoldness

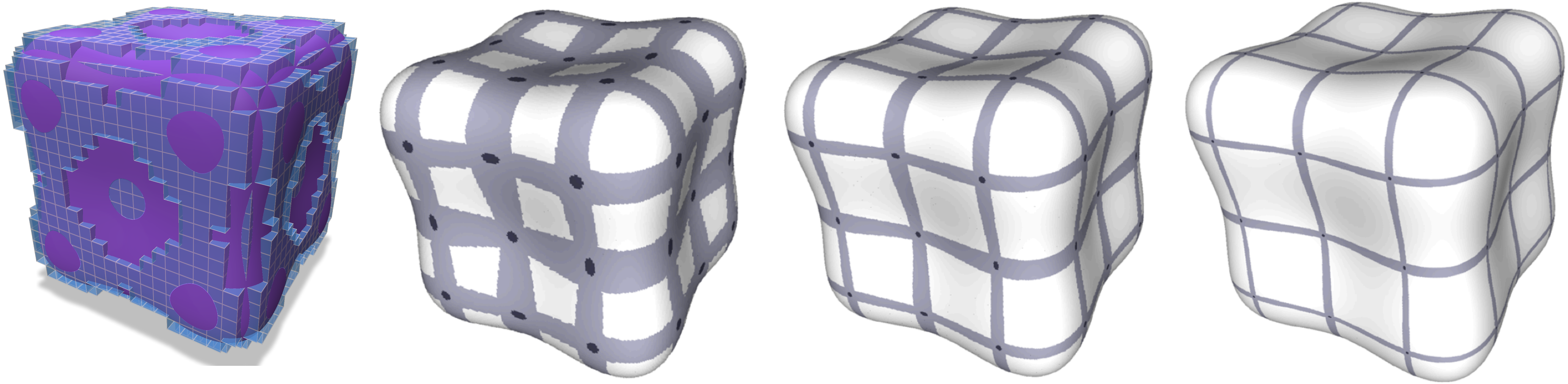

$h = 0.1$ $h = 0.05$ $h = 0.025$

[LT16]
If X has positive reach,
the size of the non-injective part of projection
$\pi_X : \partial X_h \to \partial X$ tends to zero as $h \to 0$.
(light gray + dark gray zones $\approx O(h)$)

[LT16]
If X has positive reach,
the size of the non-manifoldness part of ∂X_h
tends quickly to zero as $h \to 0$.
(dark gray zones $\approx O(h^2)$)

Multigrid convergence

For digitization process G, the discrete geometric estimator $\hat{E}$ is multigrid convergent to the geometric quantity E for the family of shapes $\mathbb{X}$, iff, for any $X \in \mathbb{X}$, there exists a grid step $h_X > 0$, such that :

$$\hat{E}(G_h(X), h) \text{ is defined for any } 0 < h < h_X,$$
$$|\hat{E}(G_h(X), h) - E(X)| < \tau_X(h)$$

where the speed of convergence $\tau_X(h)$ has null limit when $h \to 0$.

(Typically area, perimeter, integrals)

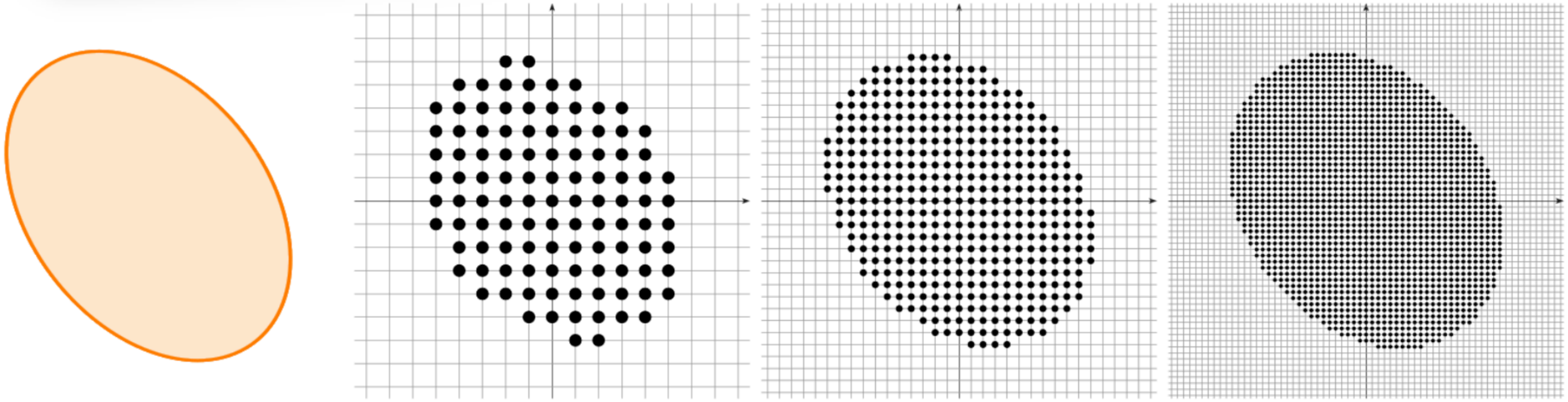

$M \in \mathbb{X}$ $\quad$ $\mathrm{G}_1(M)$ $\quad$ $\mathrm{G}_{0.5}(M)$ $\quad$ $\mathrm{G}_{0.25}(M)$

$\widehat{\text{Area}}\,(G_h(X), h) := h^2 \#(G_h(X))$ tends toward $\text{Area}(M)$ as $h \to 0$

Convergence speed is $O(h)$ and even $O(h^{\frac{22}{15}})$ for smooth enough M

Multigrid convergence (local version)

For digitization process G, the local discrete geometric estimator $\hat{E}$ is multigrid convergent to the geometric quantity E for the family of shapes $\mathbb{X}$, iff, for any $X \in \mathbb{X}$, there exists a grid step $h_X > 0$, such that :

$\hat{E}(G_h(X), \hat{x}, h)$ is defined for any $\hat{x} \in \partial[G_h(X)]_h$ with $0 < h < h_X$,

for any $x \in \partial X$, for any $\hat{x} \in \partial[G_h(X)]_h$ with $\|x - \hat{x}\|_\infty \leq h$, $\quad |\hat{E}(G_h(X), \hat{x}, h) - E(X, x)| < \tau_X(h)$

where the speed of convergence $\tau_X(h)$ has null limit when $h \to 0$.

(Typically normal direction, curvatures, ...)

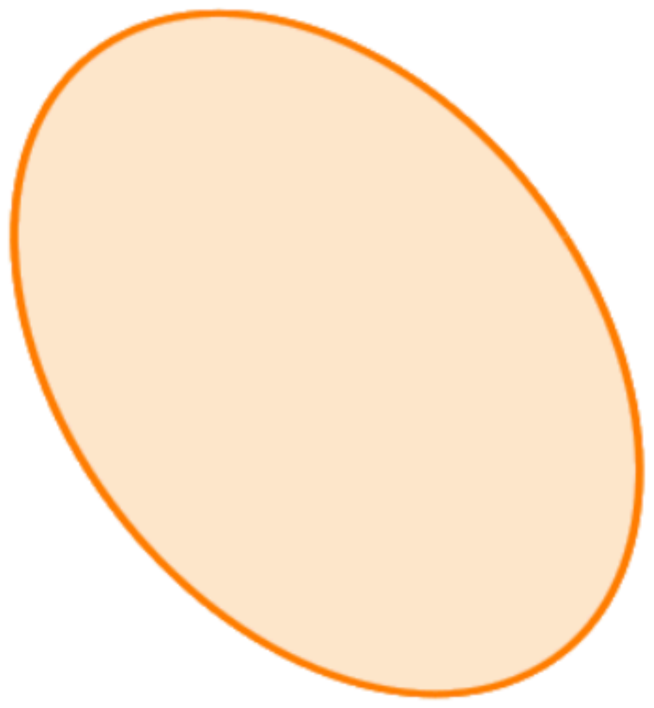

$M \in \mathbb{X}$

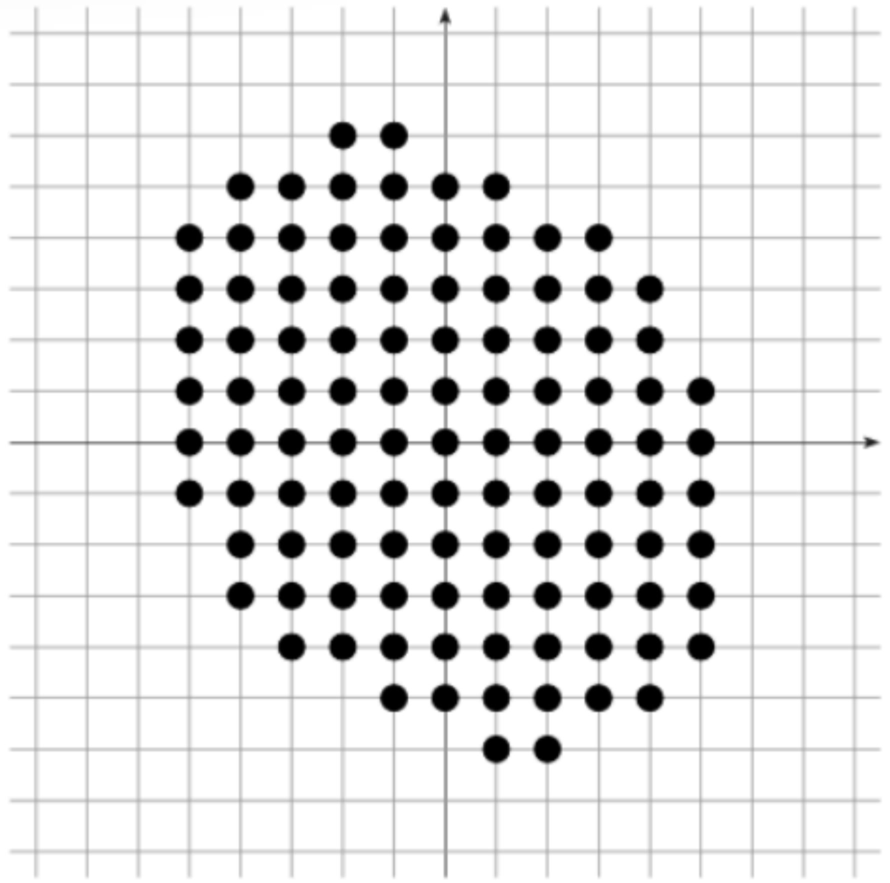

$G_1(M)$

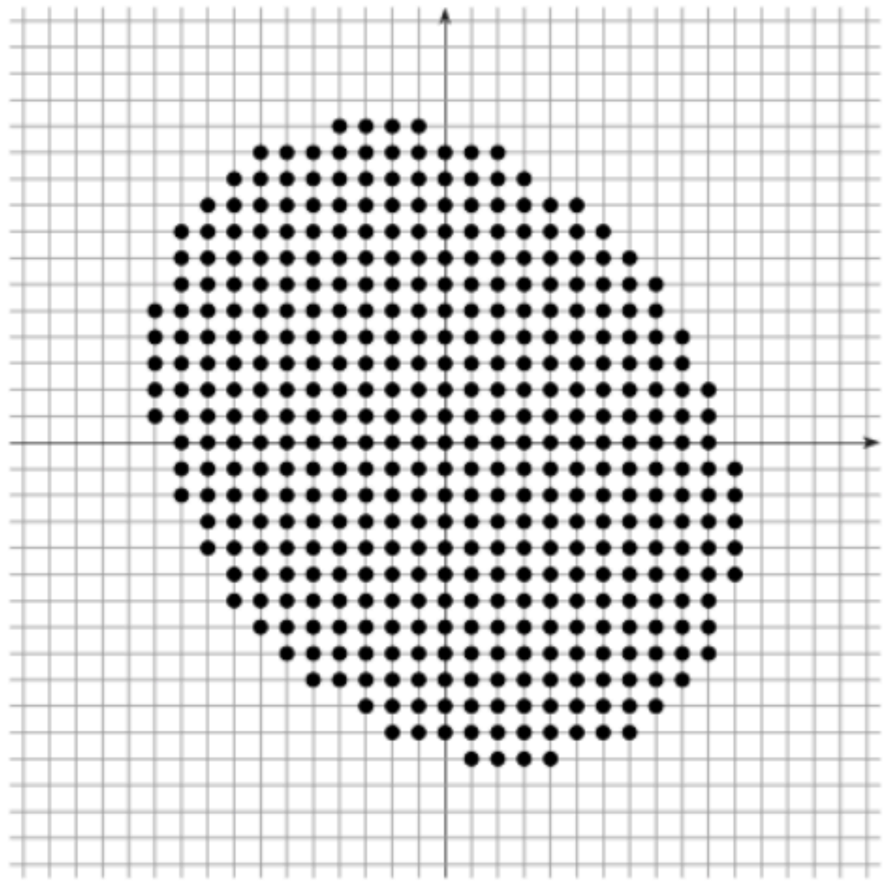

$G_{0.5}(M)$

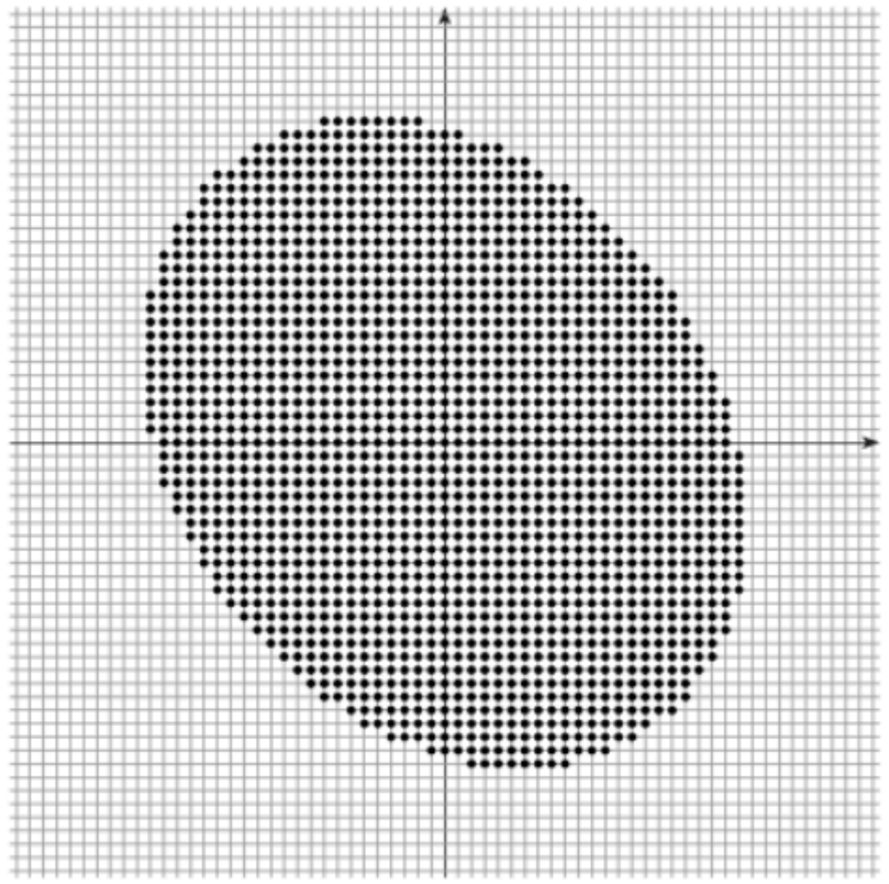

$G_{0.25}(M)$

Normal vector and curvatures estimation

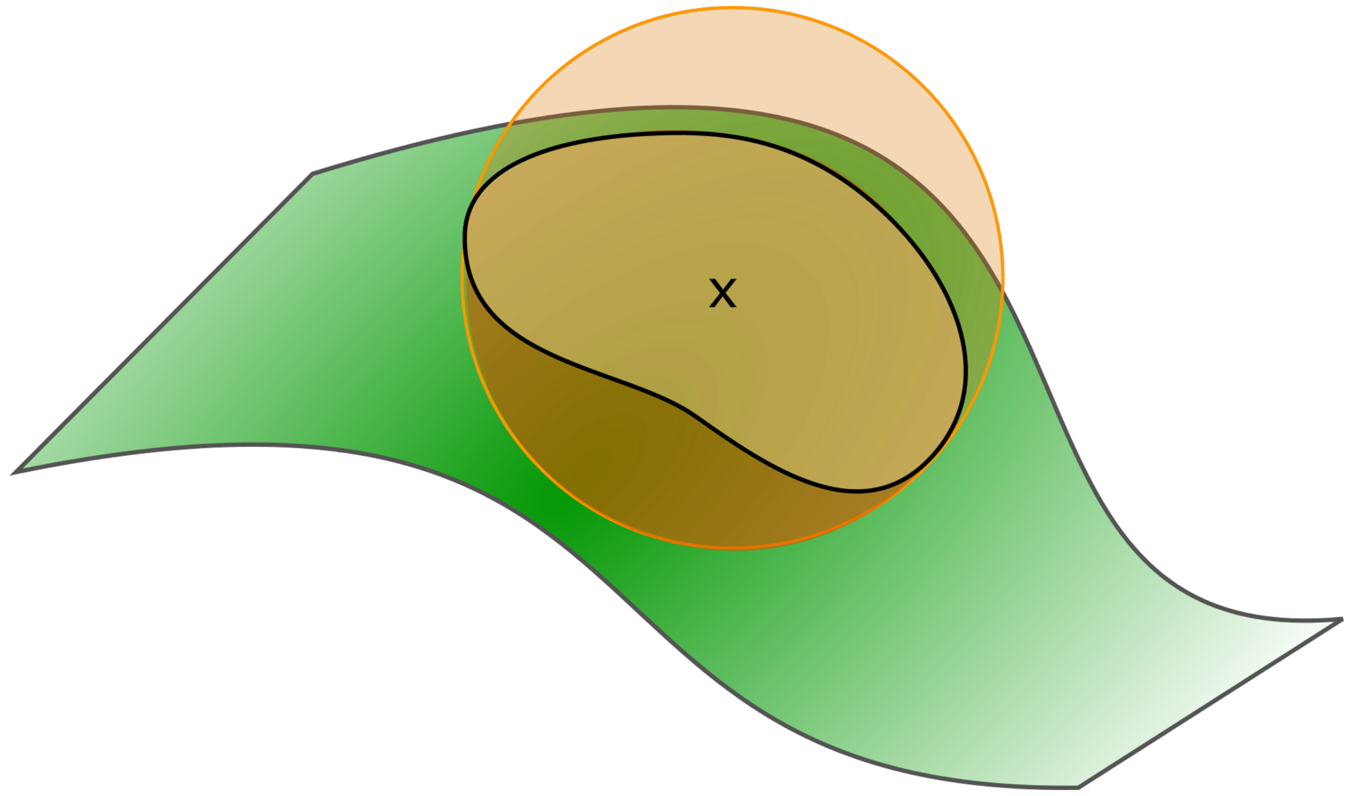

- Integral Invariants : analyzing set $B_R(x) \cap X$ gives normal vector, principal directions and curvatures [Pottmann et al. 2007]

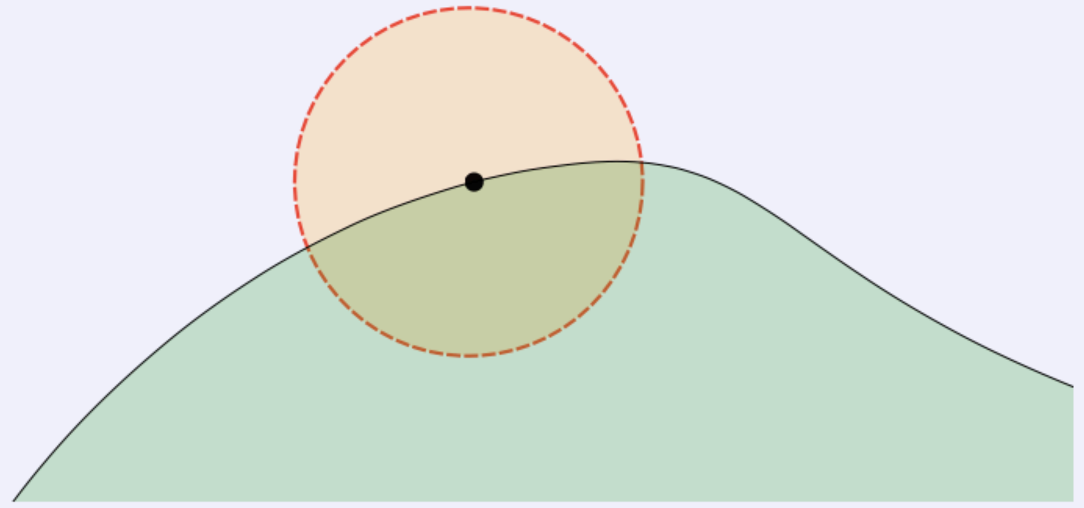

$$\kappa(M,\mathbf{x}) := \underbrace{\frac{3\pi}{2R} - \frac{3 \cdot A_R(M,\mathbf{x})}{R^3}}_{\kappa^R(M,\mathbf{x})} + O(R)$$ [Pottmann et al. 2007]

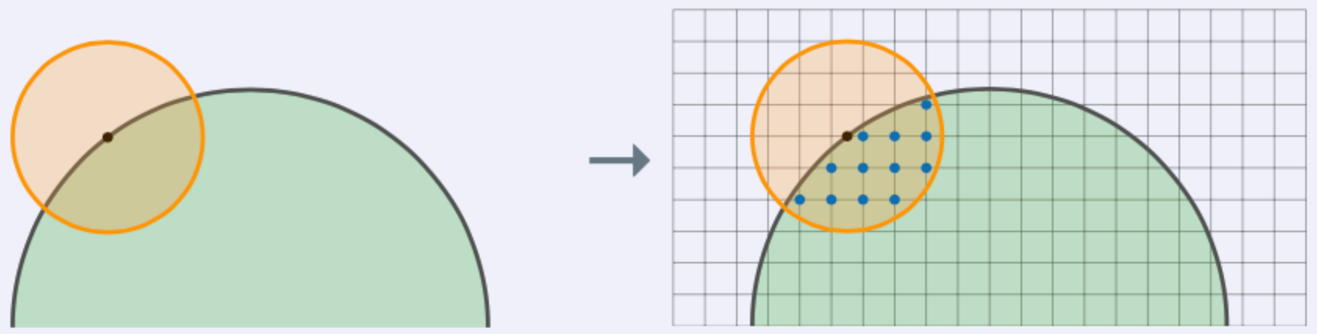

$$A_R(M,\mathbf{x}) \rightarrow \widehat{\mathrm{Area}}\,(B_{R/h}(\mathbf{x}/h) \cap \mathrm{G}_h(M))$$

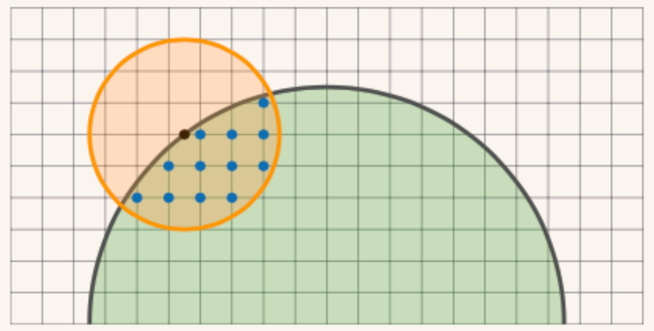

+ [Pottmann et al. 2007] $\hat{\kappa}^R(\mathrm{G}_h(M), \mathbf{x}, h)$

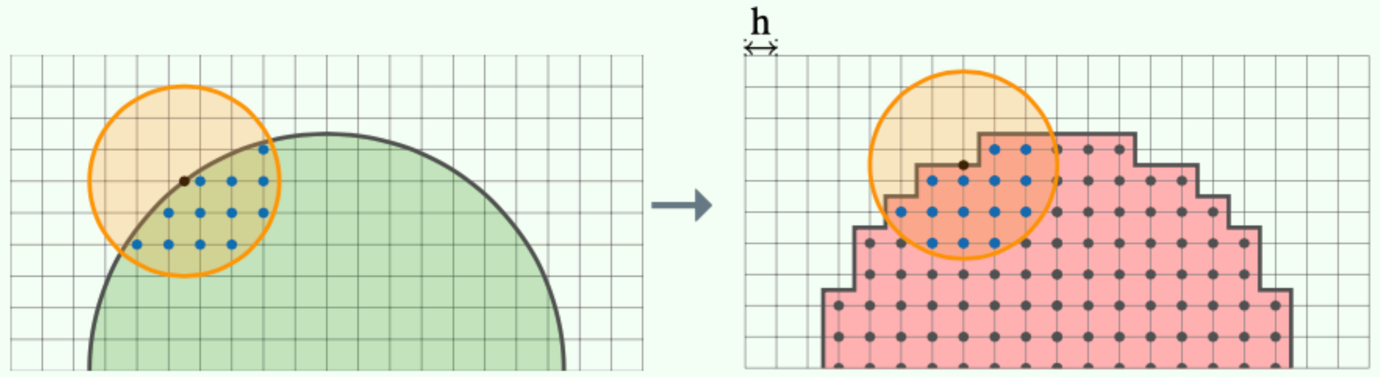

$$\hat{\kappa}^R(\mathrm{G}_h(M), \hat{\mathbf{x}}, h) \rightarrow \kappa(M,\mathbf{x})$$

[C., Levallois, Lachaud]

Let M be a convex shape in $\mathbb{R}^2$ with a C^3 bounded positive curvature boundary.

$$\forall \mathbf{x} \in \partial M, \forall \hat{\mathbf{x}} \in \partial[\mathrm{G}_h(M)]_h, \|\hat{x} - x\|_\infty \leq h \Rightarrow$$

$$|\hat{\kappa}^R(\mathrm{G}_h(M), \hat{\mathbf{x}}, h) - \kappa(M,\mathbf{x})| = O(R) + O\left(\frac{h^\beta}{R^{1+\beta}}\right) + O\left(\frac{h^{\alpha'}}{R^2}\right) + O\left(h^{\alpha'}\right) + O\left(\frac{h^{2\alpha'}}{R^2}\right)$$

Normal vector and curvatures estimation

- Integral Invariants : analyzing set $B_R(x) \cap X$ gives normal vector, principal directions and curvatures [Pottmann et al. 2007]

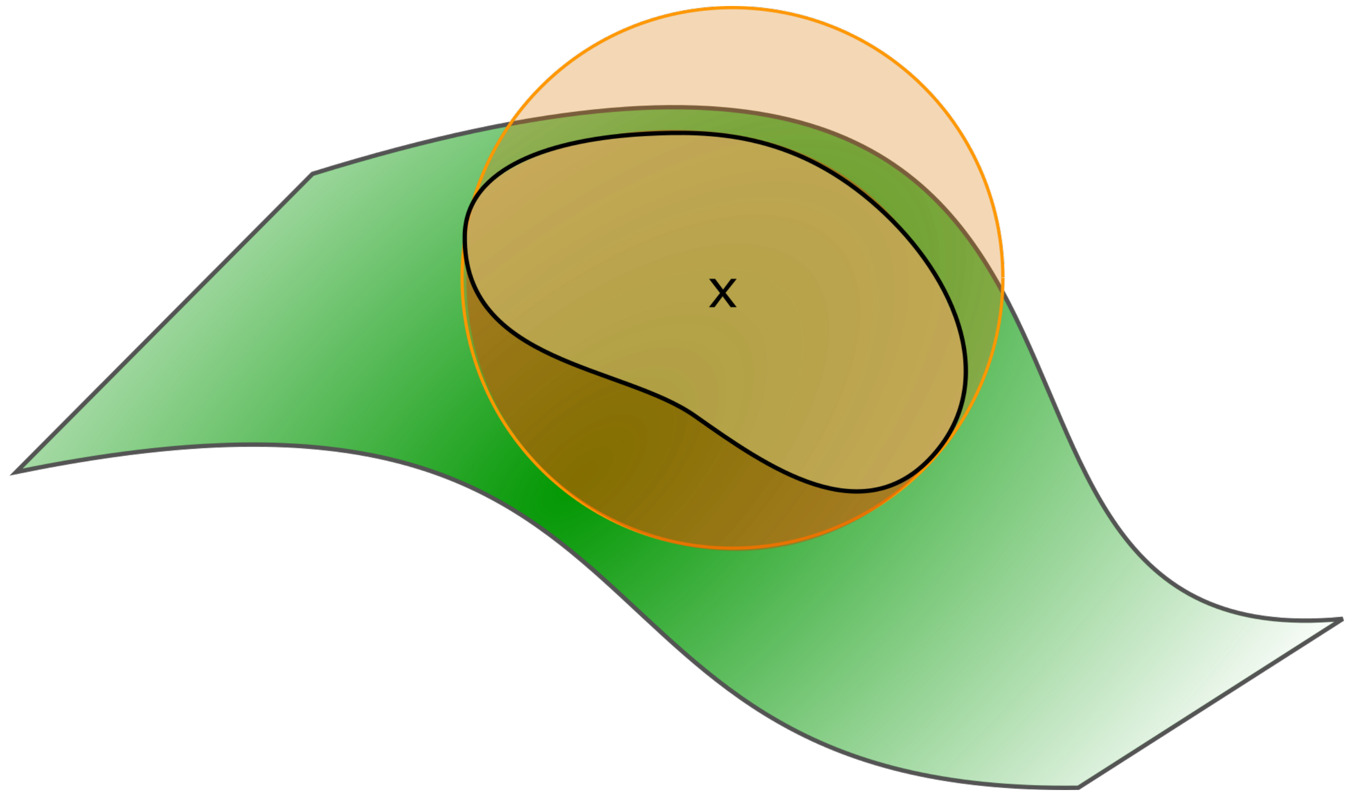

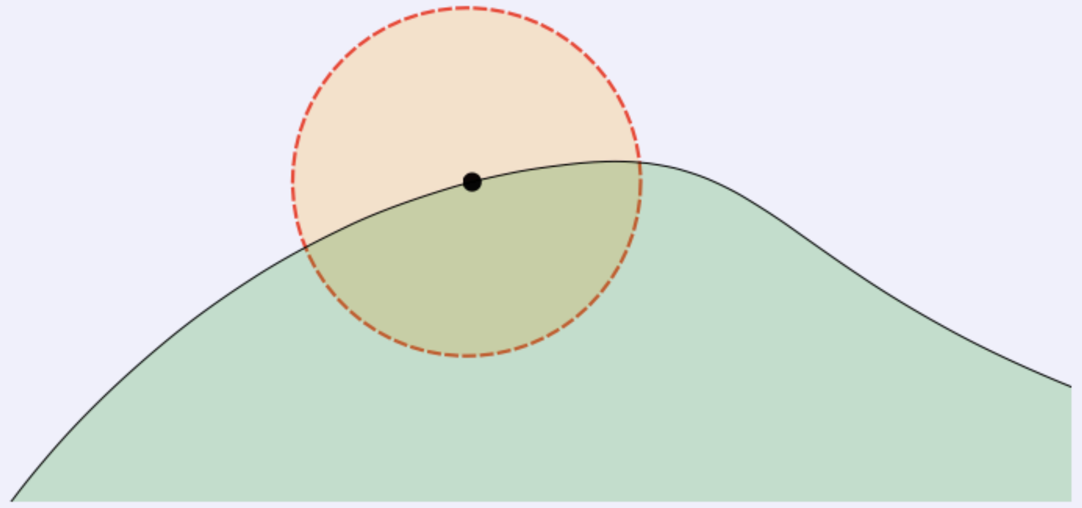

$$\kappa(M, \mathbf{x}) := \underbrace{\frac{3\pi}{2R} - \frac{3 \cdot A_R(M, \mathbf{x})}{R^3}}_{\kappa^R(M, \mathbf{x})} + O(R)$$ [Pottmann et al. 2007]

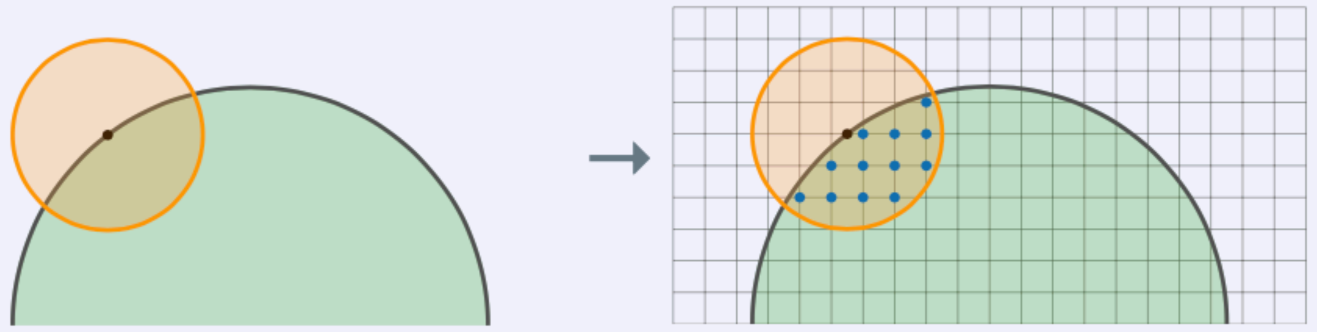

$$A_R(M, \mathbf{x}) \to \widehat{\mathrm{Area}}\,(B_{R/h}(\mathbf{x}/h) \cap \mathbb{G}_h(M))$$

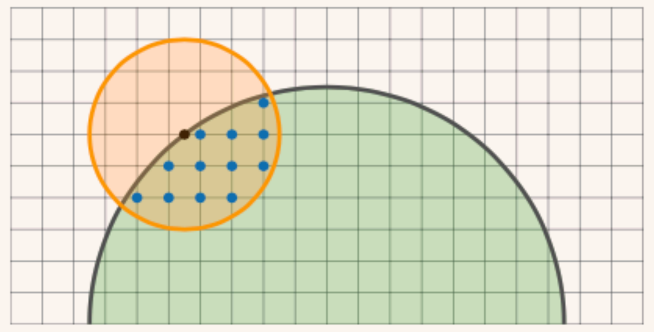

+ [Pottmann et al. 2007]

$$\kappa^R(\mathbb{G}_h(M), \mathbf{x}, h)$$

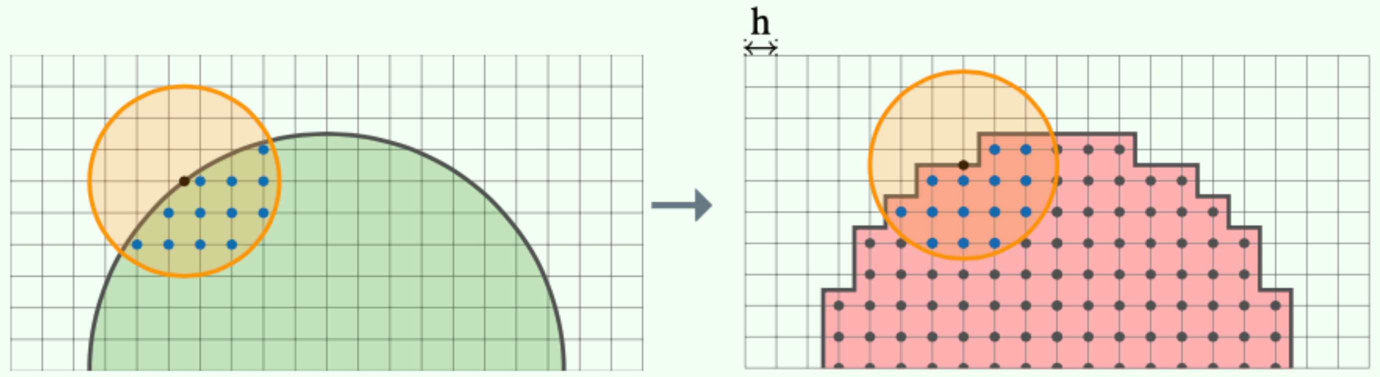

$$\kappa^R(\mathbb{G}_h(M), \hat{\mathbf{x}}, h) \to \kappa(M, \mathbf{x})$$

[C., Levallois, Lachaud]

Let M be a convex shape in $\mathbb{R}^2$ with a C^3 bounded positive curvature boundary.

$$\forall \mathbf{x} \in \partial M, \forall \hat{\mathbf{x}} \in \partial[\mathbb{G}_h(M)]_h, \|\hat{x} - x\|_\infty \leq h \Rightarrow$$
$$|\kappa^R(\mathbb{G}_h(M), \hat{\mathbf{x}}, h) - \kappa(M, \mathbf{x})| = O(R) + O\left(\frac{h^\beta}{R^{1+\beta}}\right) + O\left(\frac{h^{\alpha'}}{R^2}\right) + O\left(h^{\alpha'}\right) + O\left(\frac{h^{2\alpha'}}{R^2}\right)$$

With optimal radius $R = O(h^{\frac{1}{3}})$, then :

- normals $\left\| \hat{\mathbf{n}}(G_h(M), \xi(x), h)) - \mathbf{n}(M, x) \right\| \leq C \cdot h^{\frac{2}{3}}$
- mean curvature $\left\| \hat{\kappa}(M_h, \xi(x))) - \kappa(M, x) \right\|_2 \leq C \cdot h^{\frac{1}{3}}$
- … [CLL2014], [LCL2017]

Normal vector field estimation

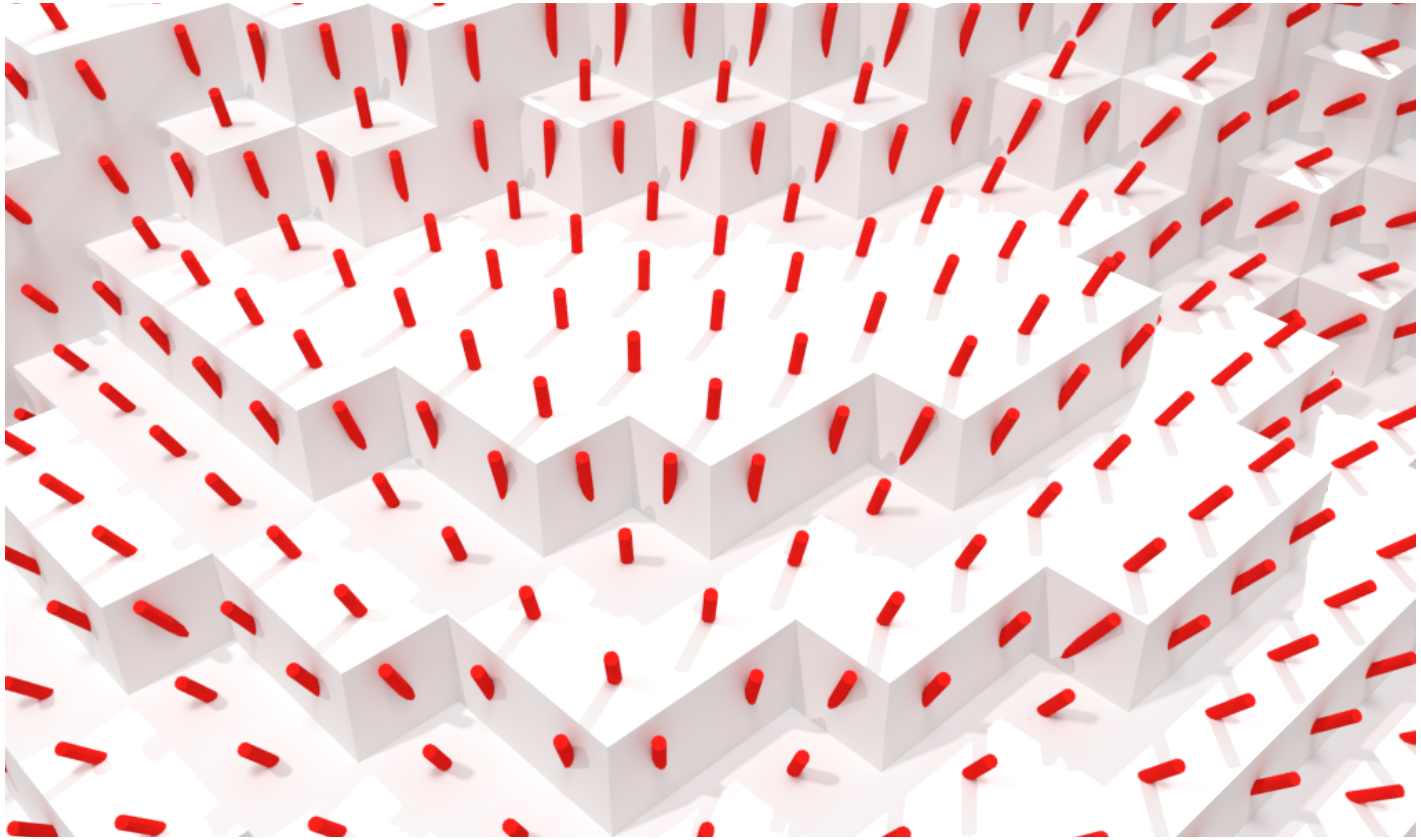

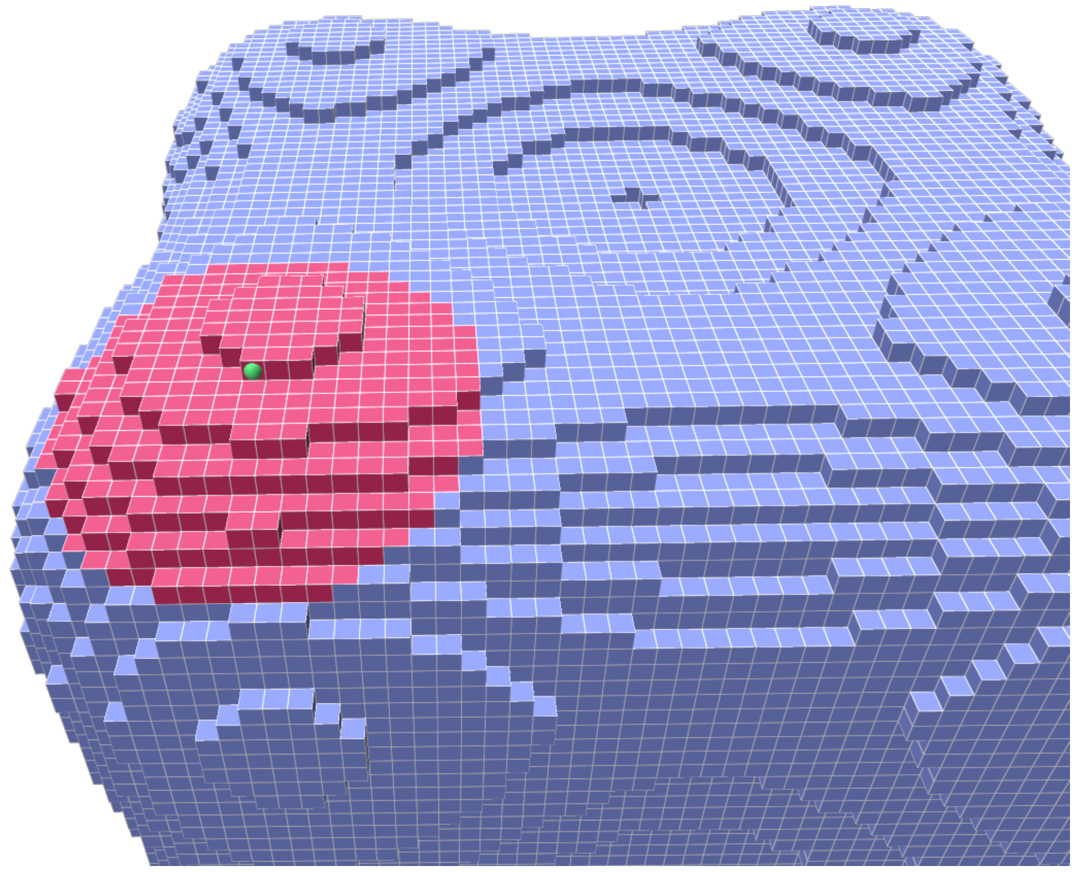

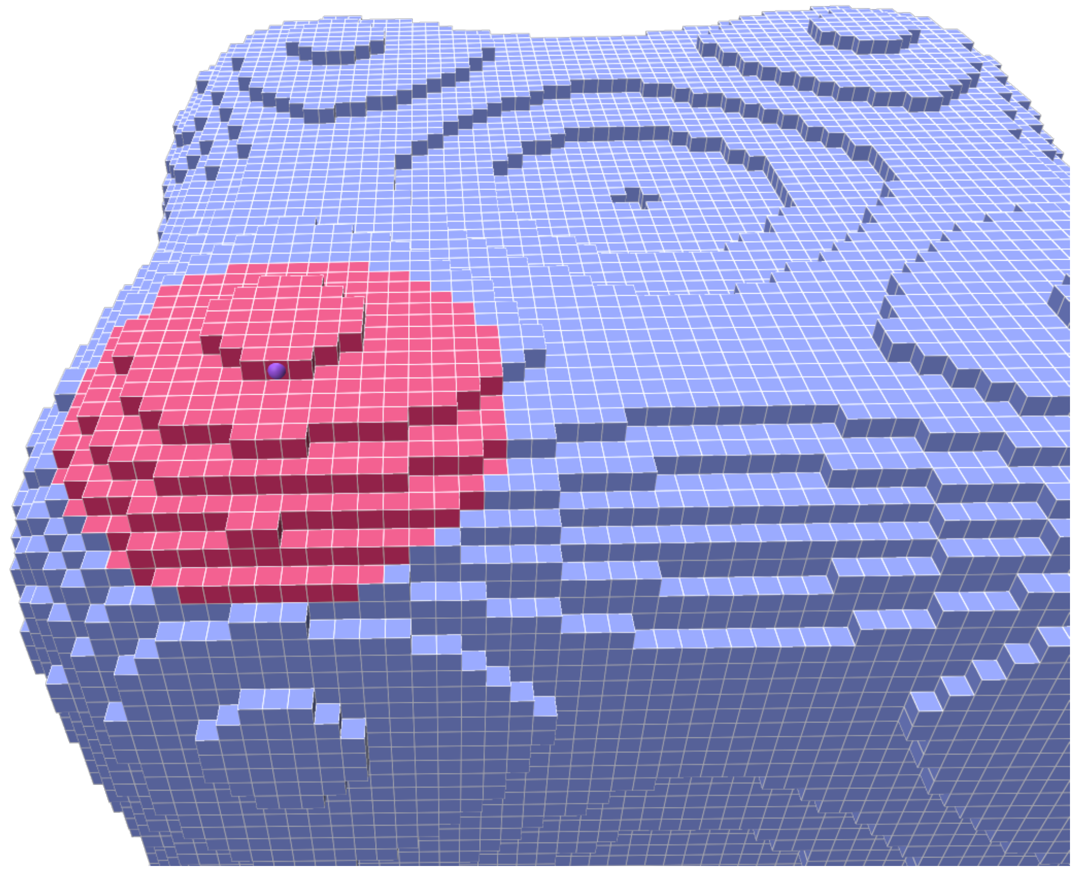

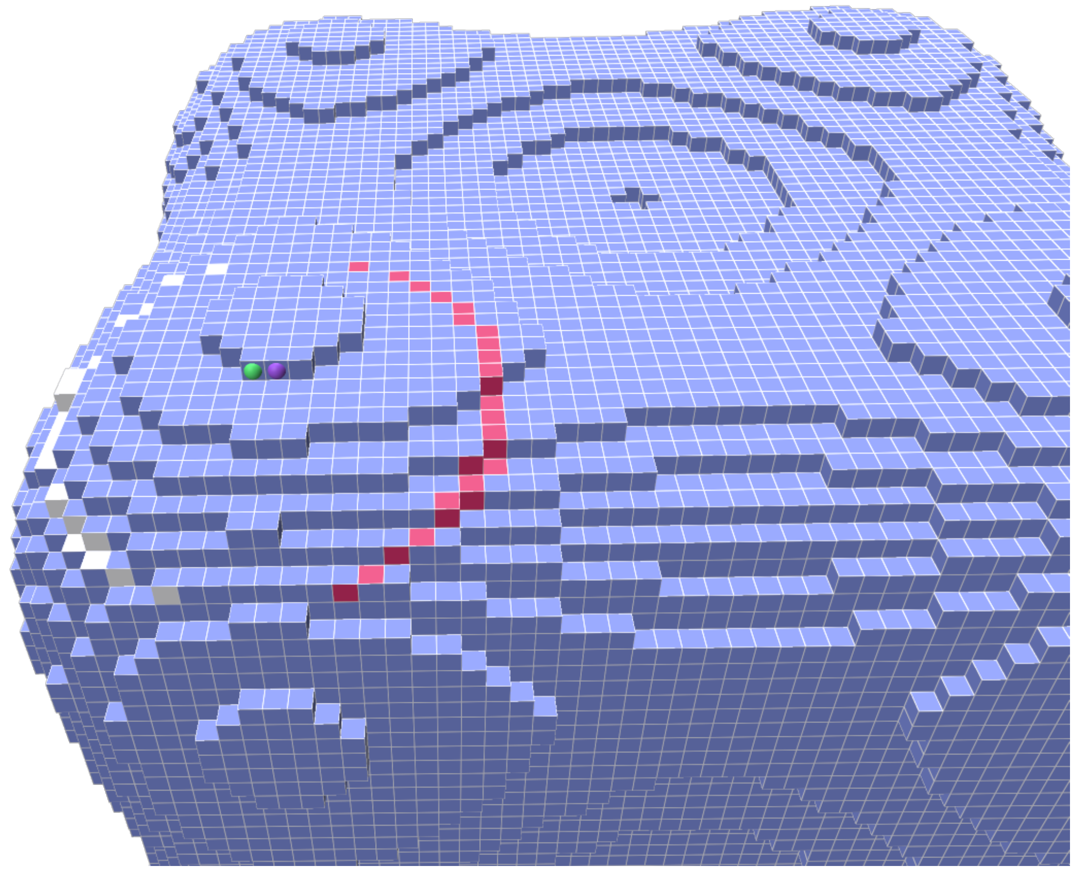

Incremental computation : estimate at y nearby x only requires preceding result + looking at points within $B_R(y) \ominus B_R(x)$

hands on…

```cpp
void oneStepAll(double h)
{
  auto params = SH3::defaultParameters() | SHG3::defaultParameters() |  SHG3::parametersGeometryEstimation();
  params( "polynomial", "goursat" )( "gridstep", h );
  auto implicit_shape  = SH3::makeImplicitShape3D  ( params );
  auto digitized_shape = SH3::makeDigitizedImplicitShape3D( implicit_shape, params );
  auto K               = SH3::getKSpace( params );
  auto binary_image    = SH3::makeBinaryImage( digitized_shape, params );
  auto surface         = SH3::makeDigitalSurface( binary_image, K, params );
  auto embedder        = SH3::getCellEmbedder( K );
  SH3::Cell2Index c2i;
  auto surfels         = SH3::getSurfelRange( surface, params );
  auto primalSurface   = SH3::makePrimalPolygonalSurface(c2i, surface);

  //Need to convert the faces
  std::vector<std::vector<std::size_t>> faces;
  for(auto &face: primalSurface->allFaces())
    faces.push_back(primalSurface->verticesAroundFace( face ));
  auto digsurf = polyscope::registerSurfaceMesh("Primal surface", primalSurface->positions(), faces);
  digsurf->rescaleToUnit(); digsurf->setEdgeWidth(h*h);  digsurf->setEdgeColor({1.,1.,1.});

  //Computing some differential quantities
  params("r-radius", 5*std::pow(h,-2.0/3.0));
  auto Mcurv      = SHG3::getIIMeanCurvatures(binary_image, surfels, params);
  auto normalsII  = SHG3::getIINormalVectors(binary_image, surfels, params);
  auto KTensor    = SHG3::getIIPrincipalCurvaturesAndDirections(binary_image, surfels, params);  //Recomputing...

  std::vector<double> Gcurv(surfels.size()),k1(surfels.size()),k2(surfels.size());
  std::vector<RealVector> d1(surfels.size()),d2(surfels.size());
  auto i=0;
  for(auto &t: KTensor) //AOS->SOA
  {
    k1[i]    = std::get<0>(t);
    k2[i]    = std::get<1>(t);
    d1[i]    = std::get<2>(t);
    d2[i]    = std::get<3>(t);
    Gcurv[i] = k1[i]*k2[i];
    ++i;
  }

  //Attaching quantities
  digsurf->addFaceVectorQuantity("II normal vectors", normalsII, polyscope::VectorType::AMBIENT);
  digsurf->addFaceScalarQuantity("II mean curvature", Mcurv);
  digsurf->addFaceScalarQuantity("II Gaussian curvature", Gcurv);
  digsurf->addFaceScalarQuantity("II k1 curvature", k1);
  digsurf->addFaceScalarQuantity("II k2 curvature", k2);
  digsurf->addFaceVectorQuantity("II first principal direction", d1, polyscope::VectorType::AMBIENT);
  digsurf->addFaceVectorQuantity("II second principal direction", d2, polyscope::VectorType::AMBIENT);
}
```

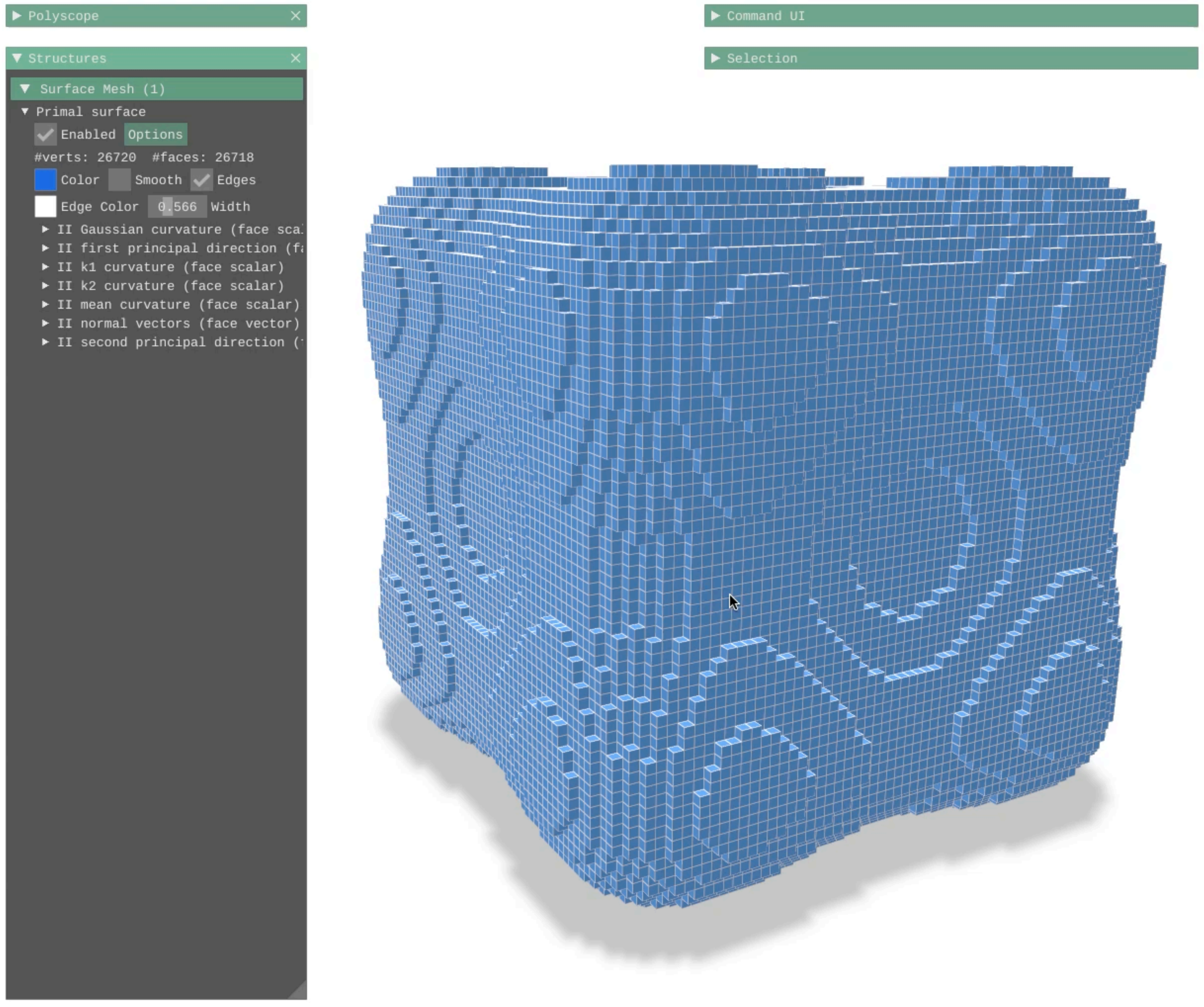

```cpp
void oneStepAll(double h)
{
  auto params = SH3::defaultParameters() | SHG3::defaultParameters() |  SHG3::parametersGeometryEstimation();
  params( "polynomial", "goursat" )( "gridstep", h );
  auto implicit_shape  = SH3::makeImplicitShape3D  ( params );
  auto digitized_shape = SH3::makeDigitizedImplicitShape3D( implicit_shape, params );
  auto K               = SH3::getKSpace( params );
  auto binary_image    = SH3::makeBinaryImage( digitized_shape, params );
  auto surface         = SH3::makeDigitalSurface( binary_image, K, params );
  auto embedder        = SH3::getCellEmbedder( K );
  SH3::Cell2Index c2i;
  auto surfels         = SH3::getSurfelRange( surface, params );
  auto primalSurface   = SH3::makePrimalPolygonalSurface(c2i, surface);

  //Need to convert the faces
  std::vector<std::vector<std::size_t>> faces;
  for(auto &face: primalSurface->allFaces())
    faces.push_back(primalSurface->verticesAroundFace( face ));
  auto digsurf = polyscope::registerSurfaceMesh("Primal surface", primalSurface->positions(), faces);
  digsurf->rescaleToUnit(); digsurf->setEdgeWidth(h*h);  digsurf->setEdgeColor({1.,1.,1.});

  //Computing some differential quantities
  params("r-radius", 5*std::pow(h,-2.0/3.0));
  auto Mcurv     = SHG3::getIIMeanCurvatures(binary_image, surfels, params);
  auto normalsII = SHG3::getIINormalVectors(binary_image, surfels, params);
  auto KTensor   = SHG3::getIIPrincipalCurvaturesAndDirections(binary_image, surfels, params);  //Recomputing...

  std::vector<double> Gcurv(surfels.size()),k1(surfels.size()),k2(surfels.size());
  std::vector<RealVector> d1(surfels.size()),d2(surfels.size());
  auto i=0;
  for(auto &t: KTensor) //AOS->SOA
  {
    k1[i]    = std::get<0>(t);
    k2[i]    = std::get<1>(t);
    d1[i]    = std::get<2>(t);
    d2[i]    = std::get<3>(t);
    Gcurv[i] = k1[i]*k2[i];
    ++i;
  }

  //Attaching quantities
  digsurf->addFaceVectorQuantity("II normal vectors", normalsII, polyscope::VectorType::AMBIENT);
  digsurf->addFaceScalarQuantity("II mean curvature", Mcurv);
  digsurf->addFaceScalarQuantity("II Gaussian curvature", Gcurv);
  digsurf->addFaceScalarQuantity("II k1 curvature", k1);
  digsurf->addFaceScalarQuantity("II k2 curvature", k2);
  digsurf->addFaceVectorQuantity("II first principal direction", d1, polyscope::VectorType::AMBIENT);
  digsurf->addFaceVectorQuantity("II second principal direction", d2, polyscope::VectorType::AMBIENT);
}
```

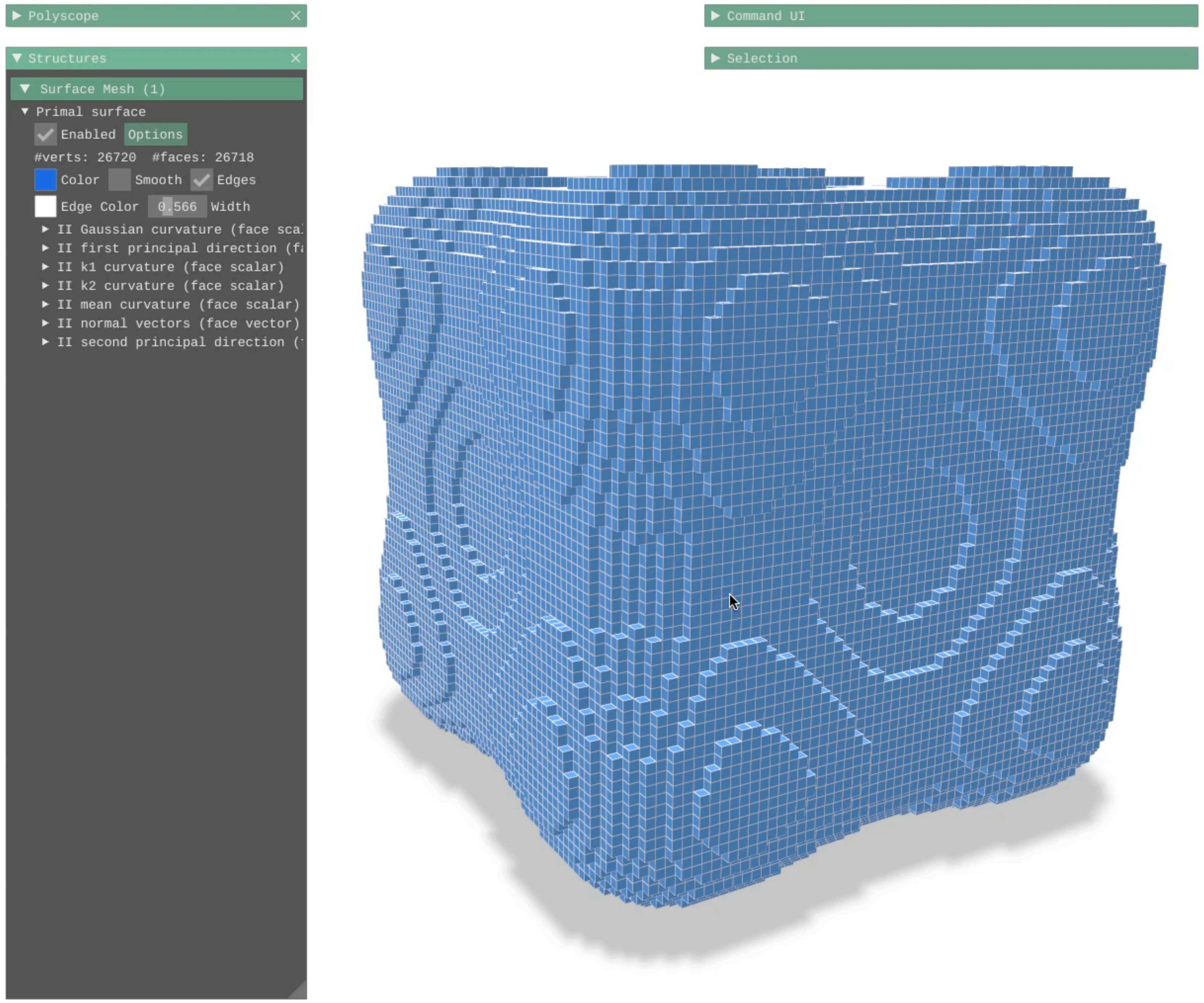

digital surface geometry processing

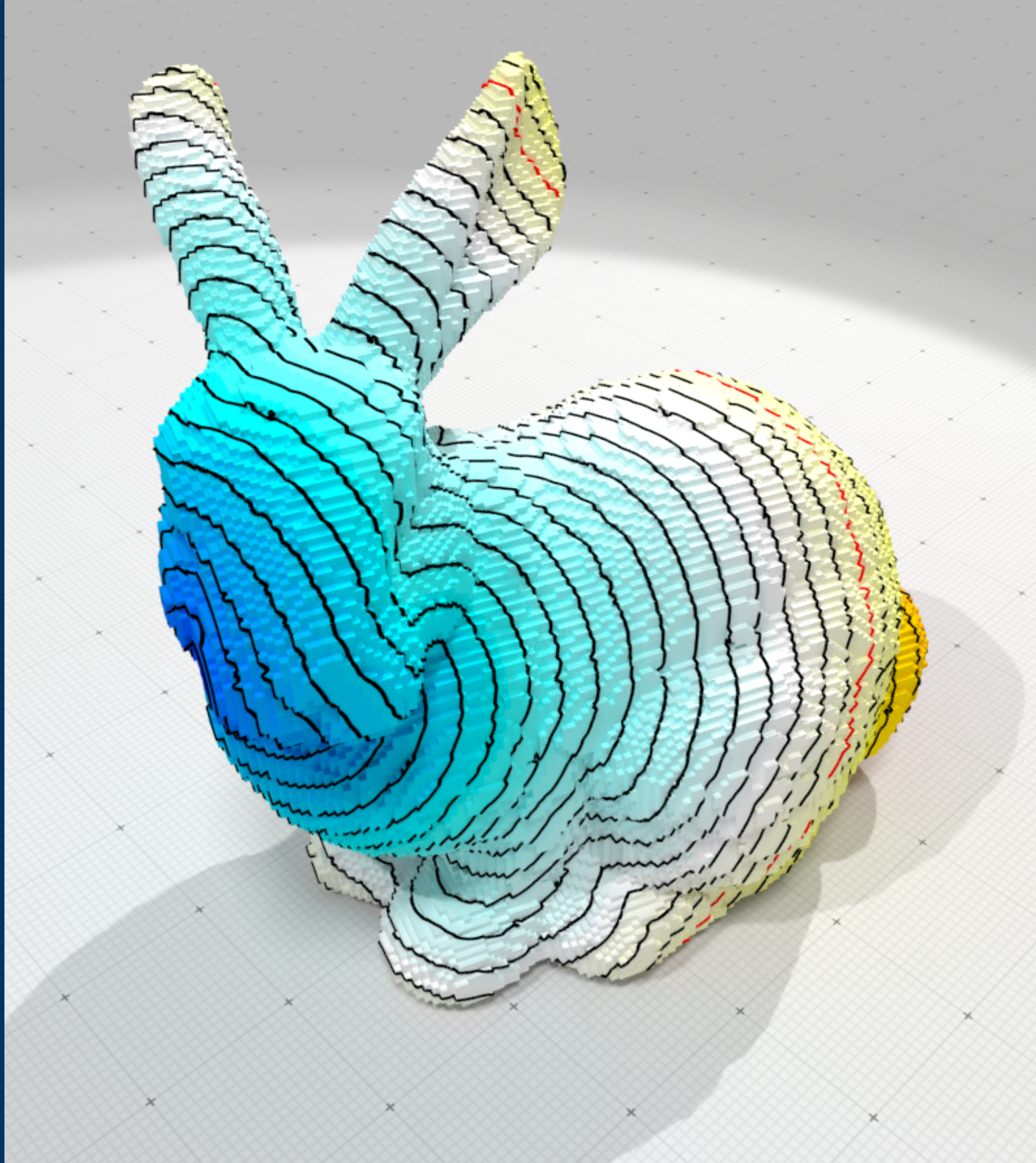

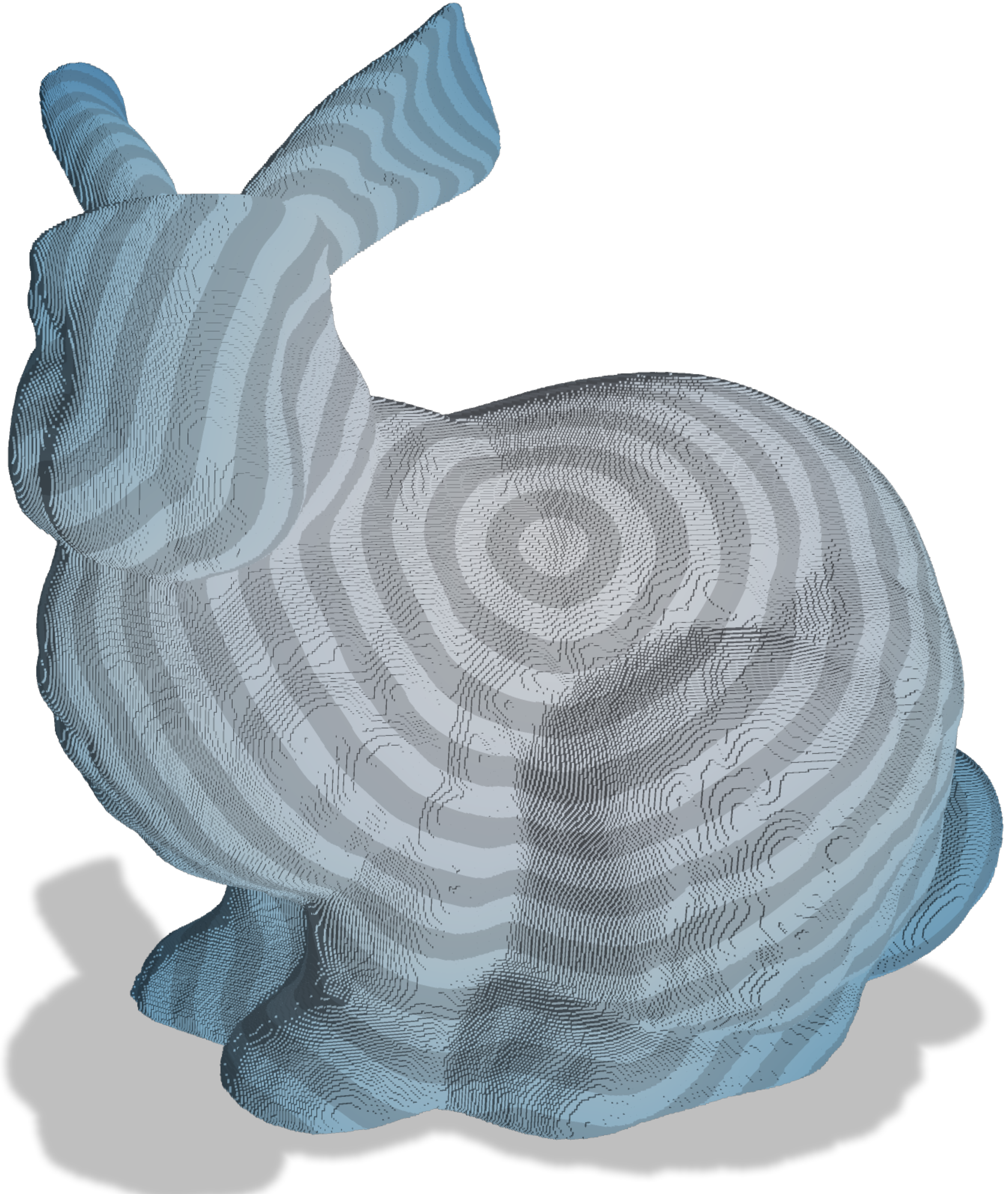

$$\dot{u} = \Delta u \qquad u(0) = u_0$$

$$\dot{u} = \Delta u \qquad u(0) = u_0$$

u

$$\dot{u} = \Delta u \qquad u(0) = u_0$$

u

∇u

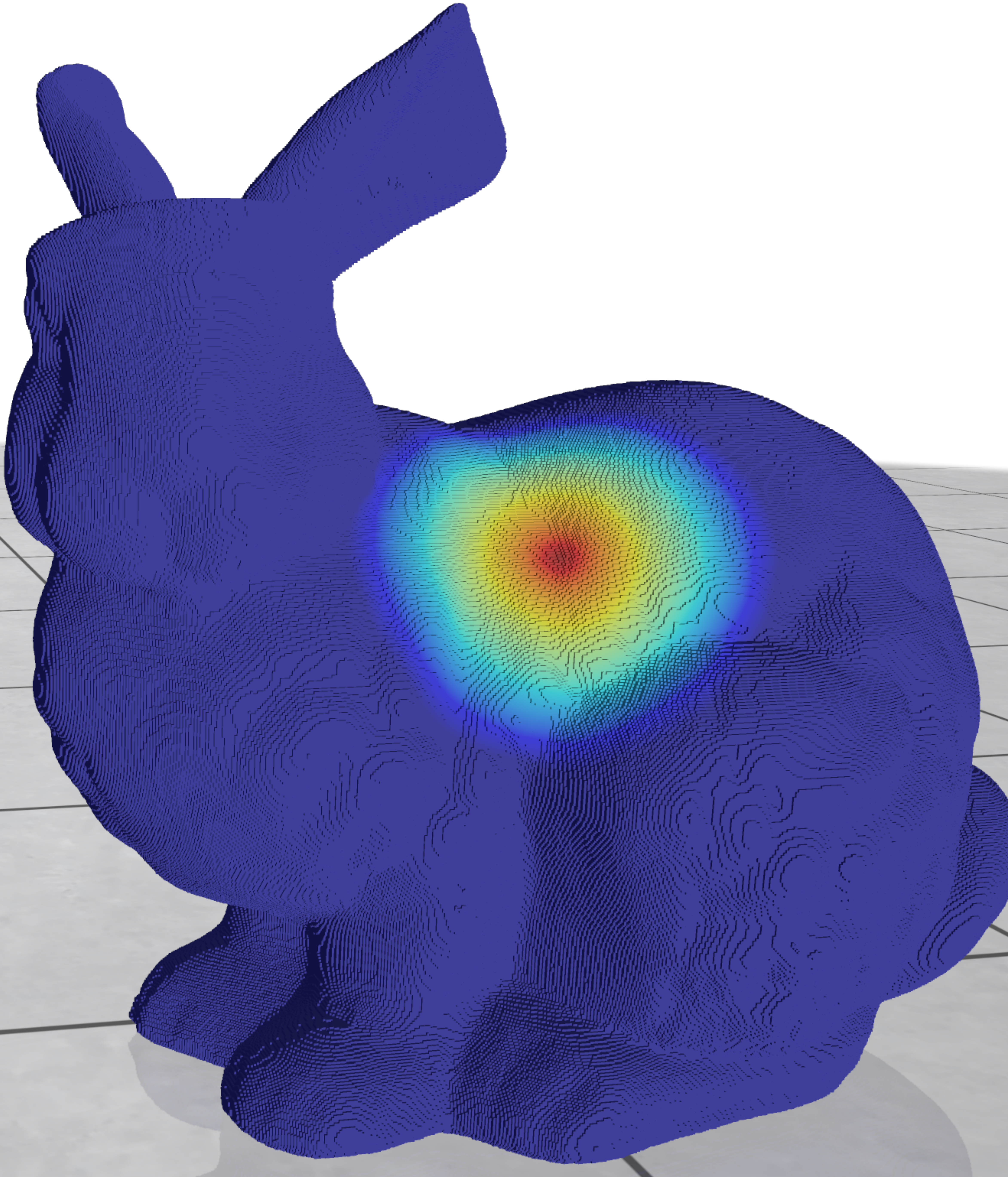

$\dot{u} = \Delta u \qquad u(0) = u_0$

u

∇u

$\operatorname{div} \vec{F}$

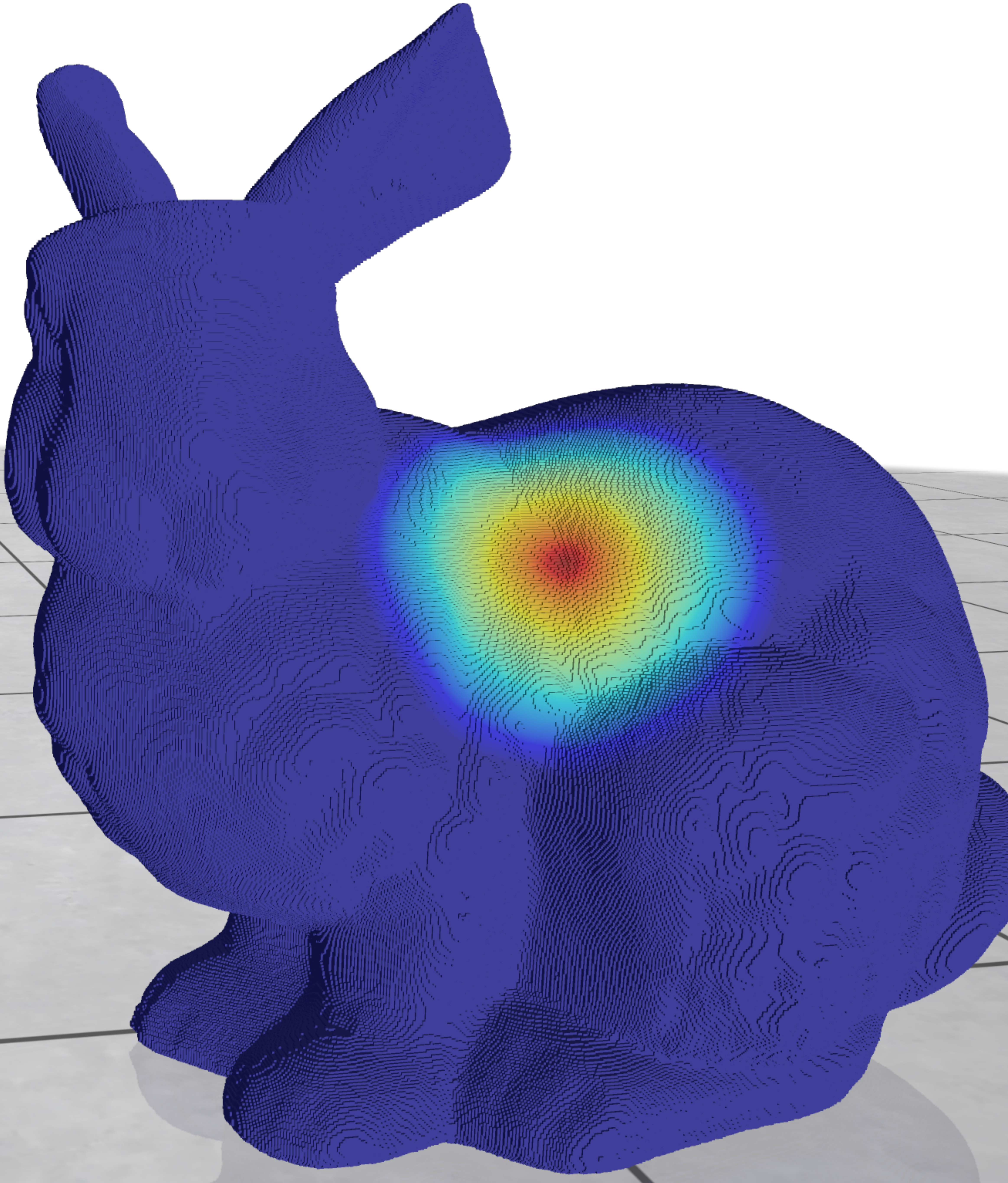

$$\dot{u} = \Delta u \qquad u(0) = u_0$$

u

∇u

$\operatorname{div} \vec{F}$

$\operatorname{curl} \vec{F}$

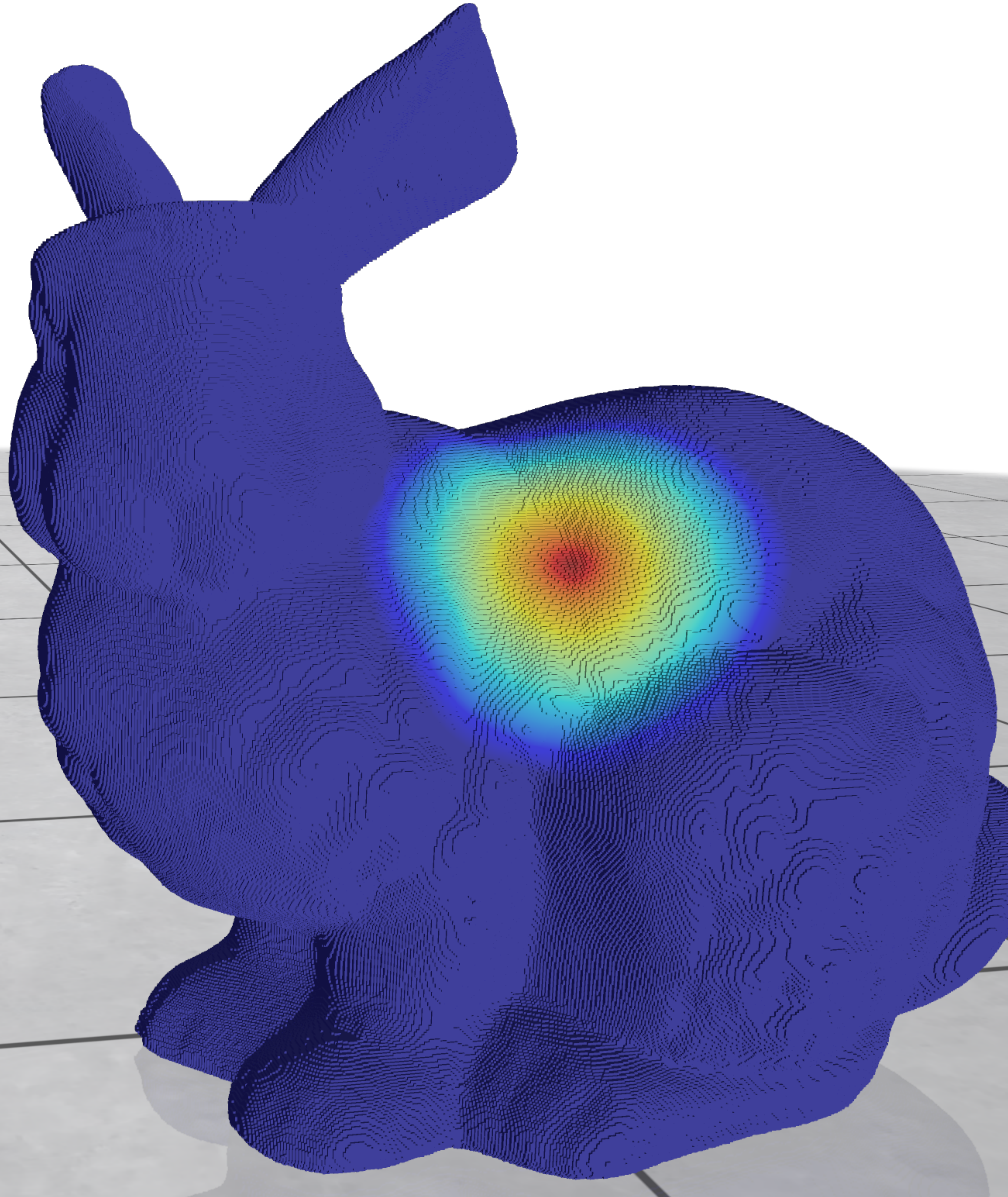

$$\dot{u} = \Delta u \qquad u(0) = u_0$$

u

∇u

$\operatorname{div} \vec{F}$

$\operatorname{curl} \vec{F}$

$\Delta u := \operatorname{div} \nabla u$

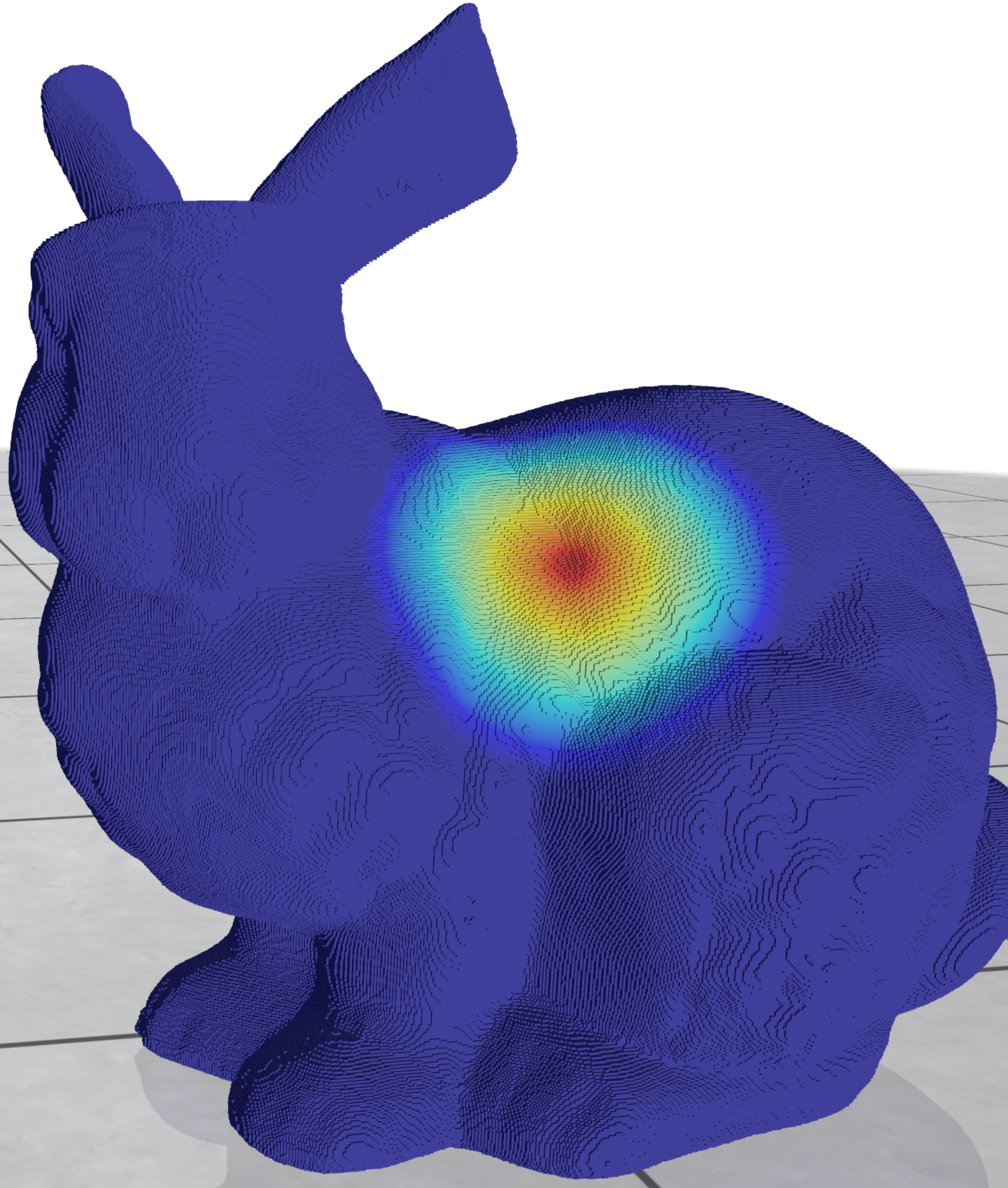

$$\dot{u} = \Delta u \qquad u(0) = u_0$$

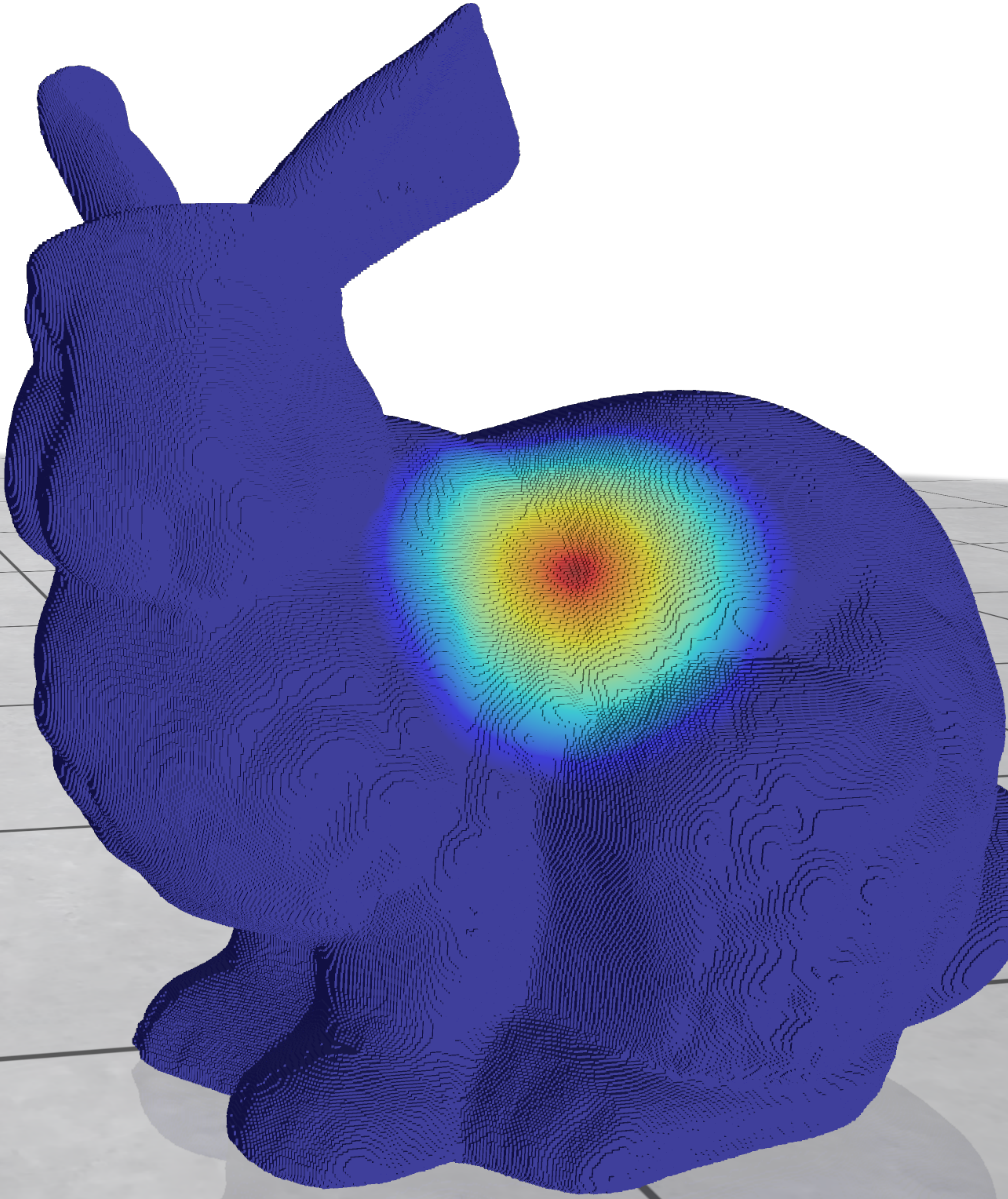

u

∇u

$\operatorname{div} \vec{F}$

$\operatorname{curl} \vec{F}$

$\Delta u := \operatorname{div} \nabla u$

$\Delta u = g$

Discrete Differential Operators on Polygonal Meshes

[de Goes et al 20]

[C. & L. DGMM2022]

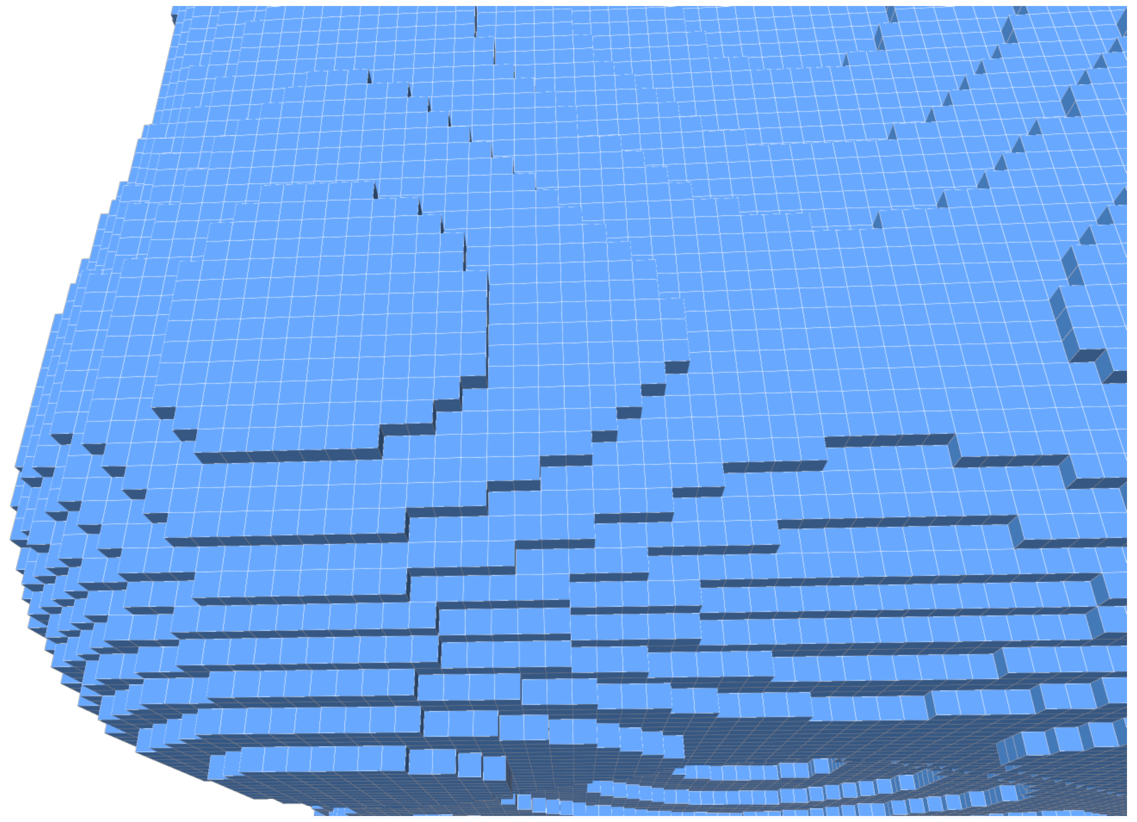

Discrete Differential Operators on Polygonal Meshes

[de Goes et al 20]

[C. & L. DGMM2022]

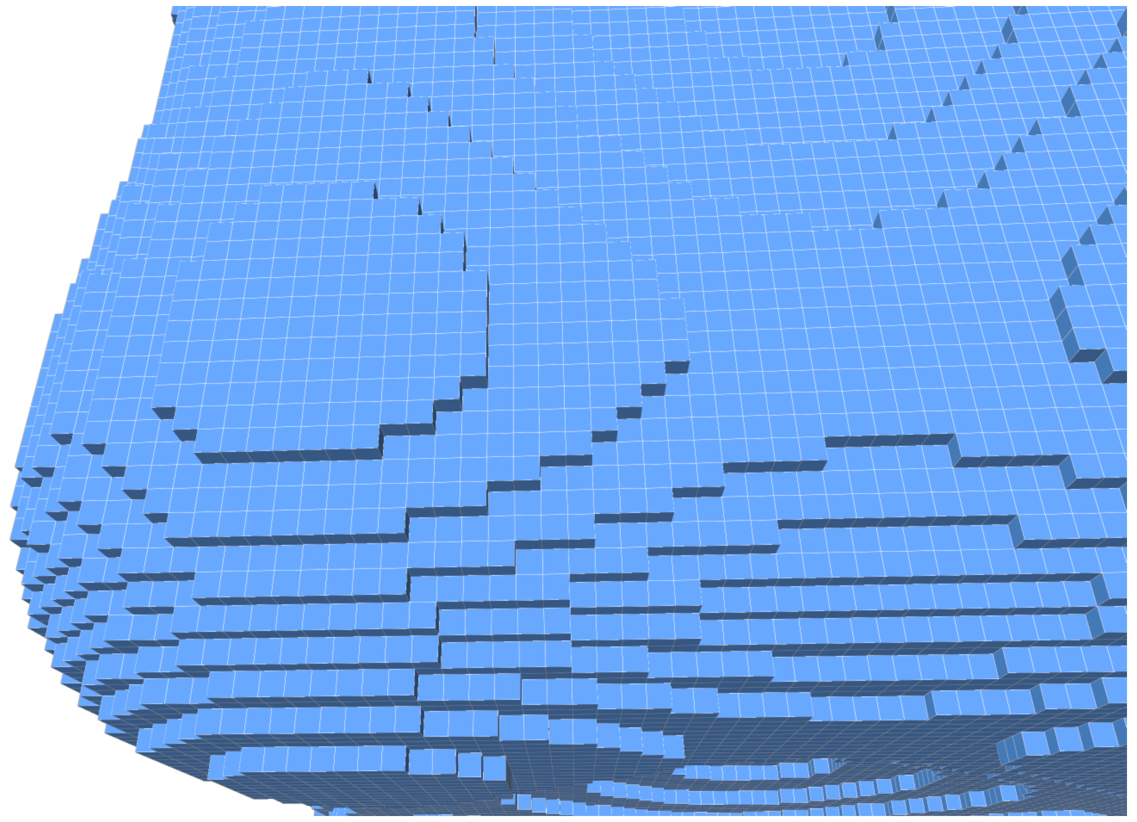

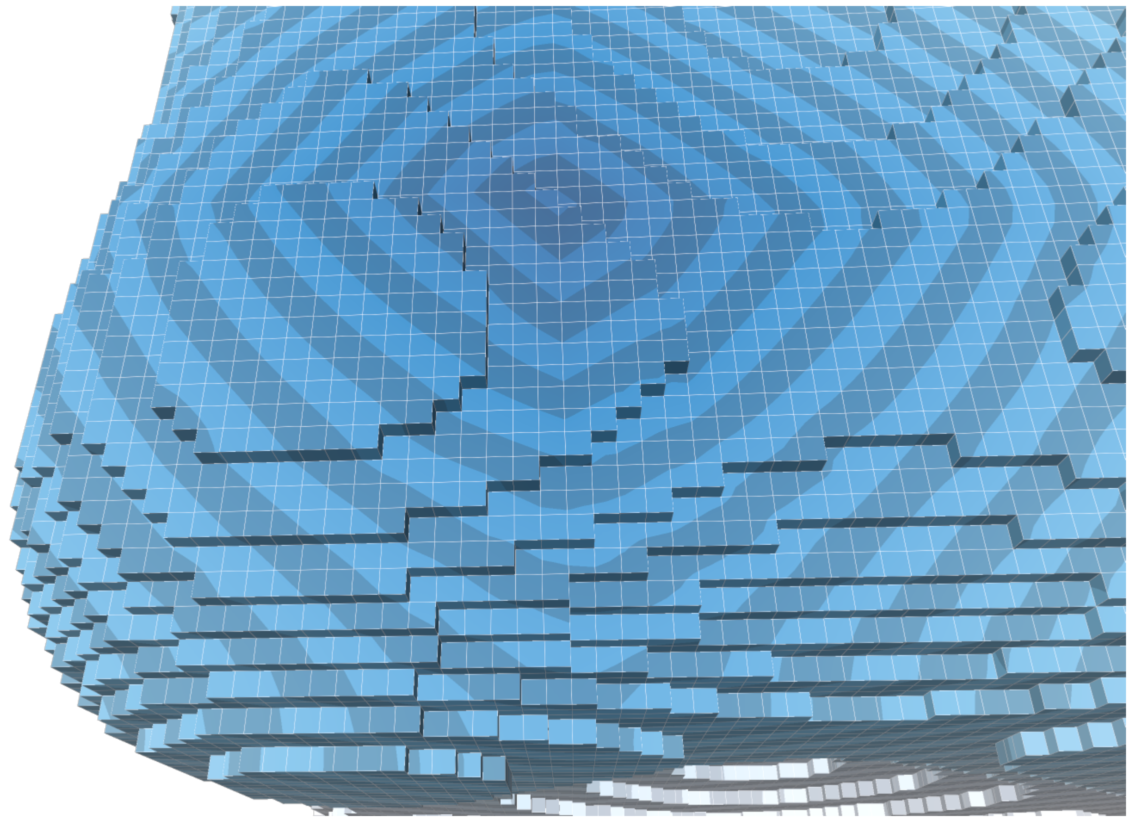

Discrete Differential Operators on Polygonal Meshes

[de Goes et al 20]
[C. & L. DGMM2022]

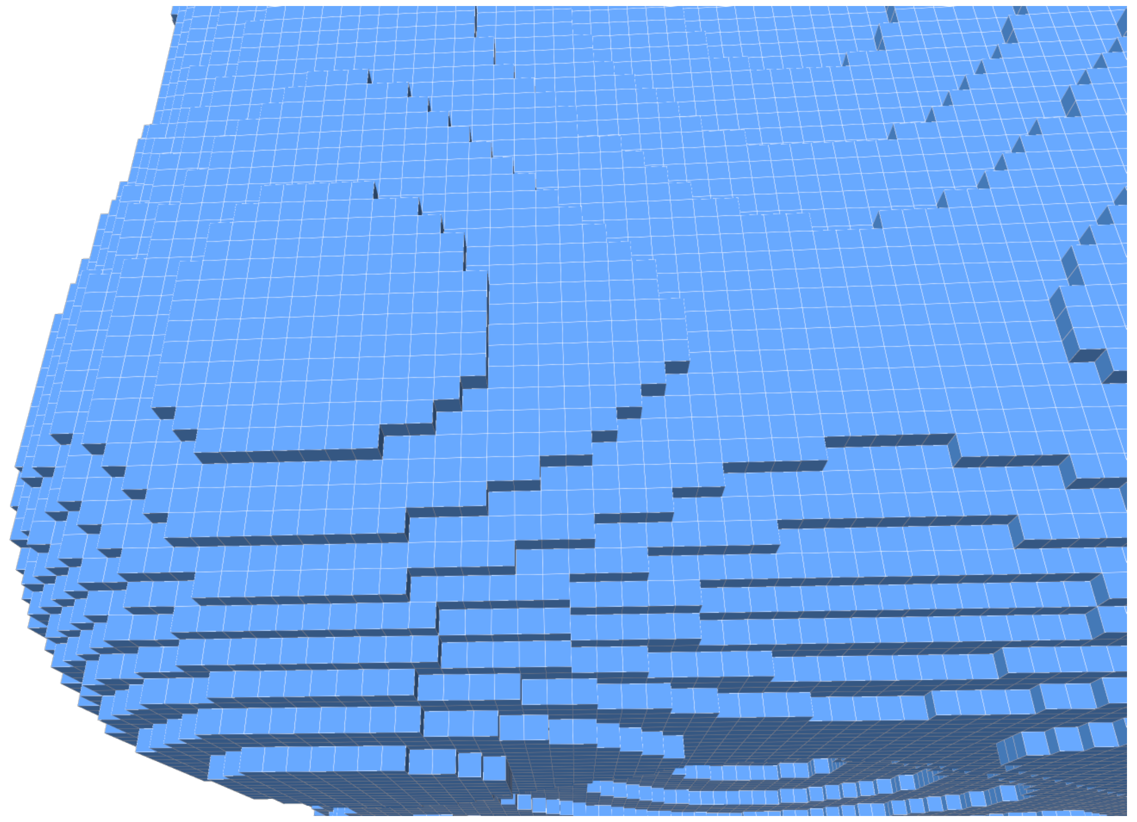

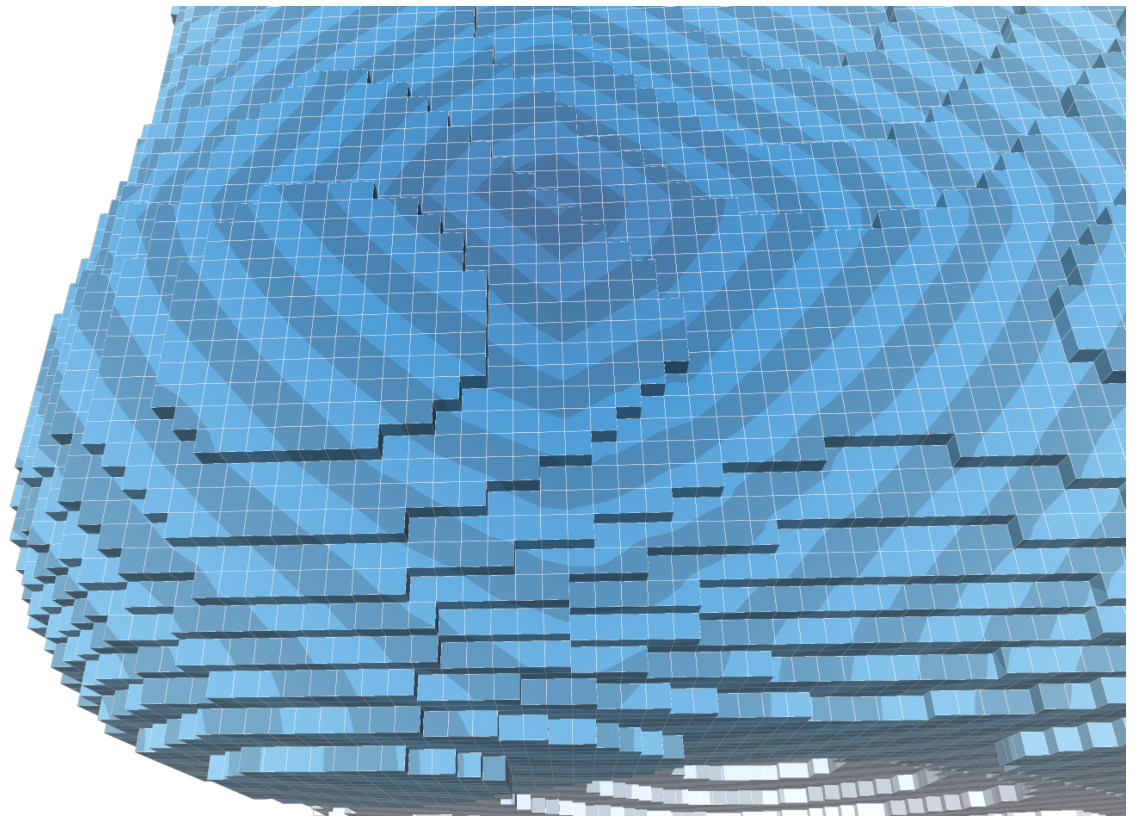

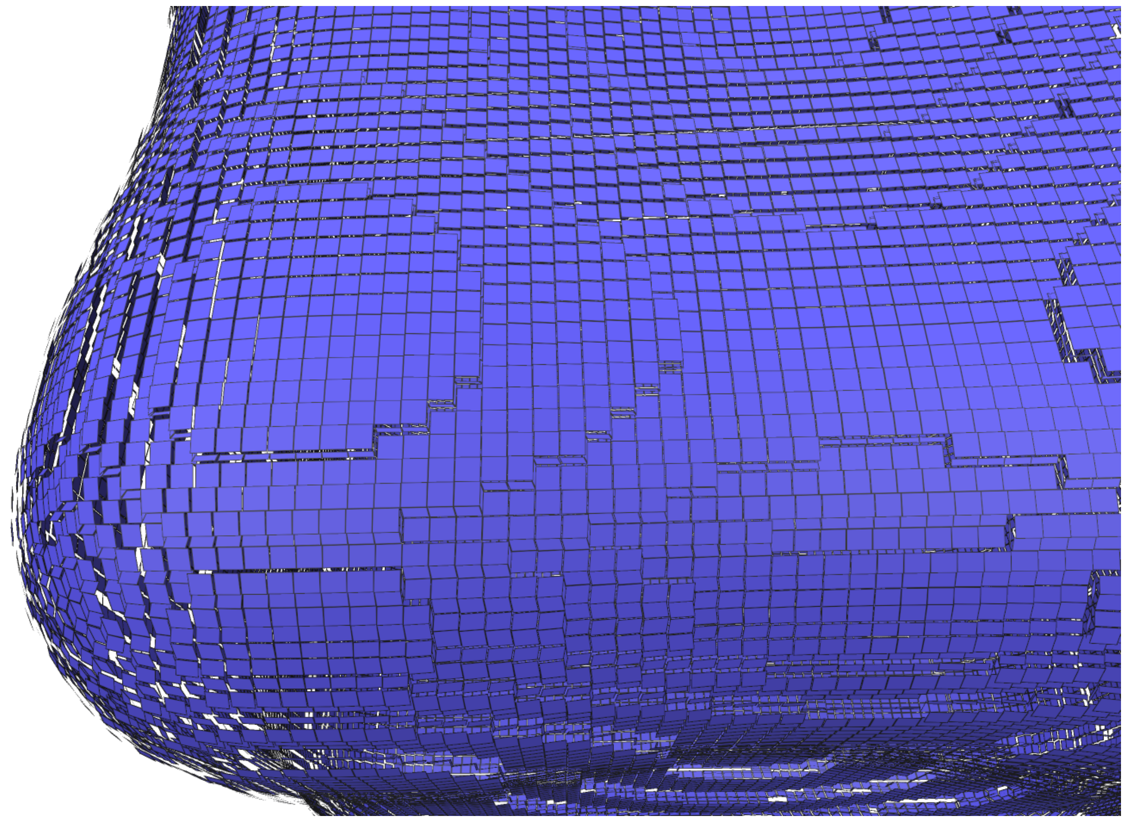

We can *correct* the face embedding using asymptotic convergence normal vector field

Challenges: advance corrections (e.g. on the Grassmanian, higher order schemes…) for asymptotic properties

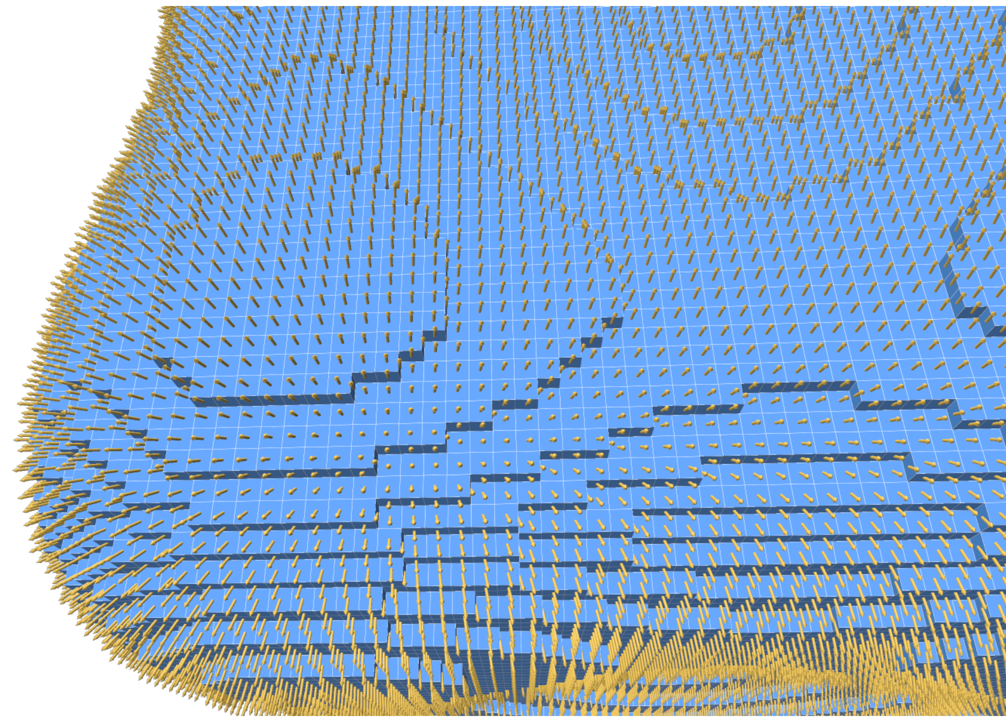

Discrete Differential Operators on Polygonal Meshes

[de Goes et al 20]
[C. & L. DGMM2022]

We can *correct* the face embedding using asymptotic convergence normal vector field

Challenges: advance corrections (e.g. on the Grassmanian, higher order schemes…) for asymptotic properties

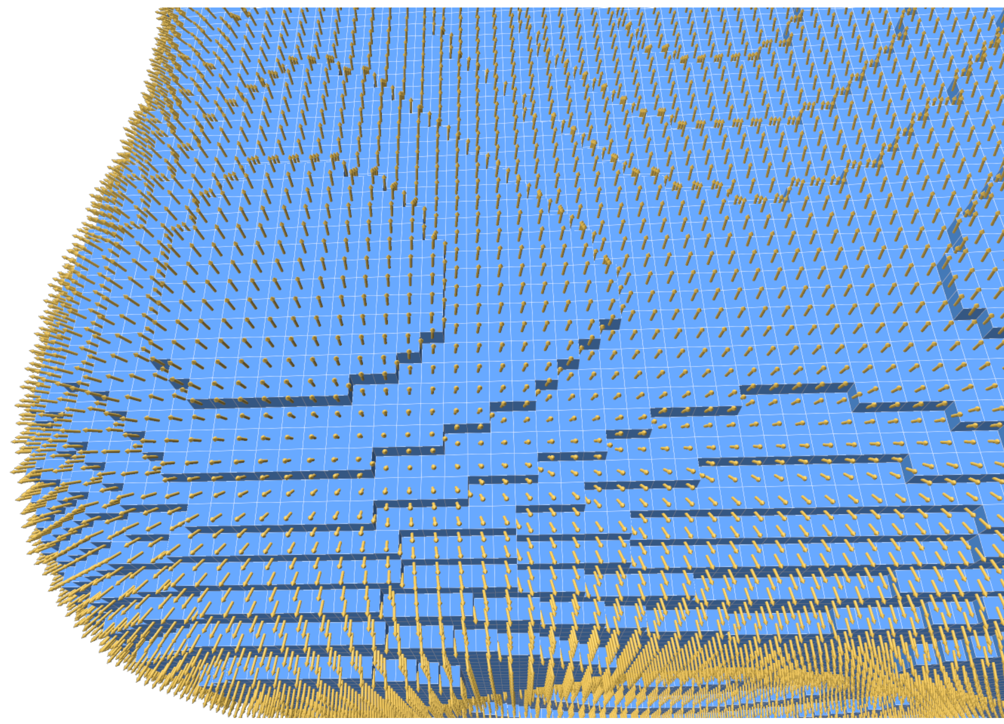

Experimental validation: stability of Laplace-Beltrami eigenvectors

Experimental validation: stability of Laplace-Beltrami eigenvectors

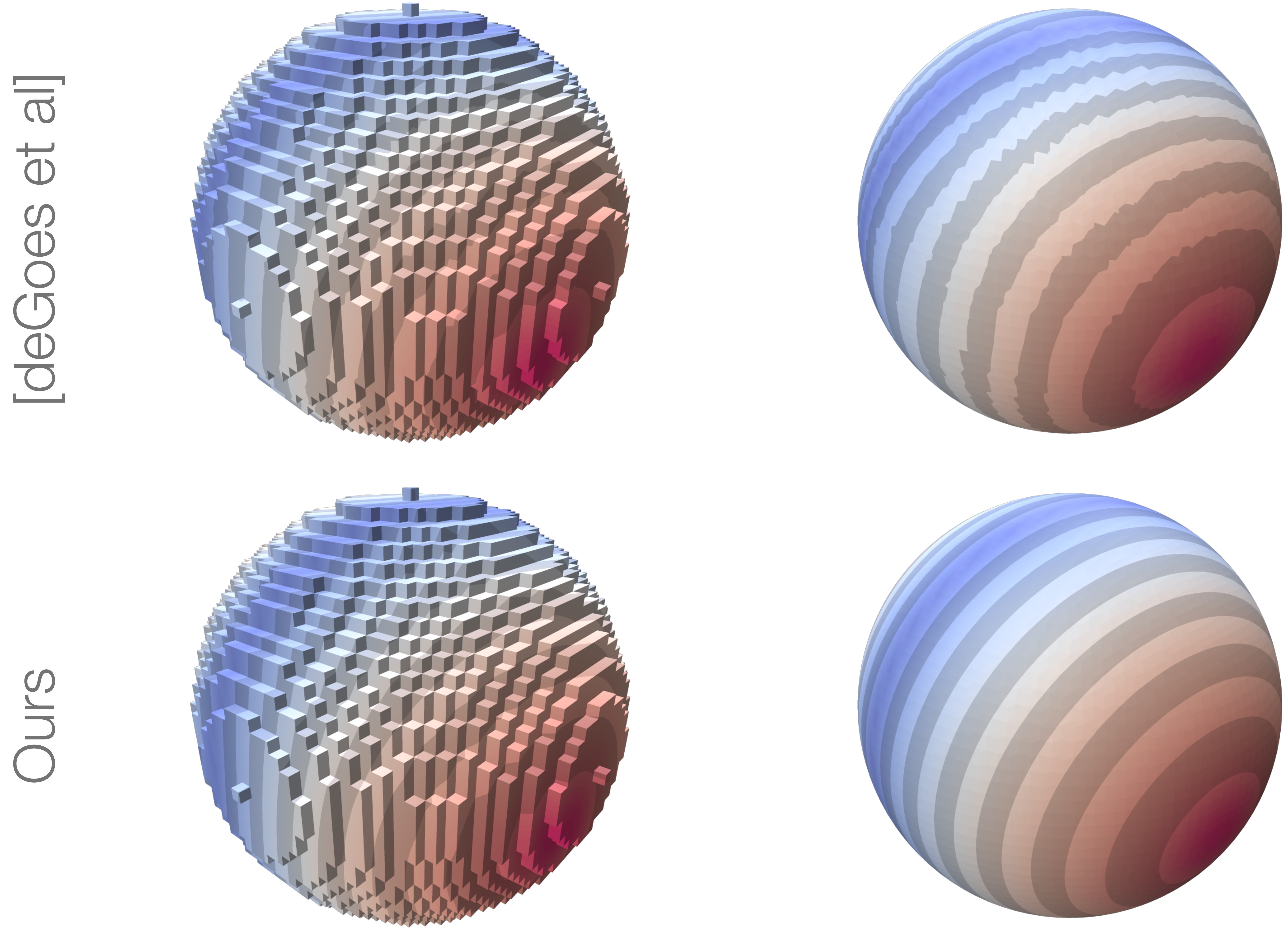

Experimental validation: Geodesics using the heat method

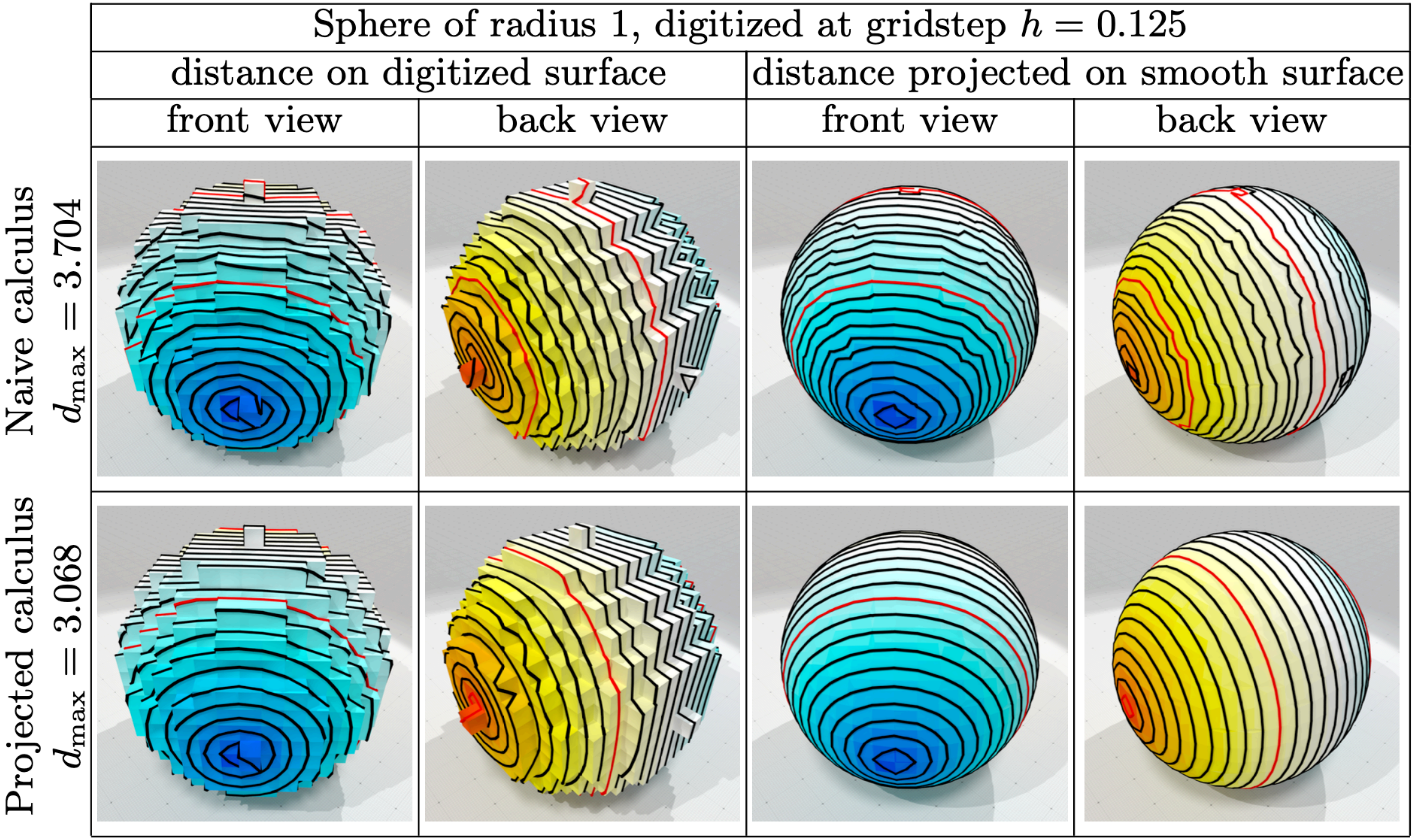

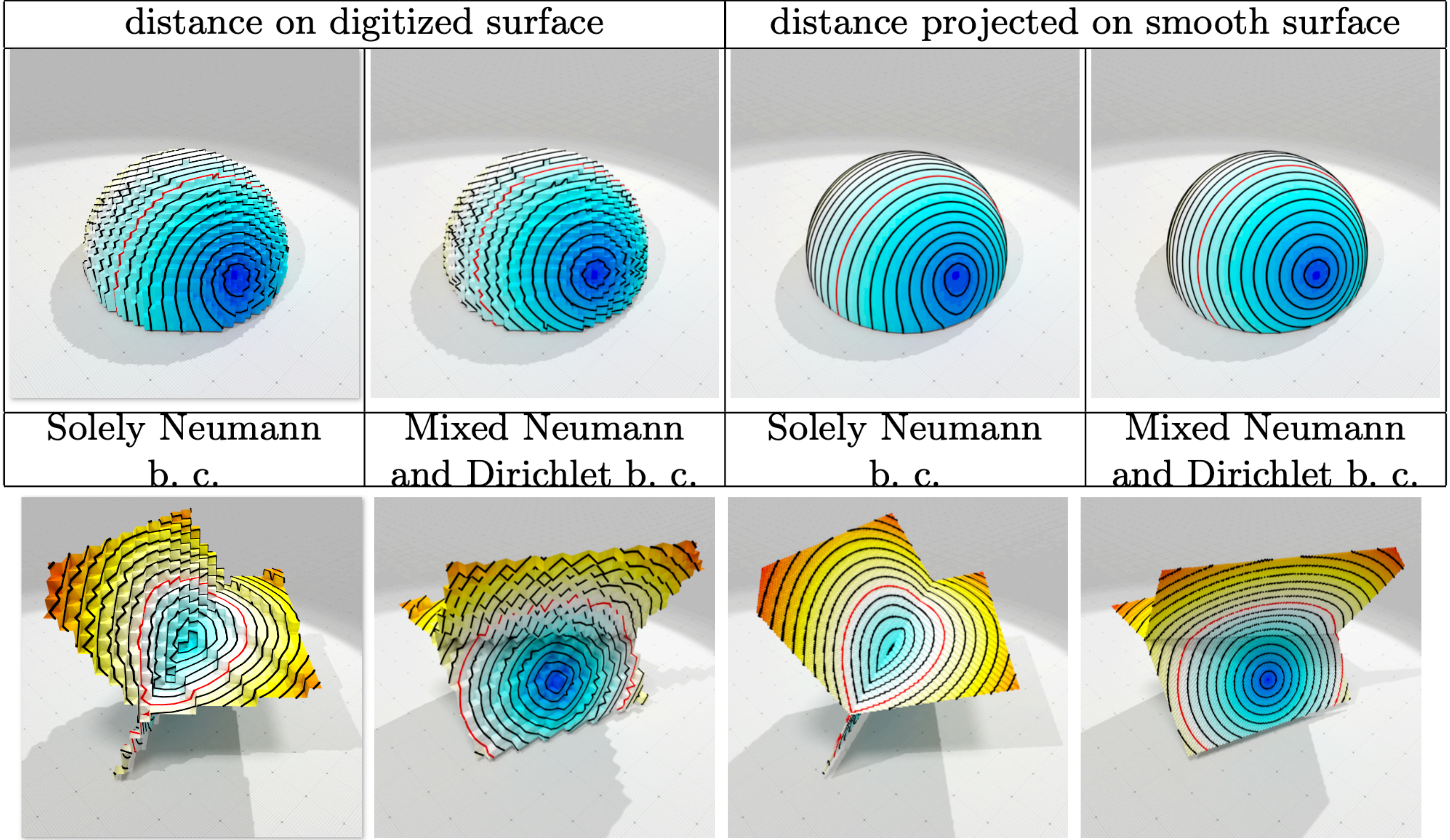
distance on digitized surface
distance projected on smooth surface
Solely Neumann b. c.
Mixed Neumann and Dirichlet b. c.
Solely Neumann b. c.
Mixed Neumann and Dirichlet b. c.

hands on…

```
void initQuantities()
{
  PolygonalCalculus<SH3::RealPoint,SH3::RealVector> calculus(surfmesh);

  std::vector<PolygonalCalculus<SH3::RealPoint,SH3::RealVector>::Vector> gradients;
  std::vector<PolygonalCalculus<SH3::RealPoint,SH3::RealVector>::Vector> cogradients;
  std::vector<PolygonalCalculus<SH3::RealPoint,SH3::RealVector>::Real3dVector> normals;
  std::vector<PolygonalCalculus<SH3::RealPoint,SH3::RealVector>::Real3dVector> vectorArea;
  std::vector<PolygonalCalculus<SH3::RealPoint,SH3::RealVector>::Real3dPoint> centroids;
  std::vector<double> faceArea;

  for(auto f=0; f < surfmesh.nbFaces(); ++f)
  {
    PolygonalCalculus<SH3::RealPoint,SH3::RealVector>::Vector ph = phiFace(f);
    PolygonalCalculus<SH3::RealPoint,SH3::RealVector>::Vector grad = calculus.gradient(f) * ph;
    gradients.push_back( grad );
    PolygonalCalculus<SH3::RealPoint,SH3::RealVector>::Vector cograd =  calculus.coGradient(f) * ph;
    cogradients.push_back( cograd );
    normals.push_back(calculus.faceNormalAsDGtalVector(f));

    auto vA = calculus.vectorArea(f);
    vectorArea.push_back({vA(0) , vA(1), vA(2)});

    faceArea.push_back( calculus.faceArea(f));

    centroids.push_back( calculus.centroidAsDGtalPoint(f) );
  }

  psMesh->addFaceVectorQuantity("Gradients", gradients);
  psMesh->addFaceVectorQuantity("co-Gradients", cogradients);
  psMesh->addFaceVectorQuantity("Normals", normals);
  psMesh->addFaceScalarQuantity("Face area", faceArea);
  psMesh->addFaceVectorQuantity("Vector area", vectorArea);

  polyscope::registerPointCloud("Centroids", centroids);
}
```

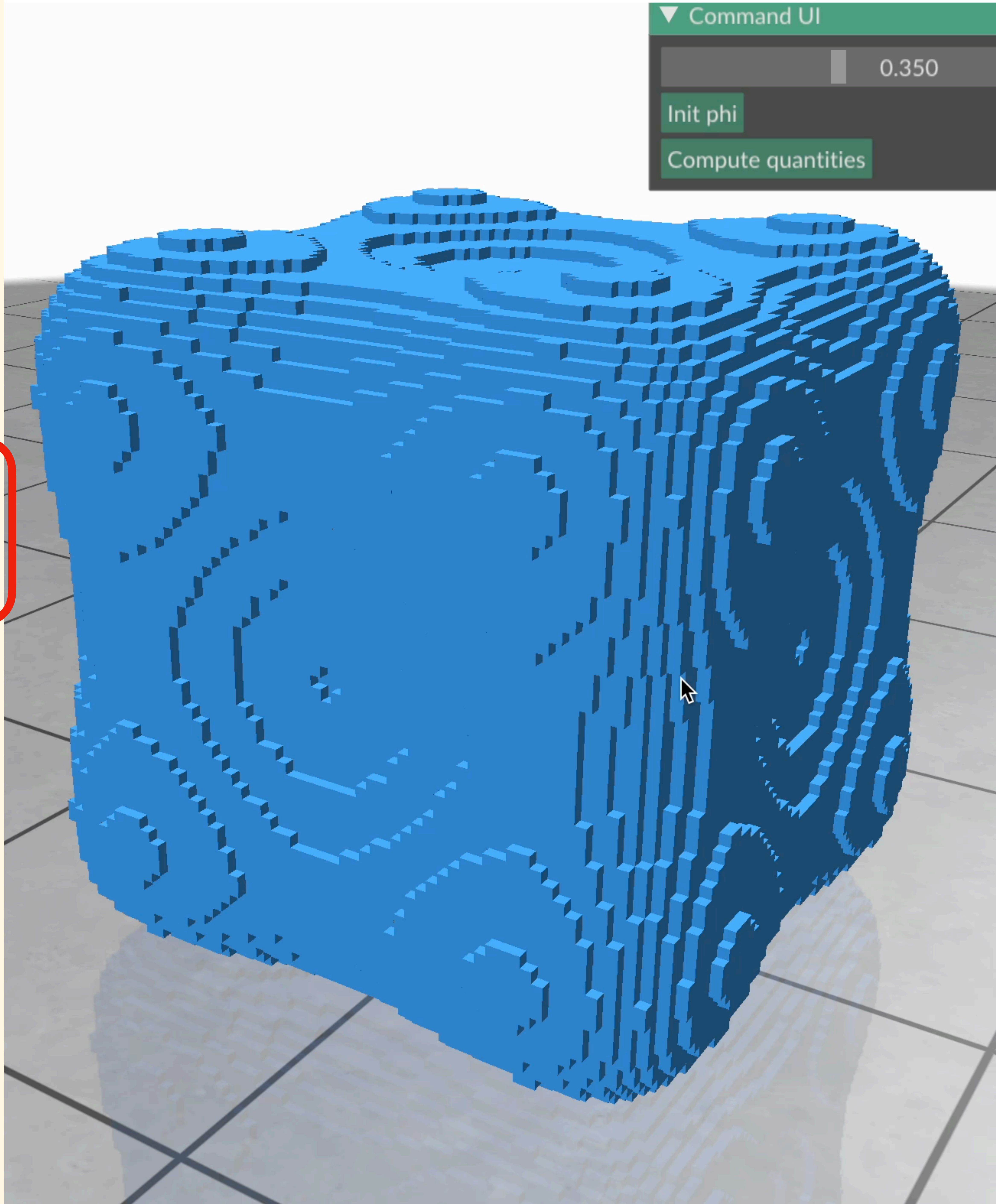

```cpp
void initQuantities()
{
  PolygonalCalculus<SH3::RealPoint,SH3::RealVector> calculus(surfmesh);

  std::vector<PolygonalCalculus<SH3::RealPoint,SH3::RealVector>::Vector> gradients;
  std::vector<PolygonalCalculus<SH3::RealPoint,SH3::RealVector>::Vector> cogradients;
  std::vector<PolygonalCalculus<SH3::RealPoint,SH3::RealVector>::Real3dVector> normals;
  std::vector<PolygonalCalculus<SH3::RealPoint,SH3::RealVector>::Real3dVector> vectorArea;
  std::vector<PolygonalCalculus<SH3::RealPoint,SH3::RealVector>::Real3dPoint> centroids;
  std::vector<double> faceArea;

  for(auto f=0; f < surfmesh.nbFaces(); ++f)
  {
    PolygonalCalculus<SH3::RealPoint,SH3::RealVector>::Vector ph = phiFace(f);
    PolygonalCalculus<SH3::RealPoint,SH3::RealVector>::Vector grad = calculus.gradient(f) * ph;
    gradients.push_back( grad );
    PolygonalCalculus<SH3::RealPoint,SH3::RealVector>::Vector cograd =  calculus.coGradient(f) * ph;
    cogradients.push_back( cograd );
    normals.push_back(calculus.faceNormalAsDGtalVector(f));

    auto vA = calculus.vectorArea(f);
    vectorArea.push_back({vA(0) , vA(1), vA(2)});

    faceArea.push_back( calculus.faceArea(f));

    centroids.push_back( calculus.centroidAsDGtalPoint(f) );
  }

  psMesh->addFaceVectorQuantity("Gradients", gradients);
  psMesh->addFaceVectorQuantity("co-Gradients", cogradients);
  psMesh->addFaceVectorQuantity("Normals", normals);
  psMesh->addFaceScalarQuantity("Face area", faceArea);
  psMesh->addFaceVectorQuantity("Vector area", vectorArea);

  polyscope::registerPointCloud("Centroids", centroids);
}
```

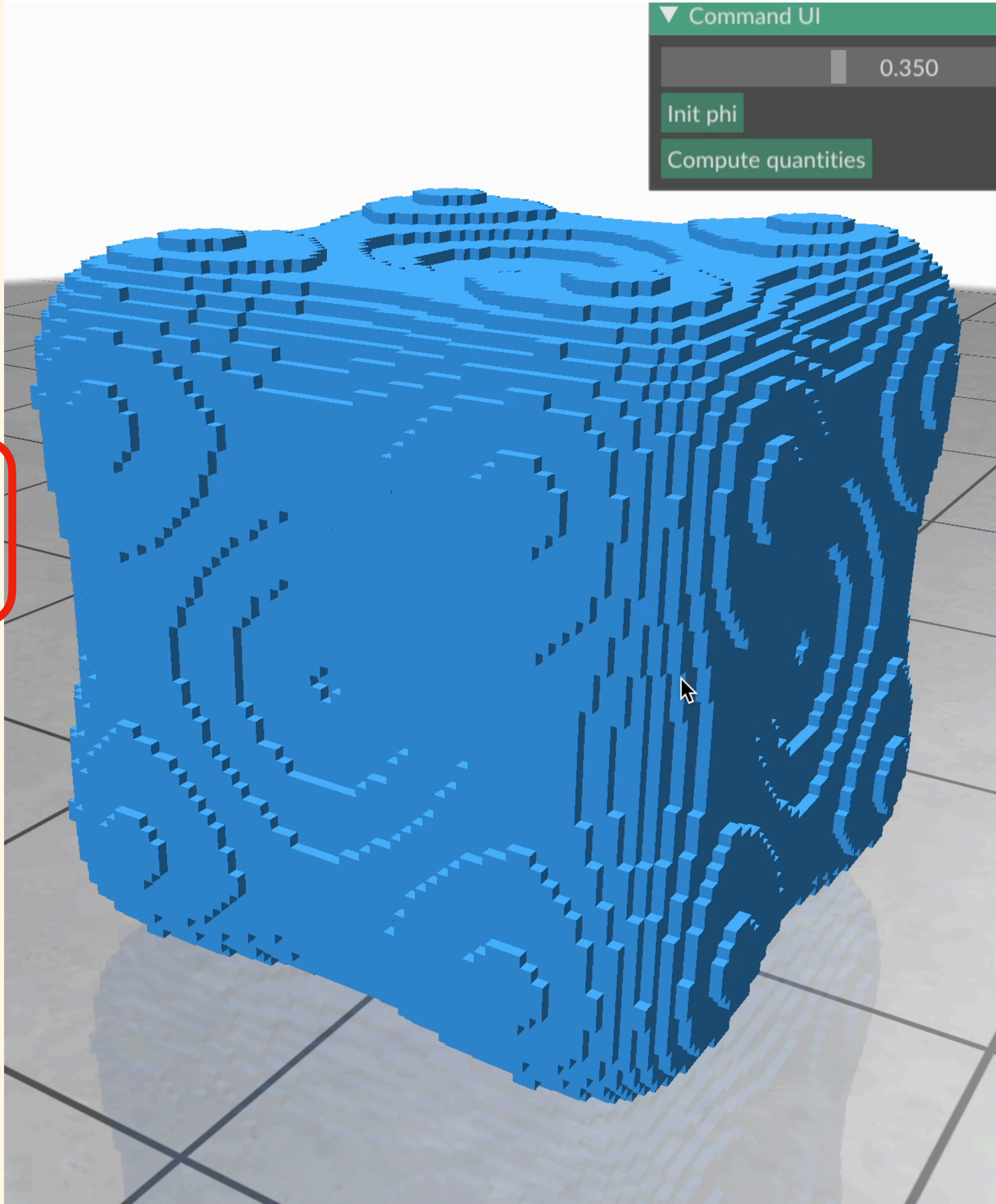

conclusion

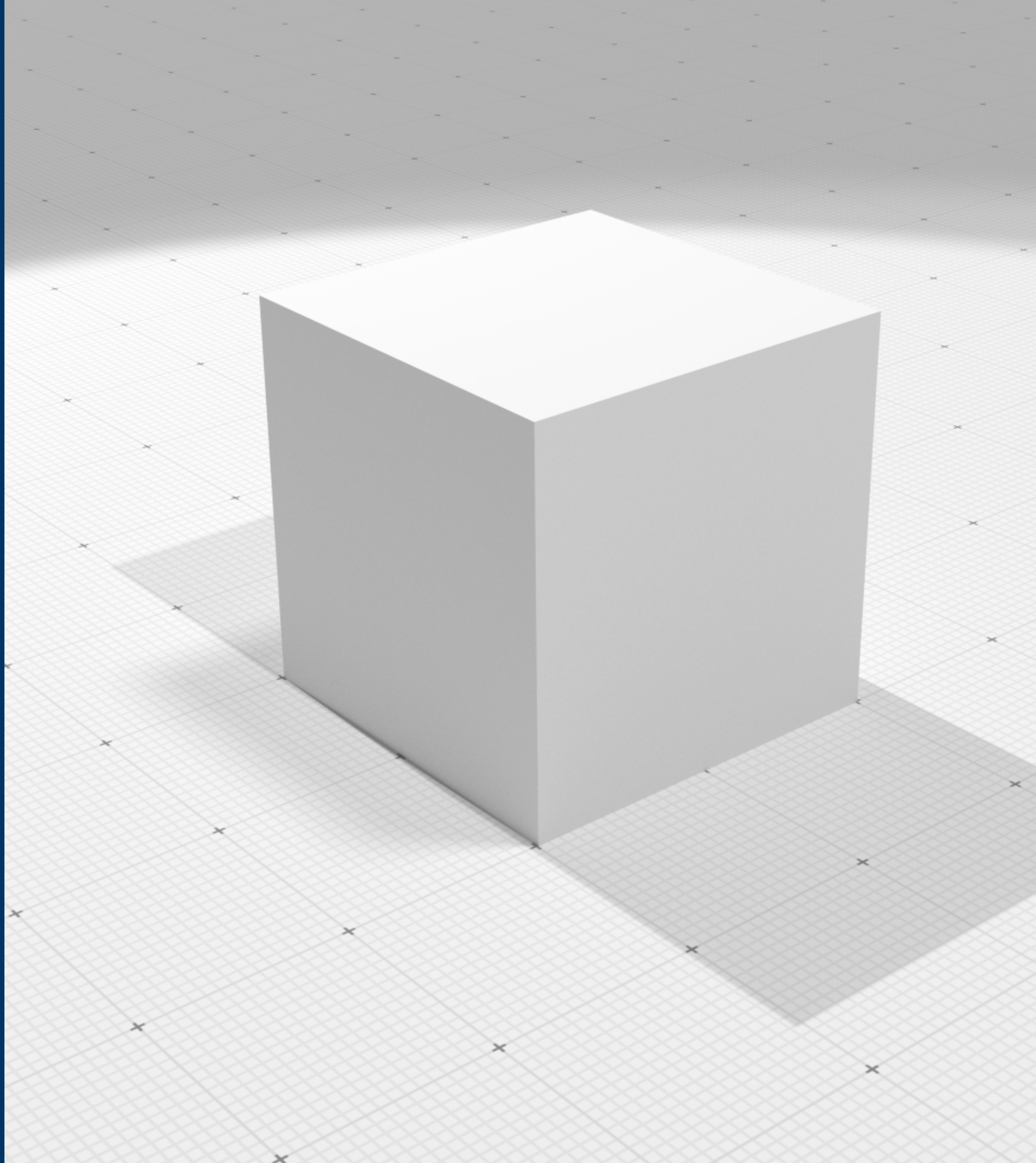

Conclusion

Topology and geometry processing on regular data:

- fast algorithms thanks to the regularity of the data
- simple topological structure
- integer based computations
- advanced surface based geometry processing

… in $\mathbb{Z}^d$

DGtal

dgtal.org

Discord

https://discord.gg/PtCk6vtS

Challenges

- **Foundation of Digital Geometry**
  - Objects (hyperplane, spheres..): arithmetical properties,
  - Digital convexity
  - Bijective transformations
  - Alternative pavings

- **Discrete <-> Continuous**
  - Digitization: stable properties (topology, geometric quantities…)
  - Unified model
  - Reconstruction (2d, 3d…)

- **Applications**
  - Material sciences
  - Image processing

References

[Villanueva et al 17] Alberto Jaspe Villanueva, Fabio Marton, and Enrico Gobbetti, Symmetry-aware Sparse Voxel DAGs (SSVDAGs) for compression-domain tracing of high-resolution geometric scenes, Journal of Computer Graphics Techniques (JCGT), vol. 6, no. 2, 1-30, 2017

[Chen et al 2020] Half-Space Power Diagrams and Discrete Surface Offsets, Zhen Chen, Daniele Panozzo, Jérémie Dumas. In TVCG, 2019.

[C. et al 07] Optimal Separable Algorithms to Compute the Reverse Euclidean Distance Transformation and Discrete Medial Axis in Arbitrary Dimension, David Coeurjolly Annick Montanvert, IEEE Transactions on Pattern Analysis and Machine Intelligence, March 2007

[Martinez et al 20] Orthotropic k-nearest Foams for Additive Manufacturing, Jonàs Martínez, Haichuan Song, Jérémie Dumas, Sylvain Lefebvre, ACM TOG 2017

[Liu et al 18] Narrow-band topology optimization on a sparsely populated grid. Liu, H., Hu, Y., Zhu, B., Matusik, W., & Sifakis, E. (2018). ACM Transactions on Graphics (TOG), 37(6), 1-14.

[de Goes et al 20] Discrete Differential Operators on Polygonal Meshes, de Goes, Butts, Desbrun SIGGRAPH / ACM Transactions on Graphics (2020)

[C. et al 21] Digital surface regularization with guarantees, David Coeurjolly, Jacques-Olivier Lachaud, Pierre Gueth, IEEE Transactions on Visualization and Computer Graphics, January 2021

[C. et al 16] Piecewise smooth reconstruction of normal vector field on digital data, David Coeurjolly, Marion Foare, Pierre Gueth, Computer Graphics Forum (Proceeding Pacific Graphics), September 2016

[Caissard et al 19] Laplace–Beltrami Operator on Digital Surfaces, Thomas Caissard, David Coeurjolly, Jacques-Olivier Lachaud, Tristan Roussillon, Journal of Mathema Imaging and Vision, January 2019

[Delanoy et al 19] Combining voxel and normal predictions for multi-view 3D sketching, Johanna Delanoy, David Coeurjolly, Jacques-Olivier Lachaud, Adrien Bousseau Computers and Graphics, June 2019

[Belkin et al 08] Belkin, M., Sun, J., Wang, Y.: Discrete laplace operator on meshed surfaces. In: M. Teillaud (ed.) Proceedings of the 24th ACM Symposium on Computational Geometry, College Park, MD, USA, June 9-11, 2008, pp. 278–287. ACM (2008)

References

[Bertrand94] Bertrand, Gilles. "Simple points, topological numbers and geodesic neighborhoods in cubic grids." *Pattern recognition letters* 15.10 (1994): 1003-1011.

[BC94] Bertrand, Gilles, and Michel Couprie. "On parallel thinning algorithms: minimal non-simple sets, P-simple points and critical kernels." *Journal of Mathematical Imaging and Vision* 35.1 (2009): 23-35.

[YLJ18] Yan, Yajie, David Letscher, and Tao Ju. "Voxel cores: Efficient, robust, and provably good approximation of 3d medial axes." *ACM Transactions on Graphics (TO* 37.4 (2018): 1-13.

[LT16] Lachaud, Jacques-Olivier, and Boris Thibert. "Properties of gauss digitized shapes and digital surface integration." *Journal of Mathematical Imaging and Vision* 54 (2016): 162-180.

[LTC17] Lachaud, Jacques-Olivier, David Coeurjolly, and Jérémy Levallois. "Robust and convergent curvature and normal estimators with digital integral invariants." *Moc Approaches to Discrete Curvature*. Springer, Cham, 2017. 293-348.

[LRTC20] Lachaud, Jacques-Olivier, Pascal Romon, Boris Thibert, and David Coeurjolly. "Interpolated corrected curvature measures for polygonal surfaces." *Computer Graphics Forum*. Vol. 39. No. 5. 2020.